

University of Southampton Research Repository ePrints Soton

Copyright © and Moral Rights for this thesis are retained by the author and/or other copyright owners. A copy can be downloaded for personal non-commercial research or study, without prior permission or charge. This thesis cannot be reproduced or quoted extensively from without first obtaining permission in writing from the copyright holder/s. The content must not be changed in any way or sold commercially in any format or medium without the formal permission of the copyright holders.

When referring to this work, full bibliographic details including the author, title, awarding institution and date of the thesis must be given e.g.

AUTHOR (year of submission) "Full thesis title", University of Southampton, name of the University School or Department, PhD Thesis, pagination

UNIVERSITY OF SOUTHAMPTON Bone & Joint Research Group Faculty of Medicine

BONE TISSUE ENGINEERING

HARNESSING INTERDISCIPLINARY
APPROACHES FOR CLINICAL APPLICATION

James Oliver Smith

Thesis for the degree of Doctor of Medicine

July 2013

UNIVERSITY OF SOUTHAMPTON

ABSTRACT

FACULTY OF MEDICINE, HEALTH & LIFE SCIENCES

Doctor of Medicine

BONE TISSUE ENGINEERING

HARNESSING INTERDISCIPLINARY APPROACHES FOR CLINICAL APPLICATION

By James Oliver Smith

There is an acute requirement for novel clinical approaches to combat loss or dysfunction of skeletal tissue. Inherent disadvantages of current reconstructive strategies combined with the ageing population and a continuing increase in musculoskeletal pathology and patient expectations, highlight a pressing need to augment current practice with osteoregenerative techniques. Tissue engineering shows promise as a discipline to meet these needs by the systematic selection and manipulation of cells, matrices and biological stimuli to produce the required tissue.

This thesis examines current and emerging clinical strategies available for replacement of skeletal tissue and discusses the requisite properties that novel approaches are required to possess before successful progress to clinical application can be achieved. Each chapter in this thesis details a specific aspect of the continuous process in the development of a novel tissue engineering strategy, considering also the wider scientific, logistical, clinical, financial and practical issues that must be addressed for successful outcomes:

- The effects of cells, cytokines and material properties are explored in the context of recreating normal biological structure and function.
- The limitations of current clinical cell enrichment techniques are discussed and a novel intra-operative strategy is shown to enrich skeletal stem cells from bone marrow by acoustic filtration, suitable for potential orthopaedic application.
- A tissue engineering approach applied to an established orthopaedic implant (Tantalum Trabecular Metal) is shown to support osteogenic differentiation and enhance bone-implant interface strength, with potential clinical applicability.
- A murine model for skeletal regeneration is used to evaluate a novel ternary polymer blend scaffold for efficacy in a tissue engineering approach.
- An ovine model for skeletal regeneration is defined and evaluated along with a candidate binary polymer blend scaffold for tissue engineering strategies.
- Many of the hurdles to successful clinical translation that are commonly overlooked are discussed with particular reference to the cellular toxicity of local anaesthetics

This thesis demonstrates the considerable potential of skeletal tissue engineering approaches, but highlights the requirement for a concerted multidisciplinary appreciation to achieve successful clinical translation.

Table of contents

Abstract	. I
Table of contents	III - XII
List of figures	XIII - XX
List of tables	XXI - XXIII
List of abbreviations	XXV - XXIX
Declaration	XXXI
Publications and presentations	XXXIII - XXXIX
Prizes and awards	XL
Acknowledgements	XLI
Chapter I: General Introduction	1 - 65
1.1 Scale of the problem in the context of clinical need	3
1.2 Composition of skeletal tissues	5 - 14
1.2.1Bone	5 - 13
1.2.1.1Fracture repair	
1.2.2Cartilage	10 - 12
1.2.3Tendon and ligament	13
1.3 Rationale for research into skeletal tissue engineering	14 - 15
1.4 Skeletal tissue engineering	16
1.5 Stem cells	17
1.6 Stem cells in skeletal tissue engineering	18 - 20
1.7 Cellular and molecular approaches to skeletal regeneration	21 - 28
1.7.1Skeletal Stem Cells and bone repair	21 - 24
1.7.2 Growth factors	24 - 27
1.7.2.1Transforming growth factor beta (TGF-β)	
1.7.2.2 Bone morphogenetic proteins (BMPs)	
1.7.2.3 Wnt signalling molecules	
1.7.2.4Local growth factors	
1.7.2.4.1 IGF-I and IGF-II	
1.7.2.4.2 FGF-1 and FGF-2	
1.7.2.4.3 PDGF	
1.7.2.4.4 Vascular endothelial growth facto	or

1.7.3Growth factors in tendon and ligament healing	27
1.7.4Platelet-rich plasma	28
1.8 Scaffolds – osteoconduction and osteoinduction	29
1.8.1Biological scaffolds	31 - 39
1.8.1.1Autogenous biological scaffolds	
1.8.1.1.1 Cancellous autograft	
1.8.1.1.2Cortical autograft	
1.8.1.1.3Autogenous cartilage graft	
1.8.1.1.4Autogenous tendon/ligamer	nt
1.8.1.2Allogeneic biological scaffolds	
1.8.1.2.1Allogeneic bone (allograft)	
1.8.1.2.1.1 Allograft proce	ssing
1.8.1.2.1.2 Enhancement	of allograft properties
1.8.1.2.1.3 Demineralised	Bone Matrix (DBM)
1.8.1.2.2 Cartilage and composite alle	ogeneic grafts
1.8.1.2.3Allogeneic tendon and ligan	nent
1.8.1.3Xenogeneic scaffolds	
1.8.2Synthetic scaffolds	40 - 57
1.8.2.1Hydrogels	
1.8.2.2Ceramics	
1.8.2.3Bioactive glasses	
1.8.2.4Osteoconductive metals	
1.8.2.5Synthetic polymers	
1.8.2.5.1Polymer scaffold fabrication	techniques
1.8.2.6Composite scaffolds	
1.8.2.7Tissue engineered constructs in maxillo	facial surgery
1.9 Future directions – scaffolds	58 - 59
1.10Considerations for the development of a tissue engineering	ı strategy60
1.10.1Funding	61
1.10.2 Regulatory requirements and research governance	e61
1.10.3Practical factors	62
1.10.3.1Scale-up for pre-clinical testing	
1.10.3.2Clinical trials	
1.11 Major null hypothesis	64
1.12 Aims	64
1.13 Objectives	65

<u>Chapter II:</u> Development of an intra-operative strategy to enrich skeletal			
stem	cells from bone marrow for orthopaedic application	67 - 94	
2.1	Introduction	69 - 70	
	2.1.1 The clinical requirement for cell enrichment strategies		
	2.1.2Sources of BMA for enrichment		
	2.1.3Cell enrichment strategies		
	2.1.3.1 Culture expansion		
	2.1.3.2 Centrifugation		
	2.1.3.3 Gradient separation		
	2.1.3.4Field-assisted separation		
	2.1.3.5 Selective cell retention		
	2.1.3.6 Filtration		
2.2	Aims	75	
2.3	Null hypotheses	75	
2.4	Materials and methods	76 - 83	
	2.4.1Patient selection	76	
	2.4.2Bone marrow harvest from the femoral canal	76	
	2.4.3Operation of the device	77 - 79	
	2.4.4Filtration time	79	
	2.4.5 Nucleated cell count and cell viability analysis	79	
	2.4.6CFU-F analysis	80	
	2.4.7 Flow cytometric analysis of stem cell markers	80	
	2.4.8Multi-lineage differentiation of concentrated and		
	unconcentrated cells	81	
	2.4.9 Histological staining and quantification of		
	differentiated cultures	82	
	2.4.10Cell seeding onto decellularised human bone graft	82	
	2.4.11 WST-1 assay for relative quantification of cell seeding	83	
	2.4.12Cell viability and imaging	83	
2.5	Results	84 - 90	
	2.5.1 BMA concentration and SSC enrichment	84 - 87	
	2.5.2Multi-lineage differentiation of concentrated and		
	unconcentrated cells.	87 - 89	
	2.5.3Cell seeding onto decellularised human trabecular		
	bone graft	89 - 90	
26	Discussion	91 - 94	

	<u>Chapter III:</u> Tantalum Trabecular Metal – addition of human skeletal cells			
	established orthopaedic implant to enhance bone-implant interfa			
stren	gth and clinical application	95 -	120	
3.1	Introduction		99	
	3.1.1Current clinical strategies for bone stock replacement	97		
	3.1.2The rationale for extending the clinical application			
	of tantalum		99	
	. Objectives			
	Null hypothesis			
3.4	Materials and methods		- 106	
	3.4.1Materials	101		
	3.4.2Cell culture	101		
	3.4.3Tantalum preparation	101		
	3.4.4Allograft preparation	102		
	3.4.5Autograft preparation	102		
	3.4.6Analysis of skeletal cell penetration and viability	102	- 104	
	3.4.6.1Live/dead immunostaining			
	3.4.6.2Collagen type I and Bone Sialoprotein immunosta	aining		
	3.4.6.3WST-1 assay			
	3.4.6.4DNA assay			
	3.4.6.5Alkaline Phosphatase assay			
	3.4.6.6Preparation for molecular analysis			
	3.4.7Analysis of cellular morphology and penetration	105		
	3.4.7.1Scanning Electron Microscopy			
	3.4.8Analysis of mechanical 'pull-apart' strength	106		
	3.4.9Statistics	106		
3.5	Results	107	- 117	
	3.5.1Cellular proliferation, viability and immunostaining	107	- 110	
	3.5.2Analysis of cell proliferation	111		
	3.5.3Analysis of DNA, ALP and specific ALP Activity	111	- 113	
	3.5.4Molecular analysis	114	- 115	
	3.5.5Analysis of cellular morphology and penetration	115	- 116	
	3.5.6Mechanical 'pull-apart' strength	117		
3.6	Discussion		- 120	

Chapt	<u>ter IV:</u> <i>In vivo</i> evaluation of novel ternary polymer blend scaffold	s
for sk	eletal tissue engineering strategies using a murine model	121 - 166
4.1	. Introduction	123 - 126
4.2	. Aims	127
4.3	. Null hypotheses	127
4.4	. Materials and methods	128 - 140
	4.4.1 Materials	128
	4.4.2Ternary polymer blend microarray fabrication	128 - 129
	4.4.3Cell acquisition and isolation	129 - 130
	4.4.4 Selection of candidate ternary polymer blends for 3D	
	fabrication	130 - 132
	4.4.4.1 Scanning Electron Microscopy	
	4.4.4.2 Cell culture on polymer microarrays	
	4.4.5 Manufacture of selected 3D polymer blend scaffolds	132 - 133
	4.4.6 Assessment of 3D scaffold characteristics	133
	4.4.7 In vitro pilot culture	133
	4.4.7.1 Characterisation of cell activity following in vitro	pilot culture
	4.4.8 Structural analysis of the chosen scaffold	134
	4.4.9 In vitro culture and analysis of single selected scaffold	134 - 136
	4.4.9.1 Immunohistochemical analysis	
	4.4.9.2 Preparation for molecular analysis	
	4.4.10 In vivo studies	137 -140
	4.4.10.1 Scaffold preparation prior to implantation	
	4.4.10.2 Implantation into the murine femoral segmental of	defect
	4.4.10.3 Preparation of murine femoral samples	
	4.4.10.4 Radiographic analysis of bone formation	
	4.4.10.5CT image analysis	
	4.4.10.6 Histological and Immunohistochemical analysis	
	4.4.10.6.1 Histochemical staining	
	4.4.10.6.2 Immunohistochemical staining	
4.5	. Results	141 - 162
	4.5.1 Physical characteristics of selected blends	141
	4.5.2 Solubility/ stability assessment	142
	4.5.3 Seven day <i>in vitro</i> pilot culture	142 - 144

4.5.4	<i>ın vitro</i> a	nalysis of selected polymer scarfold145 - 147
	4.5.4.1	Analysis of ALP production and cell viability
	4.5.4.2	Immunostaining for osteogenic bone-matrix proteins
	5.4.4.3	Molecular profiling
4.5.5	In vivo a	nalysis of Blend 4 (CS/PVAc/PLLA 50/25/25)147 - 162
	4.5.5.1	Radiographic analysis
		4.5.5.1.1Control samples
		4.5.5.1.2Polymer alone samples
		4.5.5.1.3Polymer + SSCs samples
	4.5.5.2	Analysis of change in femoral length
	4.5.5.3	Quantitative µCT analysis
	4.5.5.4	Histological analysis
		4.5.5.4.1Empty defect control samples
		4.5.5.4.2Polymer alone samples
		4.5.5.4.3Polymer + SSCs samples
4.6 Discuss	sion	163 - 166

Chapter V: In vivo evaluation	n of a candidate binary polymer ble	nd scaffold for
skeletal tissue engineering st	rategies using an ovine model	167 - 212
5.1 Introduction		169 - 175
	nt for large animal studies	
·	propriate large animal model	
	propriate defect and bone site	
•	ntal defect	
· ·	tion	
5.1.5.1Intrar	nedullary nails	
	nal plate fixation	
5.1.5.3 Exter	nal fixation	
5.1.6Binary blend po	olymer scaffold	175
5.2 Objectives		176
5.3 Null hypothesis		176
5.4 Materials and methods.		177 - 191
5.4.1Polymer fabrica	ation	177
5.4.2 Initial processing	ng of polymer scaffolds	177 - 178
5.4.3Preliminary exp	periments	178 - 180
5.4.3.1Confi	irmation of scaffold porosity and interc	connectivity
<i>5.4.</i> 3	3.1.1 Scanning Electron Microscopy	
5.4.3	2.1.2 Alcian blue penetration test	
5.4.3.2 Acqu	isition of ovine iliac crest BMA	
5.4.3.3 Isola	tion and culture of ovine SSCs	
5.4.3.4 In vit	ro incubation of ovine SSCs with test :	scaffold
5.4.4Ovine tibial seg	mental defect model	180 - 191
5.4.4.1Fixat	ion design and selection	
5.4.4.2 Cada	veric procedures	
5.4.4.3 Study	y cohorts	
5.4.4.4 Bone	marrow harvesting	
5.4.4.5 Scaff	old preparation and cell seeding prior	to implantation
5.4.4.6 Surgi	ical procedure	
5.4.4	.6.1Premedication, anaesthesia an	d preparation
5.4.4	.6.2 Operative procedure	
	5.4.4.6.2.1 Incision and appro	oach
	5.4.4.6.2.2 Fixation and creat	tion of defect
	5.4.4.6.2.3 Scaffold insertion	and stabilisation

5.4.4.6.2.4... Closure and dressings 5.4.4.6.3....Peri-operative radiography 5.4.4.6.4.... Post-operative procedure 5.4.4.7.....Post-operative analysis 5.4.4.8.....Euthanasia and specimen harvest 5.4.4.9.....Post-mortem specimen analysis 5.4.4.9.1 μCT analysis 5.4.4.9.2.... Mechanical testing 5.4.4.9.3.... Macroscopic analysis 5.4.4.9.4.... Histology 5.5.1.1.....Confirmation of scaffold porosity 5.5.1.2.....Isolation and culture of ovine SSCs 5.5.1.3.....In vitro incubation of ovine SSCs with test scaffold 5.5.2.1.....Complications of surgical procedure and anaesthesia 5.5.2.2.....Radiographic analysis 5.5.2.3....µCT analysis 5.5.2.4.....Mechanical testing 5.5.2.5.....Macroscopic analysis 5.5.2.6.....Histology

Chapter VI: Hurdles to successful clinical translation –	
The effect of commonly used local anaesthetics on skeletal stem cell	040 004
viability and function	213 - 231
6.1 Introduction	215
6.2 Aims	
6.3 Null hypotheses	
6.4 Materials and methods	
6.4.1Reagents, hardware & software	
6.4.2Cell culture	
6.4.3LA preparation	217
6.4.4Incubation in LA	
6.4.5WST-1 assay	218
6.4.6DNA assay	
6.4.7 Live/dead immunostaining	219
6.4.8Alkaline Phosphatase assay	219
6.4.9Alkaline Phosphatase stain	219
6.4.10 Statistical analysis	219
6.5 Results	220 - 227
6.5.1 Effect of LAs on skeletal cell proliferation	220 - 222
6.5.1.1Lidocaine	
6.5.1.2Bupivacaine	
6.5.1.3Levobupivacaine	
6.5.2 Effect of LAs on cell viability and necrosis	223 - 225
6.5.3 Effect of LAs on cell differentiation	225 - 227
6.6 Discussion	228 - 231
Chapter VII: Conclusions and future perspectives	233 - 241
7.1 Conclusions	235 - 238
7.2 Next steps	239 - 240
7.3 Future perspectives	241

References	242 - 288

Appendices:

Anaesthetic protocol for sheep
Peri- and post-operative protocol for sheep
Selected publications related to this thesis

List of figures

Chapter I

Fig. 1.1 Anteroposterior pelvis and lateral left hip radiographs of a female
made prior to revision total hip arthroplasty4
Fig. 1.2 High magnification images of cancellous and cortical bone 5
Fig. 1.3 Osteoclast action
Fig. 1.4 Safranin-O staining demonstrating reducing proteoglycan content of human articular cartilage with severity of osteoarthritis
Fig. 1.5 The multi-differentiation potential of stem cells derived from non-haematopoietic bone marrow stroma
Fig. 1.6 Culture-expanded human SSCs at confluence, stained with CellTracker™ Green to confirm viability
Fig. 1.7 Distraction Osteogenesis
Fig. 1.8 <i>In vitro</i> culture of human SSCs seeded onto allograft, stained with CellTracker™ Green after 7 days culture
Fig. 1.9 Impaction bone grafting technique to treat early femoral head avascular necrosis
Fig. 1.10 Laponite forms a thixotropic hydrogel when added to water 41
Fig. 1.11 'Balancing act' demonstrating the trade-off between contradictory desirable attributes of a polymer scaffold
Fig. 1.12 The collaborative tissue engineering "life cycle"

Chapter II

Fig. 2.1 Biaxial bioreactor used for bone tissue engineering	.72
Fig. 2.2 Commercially available density-gradient centrifugation devices for enrichment of BMA	. 73
Fig. 2.3 SSC enrichment strategy schematic	. 77
Fig. 2.4 Initial concept designs for the acoustic negative-pressure filtration product	. 78
Fig. 2.5 Laboratory prototype acoustic filtration device used to process all BMA samples for this study	. 79
Fig. 2.6 SSC enrichment of BMA following filtration to achieve 2- and 4-fold volume reductions	. 85
Fig. 2.7 CFU-F analysis	. 86
Fig. 2.8 Flow cytometric analysis of BMA	. 86
Fig. 2.9 Analysis of cellular concentration, viability and CFU-F concentration with respect to BMA concentration by volume	. 87
Fig. 2.10 Multilineage induction of human bone marrow stromal cell cultures derived from concentrated <i>vs.</i> unconcentrated BMA	. 88
Fig. 2.11 Enhanced cell seeding efficiency via BMA enrichment	. 90

Chapter III

Fig. 3.1 Elemental tantalum
Fig. 3.2 Trabecular tantalum as supplied by manufacturer
Fig. 3.3 Preparation of TTM for Scanning Electron Microscopy
Fig. 3.4 Cellular proliferation and viability following culture with TTM 107
Fig. 3.5 Live/dead analysis of unselected SSCs grown on TTM
Fig. 3.6 Confocal microscopy of TTM cultured with SSCs in osteogenic medium
Fig. 3.7 Sequential 'slices' of SSCs growing on TTM
Fig. 3.8 Immunocytochemistry of cells cultured on TTM
Fig. 3.9 Comparison of live/dead SSCs grown on allograft, TTM or autograft. 110
Fig. 3.10 Graph comparing cellular activity on allograft, TTM and autograft under basal and osteogenic conditions as measured by WST-1 cell proliferation assay
Fig. 3.11 Graph comparing cellular DNA activity on allograft, TTM and autograft under basal and osteogenic conditions
Fig. 3.12 Graph comparing cellular ALP activity on allograft, TTM and autograft under basal and osteogenic conditions
Fig. 3.13 Graph comparing specific cellular ALP activity on allograft, TTM and autograft under basal and osteogenic conditions
Fig. 3.14 Molecular expression of a panel of osteogenic genes of interest 114
Fig. 3.15 SEM images of control TTM section

Fig. 3.16 SEM image of TTM cultured with SSCs for 3 weeks
Fig. 3.17 Maximum mechanical 'pull-apart' stress for the different cellular constructs
Chapter IV
Fig. 4.1 SEM images of the array of ternary polymer blends
Fig. 4.2 Analysis of skeletal cell attachment and growth on ternary blend polymer spots
Fig. 4.3 Example of affinity analysis for STRO-1 positive cell adhesion (FITC) and nuclear counterstain (DAPI) for three ternary polymer blends
Fig. 4.4 Femoral specimens following harvesting
Fig. 4.5 Characteristics of polymer ternary blends as received
Fig. 4.6 Analysis of ALP staining and cell viability for discs of ternary blend 1 (CS/PVAc/PEI 50/25/25)
Fig. 4.7 Analysis of ALP staining and cell viability for discs of ternary blend 3 (CS/PEI/PLLA 50/25/25)
Fig. 4.8 Analysis of ALP staining and cell viability for discs of ternary blend 4 (CS/PVAc/PLLA 50/25/25)
Fig. 4.9 Analysis of ALP staining and cell viability for discs of ternary blend 4 (CS/PVAc/PLLA 50/25/25) following 28 days <i>in vitro</i> culture
Fig. 4.10 Immunostaining for osteogenic bone-matrix proteins of STRO-1 positive cells cultured on ternary blend 4 (CS/PVAc/PLLA 50/25/25) scaffold 146

Fig. 4.11 Radiographic analysis of the murine femoral defects at day 0 and day 28 – Control samples 1-4
Fig. 4.12 Radiographic analysis of the murine femoral defects at day 0 and day 28 – Polymer alone samples 5-8
Fig 4.13 Radiographic analysis of the murine femoral defects at day 0 and day 28 – Polymer + SSC samples 9-12
Fig. 4.14 Changes in femoral length, measured before nail insertion, immediately following nail insertion (T0), and at day 28 (T28) after the experimental period
Fig 4.15 Selected regions of interest within the osteotomy defect analysed by quantitative μCT after 28 days
Fig. 4.16 Assessment of new bone regeneration in the defect regions in femora of mice at 28 days following implantation
Fig. 4.17 Whole femur stained with A/S
Fig 4.18 Images of proximal femur and defect region of an empty control sample, stained with A/S
Fig. 4.19 Goldner's Trichrome stain – empty defect control
Fig. 4.20 Immunohistochemistry of part of an empty defect control sample 156
Fig. 4.21 Low magnification image of femoral segmental defect treated with polymer alone, along with 5 regions of interest, stained with A/S
Fig. 4.22 Collagen type I immunohistochemistry for a sample within the polymer alone group
Fig. 4.23 vWF immunohistochemistry of a polymer alone sample

Fig. 4.24 Cross-sectional overview of an entire femur from the polymer +
SSCs group160
Fig. 4.25 Regions of interest from Fig. 4.24
Fig. 4.26 Collagen type I immunohistochemistry of a sample containing
polymer + SSCs
Fig. 4.27 vWF immunohistochemistry of a sample from the polymer +
SSCs group
102
Chapter V
Onapter V
Fig. 5.1 Binary polymer scaffold177
177
Fig 5.2 Mature Northern Mule 'oull' aboon used for the study, and controlled
Fig 5.2 Mature Northern Mule 'cull' sheep used for the study, and aspiration
technique from iliac crest using needle and trocar179
Fig. 5.2 Codeverie (dr., m.m.) manadom vaina e voltale about bind limb
Fig. 5.3 Cadaveric 'dry run' procedure using a whole sheep hind limb 182
Fig. 5.4 Drawa disetion, assess the six and managering.
Fig. 5.4 Premedication, anaesthesia and preparation
F. F.F.T.
Fig. 5.5 Tibial segmental defect operative procedure
F. FO F. M. M. M. M. M. M. M. M
Fig. 5.6 Empty defect and scaffold <i>in situ</i> , immediately prior to closure 187
Fig. 5.7 Post-operative procedure
Fig. 5.8 Constructs and intact tibiae were assessed for maximum strength
under torque loading using an Instron testing rig190
Fig. 5.9 Cubes of tissue/polymer were taken from the indicated regions for
histological analysis191
Fig. 5.10 SEM images of polymer scaffold192

Fig. 5.11 Alcian blue penetration test	. 193
Fig. 5.12 Ovine BMA cells grown to confluence on monolayer tissue culture plastic	. 193
Fig. 5.13 DNA and ALP assays of ovine cells cultured with 10 mm cubes of polymer scaffold in either basal or osteogenic conditions	. 194
Fig. 5.14 Vybrant [®] Green cell viability analysis for ovine cells grown on polymer scaffold for 28 days	. 195
Fig. 5.15 Incremental lateral radiographic analysis of the fixated tibiae of sheep 1-4 in the empty defect group	. 198
Fig. 5.16 Incremental lateral radiographic analysis of the fixated tibiae of sheep 5-8 in the scaffold alone group	. 199
Fig. 5.17 Incremental lateral radiographic analysis of the fixated tibiae of sheep 9-12 in the scaffold and cells group	. 200
Fig. 5.18 The typical pattern of new bone formation in each group	. 201
Fig. 5.19 Quantitative μCT analysis at 12 weeks post-operation	. 202
Fig. 5.20 Quantitative μCT analysis of new bone formation following 12 weel incubation	
Fig. 5.21 Results of mechanical testing for the sheep tibiae under torsional compression	. 203
Fig. 5.22 Macroscopic specimen analysis following mechanical testing	. 204
Fig. 5.23 Macroscopic image of a tibia treated in the scaffold + SSCs group.	. 205
Fig. 5.24 A/S histological analysis of the ovine segmental tibial defect model	206

Chapter VI

Fig. 6.1 WST-1 cell proliferation assay at 2 hours (+ SD) for the cells from
three patients, 24 hours following exposure to different concentrations of
LAs for 2 hours
Fig. 6.2 Combined DNA assay (+ SD) of cells from all 3 patients 24 hours
following exposure to different concentrations of LAs for 2 hours221
Fig.6.3 WST-1 cell proliferation assay at 2 hours (+ SD) 7 days following
exposure to different concentrations of LAs for 2 hours
Fig. 6.4 DNA assay of cells (M39, mean + SD) following exposure to different
concentrations of LAs for 2 hours and subsequent 7 days further incubation 222
Fig. 6.5 Representative live/dead immunostains of cells after 2 hours
incubation in LAs and 24 hour recovery time
Fig. 6.6 High magnification representative live/dead immunostains of cells
after 2 hours incubation in LAs and 24 hour recovery time
Fig. 6.7 Representative live/dead immunostains of cells after 2 hours
incubation in LAs and 7 day recovery time225
Fig. 6.8 ALP assay (+ SD) of cells following exposure to different
concentrations of LAs and 7 days further incubation
Fig. 6.9 Representative photomicroscopy of cells stained for ALP, after 2
hours incubation in LAs and 7 days recovery time227

List of tables

Chapter I

Table 1.1 Extracellular Matrix proteins in bone	. 8
Table 1.2 Collagens present in articular cartilage and their functions	. 11
Table 1.3 Potential therapeutic niches for novel orthopaedic tissue engineering strategies	. 15
Table 1.4 Nomenclature for the multipotent stem cell derived from non-haematopoietic bone marrow stroma	. 19
Table 1.5 Growth factors associated with fracture repair	. 25
Table 1.6 Clinical translation of cell-based tissue engineering approaches to skeletal regeneration	. 30
Table 1.7 Synthetic polymers investigated for use in tissue engineering scaffolds for orthopaedic applications	. 46
Table 1.8 Porous 3D polymer scaffolds – evolution of scaffold fabrication techniques	. 50
Chapter II	
Table 2.1 Sources of BMA for human therapeutic clinical application	. 70
Table 2.2 Disadvantages of using culture expansion techniques for clinical tissue engineering purposes	. 71
Table 2.3 Nucleated cell counts and CFU-F concentrations pre- and post- filtration	84

Chapter III

Table 3.1 Osteogenic gene primer sequences used for RT-PCR104
Chapter IV
Table 4.1 Biodegradable synthetic polymers approved for clinical use
Table 4.2 Rudimentary homopolymers and applicable solvents used as the basis for fabrication of ternary polymer blends
Table 4.3 Structural properties of the selected polymer blend scaffold (CS/PVAc/PLLA 50/25/25) 134
Table 4.4 Osteogenic gene primer sequences used for RT-PCR136
Table 4.5 Assessment of solubility and stability of each polymer blend
Table 4.6 Analysis of cell viability, ALP staining and pH following pilot 7 day in vitro culture of SSCs on each polymer blend
Chapter V
Table 5.1 Variables within a large animal model, which need to be defined and controlled 169
Table 5.2 Inherent and procedural factors that affect the size of a critical segmental defect
Table 5.3 Previous ovine segmental defect studies 173
Table 5.4 The order of insertion of Schanz screws into the tibia was standardised for all sheep

Table 5.5 Summary of segmental tibial defect operative procedures in this	
study, presented in the order of the operative procedure19	96
Table 5.6 Factors which should be considered and modified prior to further	
large animal skeletal engineering biomaterial evaluation2	11

List of abbreviations

3D Three-Dimensional

3DP Three-Dimensional Printing

Abs Absorbance

AHSG α2HS Glycoprotein

ALCAM Activated Leukocyte Cell Adhesion Molecule

ALP Alkaline Phosphatase

αΜΕΜ Minimum Essential Medium Eagle, alpha modification

ANOVA Analysis Of Variance

A/S Weigert's haematoxylin/Alcian blue/ Sirius red

AVN Avascular Necrosis

β-actin Beta actin

BMA Bone Marrow Aspirate

BMC Bone Marrow Concentration

BMAC Bone Marrow Aspirate Concentrate

BMP Bone Morphogenetic Protein

BSA Bovine Serum Albumin

BV Bone Volume

C Celsius

 $C_2H_4O_2$ Ethanoic (acetic) acid

Ca Calcium

CAD-CAM Computer-Aided Design and Manufacture

CATK Cathepsin K

CD Cluster of Differentiation

cDNA Complementary Deoxyribonucleic Acid

CFU-F Colony Forming Unit-Fibroblastic

CHCl₃ Chloroform

CMFDA CellTracker™ Green (5-chloromethylfluorescein diacetate)

CO₂ Carbon dioxide

Col1A1 Collagen type I alpha I

Conc. Concentration

CS Chitosan

Ct Threshold cycle

CT Computed Tomography

CTG CellTracker™ Green (5-chloromethylfluorescein diacetate)

CTP Connective Tissue Progenitor

DAPI 4',6-diamidino-2-phenylindole

DBM Demineralised Bone Matrix

DNA Deoxyribonucleic acid

DO Distraction Osteogenesis

ECM Extracellular Matrix

EDTA Ethylenediaminetetraacetic acid

EGF Epidermal Growth Factor

EMA European Medicines Agency
EPC Endothelial Progenitor Cell

F Female

EU European Union FCS Fetal Calf Serum

FDA Food and Drug Administration
FDM Fused Deposition Modelling

FGF-1 Fibroblast Growth Factor 1 (acidic)
FGF-2 Basic Fibroblast Growth Factor

FITC Fluorescein isothiocyanate

GDF Growth Differentiation Factor

G Giga

GMP Good Manufacturing Practice

H⁺ Hydrogen ion

H₂O Water

HA Hydroxyapatite

HBMSC Human Bone Marrow Stromal Cell

HCI Hydrochloric acid
HCV Hepatitis C Virus

HIV Human Immunodeficiency Virus

HLA Human Leukocyte Antigen

HSS High Speed Steel
HT High Throughput

ICAM Intercellular Adhesion Molecule

IBG Impaction Bone Grafting
IGF Insulin-like Growth Factor

IL Interleukin

iPSC induced Pluripotent Stem Cell

ISO International Organisation for Standardisation
ITS Insulin, human Transferrin and sodium Selenite

LA Local anaesthetic

LREC Local Research Ethics Committee

J Joule M Male

MACS Magnetically Activated Cell Sorting

MACI Matrix induced Autologous Chondrocyte Implantation

MCAM Melanoma Cell Adhesion Molecule

M-CSF Macrophage Colony-Stimulating Factor
MEPE Matrix extracellular phosphoglycoprotein

MHRA Medicines and Healthcare products Regulatory Agency

MRI Magnetic Resonance Imaging
MSFC Marrow Stromal Fibroblastic Cell

μCT Micro Computed Tomography

n Number N Newton N₂ Nitrogen

NaCl Sodium Chloride
NC Nucleated Cell

NHS National Health Service

NMP N-methyl-2-pyrrolidinone

ns No significant difference

OA Osteoarthritis

OPC Osteoprogenitor cell
OSC Osteogenic Stem Cell

Pa Pascal

PAI Plasminogen Activator Inhibitor
PBS Phosphate Buffered Saline

PCL Polycaprolactone

PDGF Platelet Derived Growth Factor

PDLLA Poly(DL-lactide)

PDLLA co PGA Poly((DL)lactic co glycolic acid)

PDO Poly(dioxanone)

PDTE carbonate Poly(desaminotyrosyl-tyrosine ethyl ester carbonate)

PEG Polyethylene glycol

PEI Polyethylenimine

PEO Poly(ethylene oxide)

PET Polyethylene terephthalate

PGA Poly(glycolic) acid

PGA co TMC Poly(glycolic)acid co trimethylene carbonate

PHA Polyhydroxyalkanoate

PHEMA Poly(2-hydroxymethyl methacrylate)
PIPES 1,4-Piperazinediethanesulfonic acid

PLA or PLLA Poly(lactide) or Poly(lactic acid) or Poly(L)lactic acid

PLA/PCL Poly(L)lactic acid/ Polycaprolactone

PLA/PEO Poly(L)lactic acid/ Poly (ethylene oxide)

PLA/PLGA Poly(L)lactic acid /poly(glycolide)

PLDLLA Poly(L-lactide-co-D,L-lactide)

PLGA Poly(lactide-co-glycolide)

PLGA/PEG Poly(lactide-*co*-glycolide)/poly(ethylene glycol)
PLGA/PVA Poly(lactide-*co*-glycolide)/ polyvinyl alcohol

PLP Periodate-lysine-paraformaldehyde

PMMA Polymethyl methacrylate

pNNP Para-nitrophenyl phosphate

PO₄ Phosphate

P(P)EO/PBT Poly(poly(ethylene oxide) terephthalate-co-(butylene) terephthalate

PPF Poly(propylene glycol-co-fumaric acid)

ppm Parts per million

PRP Platelet-Rich Plasma
psi Pounds per square inch
PTFE Polytetrafluoroethylene

PVAc Poly(vinyl acetate)

qRT-PCR Quantitative real-time Polymerase Chain Reaction
RANKL Receptor activator of nuclear factor kappa-B ligand

RBC Red Blood Cell

RGD Arginyl-glycyl-aspartic acid DNA motif

rh Recombinant human

RNA Ribonucleic acid
ROI Region of Interest

rpm Revolutions per minute

RT-PCR Reverse Transcription Polymerase Chain Reaction

RUNX-2 Runt-related transcription factor 2
SaOs Sarcoma Osteogenic (cell line)

SD Standard Deviation

SEM Scanning Electron Microscope/Microscopy

SIBLING Small Integrin Binding Ligand N-Glycosylated (protein)

SFF Solid Freeform Fabrication

SOX-9 Sex determining region Y, box 9

SPSS Statistical Package for the Social Sciences

SSC Skeletal Stem Cell

Ta Tantalum (elemental symbol)

TCP Tricalcium Phosphate

TGF-β Transforming Growth Factor Beta

THR Total Hip Replacement

TNF-α Tumour Necrosis Factor-alpha

TRAP Tartrate-resistant acid phosphatase

Tris Tris(hydroxymethyl)aminomethane

TTM Tantalum Trabecular Metal

TV Total Volume

UK United Kingdom

US(A) United States (of America)

UV Ultraviolet

V Volt

v Volume

VCAM Vascular Cell Adhesion Molecule

VEGF Vascular Endothelial Growth Factor

Ver. Version
Vol. Volume

WST-1 2-(4-lodophenyl)-3-(4-nitrophenyl)-5-(2,4-disulfophenyl)-2H-

tetrazolium

Declaration

I hereby declare that this thesis is composed entirely of my own work, as a member of a research group. Contributions from other members of the research group, and collaborations with other institutions, are acknowledged in the appropriate sections where this has occurred. I have not submitted this thesis in candidature for any other degree, diploma or professional qualification
Mr James Oliver Smith BM, BSc(Hons), MRCS

The copyright of this thesis belongs to the author under the terms and conditions of the United Kingdom Copyrights Acts as qualified by The University of Southampton Regulation 3.8.2. Due acknowledgement must always be made of the use of any material contained in, or derived from, this thesis.

Publications

* Indicates joint first authorship

Papers

Aarvold A, **Smith JO**, Tayton ER, Jones AMH, Dawson JI, Lanham S, Briscoe A, Dunlop DG, Oreffo ROC

A tissue engineering strategy for the treatment of avascular necrosis of the femoral head

The Surgeon – accepted March 2013

Aarvold A, **Smith JO**, Tayton ER, Lanham SA, Chaudhuri J, Turner IG, Oreffo ROC The effect of porosity of a biphasic ceramic scaffold on human skeletal stem cell growth and differentiation in vivo

Journal of Biomedical Materials Research: Part A, 2013 – accepted February 2013

Tayton ER, Smith JO, Aarvold A, Evans N, Dunlop DG, Oreffo ROC

The effects of setting bone cement on tissue engineered bone graft: a potential barrier to clinical translation?

Journal of Bone and Joint Surgery (American), 2013 - accepted July 2012

Khan F*, **Smith JO***, Kanczler JM, Tare RS, Oreffo ROC, Bradley M

Discovery and Evaluation of a Functional Ternary Polymer Blend for Bone Repair -

Advanced Functional Materials, 2012, 10.1002/adfm.201202710

Translation from a Microarray to a Clinical Model

Dawson JI*, **Smith JO***, Aarvold A*, Ridgway JN, Curran SJ, Dunlop DG, Oreffo ROC Enhancing the osteogenic efficacy of human bone marrow aspirate: concentrating osteoprogenitors using wave-assisted filtration *Cytotherapy*, 2012, 10.1016/j.jcyt.2012.09.004

Smith JO, Sengers BG, Aarvold A, Tayton ER, Dunlop DG, Oreffo RO

Tantalum trabecular metal - addition of human skeletal cells to enhance bone implant interface strength and clinical application

Journal of Tissue Engineering and Regenerative Medicine, 2012, 10.1002/term.1525

Aarvold A, Smith JO, Tayton ER, Jones AMH, Dunlop DG, Oreffo ROC

From bench to clinic and back: Skeletal stem cells and impaction bone grafting for regeneration of bone defects

Journal of Tissue Engineering and Regenerative Medicine, 2012, 10.1002/term.1577

Aarvold A, **Smith JO**, Tayton ER, Edwards CJ, Fowler DJ, Gent ED, Oreffo ROC The role of osteoblast cells in the pathogenesis of unicameral bone cysts *Journal of Children's Orthopaedics*, 2012, 6(4):339-346

Tayton E, Fahmy S, Purcell M, Aarvold A, **Smith JO**, Kalra S, Briscoe A, Lanham S, Howdle S, Shakesheff K, Dunlop DG, Oreffo RO

An analysis of polymer type and chain length for use as a biological composite graft extender in impaction bone grafting: A mechanical and biocompatibility study

Journal of Biomedical Materials Research Part A, 2012, 100(12):3211-9

Tayton ER*, Smith JO*, Aarvold A, Kalra S, Dunlop DG, Oreffo RO

Translational hurdles for tissue engineering: an in vitro analysis of commonly used local anaesthetics on skeletal stem cell survival

Journal of Bone and Joint Surgery (British), 2012, 94(6):848-55

Tayton E, Purcell M, Aarvold A, **Smith JO**, Kalra S, Briscoe A, Shakesheff K, Howdle SM, Dunlop DG, Oreffo RO

Supercritical CO₂ fluid-foaming of polymers to increase porosity: a method to improve the mechanical and biocompatibility characteristics for use as a potential alternative to allografts in impaction bone grafting?

Acta Biomaterialia, 2012, 8(5):1918-27

Smith JO*, Aarvold A*, Tayton ER, Dunlop DG, Oreffo ROC

Skeletal tissue regeneration: current approaches, challenges, and novel reconstructive strategies for an aging population

Tissue Engineering Part B Reviews, 2011, 17(5):307-20

Aarvold A, **Smith JO**, Tayton ER, Tilley S, Dawson JI, Briscoe A, Lanham SA, Dunlop DG, Oreffo ROC

Taking tissue engineering principles into theatre: Retrieval analysis from a clinically translated case

Regenerative Medicine, 2011, 6(4):461-7

Chapters

Danoux C, Tare R, **Smith JO**, Bradley M, Hunt JA, Oreffo ROC, Habibovic P
Development of materials for regenerative medicine: from clinical need to clinical application. In: *Materiomics - High Throughput Screening of Biomaterial Properties*Editor: P Habibovic, Publisher: Twente University Press, 2013

Kanczler J, Dawson J, Aarvold A, **Smith JO**, Tare R, Oreffo ROC Bone Tissue Engineering. In: *Comprehensive Biotechnology, 2nd Edition* Editors: Z Cui & L Brandon, Publisher: Elsevier, 2011

Tayton ER, **Smith JO**, Aarvold A, Oreffo ROC, Zaleh W, Kassem M Clinical Applications for skeletal/ mesenchymal stem cell therapy. In: *Stem Cells: Basic Biology and Clinical Applications*.

Editor: M Kassem, Publisher: King Saud University Press, 2011

Abstracts with podium presentations

Smith JO, Dawson JI, Aarvold A, Jones AMH, Dunlop DG, Ridgway JN, Curran S, Oreffo ROC

A novel clinical strategy to enrich skeletal stem cells from bone marrow to enhance skeletal regeneration. (*Presented at BOA Congress, 2011- Dublin, Eire*)

J Bone Joint Surg Br 2012 vol. 94-B no. SUPP XXXIX 204

Smith JO, Sengers BG, Aarvold A, Tayton ER, Dunlop DG, Oreffo ROC

Tantalum Trabecular Metal – Addition of Skeletal Stem Cells to Enhance the BoneImplant Interface. (*Presented at BOA Congress, 2011 – Dublin, Eire*)

J Bone Joint Surg Br 2012 vol. 94-B no. SUPP XXXIX 163

Tayton ER, Fahmy S, Aarvold A, **Smith JO**, Kalra S, Briscoe A, Shakesheff KM, Howdle S, Dunlop DG, Oreffo ROC

The optimisation of polymer type and chain length for use as a biological composite graft in impaction bone grafting: a mechanical and bio-compatibility analysis. (Presented at BOA Congress, 2011 – Dublin, Eire)

J Bone Joint Surg Br 2012 vol. 94-B no. SUPP XXXIX 211

Tayton ER, Purcell M, Briscoe A, Kalra S, Aarvold A, **Smith JO**, Fahmy S, Shakesheff KM, Howdle S, Dunlop DG, Oreffo ROC

Does increasing PLA scaffold porosity using supercritical CO₂ strategies enhance the characteristics for use as an alternative to allograft in impaction bone grafting? (Presented at BOA Congress, 2011 – Dublin, Eire)

J Bone Joint Surg Br 2012 vol. 94-B no. SUPP XXXIX 212

Aarvold A, **Smith JO**, Tayton ER, Jones AMH, Briscoe A, Lanham S, Dunlop DG, Oreffo ROC

A tissue engineering strategy for the treatment of osteonecrosis: evaluation of efficacy in four patients. (Presented at EFORT 12th Congress 2011 – Copenhagen, Denmark)

J Bone Joint Surg Br 2012 vol. 94-B no. SUPP XXXVII 436

Tayton ER, Kalra S, Briscoe A, Aarvold A, **Smith JO**, Lanham S, Fahmy S, Howdle S, Shakesheff KM, Dunlop DG, Oreffo ROC

Optimisation of polymer and stem cells technology to produce substitute allograft for use in impaction bone grafting. (Presented at EFORT 12th Congress 2011 – Copenhagen, Denmark)

J Bone Joint Surg Br 2012 vol. 94-B no. SUPP XXXVII 20

Smith JO, Sengers BG, Aarvold A, Tayton ER, Dunlop DG, Oreffo ROC

A tissue engineering approach with tantalum trabecular metal to enhance bone-implant integration. (Presented at BORS/BRS Combined Meeting 2011 – Cambridge)

J Bone Joint Surg Br 2012 vol. 94-B no. SUPP XXXVI 30

Smith JO, Dawson JI, Aarvold A, Jones AMH, Ridgway J, Curran S, Dunlop DG, Oreffo ROC

Enrichment of skeletal stem cells from bone marrow to enhance skeletal regeneration – a novel clinical technique. (Presented at BORS/BRS Combined Meeting 2011 – Cambridge)

J Bone Joint Surg Br 2012 vol. 94-B no. SUPP XXXVI 7

Aarvold A, **Smith JO**, Tayton ER, Jones AMH, Dawson JI, Briscoe A, Lanham S, Dunlop DG, Oreffo ROC

Retrieval analysis of tissue engineered bone: a clinical and laboratory study. (Presented at BORS/BRS Combined Meeting 2011 – Cambridge)

J Bone Joint Surg Br 2012 vol. 94-B no. SUPP XXXVI 117

Tayton ER, Purcell M, Aarvold A, **Smith JO**, Kalra S, Briscoe A, Fahmy S, Shakesheff KM, Howdle S, Dunlop DG, Oreffo ROC

Enhancement of PLA for use in impaction bone grafting: The effect of production via supercritical CO₂ dissolution to increase porosity. (*Presented at BORS/BRS Combined Meeting 2011 – Cambridge*)

Bone Joint Surg Br 2012 vol. 94-B no. SUPP XXXVI 23

Aarvold A, Smith JO, Edwards CJ, Tayton ER, Gent E, Oreffo ROC

Cyst Fluid & Stem Cells: Why Unicameral Bone Cysts are so Hard to Treat. (Presented at BSCOS Meeting 2011 – Sheffield)

J Bone Joint Surg Br 2012 vol. 94-B no. SUPP XXIV 12

Smith JO, Dawson JI, Aarvold A, Ridgway JN, Curran SJ, Dunlop DG, Oreffo ROC A Clinical Strategy to Concentrate Aspirated Bone Marrow for Skeletal Stem Cells to Enhance Skeletal Regeneration (Abstract 47.013, presented at TERMIS Annual Meeting – Granada, Spain)

Histology and Histopathology, Cellular and Molecular Biology, Vol 26 (supp.1), 2011

Aarvold A, **Smith JO**, Tayton ER, Briscoe A, Lanham S, Dawson JI, Oreffo ROC, Dunlop DG

Biological Augmentation of impaction bone grafting: Retrieval analysis of human tissue engineered specimens. (Presented at BHS/BORS Combined Meeting – Torquay)

JBJS(Br), British Hip Society Proceedings

Briscoe A, Aarvold A, Street M, Tayton E, **Smith JO**, Dunlop DG, Oreffo RO
The development of a custom-made intra-medullary nail for use in an ovine tibial segmental defect model. (*Presented at OBCAS Meeting – Brunel*)

Journal of biomechanics. Vol 43, supplement 1, p71, June 2010

Aarvold A, **Smith JO**, Tayton ER, Jones AMH, Briscoe A, Dunlop DG, Oreffo ROC Retrieval analysis of femoral heads after impaction bone grafting for treatment of AVN. (Presented at BORS Meeting – Cardiff)

J Bone Joint Surg (Br), Proceedings

Poster presentations

Dawson JI, **Smith JO**, Aarvold A, Jones AMH, Ridgway J, Curran S, Dunlop DG, Oreffo ROC

Development of a novel strategy for enrichment of skeletal stem cells for clinical application

- 12th EFORT Congress 2011, Copenhagen

Aarvold A, **Smith JO**, Tayton ER, Jones AMH, Briscoe A, Lanham S, Dunlop DG, Oreffo ROC

A tissue engineering strategy for the treatment of AVN: clinical translation and analysis of retrieval specimens

-ORS (Orthopaedic Research Society) Annual Meeting, Long Beach, California, 2011

Additional first author presentations

Translational hurdles to tissue engineering: an analysis of commonly used local anaesthetics on human skeletal stem cell survival

-Gauvain Society, Hampshire, June 2012

Tissue engineering strategies to extend the orthopaedic applications of tantalum trabecular metal

-Institution of Mechanical Engineers 'Engineers and Surgeons: Joined at the Hip' Conference, London, November 2011

Cell enrichment strategies for osteosynthesis

-University of Southampton, Faculty of Medicine Centre for Human Development Seminar, May 2011

Development of a novel technique to enrich human bone skeletal stem cells for orthopaedic application

-University of Southampton, Clinical Academic Trainees' Conference, March 2011

Development of a novel orthopaedic stem cell concentrator

-Gauvain Society, Hampshire, July 2010

Prizes and awards

2012	Best Scientific Podium Presentation: 'Translational hurdles to
	tissue engineering: an analysis of commonly used local
	anaesthetics on human skeletal stem cell survival'
2011	British Orthopaedic Research Society, Cambridge
	Best presentation: 'A Tissue Engineering Approach with
	Tantalum Trabecular Metal to Enhance Bone-Implant Integration'
2011	Pfizer Award, UK National Stem Cell Network, York
	Best Conference Poster: 'Enrichment of skeletal stem cells from
	bone marrow to enhance skeletal regeneration - a novel clinical
	technique'
2011	Gauvain Society Annual Scientific Meeting, Southampton
	Second Prize for Podium Presentation: 'Extending the role of
	Tantalum Trabecular Metal using Tissue Engineering Strategies
	for Orthopaedic Application'
2011	University of Southampton Medicine and Biological
	Sciences Postgraduate Conference, Southampton
	Commendation for Podium Presentation: 'Development of a
	novel enrichment strategy for bone marrow stem cells for
	orthopaedic application'
2010	University of Southampton Micrograph Competition
	Runner up: 'Trabeculation'
2010	The Engineer Technology and Innovation Awards,
	The Royal Society, London
	Winner of the 'Medical & Healthcare' category and the overall
	'Grand Prix' Award

Acknowledgements

I would like to acknowledge the following for their support, advice, discussions and assistance:

Supervisors

Professor Richard OC Oreffo Mr Douglas G Dunlop

Bone & Joint Research Group

Mr Alexander Aarvold, Mr Edward Tayton Esther Ralph, Carol Roberts, Stefanie Inglis, Spandan Kalra Dr Jon Dawson, Dr Stuart Lanham, Dr Janos Kanczler, Dr Rahul Tare, Dr Emma-Jayne Kingham

Bioengineering Science Research Group

Dr Richard Cook, Dr Adam Briscoe, Professor Mark Taylor

Biomedical Research Unit

Jas Barley, Kerry Taylor

Biomedical Imaging Unit

Professor Anton Page, Dr David Johnston

University of Southampton Hospital NHS Foundation Trust

Mr David Higgs, Mr Ed Gent, Mr Jeremy Latham

Smith & Nephew UK Ltd. and Technology Strategy Board

Dr Steve Curran, Dr Jon Ridgway, Bridget Mathews

Royal Veterinary College, Hertfordshire

Professor Allen Goodship, Gillian Hughes

Queensland University of Technology, Brisbane, Australia

Professor Dietmar Hutmacher, Dr Johannes Reichert

University of Adelaide, Australia

Professor David Findlay, Professor Stan Gronthos, Professor Andrew Zannettino

Flinders University, Adelaide, Australia

Professor John Field

Family

Dr Tabitha Smith – my wife, who spent many hours attending to my every need during preparation of this thesis.

John and Sue Smith – my parents, who taught me the art of perseverance and have always generously supported and encouraged me.

Happy the man v	vho has been a	ble to learn the	causes of things.
			Virgil

Chapter I

General Introduction

A review article based upon the work in this chapter has recently been published in *Tissue Engineering Part B: Reviews*

Figure 1.8 of this chapter was chosen as the front cover illustration to *Tissue Engineering Part B: Reviews, October 2011*

1.1 Scale of the problem in the context of clinical need

Pathology affecting the musculoskeletal system is a global source of considerable morbidity. In addition to the acute life-threatening dangers associated with trauma, the pain and disability from chronic orthopaedic disease frequently has widespread, long-term effects on patients and their families. These impacts extend to general health and psychological status and have considerable economic implications with escalating costs of treatment, social support and loss of economic activity (Kilgore *et al.* 2009, Heckman *et al.* 1997, Dahabreh *et al.* 2007).

Bone possesses a high intrinsic regenerative potential. Consequently, the majority of fractures and bone defects heal spontaneously through a recapitulation of the embryonic developmental process (Gerstenfeld *et al.* 2003). Despite this, one of the most frequent challenges for the orthopaedic surgeon is to restore skeletal tissue that has been lost, deformed or damaged as a consequence of injury or disease. Various factors such as tissue loss, a compromised wound environment or biomechanical instability can result in persistent defects with impaired healing capacity. In addition, pathology of other skeletal tissues such as cartilage and tendon contribute to morbidity, and clinical attempts to restore these tissues have to overcome additional challenges of reduced local vascularity and the lack of inherent repair mechanisms (Khan WS *et al.* 2010). Improved surgical techniques and implant designs, as well as novel perioperative management strategies and ancillary products, have significantly decreased complication rates in such situations.

Surgical therapies for musculoskeletal pathology were initially limited to debridement of the diseased area without replacement. This often led to considerable functional loss, particularly for peri-articular pathology, where often the only method to reduce pain was by joint arthrodesis (Ahlback *et al.* 1966). More recently, with the introduction of arthroplasty, function can be restored by using biologically favourable implant materials to replace the specialised skeletal tissues lost. However, considerable disadvantages remain with this approach, which may in itself contribute to latent morbidity and complications. An example of this is the recent well-publicised failure of some metal-on-metal articulations in total hip arthroplasty, including catastrophic soft-tissue reactions (Haddad *et al.* 2011). Archetypal causes of bone loss that are targets for tissue engineering therapies include trauma, inflammation and the treatment of infection and tumours. The requirement for restoration of tissue stock and function are prerequisites to normal activities following surgical excision for osteomyelitis and bone

tumours. Additionally, there is now an escalating requirement to treat the elective cohort of patients who require bone defect reconstruction during revision arthroplasty surgery (McNamara IR 2010) (Fig. 1.1), as well as developing techniques to augment union following spinal fusion procedures and for treating morbidity associated with other skeletal tissues (see section 1.3).

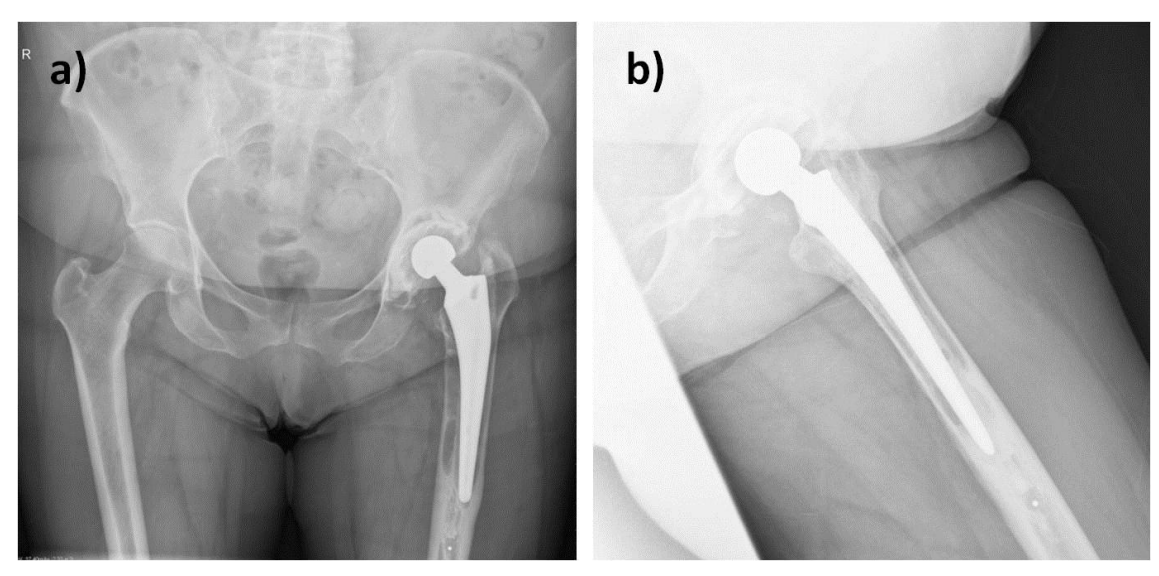


Fig. 1.1 a) Anteroposterior pelvis and b) lateral left hip radiographs of a female made prior to revision total hip arthroplasty. Substantial osteolysis is apparent around both the femoral and acetabular components, presenting a significant reconstructive challenge. *Images courtesy of University Hospital Southampton NHS Foundation Trust.*

The proportion of people aged over 65 years is projected to increase by nearly 50% in the coming 25 years in the UK (Office for National Statistics 2010), and in the US this cohort which accounted for 12.8% of the total population in 2009, will rise to approximately 20% in 2050 (Shrestha *et al.* 2011). Despite refinements in prosthetic design, manufacture and implantation, artificial joint replacements have a finite lifespan and frequently present at revision with significant lost bone stock. Given the current and historic arthroplasty implantation rates and these demographic trends, an attendant increase in orthopaedic revision surgery as well as other causes of musculoskeletal morbidity can therefore be expected, justifying the current intense research interest in this field. It is likely therefore, that in the next few years, the revision of these hip and knee arthroplasty implants will represent the biggest challenge that may be overcome by tissue engineering strategies.

1.2 Composition of skeletal tissues

Successful tissue engineering strategies to tackle the pathology detailed above are likely to closely mimic the natural processes that bring about skeletal tissue development and repair. An understanding of the normal composition of musculoskeletal tissues is therefore essential.

1.2.1 Bone

Bone, as an organ composes the largest proportion of the body's connective tissue mass and is unique in that it is constantly regenerated throughout life (Rodan 1992). The skeleton serves a variety of functions including: i) structural support; ii) locomotion; iii) protection of internal organs; iv) maintenance of mineral homeostasis and acid-base balance; v) serving as a reservoir for cytokines and growth factors, and vi) providing a space for haematopoiesis (Taichman 2005). Bone tissue can be separated into cortical (compact) and cancellous (trabecular) types, which are approximately 5% and 80% porous, respectively (Clarke 2008) (Fig. 1.2).

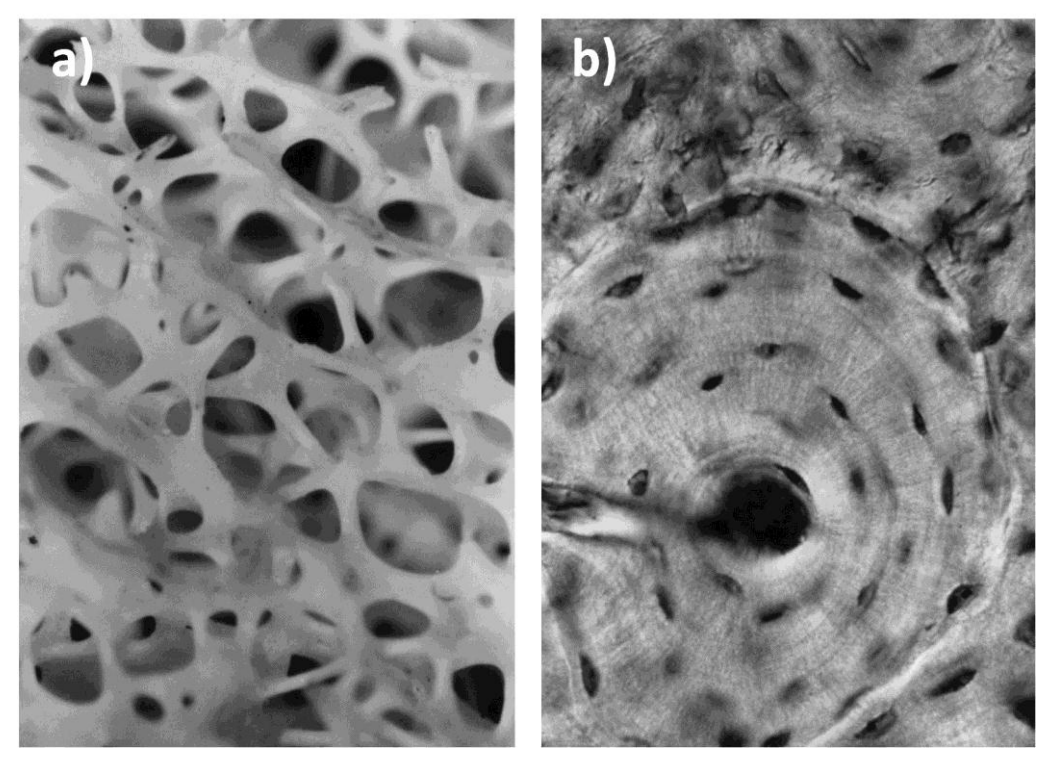


Fig. 1.2 High magnification images of a) cancellous and b) cortical bone, demonstrating the significant differences in composition and porosity. *Image from Fyhrie and Kimura 1999.*

Collagen fibrils are laid down by osteoblasts in a lamellar pattern with alternating orientations. Osteoblasts become osteocytes once they have been surrounded by mineralised bone. The cancellous compartment is filled with bone marrow, which contains haematopoietic and skeletal tissue progenitor niches (Yang *et al.* 2009).

Cortical bone is surrounded by periosteum on the outer surface and endosteum on the inner surface; both layers contain blood vessels, osteoblasts and osteoclasts, and periosteal surface activity is important for appositional growth and fracture repair. Bone undergoes longitudinal and radial growth during normal development, and continually models and remodels in response to physiological influences, in obedience to Wolff's law to meet its mechanical demands (Chen et al. 2010). The process of remodelling is normally tightly controlled by osteoblastic matrix production coupled with bone resorption by osteoclasts. Osteoblasts are derived from multipotent stem cells within the bone marrow stromal compartment, whereas osteoclasts originate from mononuclear cells of the monocyte-macrophage lineage (Del Fattore et al. 2010). Multinucleated cells are recruited by the action of Macrophage Colony-Stimulating Factor (M-CSF) and Receptor activator of nuclear factor kappa-B ligand (RANKL), which then adhere to bone and undergo differentiation into mature osteoclasts. Osteoclastic bone resorption is initiated by integrin-mediated binding to bone matrix, principally the integrin $\alpha v \beta_3$ (Robey and Boskey 2008). Upon binding, the cells develop a ruffled border that seals that portion of matrix before releasing hydrogen ions (H⁺), to dissolve the mineralised portion and also activate released enzymes, cathepsin K (CATK) and tartrate-resistant acid phosphatase (TRAP), which digest the extracellular matrix (Boyle et al. 2003) (Fig. 1.3).

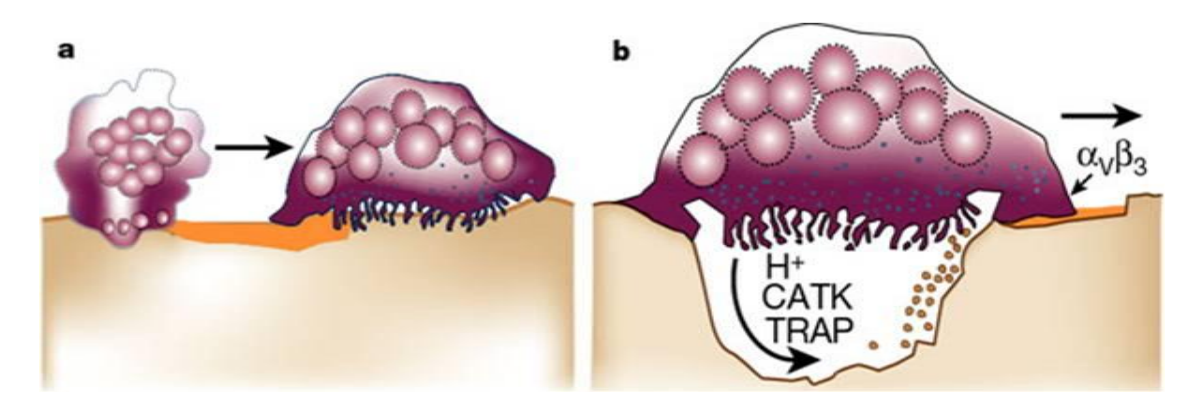


Fig. 1.3 Osteoclast action: a) A multinucleated cell is recruited by the action of M-CSF and RANKL, which then adheres to bone and undergoes differentiation into a mature osteoclast. **b)**, RANKL stimulates osteoclast activation by inducing secretion of protons (H⁺) and lytic enzymes (TRAP, CATK) into a sealed resorption vacuole formed between the osteoclast and the bone surface. Acidification of this compartment by secretion of protons leads to the enzyme activation and degradation of bone mineral and collagen matrices. *From Boyle et al. 2003*

The Extracellular Matrix (ECM) of bone consists of mineral, collagen, water, non-collagenous proteins and lipids, in decreasing proportion. The mineral phase is mostly hydroxyapatite [$Ca_{10}(PO_4)_6(OH)_2$], with small quantities of carbonate, magnesium, and acid phosphate. This provides mechanical rigidity with compressive strength, whereas the organic matrix provides elasticity and flexibility (Clarke 2008). The organic matrix is mostly composed of collagen type I with small amounts of type III, V and non-fibrillar collagens. Approximately 10-15% of the organic matrix is made up of non-collagenous proteins including serum-derived proteins (such as albumin, α_2 -HS-glycoprotein and growth factors) and non-collagenous proteins synthesised by osteoblasts (proteoglycans, glycosylated proteins, glycosylated proteins with potential cell attachment activities, and γ -carboxylated proteins) (Table 1.1).

Table 1.1 Extracellular Matrix proteins in bone

Table 1.1 Extracellular Matrix proteins in bone				
	Protein	Function/ Location	Disease (of absence or dysfunction)	
Collagen-related proteins	Type I	Binds and orientates other proteins	Osteogenesis imperfecta	
	Type X	Present in hypertrophic cartilage	Metaphyseal chondroplasia	
agen-r eins	Type III	Trace, may regulate collagen fibril diameter	Ehlers Danlos syndrome	
Collager proteins	Type V	Trace, may regulate collagen fibril diameter	Disrupted fibrils in mouse model	
	Albumin	Inhibits HA crystal growth	None	
Serum proteins	AHSG	Promotes endocytosis Monocyte chemoattractant Inhibits calcification	Ectopic calcification in mouse knockout	
Ď.	Aggrecan	Matrix organisation and strength Retention of H ₂ O, Ca, PO ₄	Spondyloepiphyseal dysplasia	
ntainir	Versican	Regulates chondrogenesis Defines space destined to ossify	Wagner syndrome	
Glycosaminoglycan containing molecules	Decorin	May regulate collagen fibril size May modulate TGF-β activity	Progeroid form of Ehlers Danlos (with double decorin-biglycan	
inogl	Biglycan	Determines peak bone mass May regulate growth factor activity	knockout)	
Glycosami molecules	Asporin	Regulates collagen structure	Human polymorphism associated with OA	
Glyc	Hyaluronan	May define space destined to ossify	None	
teins	Alkaline Phosphatase	Hydrolyses inhibitors of mineral deposition Increases local PO ₄ concentration	Hypophosphatasia – poor growth and mineralisation	
Glycoproteins	Osteonectin	Regulates collagen organisation May regulate HA deposition Regulates growth factors	Low mineral content Osteopenia in knockout mouse	
	Osteopontin	Binds to cells, controls proliferation May regulate mineralisation Inhibits Nitric oxide synthase	Poor osteoclast remodelling Increased mineral content in knockout mouse	
SIBLING proteins	Bone Sialoprotein	Binds to cells May initiate mineralisation	None	
SIB	MEPE	Regulation of PO ₄ metabolism	Oncogenic osteomalacia	
	Thrombospondins	Cell attachment Binds to collagens, platelets, thrombin, fibrinogen, laminin, plasminogen and PAI	Pseudoachondroplasia	
ining ns	Fibronectin	Cell attachment Binds to fibrin, heparin, gelatin, collagens	Lethal before skeletal development in knockout mouse	
RGD-containing glycoproteins	Vitronectin	Cell attachment Binds: collagens, plasminogen, PAI, heparin	None	
RGD. glyco _l	Fibrillin 1 and 2	Regulates elastic fibre formation	Marfan syndrome in Fibrillin 1 mutation	
amic g	Matrix Gla protein	Inhibitor of mineralisation	Keutel syndrome (excessive cartilage mineralisation)	
γ-carboxy glutamic acid-containing proteins	Osteocalcin	Regulates osteoclasts Inhibits mineralisation May coordinate bone turnover	Knockout mouse - osteopetrosis	
γ-carbo) acid-cor proteins	Protein S	May be synthesised by osteoblasts	Osteopenia	
		•	•	

HA = Hydroxyapatite, $AHSG = \alpha 2HS$ glycoprotein, $H_2O = water$, Ca = calcium, $PO_4 = phosphate$, $TGF-\beta = Transforming$ Growth Factor Beta, OA = Osteoarthritis, SIBLING = Small Integrin Binding Ligand N-Glycosylated, MEPE = Matrix extracellular phosphoglycoprotein, PAI = Plasminogen Activator Inhibitor, RGD = Arginyl-glycyl-aspartic acid DNA motif. Adapted from Robey and Boskey 2008 and Clarke 2008.

1.2.1.1 Fracture repair

Normal fracture healing is a complex of events involving a coordinated interplay of cells, growth factors and ECM. Two basic types of fracture healing exist: Primary bone healing is rare, requiring absolute contact of the bone fragments, with absolute stability, so that cells within the cortical bone can directly re-establish continuity (Giannoudis *et al.* 2007). The vast majority of fractures undergo secondary bone healing, characterised by callus formation due to the processes of intramembranous and endochondral ossification. This does not require absolute stability of bone ends; in fact the small movements associated with relative stability have to shown to be a prerequisite for callus formation (Giannoudis *et al.* 2007). Certain aspects of bone healing parallel the events of skeletal development, and although the repair process is characterised by a number of sequential cellular and molecular phases, these are, in practice, poorly delineated (Gerstenfeld *et al.* 2003):

During the initial inflammatory stage, soft tissue disruption and bleeding lead to nonspecific wound-healing pathways, stimulated by platelet degranulation and mononuclear inflammatory cell activation. These cells release cytokines and procoagulant factors, which modify the initial haematoma into a fibrinous thrombus and form a positive feedback loop, activating and recruiting further cells (Gerstenfeld et al. 2003). Over the subsequent days, infiltration of macrophages and other phagocytic cells facilitate the reorganisation of the thrombus into granulation tissue. These processes take place under the control of cytokines and growth factors (including Transforming Growth Factor Beta (TGF-β), Platelet Derived Growth Factor (PDGF), Basic Fibroblast Growth Factor (FGF-2), Vascular Endothelial Growth Factor (VEGF), Macrophage Colony-Stimulating Factor (M-CSF), Bone Morphogenetic Proteins (BMPs), Interleukin (IL) -1 and -6 and Tumour Necrosis Factor-alpha (TNF-α)) produced by the infiltrating cells. These factors recruit and stimulate the differentiation of stem cells from bone marrow, periosteum, blood vessels and surrounding soft tissue (Shapiro et al. 2008).

In the second phase of fracture healing, *endochondral ossification* commences through soft fibrocartilaginous callus formation. Growth factors stimulate chondrocytes and fibroblasts to replace areas of granulation tissue with fibrocartilage. These areas eventually fuse to form a semi-rigid cartilaginous template, which splints the fracture. Hard callus formation is then initiated by pro-angiogenic factors, such as VEGF, BMPs, FGF-1 and TGF-β, which stimulate callus vascularisation, chondrocyte hypertrophy and apoptosis. *Hard callus formation* is characterised by local ingress of Skeletal Stem

Cells (SSCs) from periosteum, bone marrow, the vasculature and surrounding soft tissues. Specific growth factors, such as the BMPs, stimulate differentiation of these cells into osteoblasts and their production of mineralised bone matrix, to produce woven bone (Schindeler *et al.* 2008).

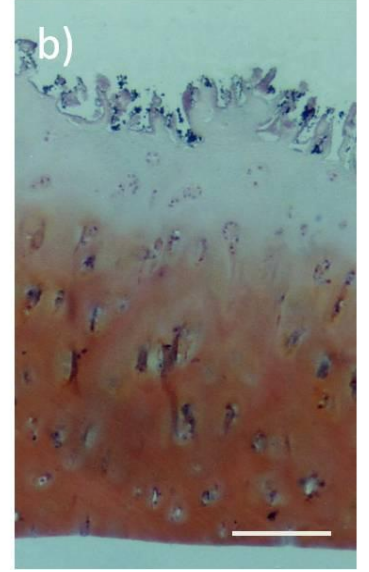
The final stage encompasses *bone remodelling* of the woven hard callus into lamellar bone and eventual restoration of the original trabecular and cortical bone conformations. This remodelling process is driven by osteoclast activity in a tightly coupled catabolic-anabolic response requiring coordinated matrix synthesis by osteoblasts. The underlying mechanism governing this has not yet been fully established, but the local release of osteoid breakdown products and growth factors during remodelling are thought to drive the osteoblastic response (Martin and Sims 2005). The final result of successful fracture healing through these means is a restoration of normal bone structure and function, without the formation of permanent scar tissue. However, it is clear that this can only take place through the complex interaction of growth factors, cells, ECM and the mechanical environment (Giannoudis et al. 2007).

1.2.2 Cartilage

Cartilage is a versatile connective tissue found in many areas of the body. It has varying properties dependent upon its exact composition to suit specific functions and requirements. Within the adult skeletal system, cartilage is found: as *hyaline articular cartilage* in synovial joints (Fig. 1.4); as *fibroelastic cartilage* within the menisci of articulations, and as *fibrocartilage* at tendon and ligament insertions into bone (Brinker and O'Connor 2008). Fibrocartilage is also formed during fracture healing (see section 1.2.1.1) and articular cartilage repair.

The ECM which provides structure and function to cartilage is produced and maintained by chondrocytes, spread sparsely throughout the matrix (Bhosale and Richardson 2008). Cartilage is avascular, aneural and alymphatic, so chondrocytes derive their nutrition primarily through matrix diffusion, driven by mechanical stimulation (Buckwalter *et al.* 1998). The avascular, anti-angiogenic nature of cartilage is important for normal function, with a loss of resistance to vascularisation being a key event in the pathogenesis of osteoarthritis (Smith *et al.* 2003).





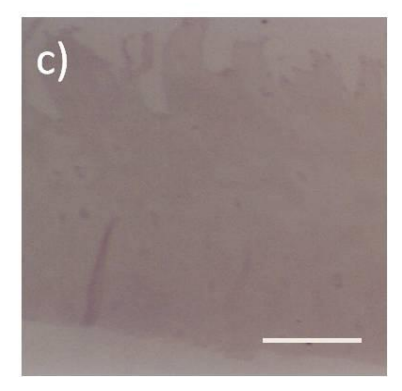


Fig. 1.4 Safranin-O staining demonstrating reducing proteoglycan content of human articular cartilage with severity of osteoarthritis in a) normal cartilage, b) early osteoarthritis, c) severe osteoarthritis. Scale bars: 400 µm, from Smith et al. 2003.

The main function of articular cartilage, to reduce friction and distribute loads, is achieved by a hydrated ECM. Indeed water is the major constituent of articular cartilage (65-80% of wet weight), which allows load-dependent deformation and provides a medium for nutrition and lubrication (Bhosale and Richardson 2008). The principal organic components are collagens (10-20% of total weight) and proteoglycans (10-15%), with collagen type II being most abundant. This forms a fibrillar meshwork around aggrecan (the most abundant proteoglycan) and provides the high tensile strength required at articular surfaces. Other collagens are present in smaller quantities and have diverse functions (Table 1.2).

Table 1.2 Collagens present in articular cartilage and their functions

Collagen type	Morphological location	Functions
II	Principal component of macrofibril (>90%)	Tensile strength
VI	Pericellular matrix	Aids matrix-cellular adherence
IX	Cross-linked to surface of macrofibril	Tensile strength Inter-fibrillar adherence
Х	Related to hypertrophic chondrocytes in calcified layer	Structural support Aids mineralisation
ΧI	Within macrofibril core	Nucleates fibril formation Limits macrofibril diameter

Adapted from Bhosale and Richardson 2008

Proteoglycans are protein polysaccharides that form large aggregates within the collagen network and are composed of highly sulphated glycosaminoglycans (keratin and chondroitin sulphate) linked to the protein core. Their high negative charge attracts water molecules and increases the osmolarity of cartilage, which provides compressive strength and elasticity (Bhosale and Richardson 2008).

Chondrocytes produce collagen, proteoglycans and some enzymes for cartilage metabolism and breakdown, including matrix metalloproteinases and tissue inhibitors of matrix metalloproteinases (TIMPs) (Brinker and O'Connor 2008). Given the avascular structure of cartilage and low chondrocyte metabolism, the tissue possesses poor inherent repair mechanisms to damage (Richter *et al.* 2009). Surface damage has a negligible healing response, whereas injury that extends into the calcified zone of the osteochondral junction causes an inflammatory reaction that may heal with fibrocartilage, produced by SSCs within the subchondral bone. This repair cartilage however, contains a high proportion of collagen type I and is thus not as durable as normal hyaline cartilage (Brinker and O'Connor 2008).

Menisci deepen the articular surface of many synovial joints, broadening the contact area and distributing load (Brinker and O'Connor 2008). Menisci are composed of specialised fibroelastic cartilage, with an interlacing network of collagen fibres (90% collagen type I), proteoglycans and glycoproteins. Fibrochondrocytes that maintain this composition are found within the ECM, but in contrast to hyaline cartilage, menisci also contain mechanoreceptor nerve endings and peripheral blood vessels (Wilson *et al.* 2009). Thus peripheral tears in the vascularised region can heal by fibrovascular scar formation, and surgical repair is often indicated, however, more central tears in the avascular region do not heal, and are therefore debrided (Jarit and Bosco 2010).

The long-term outcome following chondral, osteochondral or meniscal injury depends on many factors, including age, size and location of the defect, joint alignment and stability; however if left untreated, many of these injuries can become symptomatic and progress to osteoarthritis (Bhosale and Richardson 2008). It is clear that the inherent mechanisms of cartilage repair are not adequate in many situations, providing a strong mandate for developing alternative strategies for cartilage repair and reconstruction.

1.2.3 Tendon and ligament

Whilst this study is centred upon bone and cartilage regeneration strategies, tendons and ligaments are synthesised by cells of a comparable stromal lineage to cartilage and bone. Consequently, there is considerable overlap within and amongst research groups investigating skeletal tissue regeneration and it is therefore informative to derive data from studies into tendons and ligaments and possess knowledge of their structure and function.

Ligaments are dense connective tissues composed primarily of collagen type I with small amounts of collagen type III and elastin in a wave-like conformation (Gloria *et al.* 2010). Ligaments attach bone to bone and stabilise joints, and although their ultrastructure is similar to tendon, they have a higher elastin content and contain abundant mechanoreceptors for proprioception (Brinker and O'Connor 2008). Unstable ligamentous injuries are often reconstructed using autologous tendon, which is suitable due to its similar structure and strength characteristics. However, in many situations, such as in multiple or recurrent ligament injuries, alternatives may have to be found, and a tissue engineering approach may be appropriate (Gloria *et al.* 2010).

1.3 Rationale for research into skeletal tissue engineering

The last decade has witnessed a revolution in techniques to treat orthopaedic morbidity, with (amongst other advances) the introduction of bone tissue engineering strategies to overcome the problems inherent in entirely synthetic prosthetic materials. The gravity of this conceptual shift has been recognised by the World Health Organization and United Nations, proclaiming the years 2000-2010 'The Bone and Joint Decade' (Horan *et al.* 1999).

Bone possesses a unique capacity for regeneration upon damage together with the ability for constant turnover in response to demands of mechanical stress and mineral homeostasis (Giannoudis *et al.* 2007). Such dynamic properties imply the existence of a renewable source of progenitors able to replenish the bone-forming cells. These cells, the osteoblasts, generate mineralised bone matrix in a healing process that parallels osteochondral development pathways, following complex well-orchestrated, biological patterns (Gerstenfeld *et al.* 2003). Thus, tissue engineering principles – the use of a combination of cells, materials and biochemical factors to improve biological functions – appear particularly well suited to skeletal tissues, and in particular bone, giving substantial promise to the use of regenerative medicine techniques to tackle orthopaedic pathology (Muschler and Midura 2002).

Initial translational efforts have centred on bone and cartilage reconstruction for several reasons, not least because the differentiation pathways for osteo- and chondrogenesis are almost completely established and can now be modulated (Charbord *et al.* 2011). Once the process of bone and cartilage manipulation and regeneration has been proven in practice, such approaches may also be extended to other skeletal tissues such as tendon and ligament, although the cellular responses in these tissues appear harder to characterise (Charbord *et al.* 2011).

The development of new regenerative technology is timely, both in the nature of pathology encountered and its sheer scale. There is now a real urgency to refine these techniques and bring them to regular clinical use, in order to address the burgeoning healthcare needs of a growing population, with an ageing demographic.

The potential therapeutic niches for novel orthopaedic tissue engineering strategies are examined in Table 1.3.

Table 1.3 Potential therapeutic niches for novel orthopaedic tissue engineering strategies

Situation	Examples
Acute trauma	Segmental bone loss Chondral damage Osteochondral defects Tendon rupture Ligamentous injury Meniscal injury
Tumour	Surgically-induced bone and soft tissue defects Tissue-destructive lesions
Infection	Post-traumatic osteomyelitis Tuberculosis latrogenic
Degenerative/Inflammatory	Osteoarthritis Rheumatoid arthritis
Congenital	Dwarfism Maxillofacial defects Tendon lengthening
Prosthetic-related	Orthopaedic/Maxillofacial implants

1.4 Skeletal tissue engineering

Tissue engineering was first described by Langer and Vacanti in 1993 and can be defined as the application of scientific principles to create or induce the formation of a specific tissue, in a specific location through the selection and manipulation of cells, matrices and biological stimuli (Langer and Vacanti 1993, Muschler and Midura 2002). With respect to skeletal applications, the fundamental requisites for a successful tissue engineering approach include suitable progenitor cells delivered in conjunction with a non-toxic bio-resorbable scaffold that will maintain structural support to the construct and appropriate spatial alignment of the cells whilst incorporation into existing tissues occurs. This should take place within a local microenvironment that contains endogenous or exogenous nutrients. Success of this approach would be heralded by eventual appropriate lineage differentiation of the implanted progenitor cells. With regard to bone regeneration, this process would require a stimulation of vascular ingress, cellular infiltration and attachment, cartilage formation and eventual calcified tissue deposition, so that the construct becomes indistinguishable from regenerated native tissue. Clinical success requires structural integration with surrounding tissues and reliable remodelling to provide mechanical properties of load bearing and fatigue resistance necessary for durable function (Fleming et al. 2000). A number of elements are important for a successful bone regeneration strategy, and these same processes can be applied to other skeletal tissues (Albrektsson and Johansson 2001):

- 1. Osteoconduction The process of bone tissue growth throughout the site, supported by a physical three-dimensional (3D) scaffold or matrix.
- 2. Osteoinduction The stimulation of osteoprogenitor cells to differentiate into osteoblasts that produce bone matrix.
- 3. Osteogenesis The growth of new bone, brought about through the processes of osteoconduction and osteoinduction.

Even if all these conditions are met optimally, there is also a requirement for local vascularity and mechanical stability to prevent micromotion and non-union. These conditions are largely dependent on surgical factors and clinical expertise, and rely on meticulous tissue handling to prepare the graft bed, to ensure preservation of a good local blood supply, and to stabilise the construct and adjacent tissues (Fleming *et al.* 2000).

1.5 Stem cells

A successful skeletal tissue engineering strategy requires the isolation and delivery of progenitor cells that have been modulated or stimulated to undergo selective differentiation into the required skeletal genotype. Stem cells are found in all multicellular organisms and are defined by two properties – self-renewal and potency (Watt and Driskell 2010, Mitalipov and Wolf 2009):

- Self-renewal the ability to go through numerous cycles of cell division while maintaining an undifferentiated state. This is ensured through the processes of obligatory asymmetric replication (where cell division produces one identical undifferentiated cell and one differentiated cell) and stochastic differentiation (when one stem cell develops into two differentiated cells, another stem cell undergoes mitosis to produce two undifferentiated stem cells identical to the original) (Lin 1998).
- 2. **Potency** the capacity to differentiate into specialised cell types. *Totipotent* cells can differentiate into any of the three germ layers: endoderm, mesoderm or ectoderm, and can therefore give rise to any fetal or adult cell type and potentially develop into a whole organism (Watt and Driskell 2010). In mammalian tissue, this is only true for the zygote and early embryonic blastomeres. As embryonic development progresses, the individual blastomeres that comprise the embryo differentiate into either the inner cell mass, that gives rise to the fetus and trophectoderm, or the extra-embryonic outer layer of cells, that develops into placental tissue. These cells are pluripotent, as they can form all the cell types of the adult organism. Multipotent stem cells are lineage-restricted, but have the ability to form all the differentiated cell types of a given tissue (Lovell-Badge 2001). Most adult or somatic stem cells are multipotent and are referred to by their tissue origin (Barrilleaux et al. 2006). Their normal function is in repairing and regenerating tissues within the body (Tare et al. 2010).

1.6 Stem cells in skeletal tissue engineering

An advantage to skeletal tissue engineering is the ready supply of suitable osteoprogenitors from the non-haematopoietic stromal compartment of post-natal bone marrow. Bone marrow can be relatively easily obtained with little morbidity, and the stromal fraction can be readily isolated and separated from haematopoietic precursors (Bianco *et al.* 2006). Its use avoids the potential ethical issues of embryonic stem cell harvest and enables potential therapies to use autologous cells, essentially negating the risk of rejection. A small subset of stem cells derived from non-haematopoietic bone marrow stroma was first described by Friedenstein as spindle-shaped stromal cells (Friedenstein 1968). These cells possess the capacity for self-renewal and the ability to differentiate along multiple mesodermal lineages to generate cartilage, bone, myelosupportive stroma, adipose and fibrous connective tissue (Fig. 1.5) (Friedenstein 1976).

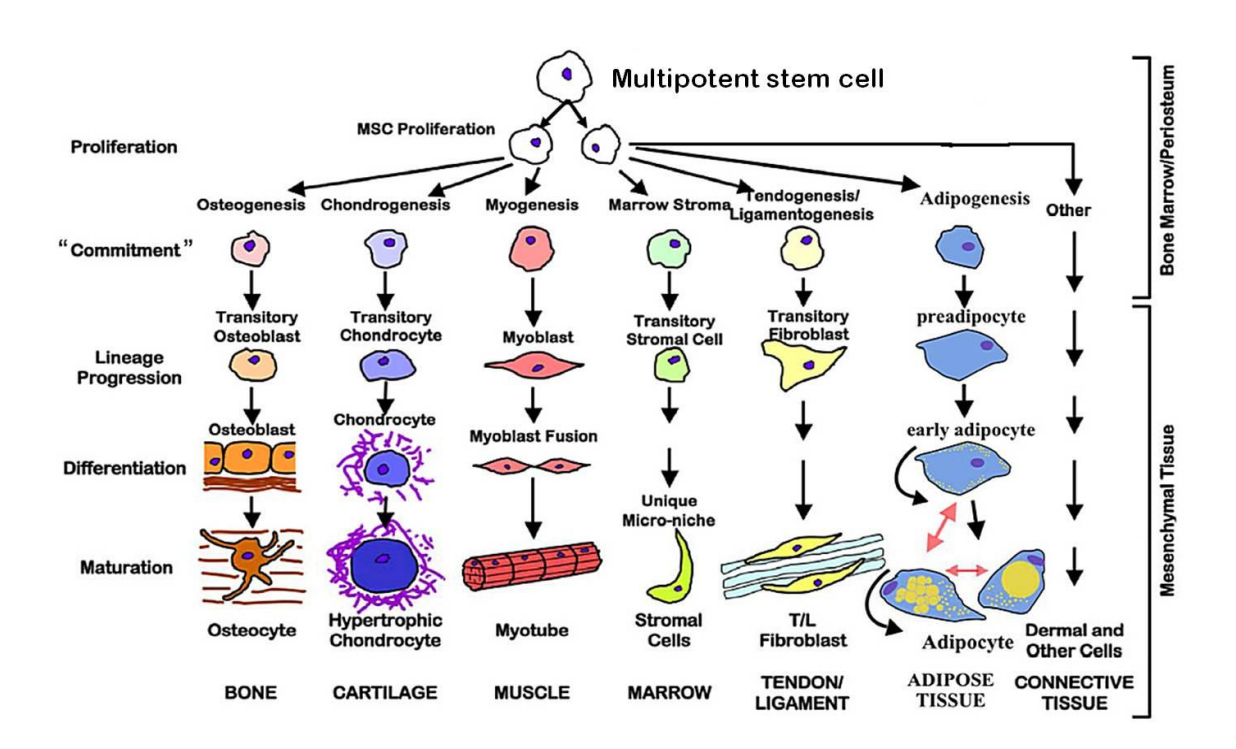


Fig. 1.5 The multi-differentiation potential of stem cells derived from non-haematopoietic bone marrow stroma. *Adapted from Caplan 2009.*

These cells form a developmental continuum within the bone marrow stromal compartment, with indistinct boundaries between cell populations, gradually losing self-renewal capacity and gaining lineage commitment with each cycle towards differentiation (Pittenger *et al.* 1999, Oreffo *et al.* 2005). Given this temporal

heterogeneity and also because no single specific skeletal stem cell marker has been defined, homogenous osteoprogenitor populations have yet to be isolated (Tare *et al.* 2010). Furthermore, the interconversion of skeletal cell precursors by dedifferentiation has also been reported, with implications in defining lineage plasticity (Park *et al.* 1999). This is particularly attractive as it may enable pluripotent stem cells to be induced from a patient's own somatic cells without the controversial use of embryos. Furthermore, use of induced Pluripotent Stem Cells (iPSCs) may avoid immunological rejection responses (Taylor *et al.* 2011). Since their discovery, varying nomenclature has been attributed to these cells (Bianco and Robey 2001, Muschler and Midura 2002, Triffitt 2002, Goshima *et al.* 1991, Tare *et al.* 2008), but for consistency the term Skeletal Stem Cell (SSC) will be used throughout this thesis (Table 1.4).

Table 1.4 Nomenclature for the multipotent stem cell derived from non-haematopoietic bone marrow stroma

Homonym	Abbreviation
Skeletal Stem Cell	SSC
Osteogenic Stem Cell	OSC
Osteoprogenitor cell	OPC
Marrow Stromal Fibroblastic Cell	MSFC
Human Bone Marrow Stromal Cell	HBMSC
Colony Forming Unit-Fibroblastic	CFU-F
Mechanocyte	None
Connective Tissue Progenitor	СТР

Note that the precise definition and biologic capabilities indicated by these terms by various authors are not entirely synonymous

Given the difficulty in defining the SSC and because all markers defined so far are non-specific, isolation and enrichment have been a challenge (Tuan *et al.* 2003). Consequently, many isolation and identification techniques exist, including tissue culture plastic adherence, induction of lineage-specific phenotypes under standard culture conditions and sorting with respect to a panel of cell surface markers. When used together, these methods can select SSCs with high discrimination (Seong *et al.* 2010) (Fig. 1.6).

An important landmark in the isolation of SSCs was the identification and generation of the STRO-1 antibody, which recognises stage – and/or lineage-specific stromal antigens expressed by a sub population of bone marrow mononuclear cells (Simmons

et al. 1991, Gronthos et al. 1994). Other cell surface markers have also been proposed for positive selection, including Cluster of Differentiation (CD) 105, CD73, CD90, CD71, CD63, CD 49a, CD44, CD166 (Activated Leukocyte Cell Adhesion Molecule: ALCAM), CD146 (Melanoma Cell Adhesion Molecule: MCAM), CD106 (Vascular Cell Adhesion Molecule-1: VCAM-1), CD54 (Intercellular Adhesion Molecule-1: ICAM-1) and CD29. Negative markers (CD45, CD34, CD14, CD19 and Human Leukocyte Antigen-DR (HLA-DR)) further distinguish SSCs from haematopoietic mononuclear cells (Kanczler et al. 2011). Research continues to identify a simple technique to reliably isolate and expand SSCs for tissue regeneration strategies (Sengers et al. 2010).

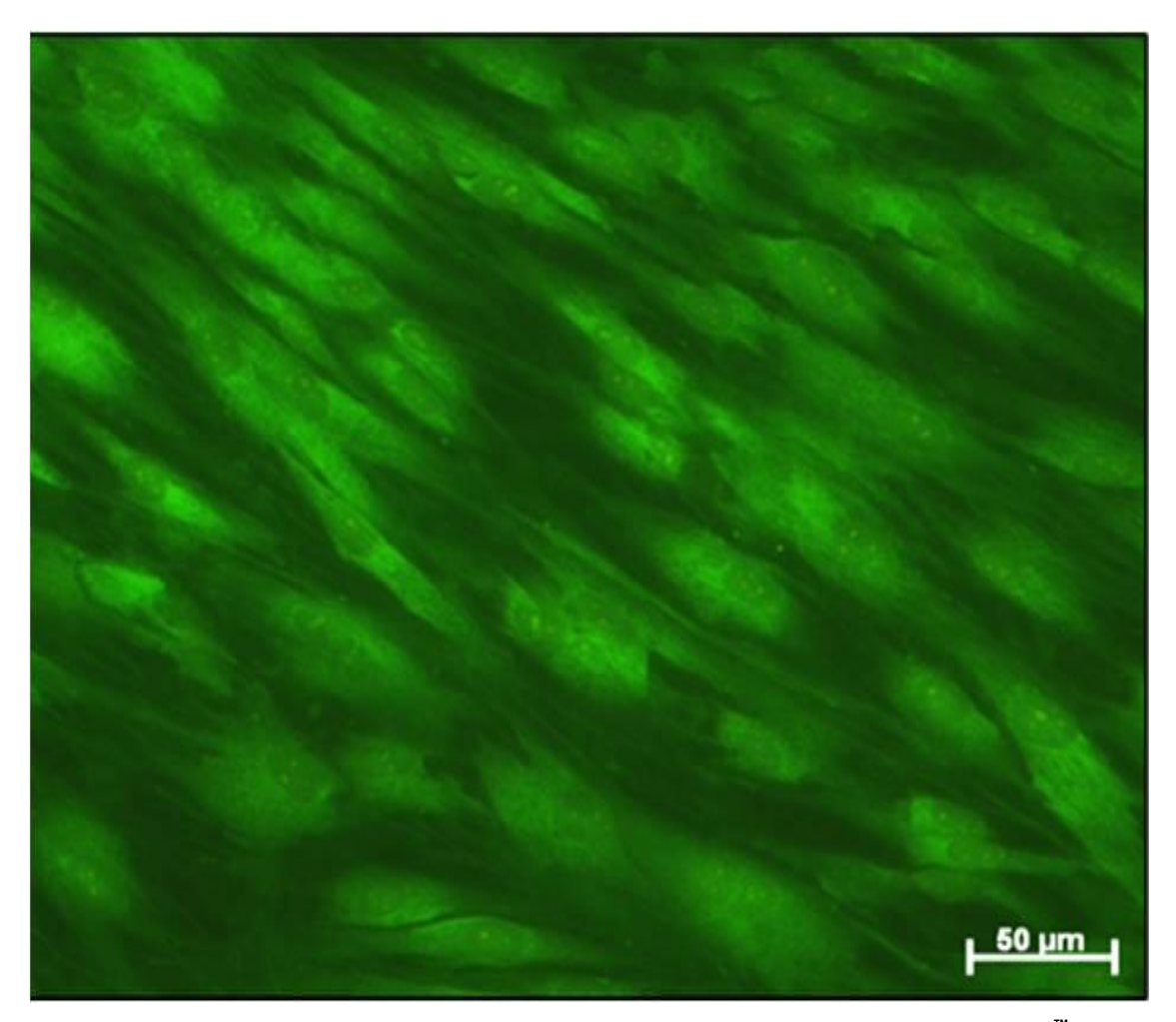


Fig. 1.6 Culture-expanded human SSCs at confluence, stained with CellTracker[™] Green to confirm viability. Scale bar: 50 μm

1.7 Cellular and molecular approaches to skeletal regeneration

1.7.1 Skeletal Stem Cells and bone repair

The use of bone marrow alone as an effective osteogenic graft has been applied to augment the healing capacity in Distraction Osteogenesis (DO) and also for the treatment of Avascular Necrosis (AVN) and fracture non-union (Hernigou *et al.* 2005a, Hernigou *et al.* 2005b, Hernigou *et al.* 2006, Hernigou *et al.* 2009, Kitoh *et al.* 2007a, Kitoh *et al.* 2007b). DO is an osteotomy-distraction technique, first described by Codivilla in 1905 to correct and lengthen limb deformities (Codivilla 2008). The procedure has since been refined by Ilizarov and others to maintain gradual lengthening of soft tissues whilst correcting bone deformities (Aronson 1997), and is frequently used with excellent functional outcomes. The traumatic or surgical osteotomy is stabilised by external fixators while distraction of approximately 1 mm per day generates ossification through the formation of microfractures (Shearer *et al.* 1992, Tsuchiya *et al.* 1997) (Fig. 1.7).

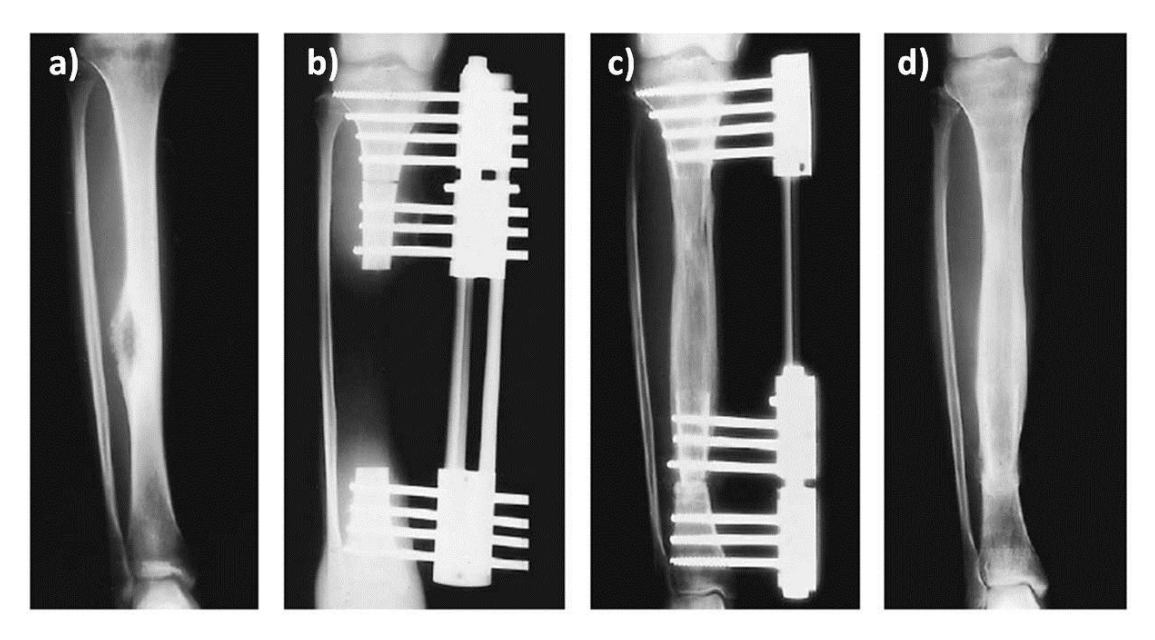


Fig. 1.7 Distraction Osteogenesis, a) in this case for treatment of a low-grade tibial osteosarcoma, **b)** following wide local excision of the tumour and application of a unilateral lengthening external fixator, note the proximal osteotomy. **c)** At the end of bone transport, note the final position of the fixator. **d)** Excellent bone formation 62 months following initial operation. *Images from Tsuchiya et al.1997.*

Current indications for DO include the regeneration of bone lost through surgical debridement, fracture non- and mal-union, congenital deformity, for limb lengthening in dwarfism and for some skeletal sequelae of poliomyelitis (Rozbruch *et al.* 2008, Schep

et al. 2009). However, because this method relies entirely on the inherent regeneration potential of bone, large defects often require extended treatment periods, with further procedures to release soft-tissues as fixation pins are distracted. Intensive specialist support, patient education and co-operation are integral to the success of this treatment. Unsurprisingly, complications occur frequently: pin tract infection is almost universal, and cellulitis, osteomyelitis, non- and mal-union and psychological consequences are common (Aronson 1997). In addition, failure to manage pain from distraction of surrounding soft tissues can affect patient compliance (Ghoneem et al. 1996).

The considerable complication rates in DO correlate with the total treatment time (Aldegheri 1999), so recent research has targeted this with the supplementation of SSCs and cellular products to reduce the total treatment time. Bone marrow alone contains SSCs, platelets and mononuclear cells that are rich in cytokines. It also provides a degradable biological fibrin matrix (Fleming *et al.* 2000). Successful treatment of 18 of 20 tibial non-unions was reported with internal fixation augmented by percutaneous local injection of autologous bone marrow (Connolly *et al.* 1991). Another study of 24 femoral and tibial osteotomies treated with concentrated autologous Platelet-Rich Plasma (PRP) and SSCs found the healing index dropped from 36.2 days/cm in the 32 control osteotomies (i.e. without additional cell therapy), to 27.1 days/cm in the treatment group (Kitoh *et al.* 2007a). However, due to the study design, it was not possible to deduce if this effect was due to the SSCs, the PRP or the combination.

Concentrated autologous SSCs from human bone marrow have also been used in the treatment of femoral head avascular necrosis (Hernigou *et al.* 2009). In a series of 534 hips in 342 patients, enduring bone architecture was demonstrated following treatment, particularly in the earlier stages of the disease. This technique was also applied to the management of tibial non-union, achieving sound bone healing in 53 of 60 cases following treatment with concentrated autologous SSCs (Hernigou *et al.* 2005a). Retrospective analysis of the seven cases that failed to unite confirmed that they were implanted with significantly lower initial SSC concentrations (less than 1000 SSCs/ml) than those cases that united soundly (between 2000 and 4000 SSCs/ml), suggesting a requirement for delivery of a critical concentration of SSCs to the defect site. The SSC concentration in untreated iliac crest aspirate is therefore often sub-therapeutic, and this emphasises the requirement for cell-enrichment approaches.

In addition to bone reconstruction, the applications of SSCs have been extended to treat osteochondral defects of articular cartilage. These focal lesions involve full thickness loss of cartilage and present most commonly in adults as a consequence of trauma, and in children from either trauma or microvascular pathology, such as osteochondritis dissecans (Green and Banks 1953, Widuchowski et al. 2008). Current therapeutic options include microfracture treatment, which involves the creation of multiple perforations (microfractures) in the subchondral bone in areas that are cartilage deficient. This stimulates a healing response through the release of endogenous factors. Unfortunately this response is mostly manifested as fibrocartilage, which is mechanically inferior to hyaline cartilage that is native to synovial joints (Salzmann et al. 2011). Despite improved function and reduced pain in the short and mid-term following microfracture treatment, substantial scope still remains for improvements in the longer term (Marder et al. 2005). A recent equine study has combined microfracture treatment with SSC implantation (Fortier et al. 2010). Twelve horses with iatrogenic full thickness cartilage defects in the lateral femoral trochlea were treated, either with microfracture alone or microfracture augmented with a concentrated fraction of Bone Marrow Aspirate (BMA). Subsequent analysis at eight months showed improved hyaline cartilage production in the group treated with the additional aspirate both in terms of amount, integration with surrounding native cartilage and quality (as judged by glycosaminoglycan and collagen type II content). Clinical trials have also shown some success, for example Haleem et al. used plateletrich fibrin glue as a scaffold to carry culture-expanded SSCs, which were implanted into 5 patients with full-thickness cartilage lesions (Haleem et al. 2010). Beneficial results were observed in all patients, both in terms of symptomatic relief, and actual cartilage regeneration as measured by magnetic resonance imaging and arthroscopically after 12 months.

Despite these successes of SSC therapy in isolation in skeletal tissue defects, these strategies do not ensure the necessary cells are distributed throughout the graft volume. Consequently, the healing response is not always contiguous and regenerated tissue may fail to integrate fully with adjacent tissue. Thus, true tissue engineering strategies for cartilage regeneration require the supportive functions of a scaffold to supply the ideal conductive and inductive stimulus for maximal tissue regeneration.

Successful translation of tissue engineering strategies to heal ligamentous damage or tendon rupture in humans remains a significant challenge and no studies have yet shown benefit in human trials. Marrow-derived SSCs used in conjunction with a collagen I construct have enhanced the biochemical and mechanical properties of tendo-achilles repairs in rabbits, however this was not seen at a functional level (Young et al. 1998). Neo-tendon formation has also been demonstrated in a rat tendo-achilles model using adenoviral modification of SSC differentiation by transfection of the biologically active Smad8 signalling molecule (Hoffmann et al. 2006). Ligament regeneration is at an even earlier stage, with current SSC strategies directed at enhancing the fibrocartilage junction strength in anterior cruciate ligament repairs in rabbits (Ekdahl et al. 2008). It appears that fibroblasts are highly sensitive to mechanical stimuli and tensile strength so stretch-loading is essential for the proper formation and alignment of ligament and tendon structure (Tuan et al. 2003). Replication of in vivo mechanical conditions to direct stem cell fate may therefore be a major hurdle for successful tissue engineering strategies.

1.7.2 Growth factors

Growth factors are a group of naturally-occurring cytokines that regulate a variety of cellular functions, such as growth, proliferation and differentiation (Yin *et al.* 2010). The pivotal role of growth factors and their complex interactions with cells, in the maintenance and healing of skeletal tissues, is widely recognised (Devescovi *et al.* 2008). It therefore follows that control of the temporal release of appropriate growth factors during tissue healing is a fundamental process in the development of successful tissue engineering strategies. Several growth factors within bone are expressed during the process of fracture healing, suggesting a role in osteochondral development and in fracture repair (Table 1.5).

1.7.2.1 Transforming growth factor beta (TGF-β)

TGF- β is a multifunctional polypeptide sequestered within the bone matrix with diverse actions: It has been shown to stimulate cellular proliferation, hypertrophy and osteogenic differentiation, and it up-regulates the production of collagen from osteoblasts, whilst enhancing mineralisation (Salgado *et al.* 2004). Despite these effects *in vitro*, fracture repair models incorporating TGF- β have produced inconclusive results, requiring continuous dosing to demonstrate efficacy, which may have unwanted effects on other non-skeletal tissues (Kanczler *et al.* 2011). Members of the TGF- β super-family (particularly TGF- β 3), have been implicated in chondrogenesis and the repair of articular cartilage following damage (Tang *et al.* 2009).

Table 1.5 Growth factors associated with fracture repair

Growth factor	Cellular source	Biologic effects	Actions on bone		
BMP-2	SSC, osteoblast, chondrocyte, endothelial cell	Chondro- and osteogenesis, Osteoinduction	SSC migration, induction, differentiation, proliferation, matrix synthesis		
FGF	Macrophage monocyte, SSC, chondrocyte, osteoblast, endothelial cell	Angiogenesis, Proliferation of fibroblasts and vascular smooth muscle cells	Chondrocyte maturation (FGF-1) Osteoblast proliferation, differentiation Inhibition of osteoblast apoptosis Induction of osteocyte apoptosis Bone resorption (FGF-2)		
IGF	Osteoblast, chondrocyte, hepatocyte, Endothelial cell	Growth regulation	Osteoblast proliferation Bone matrix synthesis Bone resorption		
PDGF	Platelet, monocyte, macrophage, osteoblast, endothelial cell	Smooth muscle cell proliferation, chemotaxis, angiogenesis	SSC migration, proliferation and differentiation		
TGF-β	Platelet, SSC, osteoblast, chondrocyte, fibroblast, endothelial cell, macrophage	Immunosuppression, Angiogenesis, stimulation of cell growth, ECM synthesis	SSC proliferation and differentiation, but inhibits terminal chondrocyte differentiation, osteoclast recruitment, ECM production		
VEGF	Osteoblast, platelet	angiogenesis	Osteoblast proliferation, vascularisation, cartilage mineralisation.		

BMP = Bone morphogenetic protein, SSC = Skeletal stem cell, FGF = Fibroblast Growth Factor, IGF = Insulin-like Growth Factor, PDGF = Platelet Derived Growth Factor, TGF- $\beta = Transforming$ Growth Factor beta, ECM = Extracellular Matrix, VEGF = Vascular Endothelial Growth Factor. Adapted from Devescovi et al. 2008 and Southwood et al. 2004.

1.7.2.2 Bone morphogenetic proteins (BMPs)

With the exception of BMP-1, BMPs are structurally considered part of the TGF-β super-family, with BMP-2, 4, 6 and 7 the most osteoinductive. BMPs are critical to the recruitment, commitment and differentiation of SSCs and they are responsible for initiating bone cell differentiation from SSCs, enhancing terminal osteoblast differentiation, and producing local signalling to control endochondral ossification (Kanczler *et al.* 2011). Given these osteoinductive properties, BMPs are already in clinical use to enhance bone union, although widespread application has been limited by their high cost (Zimmermann *et al.* 2009, Cahill *et al.* 2009).

1.7.2.3 Wnt signalling molecules

The Wnt signalling pathway has also been shown to be pivotal in the differentiation of osteoblasts and actions of osteoclasts during development and remodelling. Furthermore, the mechanisms of action of this family of glycoproteins are closely interrelated to BMP pathways (Pederson *et al.* 2008). Consistent with an important role for the Wnt protein family in humans, are the findings that activating mutations of the Wnt pathway (either primary or secondary, through the deletion of SOST (the gene encoding sclerostin), which inhibits the Wnt signalling pathway through LRP5 and 6 receptor binding) can result in increased bone mass (Semenov *et al.* 2006).

1.7.2.4 Local growth factors

Local growth factors, such as IGFs, FGFs, PDGF and VEGF are also sequestered within bone matrix, and their actions may be harnessed by developing regenerative strategies:

1.7.2.4.1 IGF-I and IGF-II activities are regulated by IGF-binding proteins, and act independently to stimulate osteogenesis and chondrogenesis. IGF-I specifically stimulates intramembranous bone formation, and whilst IGF-II has been shown to be important in skeletal development, its function in the adult skeleton is not proven (Canalis 2009). IGF-I up-regulates type I collagen and down-regulates collagenase 3 expression, resulting in maintenance of ECM, and it enhances Wnt signalling through β-catenin stabilisation, resulting in osteoblastogenesis (Playford *et al.* 2000).

1.7.2.4.2 FGF-1 and FGF-2 are polypeptides which act locally with potent angiogenic, wound healing and osteogenic properties. However, direct injection of FGF-2 into skeletal defects results in inconsistent stimulation of bone repair (Zellin and Linde 2000) This may be due to difficulties of growth factor delivery and release, rather than a lack of action of FGF itself, and research to refine carrier systems to improve bioavailability is continuing, with mixed results (Manferdini *et al.* 2010).

1.7.2.4.3 PDGF is a potent osteoblastic mitogen, enhancing proliferation, chemotaxis and collagen activity (Devescovi *et al.* 2008). Furthermore, PDGF receptors are highly expressed within newly-formed osteoid in fracture healing, and recombinant PDGF in combination with IGF-1 have shown enhanced periodontal bone formation in humans (Hollinger *et al.* 2008).

1.7.2.4.4 VEGF is a term applied to four homologous homodimeric glycoprotein family members that play an integral role in angiogenesis, osteogenesis and skeletal repair (Carano and Filvaroff 2003). VEGF is key in inducing endochondral development and its interaction with VEGF receptors regulates vascularisation, chondrocyte apoptosis, SSC recruitment and growth plate ossification (Gerber et al. 1999, Mayr-Wohlfart et al. 2002, Wang et al. 2007). Furthermore, the activities of BMPs and VEGF are intrinsically linked, aiding the coordination of vascularisation with skeletal development (Deckers et al. 2002). Several studies have incorporated active VEGF with SSCs into engineered constructs to enhance the regeneration of bone defects in rabbit radius and mouse femoral defect models (Geiger et al. 2005, Kanzcler et al. 2008). The osteogenic-angiogenic interplay between VEGF and BMPs has also more recently been exploited in such models, with newer generations of scaffold that have been engineered to release these angiogenic and osteogenic growth factors in a temporallycontrolled manner (Patel et al. 2008, Kanzcler et al. 2010, Kempen et al. 2009). Other strategies to ensure the accurate delivery of growth factors to the site of regeneration include gene therapy with various viral and non-viral vectors, which maintain high local concentrations by continuous expression of the appropriate genes (Southwood et al. 2004).

1.7.3 Growth factors in tendon and ligament healing

The role of growth factors in tendon and ligament healing is only now being elucidated: *TGF-β1* enhances cell proliferation and migration, and stimulates their production of collagen and proteoglycans, and *PDGF* may accelerate tendon and ligament healing by increasing ECM synthesis (Yin *et al.* 2010). *Growth Differentiation Factor* (GDF, a member of the BMP family) stimulates tendon and ligament formation *in vivo* in rats, and can improve healing following injury (Hoffmann *et al.* 2006). This action is orchestrated through the *Smad8 signalling pathway*, inducing fibroblastic proliferation and increasing their expression of collagen type I, scleraxis, and tenomodulin (Mendias *et al.* 2008).

Development of strategies to generate a functional vasculature at an early stage of tissue healing will facilitate the recruitment, proliferation and differentiation of cells involved in the repair of these tissues as well as providing the essential growth factors, nutrients and gaseous exchange for regeneration and homeostasis.

1.7.4 Platelet-rich plasma (PRP)

The first uses of PRP in skeletal reconstructive therapy were in maxillofacial surgery for the treatment of mandibular and periodontal defects (Alsousou *et al.* 2009). Since then its uses have been widened to orthopaedic approaches to enhance fracture union (Kitoh *et al.* 2007b) and spinal fusion (Hartmann *et al.* 2010, Initini 2009). The healing effects of PRP are mediated through the activation of the coagulation cascade, which releases growth factors from the α -granules of platelets (Cenni *et al.* 2010). These growth factors include VEGF, TGF- β , IGF, PDGF and Epidermal Growth Factor (EGF).

The combination of PRP with SSCs has been used with considerable success in the maxillofacial field: Culture expanded autologous SSCs and PRP were applied to a titanium mesh scaffold as a tissue engineered construct that demonstrated enduring and functional reconstruction of a congenital cleft lip and alveolus in a young girl (Hibi et al. 2006). The combination of autologous SSCs, PRP and Hydroxyapatite (HA) have also shown promise as grafting materials for maxillary sinus floor augmentation in 20 patients (Ueda et al. 2005). However, clinical analyses of constructs containing PRP are generally confined to case studies or small series, and many strategies also involve concurrent SSC therapy, obscuring the potential effects of PRP. Controversy therefore remains over the additional therapeutic effects provided by the growth factors within PRP, many of which only have a brief duration of action.

1.8 Scaffolds – osteoconduction and osteoinduction

Emerging strategies strive towards the ultimate therapeutic objective: to replace damaged skeletal tissues with appropriate autogenous components that have been harvested without significant morbidity and presented within a suitable matrix for cellular conduction and induction. Although biological scaffolds have been used clinically with success, their disadvantages can have serious implications. Research activity has therefore been centred upon approaches that couple material science with autogenous SSCs as true tissue engineering constructs. The ideal scaffold would be biocompatible and have structural integrity, yet be bio-resorbable, thus acting as a temporary framework until new tissue is generated (Cancedda *et al.* 2007). Research behind scaffolds and cell-based tissue engineering has culminated in their application to a number of human cases (Table 1.6).

Scaffolds for orthopaedic regeneration require particular functions and characteristics for success. In the case of load-bearing tissues, the scaffold must provide sufficient temporary mechanical support to withstand *in vivo* loading and stresses, ideally matching the mechanical properties of the host tissue (Hutmacher *et al.* 2000). Furthermore, the material must degrade at such a rate as to allow the strength of the scaffold to be maintained until the host tissue can assume its structural role (Rose and Oreffo 2002). These conditions can only be met if the construct stimulates and modulates exogenous or existing cells to produce the appropriate tissue types. This in turn requires early and sufficient angiogenesis to allow metabolic processes to proceed and for regeneration to take place (Bouhadir and Mooney 2001, Rivron *et al.* 2008).

Table 1.6 Clinical translation of cell-based tissue engineering approaches to skeletal regeneration

Tissue engineering strategy	Site/ Indication	Reference
HA scaffold seeded with culture-expanded autologous periosteum-derived cells	Right thumb distal phalanx sub-amputation	Vacanti et al. 2001
HA scaffold seeded with culture-expanded autologous marrow-derived cells	Long bone segmental defects following trauma	Quarto et al. 2001 Marcacci et al. 2007
Polymer fleece impregnated with culture- expanded mandibular periosteal cells	Maxillary sinus floor augmentation	Schimming et al. 2004
Alumina-ceramic prosthesis seeded with culture-expanded autologous SSCs	Ankle osteoarthritis	Ohgushi <i>et al.</i> 2005
HA scaffold seeded with culture-expanded autologous SSCs	Knee osteochondral defect	Adachi et al. 2005
HA scaffold seeded with autologous SSCs and PRP	Reduced maxillary crestal height	Ueda <i>et al.</i> 2005
HA and titanium scaffold seeded with autologous bone marrow	Mandibular defect following ablative tumour surgery	Warnke <i>et al.</i> 2004 Warnke <i>et al.</i> 2006
Percutaneous injection of autologous concentrated BMA	Tibial non-union	Hernigou <i>et al.</i> 2005a and b
HA seeded with culture-expanded autologous SSCs	Benign long bone tumours	Morishita et al. 2006
Titanium mesh plate seeded with culture- expanded SSCs and PRP	Alveolar cleft osteoplasty	Hibi <i>et al.</i> 2006
Percutaneous injection of autologous concentrated BMA	Femoral head avascular necrosis	Hernigou et al. 2009
PRP	Fracture non-union, spinal fusion	Alsousou et al. 2009
IBG of allograft seeded with autologous concentrated BMA	Femoral head avascular necrosis	Bolland et al. 2006 Tilley et al. 2006
DBM seeded with concentrated autologous SSCs	Unicameral bone cysts, various locations	Di Bella et al. 2010

HA = Hydroxyapatite, BMA = Bone Marrow Aspirate, SSCs = Skeletal stem cells, PRP = Platelet rich plasma, IBG = Impaction bone grafting, DBM = Demineralised bone matrix. Adapted from Smith et al. 2011

1.8.1 Biological scaffolds

1.8.1.1 Autogenous biological scaffolds

1.8.1.1.1 Cancellous autograft — Autologous cancellous bone represents the clinical gold standard for enhancing bone healing in spinal fusion, treating bone defects and for fracture repair (Marino and Ziran 2010, Burwell 1964, Burwell 1966, Kanakaris et al. 2007). Cancellous autograft bone provides an osteoconductive 3D matrix of collagen, mineral and matrix proteins, with osteoinductive proteins, whilst retaining native SSCs (Delloye et al. 2007). Cancellous autograft can be harvested from various sites and implanted during the same procedure, without provoking an immunogenic reaction. However, it is only considered osteogenic if implanted immediately (Delloye et al. 2007) and associated donor site morbidity and pain limit its use to smaller defects (Ahlmann et al. 2002). Indeed, the risk of donor site complications, such as cutaneous nerve damage, chronic donor site pain, vascular injury, infection and fracture, is reported to be approximately 10% (Younger et al. 1989).

1.8.1.1.2 Cortical autograft - Autologous cortical bone has superior mechanical strength to cancellous bone, however full incorporation into surrounding tissue can take considerably longer because it contains fewer SSCs and has a lower porosity, which inhibits vascular ingress (Delloye et al. 2007). Vascularised cortical bone grafts (implanted with or without surrounding soft tissues) can transport an immediate blood supply to the wound, and these are used in limb salvage and reconstruction scenarios following trauma, ablative tumour surgery or debridement of infection (Taylor et al. 1975, Warnke et al. 2004). However, significant donor site morbidity restricts harvesting to just a few options, such as fibula, scapula, iliac crest, and rib transplant. These bones function mainly as an attachment for muscles, and consequent functional reduction following full or partial excision can often be tolerated to improve function elsewhere (Muramatsu et al. 2004). In one study, surgically-induced long bone segmental defects following tumour resection were treated with vascularised fibular grafts in 30 patients, resulting in primary union in 23 patients within a mean of 6 months. However, over half of these had complications and 40% required re-operation for non-union, graft fracture or infection (Eward et al. 2010). Attempts have been made to improve the outcomes following this technique by placing the fibular autograft within the intramedullary canal of a cortical allograft shell (Innocenti et al. 2009). Although this provides initial structural support and promotes the biology and regeneration of host bone, the procedure is technically more challenging and high complication rates remain

(Abed *et al.* 2009). Consequently, despite significant biological, economic and practical disadvantages to its use, allograft is generally used in isolation, for the treatment of expansive defects (Emms *et al.* 2009).

1.8.1.1.3 Autogenous cartilage graft – Articular cartilage defects that are too large for microfracture treatment can be treated using mosaicplasty: Several circular (4-8 mm) autogenous grafts are harvested from non weight-bearing articular regions and then transplanted in a mosaic conformation to fill the osteochondral defect. This has yielded good results, but with the drawback of donor site morbidity (Gudas et al. 2006). Cartilage transplantation involves a smaller biopsy of a non weight-bearing area of cartilage, so is less invasive than mosaicplasty and causes less morbidity at the harvest site. Chondrocytes are isolated and cultured ex vivo prior to re-implantation during a subsequent operation, either directly into subchondral bone or onto a matrix, which is implanted into the bone (Matrix induced Autologous Chondrocyte Implantation (MACI)). These procedures are currently expensive, they require two operations to the injured joint, and the results are limited in comparison to those of mosaicplasty, both in terms of symptomatic relief and quality of cartilage regeneration (Horas et al. 2003).

1.8.1.1.4 Autogenous tendon/ligament – Tendons and ligaments have a poor intrinsic repair capability and injury of these tissues often requires therapeutic intervention. Fortunately autogenous tendon may be harvested with little morbidity from several donor sites with 'expendable' muscle-tendon units and can be used to repair or replace tendon and ligamentous structures (Yin et al. 2010). However, some reports of donor site morbidity do exist (Getgood and Bollen 2010) and the transplanted tissue may have poorer tensile strength than its native substitute, particularly if a tendon is used to replace ligamentous tissue (as in anterior cruciate ligament reconstruction of the knee using hamstring tendon) (Menetrey et al. 2008). Despite this, the orthopaedic literature contains abundant examples of tendon transfers and ligament reconstruction using autogenous material in a wide variety of conditions, with generally good outcomes (Sammer and Chung 2009).

1.8.1.2 Allogeneic biological scaffolds

1.8.1.2.1 Allogeneic bone (allograft)

Allograft is obtained from cadaveric donation or from live donors. Most frequently, the femoral head is salvaged in patients undergoing total hip replacement surgery and the donated bone is processed and stored in regional bone banks for future use. The porous, collagen-rich matrix of allograft bone contains multiple sites for SSC and endothelial cell attachment and multiple embedded growth factors which can be liberated by osteoclastic resorption (Fleming et al. 2000). These growth factors, including IGF, TGF-β, PDGF, FGFs and BMPs give allograft its osteoinductive properties, inducing cells from surrounding soft tissue to produce new bone at the hostgraft interface, which then progresses into the graft material (Delloye et al. 2007). This process requires a contiguous vascular supply and sufficient mechanical stability to permit angiogenesis and eventual bone remodelling (Hernigou et al. 2005b, Stevenson et al. 1996) - conditions that are often absent, particularly in traumatic defects, where there is frequently surrounding soft tissue disruption and instability. However, where the conditions are appropriate for bone healing, the allograft matrix is fully resorbable through normal metabolic pathways with no reactive by-products or debris (Fleming et al. 2000).

1.8.1.2.1.1 **Allograft processing** – The technique of graft milling and impaction has been used clinically in revision hip arthroplasty surgery for over 30 years. The impacted allograft provides a mechanically solid foundation and acts as a 'void filler' to support the prosthesis in the context of poor bone stock (Slooff et al. 1984). Relatively small acetabular and femoral defects have been treated with favourable outcomes at 10 and 20 years (99% (Halliday et al. 2003) and 87% (Schreurs et al. 2009) respectively). However, such surgery can be technically demanding and operator-dependent. Thus, poorer results are often reported outside specialist centres or in the treatment of larger defects, such as those encountered during revision total hip arthroplasty (Eldridge et al. 1997, van Haaren et al. 2007). Alternatively, structural allograft can be used to restore bone stock in the presence of large uncontained defects. However, structural allograft shows little remodelling or incorporation into the host bone, particularly at the host-graft interface. Furthermore, its bone mineral density decreases following implantation, and progressive microfracture accumulation results in a 50% reduction in strength at 10 years (McNamara IR 2010).

1.8.1.2.1.2 Enhancement of allograft properties – There has been significant interest in the addition of SSCs to Impaction Bone Grafting (IBG) constructs to restore the osteoinductive properties lost during processing and storage of allograft (Fig. 1.8). Recent studies have demonstrated SSC survival following the impaction process and confirm enhancement in the shear strength of the graft following culture with SSCs (Bolland *et al.* 2006, Smith *et al.* 2011).

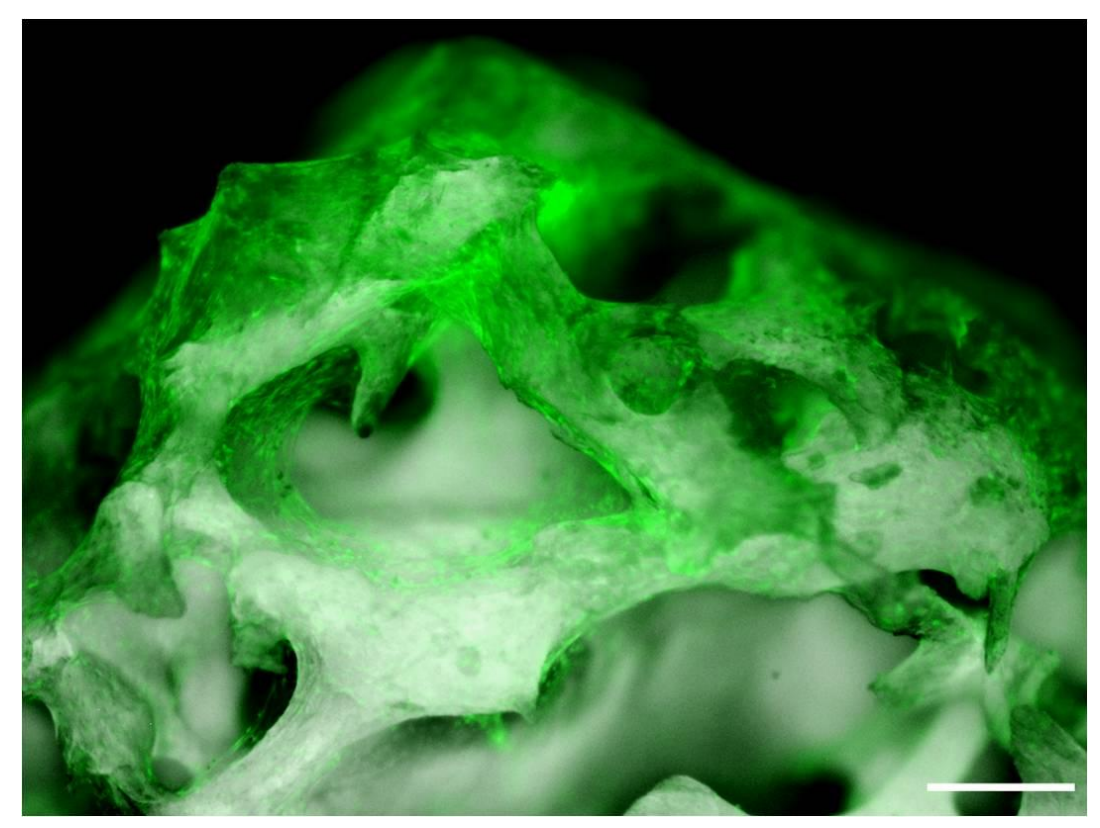


Fig. 1.8 *In vitro* culture of human SSCs seeded onto allograft, stained with CellTracker[™] Green after 7 days culture. Adherence of allograft fragments by cellular interaction is demonstrated. Scale bar: 200 μm

Regenerative efficacy has been demonstrated following clinical translation for the treatment of bone defects in two patients (due to a benign non-ossifying fibroma and AVN, both in the proximal femur) (Tilley *et al.* 2006). Despite recurrence of the cyst in the first case, this provided an opportunity for *ex vivo* analysis of the retrieved tissue-engineered bone, and confirmed remodelling of trabecular bone in the treated region (Aarvold *et al.* 2011). Increasing the concentration of SSCs applied may improve results in future cases, as further *in vitro* studies indicate a correlation between cell seeding density and the shear strength of the construct, reaching a significant difference at 2x10⁵ cells/ml, with a 16% increase in shear strength over allograft alone (Jones *et al.* 2009). The IBG technique to treat patients with early femoral head AVN (Ficat stage 1 and 2) has given encouraging clinical results at three year follow-up

(Jones *et al.* 2010). The procedure involves initial removal of necrotic bone by drilling and curettage from the avascular region, followed by impaction of allograft seeded with concentrated autologous SSCs (Fig. 1.9). The approach aims to augment mechanical support to the overlying cartilage and also improves angiogenesis and new bone formation through enhanced biology.



Fig. 1.9 Impaction bone grafting technique to treat early femoral head avascular necrosis. A. Pre-operative MRI in a patient with bilateral femoral head avascular necrosis (AVN) in the subchondral bone (arrows). **B.** Allograft from a donor femoral head is milled. **C.** The addition of concentrated BMA containing SSCs. **D.** Donor allograft in combination with concentrated aspirate. **E.** Intra-operative radiograph of a 12 mm diameter impactor in the drilled channel within the left femoral head. The SSC-seeded allograft is impacted into the necrotic segment of subchondral bone (radio-dense zone). **F.** Post-operative pelvic AP radiograph demonstrating maintenance of the architecture of left femoral head. The right total hip replacement was performed following collapse of the femoral head as a result of progressive AVN.

Despite these positive findings, several caveats to the use of allograft remain: given the concerns of potential pathogen transmission by allograft, regional 'bone banks' are required to screen and store freeze-dried, fresh-frozen or irradiated allograft for future use and provide quality assurance (Mallick *et al.* 2011). These facilities are strictly regulated in the UK under the Human Tissue Act 2004 and in the US by the American Association of Tissue Banks, with robust legislation to ensure traceability of allograft. This system has the advantage of providing a ready supply of screened and quarantined bone; however the mechanical, biological and immunological properties of

allograft may be affected differently by varying processing and storage arrangements at each facility (Schreurs et al. 2004). This can result in undesirable variation in clinical performance over and above the donor-to-donor variation in graft quality (Garbuz et al. 1998). Although it can act as an osteoconductive scaffold, the requirement to process allograft for safe storage and to reduce its immunogenic reactivity, removes much of its inherent osteoinductive properties. Nevertheless, despite stringent processing and donor screening there remains the possibility of carriage of bacteria, viruses and prions, some of which may not yet have been discovered. Indeed, many allograft recipients develop antibodies to donor antigens despite screening and processing, indicating the stimulation of an immune response (Mankin et al. 1987). Studies have reported bacterial infection rates of 0-12%, the incidence varying with donor selection criteria, processing technique and quarantine protocol (Costain and Crawford 2009, Sutherland et al. 1997, Lord et al. 1988, Kappe et al. 2010). The risk of Human Immunodeficiency Virus (HIV) transmission from screened donors has been estimated at just 1 in 1.6 million procedures (Tomford 1995), with no new reported cases since 1985 (Costain and Crawford 2009, Simonds et al. 1992), although the risk of Hepatitis C Virus (HCV) transmission is probably much greater: four cases of HCV infection were attributed to transplanted skeletal tissue harvested from a single antibody-negative donor in 2000 (Cieslak et al. 2003).

To minimise the risks of infection transmission, the Medicines and Healthcare products Regulatory Agency (MHRA) in the UK, and the US Food and Drug Administration (FDA) implemented new directives and legislations in 2004 and 2005 respectively (Mallick *et al.* 2011). Such legislations ensure traceability of allograft and provide a framework to coordinate recalls of potentially infected allograft (Mroz *et al.* 2009). However, these regulations complicate the logistics of acquisition, transport and storage of allograft, increasing its cost and reducing availability, and as requirements increase, supply will soon be outstripped by demand (Delloye *et al.* 2007).

1.8.1.2.1.3 Demineralised Bone Matrix (DBM) – DBM is cortical cadaveric allograft that has been decalcified and additionally treated to reduce immunological and potential pathogen transmission. Strict donor selection and testing procedures are observed (as above), before aseptic recovery of allograft. Processing involves the following steps: exposure to low-dose gamma irradiation; high-pressure lavage in antibacterial solution; mechanical dissection, crushing or pulverisation; ultrasonic decontamination in alcohol; demineralisation in hydrochloric acid, and copious washing

in purified water (Dinopoulos and Giannoudis 2006). The final product is supplied either pure or incorporated with a carrier (such as lecithin, calcium sulphate, hyaluronic acid, collagen or glycerol) to facilitate handling and graft containment as a gel, malleable putty, mouldable paste, injectable paste or in flexible strips (Giannoudis *et al.* 2005). The process of demineralisation removes many biologically active factors and results in a trabecular collagenous scaffold with little structural strength. However, some osteoinductivity is imparted by internal growth factors (including BMPs, osteocalcin and osteopontin) which are rendered more bio-available by the removal of the mineral phase. Thus, DBM can be more osteoinductive than standard mineralised allograft (Fleming *et al.* 2000).

DBM is widely used for filling bone defects and cavities in orthopaedic, neurosurgical and dental practice. It is used either alone or in combination with other materials (particularly autologous bone marrow) as a 'bone graft extender', however studies of efficacy show mixed clinical results and there are few prospective, randomised controlled trials (Dinopoulos and Giannoudis 2006). The paucity of robust large-scale studies reflects the wide range of clinical applications for which DBM is used. Moreover, its efficacy is determined not only by clinical factors, but may vary between manufacturers depending on the specific preparation and carrier material. Furthermore, although no report of disease transmission through DBM exists, the theoretical risk of infection or contamination from allogeneic material remains. Despite these caveats, DBM remains a useful product for the treatment of specific bone defects.

The combination of DBM with concentrated BMA has been used to stimulate bone healing in the treatment of paediatric unicameral bone cysts. (Di Bella *et al.* 2010) When compared to the standard treatment of multiple steroid injections (n = 143), healing improved after a single intralesional injection of BMA and DBM (n = 41) from 38% to 71%. The results of this series confirm the utility of DBM composites in the clinical scenario.

1.8.1.2.2 Cartilage and composite allogeneic grafts

As an alternative to autogenous cartilage transplantation, allogeneic articular cartilage may be obtained from a cadaveric donor, most commonly as an osteochondral allograft (Gortz and Bugbee 2006). The intact cartilage with underlying subchondral bone can be implanted *en bloc* into a defect with the advantage of immediate viable cartilage restoration and no donor site morbidity to the recipient (Getgood and Bollen 2010).

Given cartilage is avascular and thus relatively immunoprivileged, transmission of viral disease has not been reported following cartilage transplantation alone (Tomford 1995), however the risks of bacterial infection and transmission from the osseous portion of grafts remain, particularly as the use of screened fresh osteochondral grafts is routine to avoid chondrocyte damage by storage and processing techniques (Gortz and Bugbee 2006). Immunological incompatibility is also an issue, and bone must be thoroughly washed with pulsatile lavage before implantation to reduce its antigenic load (Getgood and Bollen 2010). Despite these shortcomings, several large trials have reported successful medium-term outcomes of osteochondral allograft transplantation in 72 to 88% of patients with corresponding radiological incorporation (Gortz and Bugbee 2006, Bedi *et al.* 2010). This technique is expensive however, and the procedure requires significant skill and logistical support. Furthermore, the procedure is dependent upon a reliable supply of screened cadaveric material with the inherent risks of disease transmission therein.

Commercial allograft composites (such as Osteocel® and Trinity™) containing allogeneic skeletal stem cells (SSCs) have recently become available (Rush 2010, Rush *et al.* 2009, McAllister *et al.* 2009). These composites employ a combination of immuno-depleted cellular cortical allograft with particulate demineralised bone matrix, which have been cryopreserved to retain cell viability and multipotency, thus demonstrating osteoinduction, osteoconduction and osteogenesis. Encouraging case series confirm therapeutic utility of these products in maxillofacial reconstruction (McAllister *et al.* 2009) and revision foot and ankle surgery (Rush 2010, Rush *et al.* 2009) as an alternative to autogenous bone, although the caveats of using allogeneic material remain.

1.8.1.2.3 Allogeneic tendon and ligament

The use of cadaveric tendon allograft has increased markedly over the last 20 years (McDermott *et al.* 2006). It is mainly used for the treatment of knee and shoulder pathology, particularly in cases requiring multiple ligamentous reconstruction or in revision surgery, where the most appropriate autogenous candidate has already been harvested (Getgood and Bollen 2010). Allograft has the advantage of eliminating donor site morbidity, whilst allowing shorter operation times and smaller scars. Furthermore, some studies have demonstrated superior implant strength and better clinical outcomes compared to tendon autograft (Krych *et al.* 2008). However, the risks of

immunogenic reaction, disease transmission, delayed graft incorporation, high cost and restricted availability, limit its use for routine cases (Getgood and Bollen 2010).

Cadaveric human skin can also be processed into acellular dermal matrix, which is commercially available for tendon and ligament repair as Graftjacket[®] (Wright Medical Technology Ltd) (Longo *et al.* 2010). Following processing and freeze-drying, the acellular graft is mainly composed of Collagen I, III, IV and VII, elastin, chondroitin sulphate, proteoglycans and fibroblast growth factor, and because the basement membrane and vascular channels remain intact, rapid revascularisation and graft incorporation are claimed (Derwin *et al.* 2006). This product is licensed for tendon repairs, ligament reconstructions, capsular reinforcement and periosteal covering (Coons and Alan 2006). A study using Graftjacket[®] to repair chronic tendo-achilles ruptures in nine patients confirmed no re-ruptures or chronic pain in any patient followed up beyond two years (Lee MS 2004).

1.8.1.3 Xenogeneic scaffolds

Xenogeneic scaffolds have found widespread orthopaedic acceptance in soft-tissue reconstructive strategies, but are rarely used for skeletal reconstruction *per se.* The most frequent sources are porcine (e.g. Cuffpatch® (Arthrotek, IN USA), Restore™ (DePuy, IN USA), bovine (e.g. Bio-Blanket® (Kensey Nash, PA, USA)) or equine (e.g. OrthADAPT® (Pegasus Biologic Inc, CA, USA)) (Longo *et al.* 2010). Tissue is harvested from sites such as small intestinal submucosa, pericardium, renal capsule or dermis. The ECM is processed, denuded and combined with chemically cross-linked collagen. Initially limited to rotator cuff repair, these products have now been shown to be effective for the reconstruction of many different tendons and ligaments, including tendo-achilles, biceps and triceps tendons and the posterior hip capsule. Retrieval analyses confirm well-integrated tissues with organised bundles of tissue and resolution of fibrous scar tissue; however the significant disadvantages of using xenogeneic tissues will still exist until a solution has been found for problems such as immunological reactions and disease transmission (Badylak 2004).

1.8.2 Synthetic scaffolds

As a consequence of the disadvantages of using autograft and allograft bone, there has been a significant drive for the development of bio-resorbable synthetic scaffold materials which aim to mimic the beneficial characteristics of biological material whilst avoiding their drawbacks. Hydrogels and collagen are particularly favoured as scaffold materials because they occur naturally, although other promising candidates include polylactic acid, a synthetic polymer, and the minerals hydroxyapatite (HA) and betatricalcium phosphate (TCP) (Hutmacher et al. 2007). These scaffolds can be fabricated to possess desirable osteoconductive properties and the constituent materials are readily available subject to manufacturing processes. Work is ongoing to improve their structural and osteoinductive properties and to ensure their degradation within the body is safe, predictable and complete. The distinction between biological and synthetic materials is rather arbitrary in this context as the majority of the following scaffolds are initially derived from natural biological sources, albeit with significant chemical manipulation during manufacture and processing. Materials that are natural in origin have the distinct advantage of reduced toxicity and inflammatory reactions and they are more rapidly degraded by enzymes, however they may suffer from natural structural variability (Hutmacher et al. 2007).

1.8.2.1 Hydrogels

Hydrogels, such as gelatin, agar, collagen, hyaluronan or fibrin, form 3D networks of hydrophilic polymers that absorb large quantities of water and biological fluids. Their high water-content, elasticity, biocompatibility and ability to permit diffusion of nutrients and bioactive molecules make them well-suited to cartilage tissue engineering strategies, but their strength and structural characteristics render them unsuitable for structural roles (Kessler and Grande 2008). Fibrin glue has been used to encapsulate chondrocytes in articular cartilage restoration techniques, but the resulting gel is weak with little spatial control over matrix formation (Elisseeff *et al.* 2005). *Alginate* and *agarose* gels have also been used in craniofacial cartilage regeneration applications, but the problems of cell encapsulation and regulation of final scaffold shape after polymerisation remain (Rowley *et al.* 1999, Elisseeff *et al.* 2005).

The properties of clay gels such as *laponite* have recently been harnessed for their ability to deliver cells, angiogenic and osteogenic factors for a regenerative medicine strategy (Dawson *et al.* 2011) (Fig. 1.10).

Collagen, the main component of the ECM functions poorly as a graft material by itself (Drury and Mooney 2003). However, it has shown efficacy as a delivery system for ceramic granules, BMPs and SSCs in animal models and a composite of collagen gel with granules of HA and TCP has been marketed for bone regeneration strategies (Collagraft®) (Fleming *et al.* 2000).

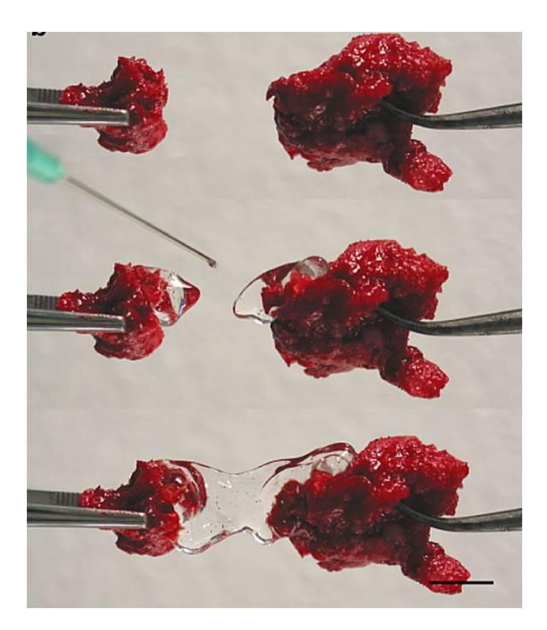


Fig. 1.10 Laponite forms a thixotropic hydrogel when added to water, allowing it to be dispensed onto allograft bone through a hypodermic needle before re-establishment of a gel network. Scale bar: 250 μm. *Image courtesy of Dr JI Dawson.*

The application of these hydrogels with autologous cells, growth factors and even prevascularised composite systems is likely to be a productive avenue for the treatment of certain musculoskeletal conditions (Rath *et al.* 2012); however the absence of structural integrity of hydrogels in themselves restricts them to limited load bearing applications.

1.8.2.2 Ceramics

Calcium phosphate ceramics, such as *hydroxyapatite* (HA) and *tricalcium phosphate* (TCP) have been used extensively in clinical orthopaedic practice. Several formulations with varying viscosities are available for different applications, allowing

either rapid or slow absorption, or use as an injectable cement (Fleming *et al.* 2000). In addition, HA can be used as a coating on metal implants to reduce the rate of aseptic loosening in applications such as hip arthroplasty and reconstructions following tumour resection (Trikha *et al.* 2005, Spiegelberg *et al.* 2009).

Porous TCP has been in clinical use for several years, however because the porosity of bulk TCP is only around 35% and pore interconnections are incomplete, only modest bone in-growth is permitted before re-absorption of the TCP matrix. Therefore TCP is normally supplied as granules to increase the bioavailable surface, but at the cost of short-term strength.

Natural coral (calcium carbonate (CaCO₃)) exists in a variety of porous conformations with highly reproducible pore sizes and interconnecting fenestrations depending upon the genus, with structures similar to human cortical or cancellous bone (Chiroff *et al.* 1975). Despite its favourable microstructural composition, which facilitates the ingrowth of host fibrovascular tissue and bone, its high dissolution rate, poor longevity and stability renders it unsuitable for weight-bearing implants (Hutmacher *et al.* 2007). However, a simple hydrothermal exchange process converts delicate coral into mechanically superior HA $[Ca_{10}(PO_4)_6(OH)_2]$ without altering its structure. These scaffolds are biocompatible and readily invaded by fibrovascular tissue, which is later converted to mature lamellar bone nearly identical to autogenous bone, which undergoes active remodelling and resorption (Chapman *et al.* 1997). However, host bone in-growth relies on rigid stability and rapid opposition, which is inhibited by the lack of completely interconnected pores and slow resorption. Furthermore, its inherent brittleness and susceptibility to fracture in compressive loading prevent the use of scaffolds with more open porosity, and limit its translation to clinical application.

Despite these drawbacks, the application of tissue engineering strategies to ceramic scaffolds has been successful. Following ovine trials, (Kon *et al.* 2000) autologous SSCs from three patients were culture-expanded *ex vivo* and seeded onto HA scaffolds to treat extensive segmental long bone defects (between 4 and 7 cm). Radiological osseointegration and surrounding callus was observed after just two months, with subsequent functional recovery (Quarto *et al.* 2001) and ongoing clinical success at 6-7 year follow-up (Marcacci *et al.* 2007). The radiographic signs of bone healing presented in this study should be interpreted with caution however: the layer of new bone surrounding each of the scaffolds remains limited, even at several years' follow-up and additional evidence of bone formation and integration within the pores of the scaffold

would be required for clinical confidence. The presence of such ossification within the implant is difficult to assess, even from the Computed Tomography (CT) sections presented, not least because the implanted porous HA scaffold is radio-opaque and non-absorbable, and no immediate post-operative comparative CT scans are presented. Nevertheless, despite these limitations, these were clearly challenging cases, and it is important to note the patients reached good clinical outcomes with no subsequent fractures reported to date.

A porous HA scaffold, inoculated with autologous culture-expanded cells derived from periosteum, has also been used to re-create a human distal phalanx following traumatic amputation (Vacanti *et al.* 2001). Although the resultant construct was limited in function with significant dorsal subluxation and no active range of movement at the interphalangeal joint, the resultant thumb was sufficiently functional for the patient to return to work within three months and the case may be regarded as 'proof of concept' to create new bone using in essence, tissue engineering principles.

Ceramics have also been used as part of a tissue engineering strategy in the treatment of benign bone tumours: an aneurysmal bone cyst of the proximal tibia, a giant cell tumour of the proximal tibia and fibrous dysplasia of the proximal femur were treated by implanting autologous culture-expanded SSCs seeded onto a HA scaffolds (Morishita et al. 2006). Early mechanical strength was achieved and all three patients were able to bear weight within 3 weeks with no adverse clinical or radiological sequelae. The same group successfully applied a tissue engineering approach to prevent aseptic loosening following ankle arthroplasty in three patients with osteoarthritis (Ohgushi et al. 2005). The authors culture-expanded autologous SSCs, then applied these to the bone-ceramic interfaces of the prostheses, culturing ex vivo for a further two weeks before implanting the constructs. The authors emphasise several drawbacks of the study, including lack of a control group, a small cohort with short patient follow-up and the need for an additional procedure to harvest the bone marrow. Nevertheless, this highlights an exciting new technique to enhance the integration at the prosthesis-bone interface.

In a recent preliminary study, 22 patients were treated for femoral head AVN with porous calcium-HA implants seeded with autologous concentrated bone marrow SSCs. Radiological and clinical improvements were apparent in the majority of patients in the treatment group, with only three patients showing disease progression at two years follow up, compared to severe femoral head collapse in six of the eight control patients

(calcium-HA implant alone) (Yamasaki *et al.* 2010). The authors point out several weaknesses of their study, including the lack of a true negative control group, however this pilot study provides encouraging results for future trials.

1.8.2.3 Bioactive glasses

Commercial bioactive glasses (e.g. Bioglass®) with selected compositions of silicate and phosphate have been in clinical use for over 20 years (Yang *et al.* 2006). These glasses react with physiological fluids and form strong bonds with tissues through cellular activity, and biodegrade safely within a physiological environment. Most recent research activity surrounding bioactive glasses has been in combining them with other synthetic scaffold types to enhance their mechanical competence, impart bioactivity and modulate degradation (Hutmacher *et al.* 2007).

1.8.2.4 Osteoconductive metals

Metal implants have long been used in orthopaedic surgery for the reconstruction of bone defects or as a supportive mesh for reconstructive strategies, although the structural modification of the bulk material itself to enhance osseointegration and stimulate bone regeneration in its own right has only relatively recently been realised (Navarro *et al.* 2008). The main advantage of metal implants is their excellent mechanical properties, although the low rate of degradation results in the need for either permanent implantation with the associated risks of metal toxicity, or a further surgical procedure for implant removal (Karageorgiou and Kaplan 2005).

The osteoconductive properties of *Tantalum Trabecular Metal (TTM)* are already exploited in several orthopaedic applications, such as hip and knee arthroplasty, spinal fusion, for the treatment of AVN and for reconstruction following skeletal tumour excision (Findlay *et al.* 2004). In a recent series to evaluate trabecular tantalum for the management of severe acetabular bone defects in revision hip arthroplasty, mechanical integrity was maintained in all 23 patients at 35 months follow-up (Flecher *et al.* 2008). The treatment of femoral head AVN using TTM rods represents a pragmatic alternative to vascularised fibular grafting, and has potential advantages of immediate construct stability, expediting safe weight-bearing and return to function. The procedure can be performed using a minimally-invasive technique and without the

disadvantage of donor site morbidity, however in cases where subchondral bone collapse does occur, the implant can become prominent, causing pain and acetabular degeneration. In addition, on eventual removal of the metal implant to allow joint reconstruction, the result is a sizeable defect that ultimately requires further grafting.

The combination of TTM with human SSCs has also previously been reported *in vitro* (Findlay *et al.* 2004, Matsuno *et al.* 2001, Sagomonyants *et al.* 2011, Stiehler *et al.* 2007, Welldon *et al.* 2008, Smith *et al.* 2012). These studies show excellent osteoconductive properties of TTM and pave the way for new clinical approaches that extend its current applications.

Titanium has also been recognised as a bioactive metal, with bone induction first reported in 2004 after manufacture of macroporous titanium using a plasma spraying technique (Fujibayashi *et al.* 2004). More recently, an open-porous titanium foam has been fabricated that supports and encourages the growth of SSCs throughout the scaffold *in vitro* (Muller *et al.* 2006). Electron Beam Melting technology has also been applied to titanium to create a trabecular conformation with various different pore sizes to enhance cellular infiltration (Marin *et al.* 2010). In comparative studies, adiposetissue derived stem cells grown on trabecular titanium in osteogenic conditions produced significantly more calcified ECM than comparable polymer scaffolds (Asti *et al.* 2010, Gastaldi *et al.* 2010).

Osteoconductive metals possess some important disadvantages that limit their use in skeletal tissue engineering: metals in isolation lack osteoinductive capacity and as such may not be appropriate for use in large unsupported defects. In a goat femoral diaphyseal defect model for example, the use of trabecular tantalum cylinders required the preservation of native periosteum in order to achieve bony union (Bullens *et al.* 2009). This indicates potential limitations in the application of tantalum to reconstruction following trauma, infection or tumour excision, because periosteum is often deficient in such scenarios. Furthermore, metals are not biodegradable and removal can cause considerable collateral damage to surrounding bone should subsequent revision be required.

1.8.2.5 Synthetic polymers

Chemically synthesised polymers are versatile and enable the fabrication of scaffolds with appropriate characteristics to suit a variety of different applications (Table 1.7).

Table 1.7 Synthetic polymers investigated for use in tissue engineering scaffolds for orthopaedic applications

Polymer	Abbreviation	Examples			
Poly(lactide) or Poly(lactic acid) or Poly(L)lactic acid	PLA or PLLA	Freed et al. 1993, Kanczler et al. 2010			
Poly(DL-lactide)	PDLLA	Wildemann et al. 2005			
Poly(glycolic) acid	PGA	Freed et al. 1993			
Poly (L) lactic acid poly(glycolide)	PLA/PLGA	Bostman et al. 1989			
Poly(L-lactide-co-D,L-lactide)	PLDLLA	Coe et al. 2004			
Poly(lactide-co-glycolide)	PLGA	Goldstein et al. 1999, Borden et al. 2003			
Poly(lactide-co-glycolide)/poly(ethylene glycol)	PLGA/PEG	King <i>et al.</i> 2000, Schaefer <i>et al.</i> 2000			
Poly(lactide-co-glycolide)/ polyvinyl alcohol	PLGA/PVA	Oh <i>et al.</i> 2003			
Polyethylene terephthalate	PET	Takahashi et al. 2004			
Poly(propylene glycol-co-fumaric acid)	PPF	Hile et al. 2003			
Poly(desaminotyrosyl-tyrosine ethyl ester carbonate)	PDTE carbonate	Simon et al. 2003			
Polyethylene glycol	PEG	Terella et al. 2010			
Polycaprolactone	PCL	Yoshimoto et al. 2003, Schantz et al. 2006			
Polymethyl methacrylate	PMMA	Shimko and Nauman 2007			
Polyhydroxyalkanoates	PHAs	Chen and Wu 2005			
Poly(poly(ethylene oxide) terephthalate- co-(butylene) terephthalate	P(P)EO/PBT	Bulstra et al. 1996			
Poly (L) lactic acid/ Poly (ethylene oxide)	PLLA/PEO	Coraca et al. 2008			
Poly (L) lactic acid/ Polycaprolactone	PLLA/PCL	Khan et al. 2010			

Adapted from Zippel et al. 2010, Karageorgiou and Kaplan 2005

Well-defined changes in variables such as solvent type, precipitation temperature, chemical formulation and pressure allow the precise manipulation of the scaffold, thus tailoring its overall shape, pore interconnectivity and size, degradation rate, molecular weight, mechanical properties and handling properties (Karageorgiou and Kaplan 2005).

However, synthetic materials are more likely than natural scaffolds to have undesirable effects within the body, so care is needed to ensure the scaffold is fabricated from a highly biocompatible material that has no potential to elicit an immunological or foreign body reaction (Muschler et al. 2004). Furthermore, suitable polymers should be chosen for the intended application not only to support sufficient load, but also to degrade and resorb at an appropriate rate, and release non-toxic degradation products (Hutmacher 2001). Most synthetic polymers in trials and in clinical use undergo bulk degradation to lactic and/or glycolic acid (Hutmacher 2000). Substantial local concentrations of degradation products produced either by a large quickly resorbing scaffold, or through poor elimination capacity of local tissues, can lead to a reduced local pH and increased osmotic pressure (Bostman et al. 1989, Bostman et al. 1990). This hostile environment can damage the local cells, potentially negating the regenerative effects of the strategy and further, the local acidification can increase the rate of polymer breakdown, exacerbating the problem and leading to further inflammation, giant cell activation and cytotoxicity (Hutmacher 2000).

The design of synthetic polymers for orthopaedic regenerative applications requires a trade-off between desirable properties that contribute to the strength of the construct and properties that allow consistent degradation (Fig. 1.11). A cardinal requirement for successful synthetic polymer scaffolds is an open, interconnecting porous architecture (Karageorgiou and Kaplan 2005). Porosity is defined as the percentage of void space within a solid, and is necessary for migration and proliferation of progenitor and vascular cells and also for diffusion of nutrients into and waste products away from the construct. Surface porosity also increases the stability of the scaffold by providing mechanical interlocking at the interface with surrounding tissue. Optimal pore size has not been fully established, but for bone formation, most strategies aim for pores of 100-500 µm diameter to allow adequate blood vessel ingress (Zippel *et al.* 2010, Hutmacher 2000).

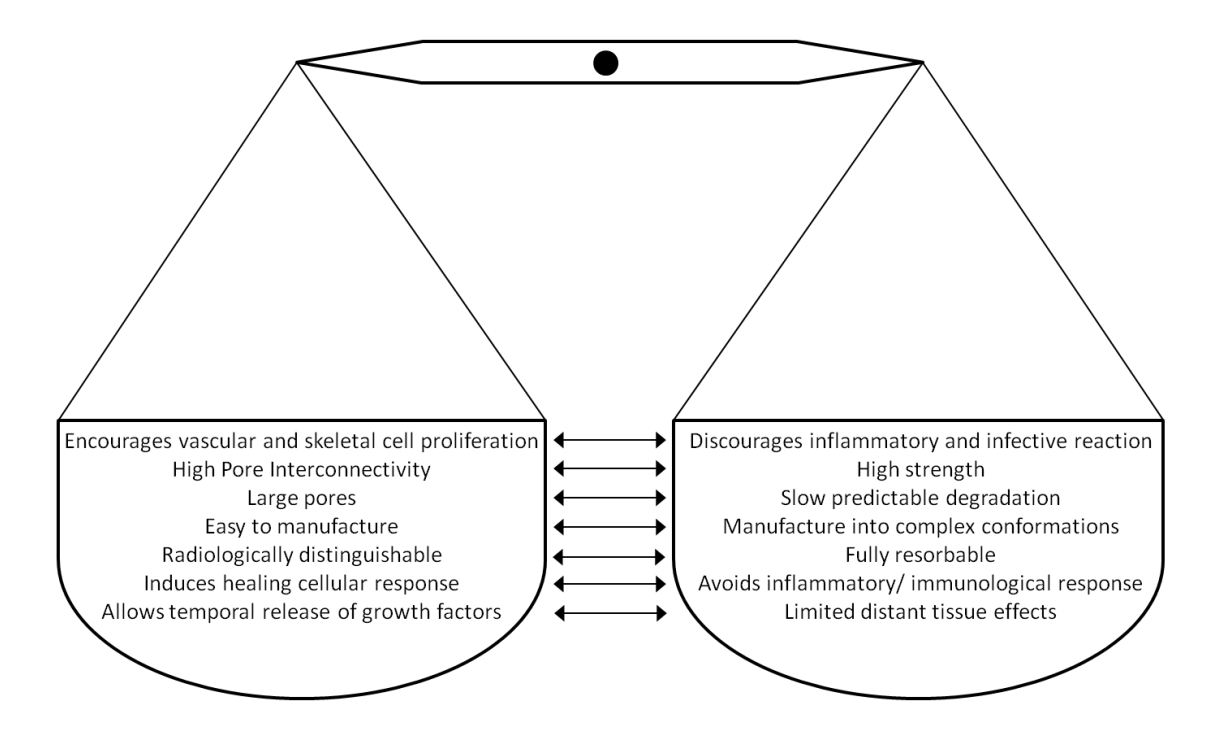


Fig. 1.11 'Balancing act' demonstrating the trade-off between contradictory desirable attributes of a polymer scaffold

1.8.2.5.1 Polymer scaffold fabrication techniques

Techniques to fabricate porous 3D scaffolds have evolved over the last two decades (Table 1.8). Modern strategies tend to be automated and are capable of producing larger quantities of scaffold with more complex designs over a shorter timeframe, with high fidelity to the intended architecture. Newer methods are also capable of incorporating more materials in spatially defined configurations to encourage robust regeneration throughout the entire volume. However, not all fabrication techniques work for every polymer, so the choice of scaffold for an intended application and the properties that are induced by its various fabrication options must be identified at an early stage.

Initial techniques for scaffold fabrication involved dissolving the polymer in organic solvents such as chloroform, before casting the polymer into the desired shape. Porosity was induced by including salt microspheres or gelatin in the solution which were then leached out following evaporation of the solvent (Mikos *et al.* 1993a, Thomson *et al.* 1995). These constructs only produce thin sheets or membranes with reliable porosity and attempts to create thicker 3D scaffolds result in residual solvent encapsulation, which is cytotoxic and reduces porosity. Furthermore, the product is brittle and therefore unsuitable for soft tissue applications. A modification of this

technique, which included lamination of multiple layers of this construct with a solvent binder, was demonstrated to produce 3D scaffolds, but the problem of residual chloroform remained and pore interconnectivity was not consistent (Mikos *et al.* 1993b). Alternatively, the solvent-casting and particulate-leaching approach can be followed by an extrusion step where the composite is heated and extruded as a tube through a nozzle at high pressure. After cooling, the scaffold is leached as before, prior to vacuum drying. This allows good control over pore size and number, although thermal degradation of the polymer is a risk (Widmer *et al.* 1998).

Another early technique to produce 3D scaffolds made use of technology from the textile industry. Fleeces or meshes can be manufactured by laying fibres side by side with the next layer laid in a perpendicular conformation. Bonding at the cross-links can be achieved through heating or local application of solvent (Hutmacher 2001). Despite having a large surface area to volume ratio necessary for successful cell infiltration, these scaffolds lack structural stability for use in weight-bearing orthopaedic applications and are prone to contractile deformation (Hutmacher *et al.* 2007).

Phase separation allows the incorporation of biologically active molecules into the biodegradable polymer. The polymer is dissolved with a solvent such as phenol or naphthalene before addition of the bioactive molecules. However, subsequent removal of the solvent during sublimation is often incomplete, with potentially harmful consequences when incorporated into the body. Furthermore, the technique gives a scaffold with low porosity, and incorporation of larger proteins and drugs reduces their activity (Sachlos and Czernuszka 2003).

Table 1.8 Porous 3D polymer scaffolds – evolution of scaffold fabrication techniques

	.6 F0	lous 3D	polyllic	er scarr							res
References	Mikos 1993a	Mikos 1993a	Mikos 1993b	Sachlos 2003	Thomson 1995	Widmer 1998	Whang 1995	Mooney 1996, Harris 1998	Mathieu 2006	Hutmacher 2001	Hutmacher 2001, Sachlos 2003
Properties	Scarty spherical pores with large insoluble salt particles remain. High porosity only maintained for thin membranes. Time-consuming manufacture. Remaining chloroform is cytotoxic. Brittle scaffolds are inappropriate for soft tissue applications.	Used with solvent-casting to increase 3D capability. Irregular pores, variable mechanical properties, residual chloroform is cytotoxic.	Large surface area: volume ratio. Poor mechanical properties, lack of stability, contractile deformation, poor control of porosity and size.	Allows incorporation of small biologically active molecules (e.g. ALP). Incorporation of large proteins and drugs without loss of activity remains a challenge. Low porosity and small pore size.	Any shape can be fabricated depending on mould. Porosity and pore size can be controlled independently by varying quantity and size of gelatin microspheres. Requires high temperature, which excludes addition of drugs or growth factors.	Pore size and porosity can be tailored by varying salt weight and crystal size and temperature of extrusion.	High volume of interconnected micropores. Can make thick scaffolds (>1 cm thick) Limited ability to customise pores. Low mechanical strength. Operator sensitive.	Avoids use of organic solvents. Closed pore morphology, although can be combined with particulate-leaching to create open, interconnected morphology.	Combined with particulate-leaching to improve pore- interconnectivity. Good control of pore size by varying particle: polymer ratio and particle size.	Allows varying multiple-layer design. Fabrication at room temperature avoids damage to incorporated biological agents. Tightly controlled pore size and porosity, very accurate. Timeconsuming manufacture and design. Requires organic solvents. Unbound powder must be removed following fabrication.	Allows varying multiple-layer design. Tightly controlled pore size and porosity, very accurate. Time-consuming manufacture and design, requires heating of polymer.
Poros ity (%)	20-90	<85	<95	23-56	<80	<85	<97	<97	<97	09>	89
Pore size (µm)	30-300	30-300	20-100	2-100	50-500	<100	15-200	100-500	Micro <50 Macro >400	45-150	>150
Reproducibility	Operator, technique and material dependent	Operator, technique and material dependent	Mechanised	Operator, technique and material dependent	Mechanised	Mechanised	Operator, technique and material dependent	Operator, technique and material dependent	Operator, technique and material dependent	Computerised and mechanised	Computerised and mechanised
Material properties during processing	Soluble	Soluble	Fibres	Soluble	Thermoplastic	Thermoplastic	Soluble	Soluble	Amorphous	Soluble	Thermoplastic
Processing techniques	Casting with salt particles in solvent. Salt particles are leached in water following solvent evaporation	Solvent bonding following solvent-casting and particulate-leaching	Carding, needling, plate pressing and heating to bond cross-links	Solvent dissolution and sublimation	Polymer molten above glass-transition temperature within Teflon mould. Gelatin microspheres introduced, then dissolved to leave pores.	Following casting, polymer is extruded through a custom-made die at high temperature. Salt is then leached-out before vacuum-drying	Water added to polymer in solvent. Immiscible layers are homogenised to form an emulsion. Freeze-dried in liquid nitrogen and casted into a mould	Polymer pellets compressed into moulds then saturated with high pressure CO_2 , then pressure reduced.	High pressure gas (CO ₂ or N ₂) plasticises the polymer granules and diffuse into matrix to create low viscosity, porous construct.	A 3D printer follows a Computer Aided Design (CAD) model by printing a solvent binder onto layers of polymer powder. Sequential layers are built-up as required.	CAD and imaging data allow design of a conceptual model. Semi-liquid polymer is extruded in ultra-thin layers. Each layer laminates to the previous layer as it sets.
Fabrication technique	Solvent-casting and particulate-leaching	Membrane lamination	Fibre meshes/fibre bonding	Phase separation	Melt moulding and gelatin leaching	Extrusion plus particulate leaching	Emulsion plus freeze drying	Gas foaming +/- particulate-leaching	Supercritical fluid processing +/- particulate-leaching	3-D printing (rapid prototyping/ Solid free- form fabrication)	Fused deposition modelling (Solid free- form fabrication)

Porosity can also be induced in a solid block of polymer by emulsion freeze-drying. The polymer is dissolved in a solvent before adding to water. The two immiscible layers are then homogenised to form an emulsion, which is subsequently quenched in liquid nitrogen and freeze-dried to produce a porous structure. This has the advantage of producing large 3D scaffolds with multiple interconnected pores. However, mechanical strength is low and exact conformation is operator-dependent (Whang *et al.* 1995).

All the above techniques make use of solvents (chloroform, methylene chloride, phenol or naphthalene) in order to solubilise the polymer and allow its manipulation. The exact solvent depends on the technique and polymer involved, but residual solvent has been identified in these methods despite attempts to remove them through thorough washing and evaporation techniques. The risks of toxicity, inflammation and potential carcinogenicity must therefore be taken into consideration (Sachlos and Czernuszka 2003).

Techniques to produce a 3D polymer without using solvent include melt-moulding and gelatin-leaching. Here, the polymer is melted rather than solubilised by heating above its glass-transition temperature, and the addition of gelatin microspheres induces porosity on their subsequent dissolution (Thomson et al. 1995). This process allows tight control of porosity by varying the size and number of gelatin microspheres, but the high temperatures can alter the mechanical properties of the polymer and denature or inactivate any added drugs or growth factors. Alternatives to thermal or solvent techniques include the use of high pressure gasses: In gas foaming, polymer pellets are compressed into custom made moulds, then saturated with high pressure carbon dioxide (CO₂) gas. As the pressure is reduced, the solubility of gas in the polymer is decreased, leaving nucleation and growth of gas cells of 100-500 µm diameter (Mooney et al. 1996). In order to produce an interconnected open pore morphology, this method has been combined with particulate-leaching (Harris et al. 1998). Supercritical fluid processing also makes use of high pressure gas (either CO₂ or N₂), which plasticises polymer granules and creates air cells, which reduces the viscosity and allows the incorporation of heat sensitive pharmaceuticals or biological agents. The resultant pores are only on average 10-30% interconnected, although the combination of this technique with particulate-leaching produces a controllable highlyinterconnected porosity. The resultant scaffolds have been used with incorporation of growth factors with success in vivo (Mathieu et al. 2006, Harris et al. 1998).

Although the latter techniques dispense with the requirement for solvents in their fabrication, several limitations still exist. These techniques are not capable of precisely controlling pore size, their geometry, spatial distribution and interconnectivity. This has a negative impact on cellular migration and infiltration into the scaffold and restricts diffusion of nutrients and oxygen and removal of waste products. Furthermore, scaffolds produced by casting tend to form a thin external coating or 'skin' which requires removal before use (Sachlos and Czernuszka 2003).

As a result of the disadvantages of scaffolds produced by these techniques, the technology transfer of *Solid Freeform Fabrication* (SFF, also known as rapid prototyping or advanced manufacturing technologies) to tissue engineering has led to great advances. This involves building 3D objects using layered manufacturing strategies and allows scaffolds to be designed and manufactured with customised external shapes and pre-defined, reproducible internal morphology. The process makes use of Computer-Aided Design and Manufacture (CAD-CAM), whereby a conceptual 3D model (which could be derived clinically from CT or Magnetic Resonance Imaging (MRI) images of the defect region) is expressed as a series of cross-sectional layers. Repetitive deposition and processing of these physical layers is then accurately controlled through an entirely computerised and mechanised process to produce an accurate and reproducible 3D construct. This has the potential advantage of providing a custom-built implant for any specific clinical scenario, although all techniques currently in use involve considerable time-consumption in manufacture (Hutmacher 2001, Sachlos and Czernuszka 2003).

Several techniques have been developed for final deposition of the layered construct: in Three-Dimensional Printing (3DP) the powdered polymer is first spread in a thin layer over the surface of the powder bed. A jet head with x- and y-axis control moves over the powder and ejects a binder material in accordance with Computer-Aided Design (CAD) cross-sectional data onto the polymer surface, which locally dissolves the polymer, allowing adherence to subsequent layers. The chamber is lowered following each pass of the jet head to allow incremental build-up of bound layers. The whole process can be achieved at room temperature, and water-based binders can be used; however the unbound powder must be completely removed following component completion (Hutmacher 2000). Stereolithography uses similar co-ordinated control systems, but makes use of an ultraviolet laser beam to selectively polymerise a liquid photocurable monomer as it is lowered into the monomer liquid-filled vat. In Fused Deposition Modelling (FDM), a fibre of thermoplastic polymer is extruded from a

moving nozzle in semi-liquid state, and deposited layer-by-layer. As the material solidifies, it laminates to the preceding layer. This process requires heating of the polymer (up to 120°C), which eliminates the possibility of incorporating biological molecules. However it, results in a highly accurate, reproducible product with high porosity and strength (Hutmacher 2001).

Polymers have also been fabricated for tendon and ligament reconstruction. Synthetic scaffolds manufactured for clinical use are made of polyester, polypropylene, polyarylamide, polyethylene terephthalate, carbon and nylon (Chen et al. 2009). Despite having superior mechanical properties as compared to biological scaffolds for tendon/ligament reconstruction, they are designed as permanent replacements for the native tissue, rather than as true tissue engineering constructs. Consequently, these materials often have poor biological compatibility and major longer-term complications have been reported for some scaffolds (e.g. polytetrafluoroethylene (PTFE)). Inflammatory reactions are common and may extend to synovitis, osteolysis and foreign body rejection, resulting in failure of the construct and further collateral damage. Given these concerns, current developments are focusing on improving the biological compatibility of future scaffolds and applying tissue engineering principles to their design to improve the healing process at the enthesis (Longo et al. 2010). Fibroblasts cultured on cross-linked collagen, silk and PLGA scaffolds have shown encouraging results in vitro and in small animal studies, particularly with the addition of exogenous growth factors, such as TGF, EGF, IGF and PDGF (Rahaman and Mao 2005). However, challenges in culturing fibroblasts and limitations of the properties of bioresorbable scaffolds mean that no tissue engineering strategy to date has shown resilient neo-tendon formation with sufficient tensile strength for potential clinical application.

1.8.2.6 Composite scaffolds

The use of single scaffolds to replace skeletal tissues in tissue engineering strategies is unlikely to achieve adequate functional results in the clinical scenario because each skeletal tissue is in itself a composite material in many senses. The mechanical properties of bone, for example depend on its local structure with respect to porosity and lamellar architecture and also its composition of collagen-rich organic matrix and mineral hydroxyapatite (Hutmacher *et al.* 2007). In addition, the composition and mechanical characteristics of bone change with age, activity, nutritional state and

disease status, adding to the challenge of fabricating an appropriate scaffold for individual requirements (Karageorgiou and Kaplan 2005). Clearly then, a successful tissue engineering scaffold will have to take account of this complex of properties to act as a functional surrogate for native tissue until regeneration is complete.

Collagen has been demonstrated to encourage osteogenesis, but provides minimal structural support, so in isolation it functions poorly as a graft material (Mizuno and Kuboki 2001). Once coupled with SSCs, growth factors, or scaffold materials, its properties can be enhanced considerably (Giannoudis *et al.* 2005). A composite strategy, using collagen type I pre-coated onto allograft, has been shown to enhance osteogenic differentiation of SSCs in basal culture, augmenting the mechanical properties of the allograft (Jones *et al.* 2009).

HA has been combined with chitosan to form a bioactive scaffold for bone tissue engineering (Venkatesan and Kim 2010). Chitosan is produced from chitin, an abundant natural polysaccharide found in marine crustacean shells. Alone, it is highly biocompatible, biodegradable, antibacterial, and can be moulded into various forms with a porous structure (Di Martino et al. 2005). However, it is flexible, with poor loading characteristics and is not, in itself, osteoconductive. The combination of chitosan with HA vastly improves osteoconductivity and to some extent also its mechanical strength, so that the composite closely mimics both the organic and inorganic portions of natural bone. Several in vitro studies have been performed that confirm its osteogenic utility; however translation has been prevented because its compressive strength is still inadequate (Hu et al. 2004, Thein-Han and Misra 2009). The combination of chitosan-HA composite with carbon nanotubes have been produced, and they possess superior mechanical properties, although these scaffolds come at a potential risk of cytotoxicity, display poor bioresorption profiles and there have been difficulties ensuring uniform dispersion of the carbon skeleton within the scaffold (Venkatesan and Kim 2010). The most promising strategy for skeletal tissue regeneration is therefore likely to lie in the combination of growth factors with enriched autologous SSCs added to a suitable composite scaffold.

The fabrication of synthetic composite scaffolds initially centred on achieving the appropriate scaffold properties to replicate the overall 'bulk' properties of the host tissue. In addition to the composite of two or more polymers, composites of polymers with ceramics or other materials have been trialled with beneficial effects. Not only do these materials have the potential to complement and enhance the structural and

osteoconductive performance of the composite, but biochemical advantages also exist. For example, when HA or TCP is used in combination with polymers, the basic resorption products of the ceramic buffer the acidic resorption by-products of polymer breakdown and help to avoid the formation of an unfavourable acidic environment. (Agrawal and Athanasiou 1997) Consequently a wide variety of such composites, some containing additional biological materials such as collagen, have been investigated for use as orthopaedic scaffolds (Zippel *et al.* 2010).

A further challenge is in the synthesis of tissue-engineered constructs containing a single tissue-type, but with a heterogeneous biochemical composition and mechanical properties. Replication of the four distinct anatomical and functional regions in native human articular cartilage has recently been achieved *in vitro* (Nguyen *et al.* 2011). A spatially organised scaffold was formulated using distinct hydrogel layers, each containing a specific combination of synthetic and natural biomaterials, which was able to direct appropriate zone-specific chondrogenesis with corresponding mechanical properties.

An additional requirement for composite scaffolds is in the regeneration of structures at the interface of two tissue types. Previous attempts encountered difficulty securing the regenerative scaffold to underlying tissues, such as in osteochondral defects of articular cartilage or meniscus (Elisseeff et al. 2005). Success has been achieved by the development of a multilayered hydrogel scaffold with different cell types in each layer, which were then co-cultured in tandem to produce the appropriate matrix for the tissue being engineered, in this case articular cartilage and subchondral bone (Kim et al. 2003). The production of a bilayered scaffold to re-create the tissues within a temporomandibular joint has also been implemented in a rat model (Alhadlaq et al. 2004), providing just one example of many where maxillofacial surgery has been at the forefront of skeletal tissue engineering research.

1.8.2.7 Tissue engineered constructs in maxillofacial surgery

Tissue engineering principles are particularly suited to the field of maxillofacial surgery given the region's high vascularity and because there is limited intra-oral bone suitable for grafting as an alternative (Schmelzeisen *et al.* 2003). Knowledge of the maxillofacial progress is essential for researchers in the field of orthopaedics as pioneering techniques are often first instigated in this arena, and many lessons can be learnt from their results before application of the techniques in the orthopaedic field, whilst avoiding repetition of work.

In cases of deficient maxillary alveolus bone, maxillary sinus floor augmentation is required to ensure stability before dental implant insertion. This clinical necessity has provided further novel strategies for skeletal regeneration with some larger-scale studies. Schimming et al. demonstrated successful maxillary sinus floor augmentation at three months in 18 of 27 patients using a polymer fleece with impregnated cultureexpanded mandibular periosteal cells (Schimming et al. 2004). 12 of these patients underwent a one-stage procedure, and although one patient from this group sustained an early post-operative infection, and the graft was removed, good bone formation was demonstrated in all the other patients from this group. 15 patients underwent a twostage procedure, where the dental prosthesis was implanted three months following augmentation. In eight of these patients the engineered matrix underwent resorption and replacement with connective tissue, and they required supplementary augmentation with autologous bone. One reason cited by the authors for the poorer results in the two-stage procedures is the lack of adequate oxygen and nutrient supply to cells deep within these larger constructs. Current work to improve the induction of vascularisation in such constructs will enhance their application to long bone defects, where the extra-osseous blood supply is often significantly impaired (Johnson et al. 2011).

Tissue engineering principles have also been applied to fabricate an entire mandible *de novo* using autologous bone marrow cells seeded onto BMP-7-coated HA blocks, supported within a titanium mesh scaffold (Warnke *et al.* 2004). The construct was grown in the patient's latissimus dorsi muscle before final implantation. Despite complications including infection, heterotopic ossification and mesh fracture, a second patient has subsequently undergone the procedure (Warnke *et al.* 2006). Although the resulting mandible provides a good cosmetic result, the report detailed limited evidence

of normal function or structural integration with the surrounding native tissues. The application of these techniques to weight-bearing bones in an orthopaedic context may therefore require significant refinement (Gronthos 2004).

Maxillofacial applications have also been described for the induction of bone formation in extra-skeletal sites using growth factors and scaffolds without the requirement for exogenous SSCs. In one report, a mandibular defect following surgical tumour resection was reconstructed using an HA implant impregnated with BMP-7 (Heliotis *et al.* 2006). The construct was implanted into a patient's pectoralis major muscle for three months before being harvested and transplanted to the mandibular defect as a pedicled 'myo-osseo-HA' flap. Unfortunately, despite promising initial integration, the graft soon became infected and required excision after five months.

1.9 Future directions – scaffolds

The inherent disadvantages of currently utilised reconstructive strategies (metal implants, cement, autograft and allograft) combined with the ageing population and a continuing increase in musculoskeletal pathology and patient expectations, highlight a pressing need to augment or replace current practice with osteoregenerative techniques. However, these strategies will need to act as a functionally and physiologically appropriate surrogate for a patient's lost or damaged skeleton. In addition to the need to reconstruct bone defects, much orthopaedic morbidity is derived from cartilage disease and tendon pathology (Khan *et al.* 2010, Getgood *et al.* 2009). It is envisaged that novel technologies to address bone defects will also be readily transferrable to these applications.

The design of biomaterial scaffolds is now focussed on biological stimulation to ensure infiltration and regeneration of the appropriate tissue type with coincident promotion of angiogenesis (Bouhadir and Mooney 2001). The scaffold can either be functionalised on the surface by peptides or growth factors that mimic ECM chemistry, or they can be included in the scaffold composition, to allow physical and temporal control of their delivery during degradation (Navarro *et al.* 2008). Due to the high number of combinations and permutations possible, many studies examining various composites of scaffold, cell, and growth factor interaction on skeletal tissue regeneration have been published (Yang *et al.* 2003, Kanczler *et al.* 2010, Zippel *et al.* 2010).

Although there is intense interest in augmenting the potential of SSCs by combining them with growth factors and biomimetic scaffolds as a self-contained implantable unit, some commentators believe the addition of exogenous SSCs is not necessary for appropriate regeneration (Watt and Driskell 2010). A recent rabbit study has exploited the potential for the contents and structure of the scaffold itself to manipulate the surrounding environment, hence stimulating and incorporating the host's own local SSCs and removing the need for *ex vivo* cell culture and scaffold seeding (Lee CH *et al.* 2010). In the study, the articular surface of the proximal humerus of a group of rabbits was completely excised and replaced with an anatomically correct bioscaffold spatially infused with TGF-β3-adsorbed or TGF-β3-free collagen hydrogel. Four months following surgery, the articular surfaces of TGF-β3-adsorbed bioscaffolds were entirely covered with hyaline cartilage, whilst TGF-β3-free bioscaffolds supported only isolated cartilage growth. Furthermore, there was no difference in shear and compressive characteristics of TGF-β3-mediated articular cartilage, compared to those

of native articular cartilage, although these properties were significantly reduced in the group without TGF- β 3. In addition, TGF- β 3 delivery recruited approximately 130% more cells in the regenerated articular cartilage than in the group without TGF- β 3. Clearly the reconstruction of a complex human joint is still some way off, but this study demonstrated proof of concept for development of novel scaffolds and carrier materials as potential treatments for advanced arthritis.

1.10 Considerations for the development of a tissue engineering strategy

The successful development of an emergent tissue engineering approach requires a series of tightly coordinated processes to take place within a limited timeframe and budget (Smith *et al.* 2011) (Fig. 1.12). The initial concept must be based upon an accurate insight into the current clinical needs and a realistic vision of future potential. Progression to each subsequent stage in the development process requires close collaboration between multiple agencies with wide-ranging expertise and a high degree of discrimination to select the most promising cell, candidate material and protocol. Several factors have particular relevance to the development of an effective emergent tissue engineering strategy, and without which the process inevitably fails.

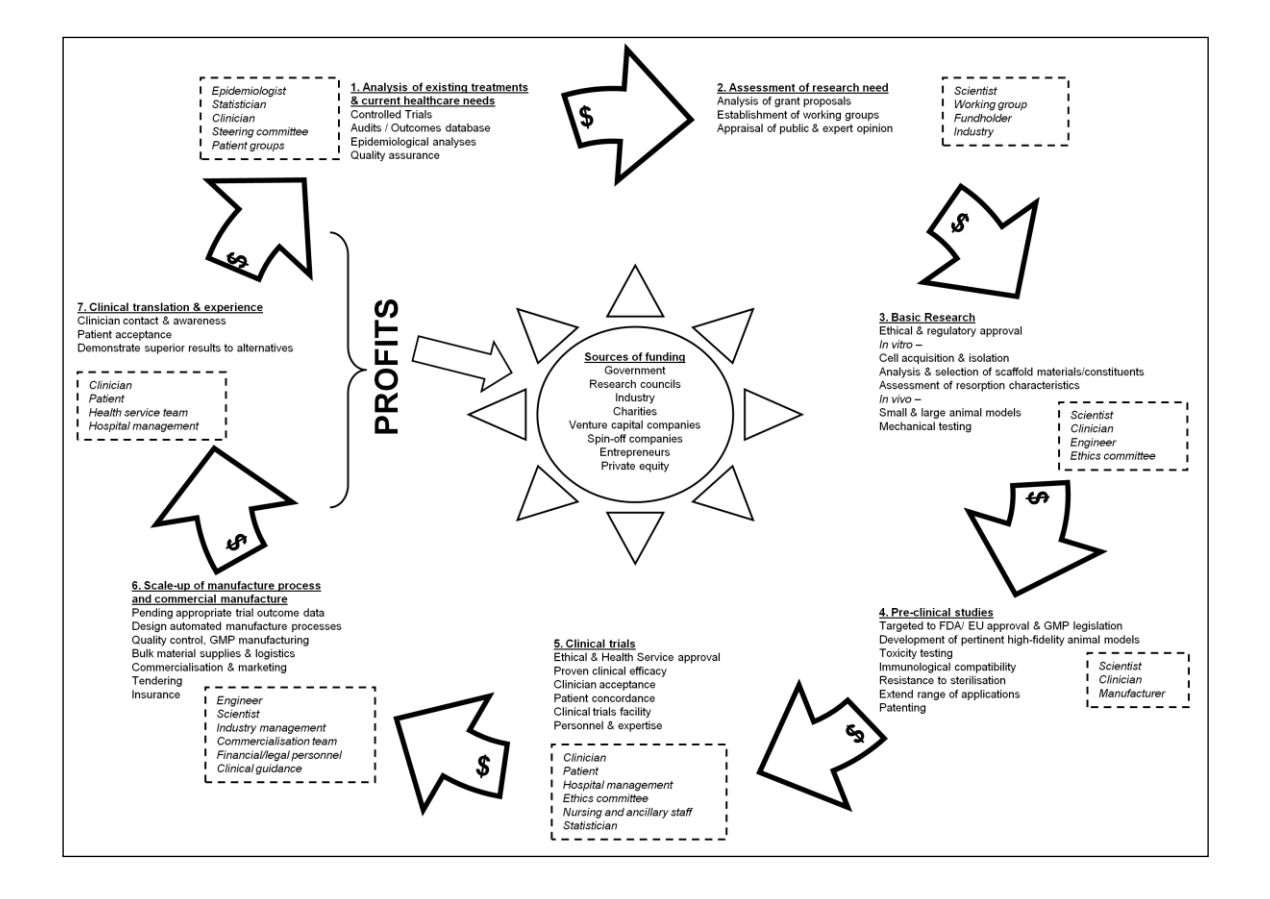


Fig. 1.12 The collaborative tissue engineering "life cycle". The process is driven at all stages by informed allocation of funding (denoted by \$). The speed of the cycle is not only dependent upon the success of scientific research and testing, but also heavily relies on the collaboration of multiple agencies (dashed boxes).

1.10.1 Funding

Informed allocation of adequate funding is required at each step, particularly after upscaling to pre-clinical studies, and although this has, to date, been available, there remains a disparity between early-stage funding and final clinical output (Mason and Manzotti 2010, Griffith and Naughton 2002). This contrast may reflect the sources of funding: late-stage projects are often funded for a specific product by industry or venture capital companies, where given the associated risk, potential losses can be high – this restricts funding to only a few selected therapies or approaches. Economic modelling has been advocated as a solution to determine the likely cost-benefit of a putative tissue engineering construct before product development is considered, allowing stakeholders to assess convincing data on value and clinical efficacy before investing (Archer and Williams 2005). However, the tissue engineering 'life-cycle' remains an exhaustive process, such that even for the successful strategies that progress to sustained production, there is often a significant lead-time to financial return.

1.10.2 Regulatory requirements and research governance

Regulatory hurdles must be overcome at all stages of research. *In vivo* laboratory work must adhere to the principles of replacement, reduction and refinement and is subject to licence, under the Animals (Scientific Procedures) Act 1986 in the UK, following scrutiny of the facilities, research programme and prior assessment of the researchers' training and competence (Kolar 2006). Removal, storage and use of human tissue as part of pre-clinical evaluation of strategies involving human cells are regulated in the UK by the Human Tissue Act 2004. The conduct of any clinical trial requires prior approval by the appropriate ethics committee as part of the quality and accountability Research Governance Framework within which research is undertaken in the National Health Service (NHS). Before any biomaterial may be used in the clinic, it must comply with stringent production and safety standards such as ISO (International Organisation for Standardisation), USFDA (United States Food and Drug Administration) and GMP (Good Manufacturing Practice) (Reichert et al. 2010). Even if a particular device or material has already been approved for clinical use, such approval may be indicationspecific, thus a novel application may require further evaluation and approval. Furthermore, the addition of biologically active molecules to a previously approved material may change its classification, in certain standardisation systems, to a drug, requiring a different or additional evaluation protocol before clinical use is sanctioned.

These regulatory frameworks provide an important system of governance which is required to ensure research protocols are necessary, in the interest of the population, and produce the maximum impact for any harm caused through the process itself, and with minimal unnecessary repetition of established results. However, these regulatory processes must in themselves be overseen and regulated to ensure they serve their purpose and do not create additional repetition of work through bureaucratic justification by these agencies.

1.10.3 Practical factors

1.10.3.1 Scale-up for pre-clinical testing

Practical obstacles to in vivo scale-up must also be addressed to reliably assess new strategies for skeletal tissue engineering before pre-clinical studies can take place. Challenges include the establishment of appropriate large animal models for the clinical scenarios to be modelled, the requirement to manufacture larger biomaterials and the need to culture cells on a much greater scale than is routine in most research laboratories (Reichert et al. 2009). Although the bone composition of the dog, sheep, goat and pig is similar to those of humans, the age and rate at which osteonal remodelling occurs varies between these groups. In addition, cost, local availability, temperament and husbandry expertise are important factors (Muschler et al. 2010). For bone regeneration models, sheep and goats are particularly relevant as their bodyweight is comparable to humans and the dimensions of their long bones allow for the use of human implants and fixation techniques (Reichert et al. 2010, Newman et al. 1995). The equine knee is often the favoured model for cartilage repair strategies, because the thick hyaline cartilage allows investigation of both partial and full-thickness defects (Chu et al. 2010). Furthermore, horses have large joints that permit arthroscopy and they are typically more compliant with post-operative rehabilitation protocols compared to pigs and ruminants (Sah and Ratcliffe 2010).

The technicalities of large-scale manufacture are often very different to the protocols involved in producing small quantities of a test substance for analysis. These processes must not be (but often are) neglected until a late stage in product development, when modification of manufacturing processes may be costly or require regulatory re-approval. The difficulties associated with mass-production of complex biocomposites or cell production processes may be overcome by incorporating commercial interests and production strategies in the initial research and development.

This would provide a platform for progression in parallel with translation (Archer and Williams 2005).

1.10.3.2 Clinical trials

Once efficacy has been demonstrated in a large animal model and pre-clinical safety approval has been granted, the successful product can then undergo clinical trials prior to commercial manufacture. Clinical trials present further challenges including a requirement for significant clinician involvement, patient concordance, organisation and appropriate clinical facilities to undertake such studies. It is often at this stage that important practical aspects of the novel treatment are considered. Routine supplementary procedures intrinsic to the patient's treatment may have unexpected effects on the new tissue engineering approach, and these may initially be overlooked. Typically, strategies that incorporate the use of stem cells as part of therapeutic procedures remain comparable to current surgical protocols, with only modest changes advocated to accommodate the novel construct. Without specific implementation however, the efficacy of the new technique may be adversely affected and there remain a number of factors in a clinical protocol whereby cell populations may be compromised. These include temperature changes, infection, wound cleansing (e.g. pulsatile lavage) as well as the use of ancillary products such as antibiotic or local anaesthetic (LA) agents. It therefore makes sense to assess the impact of each of these modifiable factors on the components of a tissue engineering construct before clinical translation, so that adverse effects may be minimised and ideal conditions be established to ensure optimal therapeutic efficacy.

1.11 Major null hypothesis

Enriched skeletal stem cells applied as tissue engineered constructs do not augment bone formation.

1.12 **Aims**

Following on from this examination of current knowledge surrounding skeletal tissue regeneration, the aims of this thesis are to evaluate and refine a clinically appropriate stem-cell enrichment strategy, for use within a tissue engineered construct (Chapter II), then to apply these concentrated stem cells to putative scaffolds within selected *in vitro* and *in vivo* models as a precursor to clinical application (Chapters III-V). The application of tissue engineering strategies to enhance the properties of a material already in widespread orthopaedic use will be determined (Chapter III), as well as an assessment of the appropriate properties of novel scaffold materials (Chapter IV and V). As a precursor to clinical evaluation of a further new scaffold, the establishment of a large animal *in vivo* model of skeletal regeneration will also be examined (Chapter V), including potential hurdles that must be overcome prior to successful clinical translation (Chapter VI).

1.13 Objectives

- 1. To demonstrate the potential to efficiently concentrate the nucleated fraction of BMA, obtained from a clinically relevant elderly cohort, adopting an approach to cell filtration applicable within the sterile field of an operating theatre.
- To demonstrate the significance of cell enrichment for osteogenic and chondrogenic cell differentiation, and seeding efficiency onto allogeneic bone graft.
- To examine the osteoconductive and inductive capacity of Tantalum Trabecular Metal (TTM) in relation to allograft and autograft
- 4. To determine the potential of TTM with the addition of human skeletal stem cells in tissue engineering applications as an alternative to the current accepted standard treatments for loss of skeletal tissues.
- 5. To perform *in vitro* and *in vivo* analyses for skeletal regeneration applications of candidate polymer scaffolds selected by a High Throughput (HT) screening approach.
- To establish a consistent and reproducible technique for stabilisation of a 35 mm tibial critical defect in sheep, for subsequent trialling of tissue regeneration strategies.
- To demonstrate a living cell composite using cultured skeletal stem cells on synthetic scaffold to augment bone formation in a large animal segmental defect model.
- 8. To investigate the effects of three local anaesthetic agents, in routine use in orthopaedic practice, on skeletal stem cell function and survival and instruct the implementation of appropriate analgesia during the application of skeletal tissue engineering strategies.

Chapter II

Development of an intra-operative strategy to enrich skeletal stem cells from bone marrow for orthopaedic application

This study was performed with Dr Jonathan Dawson and Mr Alexander Aarvold. I gratefully acknowledge their support, in addition to Mr Andrew Jones for obtaining ethical approval and Mr Doug Dunlop and Mr David Higgs for provision of aspirated bone marrow. Initial development and testing of the device was performed by Dr Jonathan Ridgway and Dr Steven Curran at the Smith & Nephew Product Development Centre in York, prior to the work described in this chapter and has been published separately. Initial steps in the development of the aspiration and filtration technique have already been documented in Mr Aarvold's thesis. All experimental and analytical components presented in this chapter were conducted jointly by Dr Dawson and me. This work was funded by the Technology Strategy Board (AG280K) and Engineering and Physical Sciences Research Council (TS/G001650/1)

A paper detailing this study has recently been published in *Cytotherapy* under joint first authorship

The collaboration between clinician, scientist and industry in developing and evaluating this novel technique was recognised nationally by 'The Engineer' Technology & Innovation Awards 2010, winning both the 'Medical and Healthcare' category and the overall 'Grand Prix'

A presentation based on this study received the Pfizer Award for best conference poster at the UK National Stem Cell Network, York, 2011

2.1 Introduction

2.1.1 The clinical requirement for cell enrichment strategies

Tissue engineering strategies seek to harness the regenerative potential of stem or progenitor cells to replace tissue lost or damaged through injury or disease. With respect to skeletal tissues, aspirated bone marrow possesses considerable potential in such applications as an autologous source of SSCs able to regenerate bone and cartilage tissue. While connective tissue progenitors are resident in many tissues, bone marrow serves as the richest and most readily available repository of SSCs (Block 2005). Indeed, much of the osteogenic capacity of autologous bone graft derives from the bone marrow component (Nade and Burwell 1977). Despite some notable isolated successes however, where the regenerative capacity of autologous BMA has been successfully applied in the treatment of chronic wounds (Badiavas and Falanga 2003), or in combination with DBM for the treatment of aneurysmal (Docquier and Delloye 2005) and unicameral (Rougraff and Kling 2002) bone cysts, variable results obtained with aspirated cells suggest that concentration of BMA for SSCs is required to sustain robust skeletal regeneration (Warnke et al. 2004, Connolly et al. 1991, Tilley et al. 2006). The proportion of SSCs present in bone marrow is typically only 0.005% of total nucleated cells. These numbers are variable and dependent on sampling technique, volume, and site (Muschler and Midura 2002). Although this low cell concentration is sufficient when transplanting bulk autograft bone, where cells are translocated within their existing osteoinductive environment, robust skeletal regeneration using BMA appears likely to require pre-emptive cellular enrichment (Hernigou et al. 2005a and b, Jäger et al. 2011, Quarto et al. 2001).

Key clinical and pre-clinical studies have established the importance of SSC concentration and number on bone repair. Early clinical and pre-clinical studies by Connolly *et al.* indicated that the nucleated cell concentration of BMA was significant for bone formation and repair (Connolly *et al.* 1989, Connolly *et al.* 1991). More recently, Hernigou and colleagues successfully treated 53 out of 60 patients with femoral head AVN or fracture non-unions using percutaneous injection of BMA concentrated for SSCs (Hernigou *et al.* 2005b). Retrospective analysis of SSC number (by Colony Forming Unit-Fibroblastic (CFU-F) analysis) revealed that the seven atrophic non-unions that failed to heal had significantly lower number and concentration of SSCs (reviewed in detail in Chapter I, section 1.7).

2.1.2 Sources of BMA for enrichment

Several sites for BMA harvesting have been described (Table 2.1). Each aspiration site has its particular advantages, disadvantages and technique of acquisition. Most commonly a proprietary sterile aspiration kit consisting of a needle with introducing trocar is used, although novel methods include collection from the intramedullary canal using a reamer-irrigator (Cox et al. 2011). For clinical application, certain sampling procedures can be performed under local anaesthesia, or in conjunction with the principal operation, although frequently a separate anaesthetic is required. These factors should be considered for each case to maximise sample size and quality but minimise associated morbidity.

Table 2.1 Sources of BMA for human therapeutic clinical application

Source	Application	Example	
Iliac crest (anterior or posterior)	Most common approach, minimally invasive	Brodano et al. 2012 Smith et al. 2011 Kitchel et al. 2005	
Mandible	Maxillofacial surgical reconstruction	Lee BK <i>et al.</i> 2011	
Supra-acetabular sulcus	Facile approach during total hip arthroplasty	Fennema et al. 2009	
Vertebral body	Facile approach during preparation for pedicle screw insertion in spinal fusion	Kitchel <i>et al.</i> 2005 McLain <i>et al.</i> 2005	
Intramedullary canal	By-product of using the 'Reamer-Irrigator Aspirator' to prevent fat embolism during arthroplasty/ intramedullary surgery	Porter <i>et al.</i> 2009 Cox <i>et al.</i> 2011	
Distal femur	Performed during arthroscopic knee surgery	Beitzel et al. 2012	
Proximal humerus	Performed during arthroscopic rotator cuff repair	Mazzocca et al. 2010	
Sternum	BMA implanted into myocardium during coronary artery bypass grafting	Holinski et al. 2011	

BMA = Bone Marrow Aspirate

2.1.3 Cell enrichment strategies

In response to the critical requirement for the operative delivery of stem cells into a tissue engineering construct, several cell enrichment strategies have been developed. Many of these systems are already in clinical use in the orthopaedic field, although each has its own advantages and disadvantages and therefore a pragmatic approach is required to evaluate each option for its suitability before undertaking a procedure using one of these strategies.

2.1.3.1 Culture expansion

For this technique, autologous BMA is acquired from a patient often several weeks prior to the planned implantation of the tissue engineered construct. The BMA is transported under sterile conditions to the laboratory for processing and culture to selectively expand the required cell fraction *in vitro*. Expanded cells are released from culture and seeded onto a suitable scaffold either immediately prior to implantation, or cultured with the scaffold *in vitro* for several days to establish confluence prior to implantation. This technique has been used successfully to treat various osteochondral and osseous defects (Vacanti *et al.* 2001, Quarto *et al.* 2001, Schimming and Schmelzeisen 2004, Ohgushi *et al.* 2005, Adachi et al. 2005, Morishita *et al.* 2006, Hibi *et al.* 2006, Marcacci *et al.* 2007) (see Chapter I, Table 1.6). Although culture expansion reliably provides a high concentration of required stem cells, several inherent disadvantages to this technique exist (Table 2.2).

Table 2.2 Disadvantages of using culture expansion techniques for clinical tissue engineering purposes

Requirement	Potential consequences		
Interval operative procedures – for aspiration and subsequent implantation	Increased anaesthetic and surgical risk Delay in treatment		
Removal of cells from the operating theatre for culture expansion	Infection, contamination or donor cross-contamination		
Artificial culture conditions, potential use of animal-derived culture media	Altered cellular phenotype, contamination, disease transmission		
Laboratory expertise, accreditation and licensing, personnel, specialist equipment	Considerable capital expense		

Attempts to overcome some of these hurdles include the development of bioreactors, which allow continuous culture perfusion and increase mass transport to mitigate the diffusion limitation during the cultivation of clinically-sized tissue engineering constructs (Koller *et al.* 1993). Serum-free bioreactor models have demonstrated some efficacy, but non-homogenous distribution of cells on scaffolds and cellular 'wash-out' due to turbulent flow of media has hindered clinical application (Zhang *et al.* 2012). Consequently attempts have been made to identify alternative cell concentration strategies.

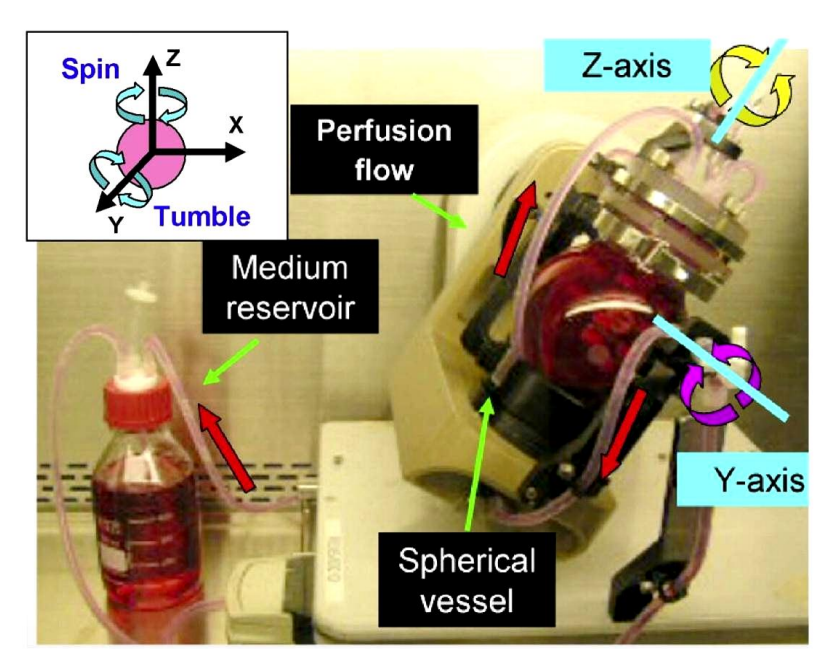


Fig. 2.1 Biaxial bioreactor used for bone tissue engineering. It is designed to rotate around two perpendicular axes simultaneously, with continuous media perfusion occurring between the culture vessel and a medium reservoir. *From Zhang et al. 2012.*

2.1.3.2 Centrifugation

Density gradient centrifuge-based devices are the most commonly used systems that rapidly and effectively concentrate the nucleated cell content of BMA for operative use (Jäger *et al.* 2011, Hernigou *et al.* 2005b, Hernigou *et al.* 2006, Hernigou *et al.* 2009). Following concentration, cells are either applied directly to the operative site, or infiltrated into a scaffold. Current products include the Res-Q™ Bone Marrow Concentration (BMC) System (Thermogenesis, Rancho Cordova, USA), Marrowstim™ (Biomet Biologics Inc, Indiana, USA) and Bone Marrow Aspirate Concentrate (BMAC) SmartPrep2™ (Harvest Technologies Corp., Plymouth, USA), which have been used for a wide range of orthopaedic, maxillofacial, soft tissue and cardiovascular applications (Hernigou *et al.* 2005b, Badiavas *et al.* 2003, Rougraff and Kling 2002).

Although cellular enrichment can be achieved within the time-constraints of most operations, it involves the removal of aspirated marrow from the sterile operative field for processing, significant capital equipment expenditure and a risk of donor cross-contamination (Ridgway *et al.* 2010).

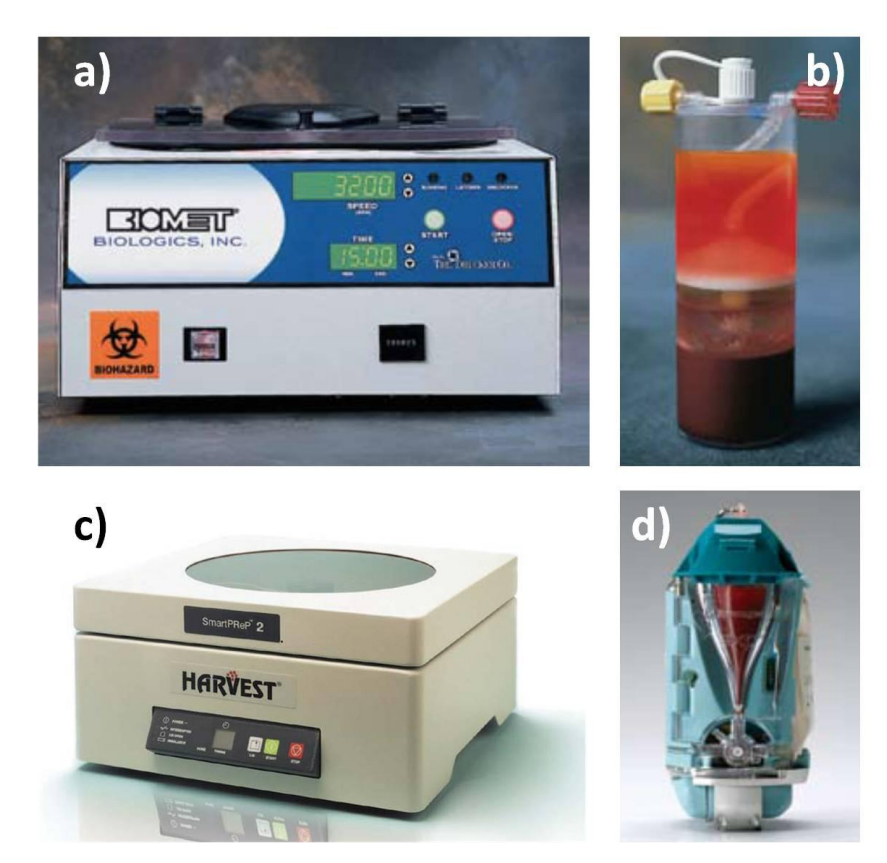


Fig. 2.2 Commercially available density-gradient centrifugation devices for enrichment of BMA. a) Biomet Marrowstim[™] centrifugation unit, b) Disposable Marrowstim[™] concentration tube following centrifugation, demonstrating layers of cell poor plasma (top), nucleated cell concentrate (middle), erythrocytes (bottom), c) Harvest BMAC SmartPrep2[™] centrifugation unit, d) Thermogenesis Res-Q[™] BMC module. *Images a) and b) from www.biomet.co.uk, c) from www.harvesttech.com and d) from www.thermogenesis.com.*

2.1.3.3 Gradient separation

Gradient separation techniques are frequently employed to isolate cells for diagnostic purposes and require addition of a graded density solution such as Ficoll or sucrose (Hunter *et al.* 1987). Although this technique has been shown to separate cells with reasonable sensitivity and specificity, the process is time consuming and addition of graded solutions is likely to interfere with clinical use.

2.1.3.4 Field-assisted separation

Cells, bio-macromolecules and micro-organisms have been successfully separated using various field-assisted techniques, including electric, magnetic and acoustic phenomena (Karumanchi *et al.* 2002). These processes have largely been limited to laboratory use as they are complex, rely on constant adjustment and tuning to maintain effectiveness and tend to operate on a small-volume scale. Consequently, direct transference of these techniques to large-scale clinical application has not been forthcoming.

2.1.3.5 Selective cell retention

Several animal studies have successfully used selective cell retention as a method of seeding scaffolds with enriched BMA prior to implantation (Muschler *et al.* 2005, Brodke *et al.* 2006). The technique relies on the principles of an affinity column to populate a porous matrix with a high proportion of SSCs found in bone marrow by establishing a controlled flow of aspirate through the scaffold. The nucleated cells attach to the matrix while haematopoietic cells pass through, resulting in a graft material that contains an increased concentration of SSCs. Although studies report a higher union rate in animal models using this technique, the fold enrichment of nucleated cells produced (up to 3-fold) is unlikely to have therapeutic benefit in the human clinical scenario.

2.1.3.6 Filtration

Various filtration techniques have been successfully used to separate mammalian cells including spin filters, vibrating and rotating disc filters, cross-flow micro-filter devices and controlled shear filtration (Ridgway *et al.* 2010). In this study, a combination of negative pressure-assisted filtration and acoustic vibration has been evaluated, as a technique to separate cells by size to provide therapeutic enrichment of the SSC fraction of human BMA.

2.2 Aims

The aim of this study was to demonstrate the potential to efficiently concentrate the nucleated fraction of BMA, obtained from a clinically relevant elderly cohort, adopting an approach to cell filtration applicable within the sterile field of an operating theatre (Ridgway *et al.* 2010). A further aim was to demonstrate the significance of cell enrichment for osteogenic and chondrogenic cell differentiation, and seeding efficiency onto allogeneic bone graft.

2.3 Null hypotheses

- 1. Negative pressure-assisted filtration does not significantly enhance the concentration of SSCs in human BMA.
- 2. Enrichment of SSCs in human BMA by negative pressure-assisted filtration does not enhance osteogenic and chondrogenic cell differentiation and seeding efficiency onto allogeneic bone graft.

2.4 <u>Materials and methods</u>

2.4.1 Patient selection

Volunteers were selected from haematologically normal patients undergoing primary Total Hip Replacement (THR). Exclusion criteria were pre-existing conditions that may have confounding effects on cellular activity: a history of Paget's disease of bone; malignancy; infection; clotting disorders; osteogenesis imperfecta; rheumatoid arthritis; avascular necrosis of the femoral head; long term bisphosphonate or glucocorticoid therapy, and known transmissible disease (e.g. hepatitis, HIV, malaria) or sickle cell disease. Patients provided fully informed consent after receiving a lay summary of the trial, together with a verbal explanation and an opportunity for questioning. Ethical approval of the study was obtained locally (LREC194/99/1) and regionally (Research Ethics Committee 09/H0505/5). Medicines and Healthcare products Regulatory Agency (MHRA) registration was unnecessary at this stage as the device was not being used for direct therapeutic intervention.

2.4.2 Bone marrow harvest from the femoral canal

BMA for *in vitro* experimentation was harvested as waste tissue from the femoral canal during THR surgery (Fig. 2.3A). Prior to aspiration of bone marrow, a 20 ml Luer lock syringe containing 5000 IU heparin in 5 ml normal saline was prepared and the needle was flushed with heparin. Bone marrow was aspirated from a location proximal to the pending neck osteotomy into the heparinised syringe, then transferred to a sterile universal container for transport from operating theatre to laboratory for filtration.

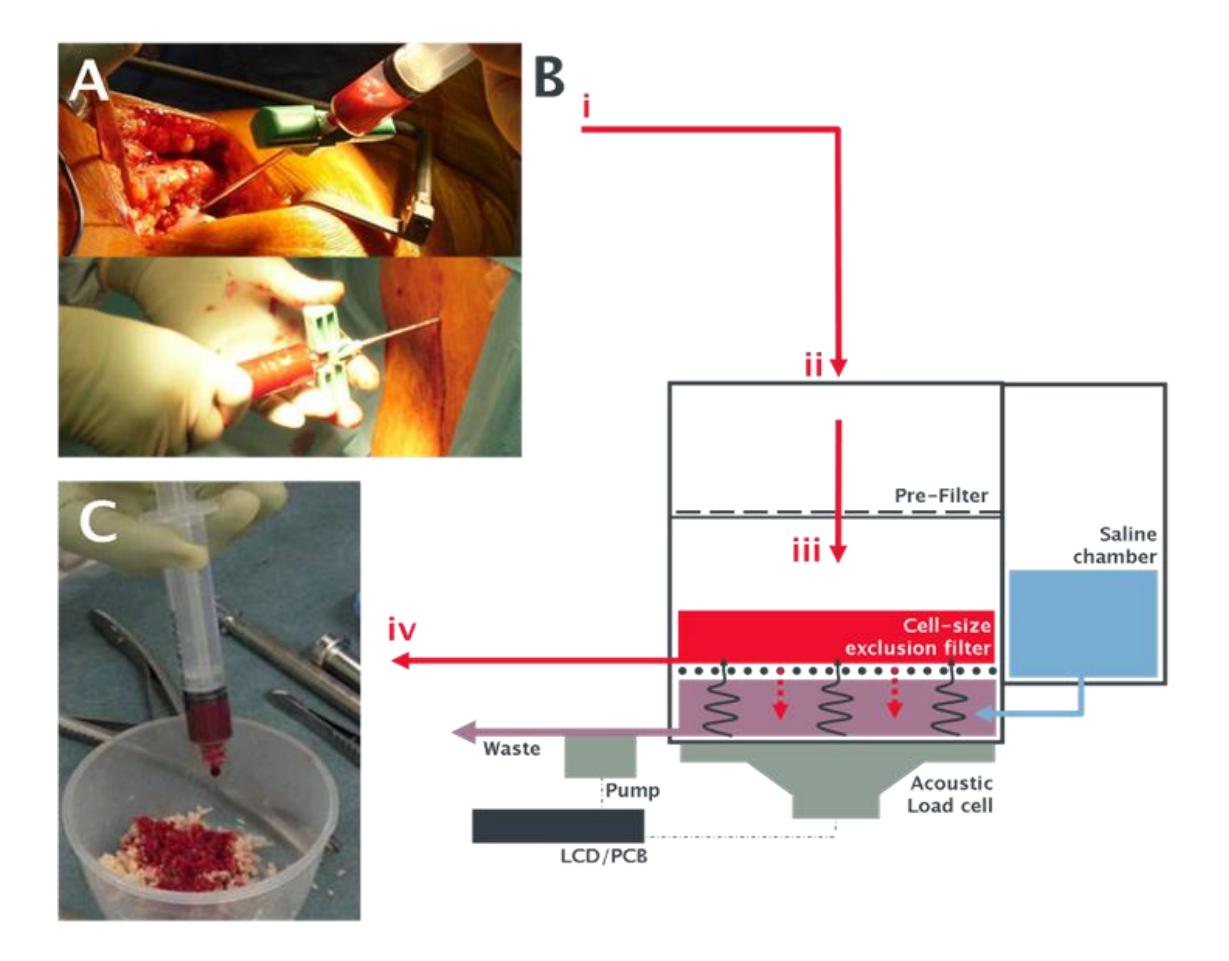


Fig. 2.3 SSC enrichment strategy schematic. (A) Bone marrow aspiration from the femoral canal during a total hip replacement (top) and from iliac crest (bottom). (B) BMA enrichment process (projected to occur immediately following aspiration and within the sterile field for clinical application) (i), BMA is injected into the unit (ii). After passing through a pre-filter to remove debris the BMA is applied to a secondary filter (iii) and an acoustic wave applied to agitate the sample and ensure an even cell suspension. Negative pressure draws erythrocytes and platelets through the filter retaining nucleated cell fraction via size exclusion. (iv) Enriched nucleated cells, retained above the filter, are removed for analysis (projected use for therapeutic application). (C) Concentrated bone marrow being applied to allogeneic bone graft (allograft) prior to bone grafting in the clinical scenario.

2.4.3 Operation of the device

BMA was concentrated via a vacuum assisted filtration approach facilitated by acoustic agitation (Figs. 2.3 - 2.5). Filters were manufactured from 23 µm thick polyethylene terephthalate (PET) to achieve a range of uniform pore sizes (between 1.2 and 4.1 µm diameter) and porosities (between 150,000 and 1.5 million pores/ cm²) using a track etching process (it4ip, Seneffe, Belgium). Acoustic vibration was applied using a voice-coil (model RM-ETNC0033K19C-2KOI, NXT Technology, Cambridge, UK). Vacuum pressure was produced with a 6 V miniature diaphragm pump (Kage KPV14A-GA, Taiwan).

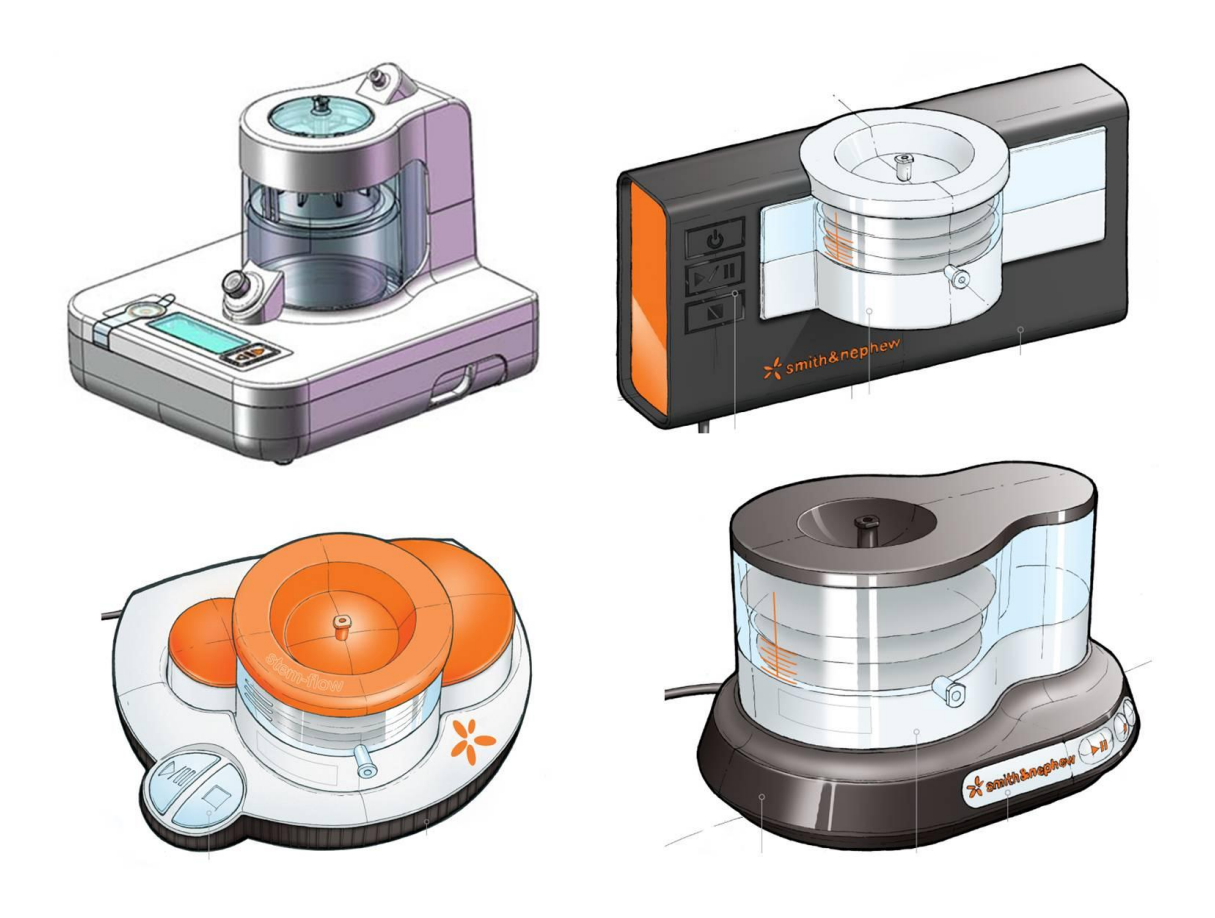


Fig. 2.4 Initial concept designs for the acoustic negative-pressure filtration product.

Courtesy of Smith & Nephew

Following straining through a 70 μ m pore-size pre-filter (Fig. 2.3B ii), BMA samples were applied to a size-exclusion filter positioned above a reservoir of Phosphate Buffered Saline (PBS) (Fig. 2.3B iii). A resonant frequency wave was passed through the PBS reservoir, agitating the filter and BMA above it. This produced a geometric standing waveform pattern on the aspirate fluid surface. The frequency was manually adjusted as the remaining unconcentrated volume reduced, in order to maintain a standing wave and the resultant stable cell suspension. A negative pressure (25 psi) was applied from below the filter, to preferentially filter out the smaller cells (erythrocytes (diameter 5-8 μ m) and platelets (1-3 μ m)), whilst retaining the nucleated cell fraction above the filter.

Following filtration, the volume of aspirate remaining above the filter was recovered as concentrated BMA for analysis (Fig. 2.3B iv). 2-5 ml of fresh heparinised BMA was set aside prior to filtration as unconcentrated control BMA.

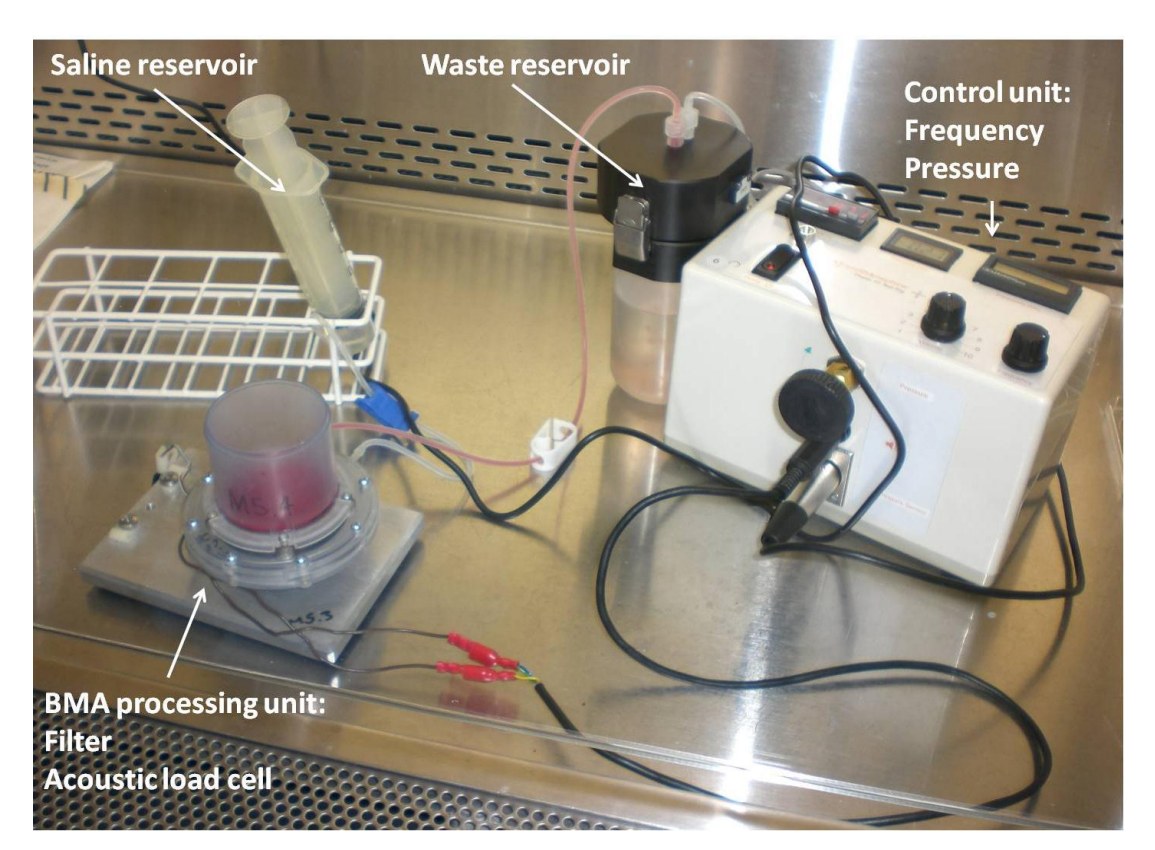


Fig. 2.5 Laboratory prototype acoustic filtration device used to process all BMA samples for this study. Final product concept is a single self-contained automated unit.

2.4.4 Filtration time

Filtration was continued to achieve either a minimum 4.0-fold volume reduction, or until flow through the filter became laborious. Start and end time-points, starting volume and final volume were recorded for each sample filtered.

2.4.5 Nucleated cell count and cell viability analysis

Nucleated cell counts of unconcentrated and concentrated BMA were determined on 15 samples using Guava Easycyte (Millipore Corp., Billerica, USA) flow cytometry and confirmed by manual count on a haemocytometer. Guava Viacount Reagent was used to differentiate live and dead cells, and the viable cell count value was used in all calculations. Statistical analysis was performed using Microsoft Excel and SPSS Ver.18 (SPSS Inc, Chicago, IL, USA).

2.4.6 CFU-F analysis

CFU-F assay was used as an indicator of SSC number present in the aspirate pre- and post- filtration through the device, and was performed on 15 samples. Following determination of viable nucleated cell count using Guava Easycyte flow cytometry, unconcentrated and concentrated BMA was seeded into T25 culture flasks (n=3) according to the Friedenstein protocol for density independent growth (Bianco et al. 2006). Briefly, aspirates were diluted in basal medium (aMEM (Minimum Essential Medium Eagle, Alpha Modification) containing 10% Fetal Calf Serum (FCS)) to achieve clonal seeding densities of 1x104 and 1x105 nucleated cells/ml, strained to ensure a single cell suspension, and seeded at 0.2 ml/cm². After three hours at 37°C and 5% CO₂, plates were washed twice with PBS to remove non-adherent cells and incubated at 37°C and 5% CO₂ in basal medium for 14 days. Following fixation in 95% ethanol, and staining for Alkaline Phosphatase (ALP) activity against Gill's haematoxylin nuclear counter-stain, colony number was counted and the CFU-F/ml value for each aspirate was calculated taking into account the dilution factor required to achieve clonal seeding densities. Parallel assays of like-for-like volumes of unconcentrated and concentrated BMA were also performed to illustrate differences in CFU-F concentration.

2.4.7 Flow cytometric analysis of stem cell markers

Unconcentrated and concentrated BMA were washed in PBS with 1% Bovine Serum Albumin (BSA) before being incubated in blocking buffer (PBS, 1% BSA, 10% human serum, 5% FCS) at room temperature for 30 minutes. Cells were then immuno-labelled with antibodies against STRO-1 (undiluted culture supernatant from the STRO-1 hybridoma provided by Dr J. Beresford, University of Bath), CD146 (1:50, mouse monoclonal [P1H12], BD Pharmingen, Oxford, UK) and CD105 (1:50, chicken polyclonal, Abcam, Cambridge, UK) for 60 minutes at room temperature and then washed and incubated with fluorescently labelled secondary antibodies (1:100). Labelled populations from each sample were quantified against the relevant isotype control using Guava Easycyte flow cytometry.

2.4.8 Multi-lineage differentiation of concentrated and unconcentrated cells

Following filtration, equal volumes of unconcentrated and concentrated aspirate were seeded across culture vessels and culture expanded for 12 days. After expansion, cells (which were at less than 80% confluence) were released with trypsin, counted and reseeded, at densities consistent with the fold difference in cell number (2.54-fold) obtained from expanded concentrated *vs.* unconcentrated samples, into 12-well plates for osteogenic, adipogenic and chondrogenic differentiation. Control cultures were refreshed with basal medium every 3 days.

Osteogenic culture: After a further 14 days in basal conditions, monolayer cultures of concentrated and unconcentrated BMA were transferred to osteogenic media (αMEM with 10% FCS, 100 μM ascorbate (ascorbic acid 2-phosphate) and 10 nM dexamethasone) for 14 days. Media were refreshed every 2-3 days.

Adipogenic culture: After a further 14 days in basal conditions, monolayer cultures of concentrated and unconcentrated BMA were transferred to adipogenic media consisting of basal cell culture media containing additional 2 g/L D-glucose and 0.5 mM 3-isobutyl-1-methylxanthine, 1 μ M dexamethasone, 1% ITS (Insulin, human Transferrin and sodium Selenite) solution (equal to 10 μ g/ml insulin (Sigma-Aldrich, Gillingham, UK)), and 100 μ M indomethacin, for three days followed by 1 day in basal cell culture medium containing 1% ITS solution. Both cycles were repeated for 28 days.

Chondrogenic culture: Monolayer expanded cells were seeded at high density (unconcentrated BMA 1.475×10^6 cells/ml; concentrated BMA 3.75×10^6 cells/ml) in 20 μl volumes at the centre of each well and following 30 minutes incubation to allow cell-adhesion, cultured in chondrogenic medium (serum-free αMEM supplemented with 10 ng/ml TGF- $\beta 3$, 10 nM dexamethasone, 100 μM ascorbate, and 10 μl/ml 100 × ITS Solution) for 21 days. Media were refreshed every 2-3 days.

2.4.9 Histological staining and quantification of differentiated cultures

Osteogenic differentiation was determined using ALP histochemical staining, demonstrated with naphthol AS-MX phosphate and Fast Violet B Salts. Relative ALP staining intensity was quantified using Cell Profiler image analysis software (www.cellprofiler.org).

Adipogenic differentiation was identified by adipocyte accumulation of lipid droplets observed under light microscopy using a Zeiss microscope and following staining for lipid with Oil Red O histochemistry. In brief, cells were fixed in Baker's formal calcium, rinsed in 60% isopropanol, and stained using double-filtered Oil Red O solution. Following imaging, Oil Red O staining was leached from the cells in 100% isopropanol, and absorbance measured via spectrophotometry.

Chondrogenic differentiation was determined by staining for proteoglycan with Alcian blue. Following imaging, Alcian blue staining was leached using 0.5% Triton X-100 and absorbance measured via spectrophotometry.

2.4.10 Cell seeding onto decellularised human bone graft

For this part of the study, BMA was filtered through the device to achieve a 7.4-fold reduction in volume and a corresponding increase in the concentration of nucleated cells was confirmed via flow cytometry. Equal volumes of unconcentrated BMA and concentrated BMA were applied to bone graft to assess the affect of concentration of BMA on seeding. Two further preparations were applied to bone as controls: 1) a 7.4-fold reduced volume of concentrated BMA to normalise to unconcentrated BMA by nucleated cell number, and 2) a 7.4-fold reduced volume of concentrated BMA rediluted in PBS to normalise to unconcentrated BMA by both volume and nucleated cell number. Aspirates were applied so as to immerse approximately 5 mm³ pieces of decellularised human trabecular bone. After incubation for 18 hours under gentle agitation, excess BMA was removed and samples were washed twice with PBS before being re-immersed in αMEM with 10% FCS. Samples were cultured for a further 48 hours before cell quantification and viability analysis.

2.4.11 WST-1 assay for relative quantification of cell seeding

Following seeding and a 48 hour culture period the extent of cell seeding and growth on decellularised human trabecular bone matrix was assessed using the colorimetric WST-1 (2-(4-lodophenyl)-3-(4-nitrophenyl)-5-(2,4-disulfophenyl)-2H-tetrazolium) assay for metabolic activity (Roche, Burgess Hill, UK). Seeded matrices were washed twice with PBS, re-immersed in 9% WST-1 reagent and transferred to an incubator. After 2 hours the absorbance was read at 450 nm on an ELx800 microplate reader (BioTek Instruments, Potton, UK).

2.4.12 Cell viability and imaging

Prior to fixation, cell cultures were incubated for 45 minutes (37°C and 5% CO₂) in the presence of αMEM containing 10 $\mu\text{g/ml}$ CellTracker[™] Green (CTG, 5-chloromethylfluorescein diacetate (CMFDA)) and 5 $\mu\text{g/ml}$ Ethidium Homodimer-1 (EH-1) to label viable and necrotic cells respectively. Cells were then incubated in fresh αMEM for a further 45 minutes before fixing in 95% ethanol for 15 minutes. Fluorescent imaging was conducted on a Zeiss Axiovert 200 inverted microscope equipped with an AxioCam MRm monochrome camera and an X-Cite 120 fluorescence light source.

2.5 Results

2.5.1 BMA concentration and SSC enrichment

Femoral BMA sampled from 15 patients from an elderly cohort was concentrated up to 4-fold with a corresponding enrichment of SSCs (Table 2.3).

Table 2.3 Nucleated cell counts and CFU-F concentrations pre- and post- filtration

Table 2.0 Radicated cell counts and of 6 T confernations pre- and post intration								
Sex	Age (years)	ج <u>(</u>	(p	ne	Pre-filtration		Post-filtration	
		Aspirated Volume (ml)	Conc. by	Filtration time (mins)	Viable NC conc. (x10 ⁶ cells/ml)	CFU-F conc. (per ml BMA)	Viable NC conc. (x10 ⁶ cells/ml)	CFU-F conc. (per ml BMA)
F	77	20	2.4	8	6.6	71	13.2	141
М	75	40	4.7	10	6.1	29	23.8	143
F	91	18	2.7	29	6.8	89	14.9	198
F	70	40	4.0	16	27.8	115	89.3	357
М	70	19	5.2	21	12.5	158	43.7	554
F	82	20	4.0	15	19.6	116	41.0	611
F	78	20	4.0	8	16.9	202	78.1	703
F	75	40	5.5	25	44.8	131	195.8	703
F	71	40	4.0	20	17.7	215	59.2	977
F	69	20	4.0	20	14.2	426	52.3	1152
М	55	40	4.0	20	12.1	317	40.3	1379
F	89	20	6.0	25	32.4	330	126.0	1418
М	52	20	4.0	15	18.5	368	61.6	1493
F	78	40	4.3	15	37.7	2108	95.4	3955
М	68	20	4.0	25	70.2	1032	234.1	4003
Mea	Mean 27.8 4.2 18.1		18.1	22.9	380.3	77.9	1185.8	
SD		10.3	0.9	6.5	17.4	536.9	64.0	1220.9

Concentrations corrected for BMA dilution with heparin at time of harvest. Samples below the double line displayed post-filtration CFU-F concentrations above the critical therapeutic threshold of 1000 CFU-F/ml suggested by Hernigou and colleagues (Hernigou et al. 2005a and b). M = Male, F = Female, Conc. = concentration, CFU-F = Colony Forming Unit (Fibroblastic), BMA = Bone Marrow Aspirate, NC = Nucleated Cell

Samples were obtained from five male and ten female patients, with a mean age of 73 years (range 52-91, SD 10.3). All samples were analysed for nucleated cell number and viability, and cultured for CFU-F analysis. No significant difference in filtration time or initial nucleated cell count was observed between the sexes or across the age range of this elderly cohort.

The 15 freshly obtained samples of BMA were filtered to achieve between a 2- and 6-fold reduction in volume (mean = 4.2) with an average filtration time of 18.1 minutes. Eight samples were filtered to achieve the target 4-fold volume reduction and a further five samples were filtered to achieve a volume reduction in excess of 4-fold.

Counts of viable cells following a 2-fold and then 4-fold reduction in volume revealed a corresponding increase in the concentration of nucleated cells in the concentrated aspirate relative to both volume and erythrocyte concentration (Fig. 2.6).

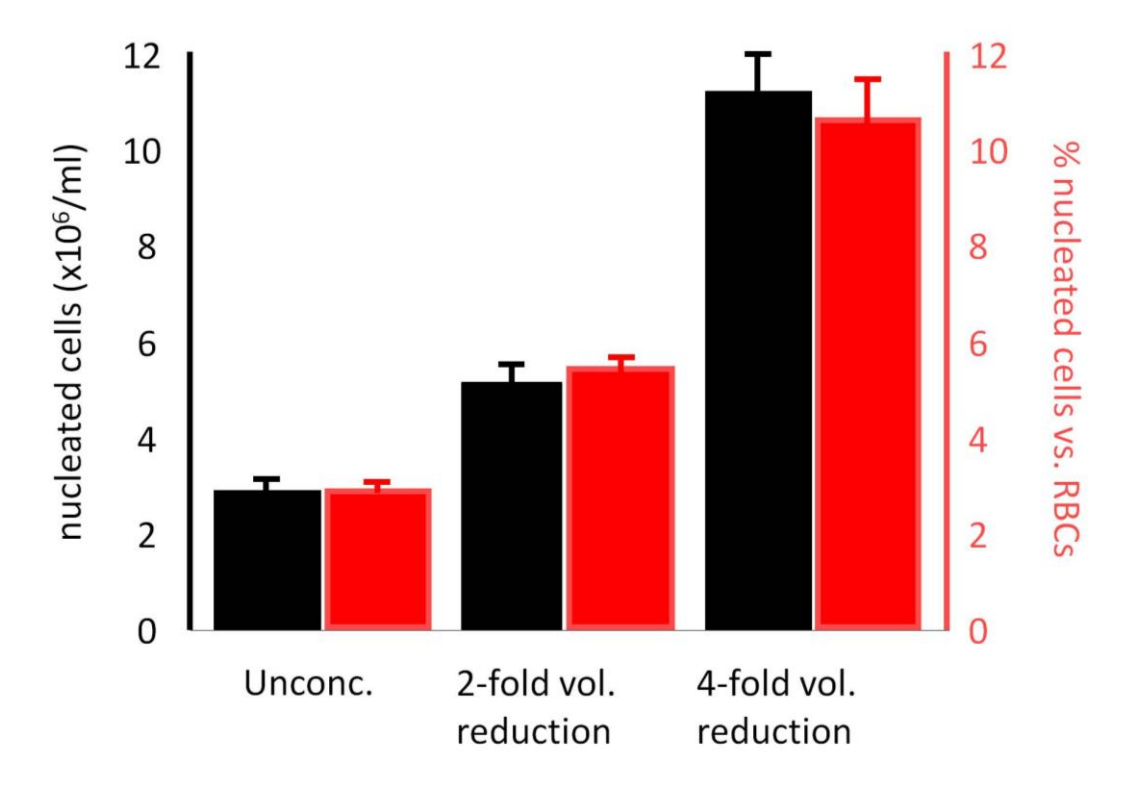


Fig. 2.6 SSC enrichment of BMA following filtration to achieve 2- and 4-fold volume reductions, a corresponding concentration of total NCs relative to erythrocytes/red blood cells (RBCs) was observed. Error bars: +/- SD of replicates.

An increase in the concentration of CFU-F was also observed (Fig. 2.7).

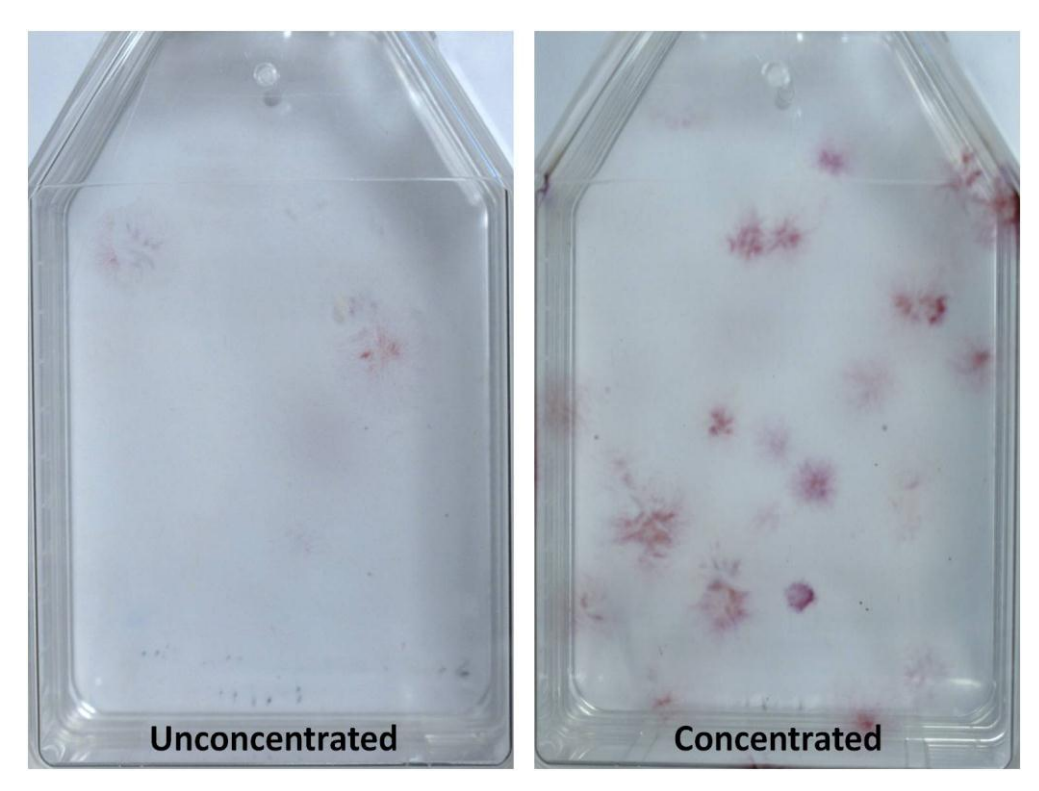


Fig. 2.7 CFU-F analysis. Equal volumes of unconcentrated and concentrated BMA were cultured for 14 days and colonies were counted after staining for ALP. In this case, a 3.7-fold increase in CFU-F number was observed.

Flow cytometry analysis of commonly used markers for SSCs (STRO-1, CD105 and CD146) revealed enrichment of these cells in the concentrated BMA volume (Fig. 2.8)

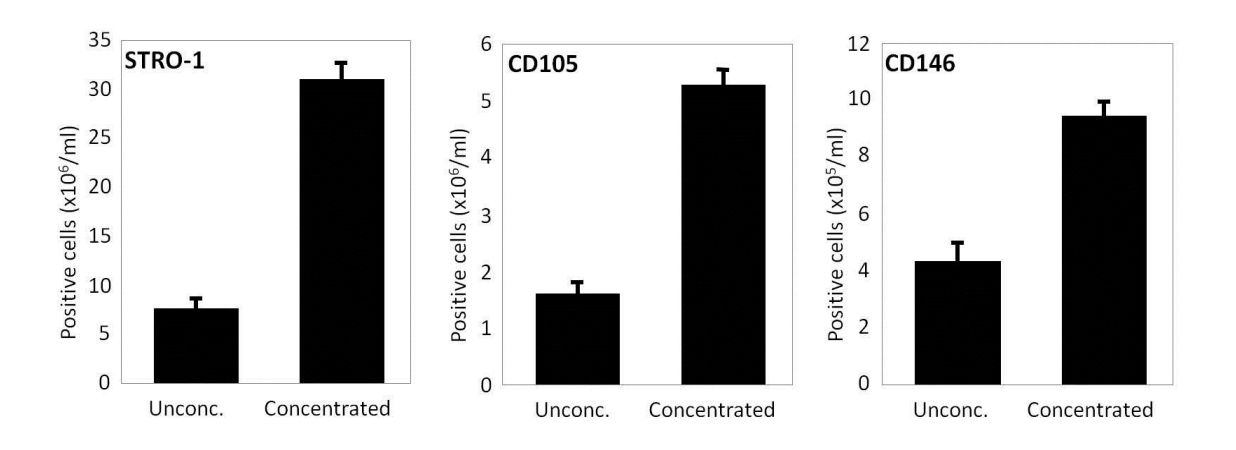


Fig. 2.8 Flow cytometric analysis of BMA, immuno-labelled for markers associated with SSCs revealed a corresponding enrichment in concentrated samples. Error bars: +/- SD of replicates.

A viable nucleated cell concentration of mean 3.65 (+/-0.52) was observed following 4-fold volume reduction (Fig. 2.9A) indicating 88% (+/-12.83) of nucleated cells were recovered subsequent to filtration (Fig. 2.9B). An equivalent CFU-F concentration of 3.88 (+/-1.17) was observed (Fig. 2.9C). When BMA was filtered to achieve >4-fold volume reduction a drop in nucleated cell recovery (mean = 68.3% +/- 10.47) was observed (Figure 2.9B).

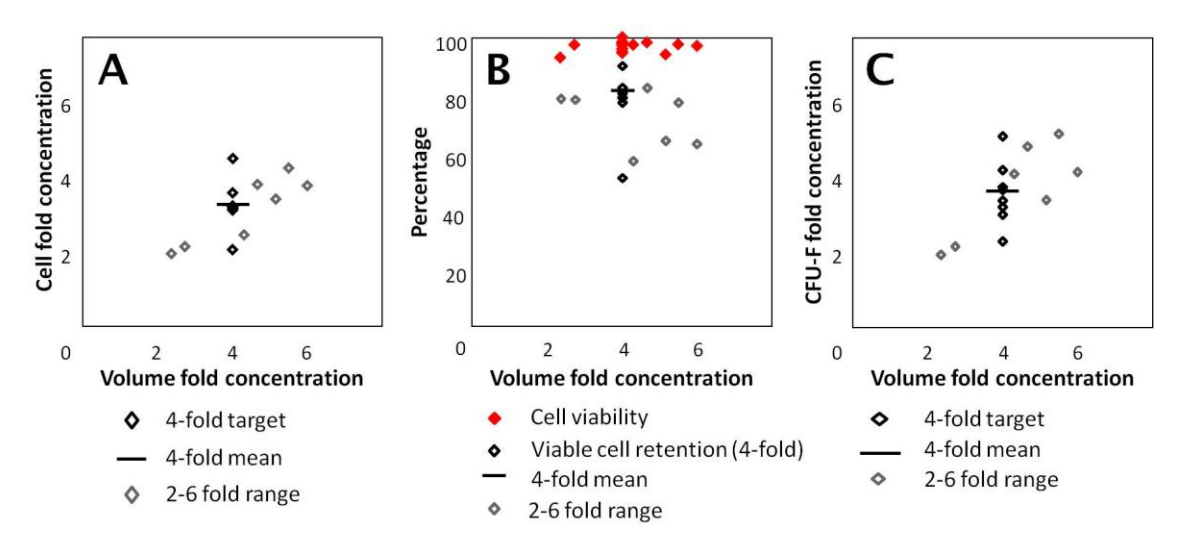


Fig. 2.9 Analysis of cellular concentration, viability and CFU-F concentration with respect to BMA concentration by volume. (A) Across the 15 samples a corresponding enrichment of total NCs was observed in relation to the volume filtered. (B) While cell viability was maintained during filtration, a reduction in the percentage retention of NCs was observed when samples were filtered to achieve >4-fold reduction in volume. (C) A corresponding enrichment of CFU-F relative to the aspirate volume filtered was observed.

2.5.2 Multi-lineage differentiation of concentrated and unconcentrated cells

Following a 2.54-fold concentration of nucleated cells via acoustic-mediated filtration, aspirates were seeded at equal volumes and cells expanded before being transferred to differentiation conditions to assess the effect of cell concentration on the response to multi-lineage induction. After 14 days, cells from concentrated BMA seeded onto tissue culture plastic at an equal volume to unconcentrated BMA displayed significantly higher ALP activity (P<0.05) in both osteogenic and basal conditions (Fig. 2.10A).

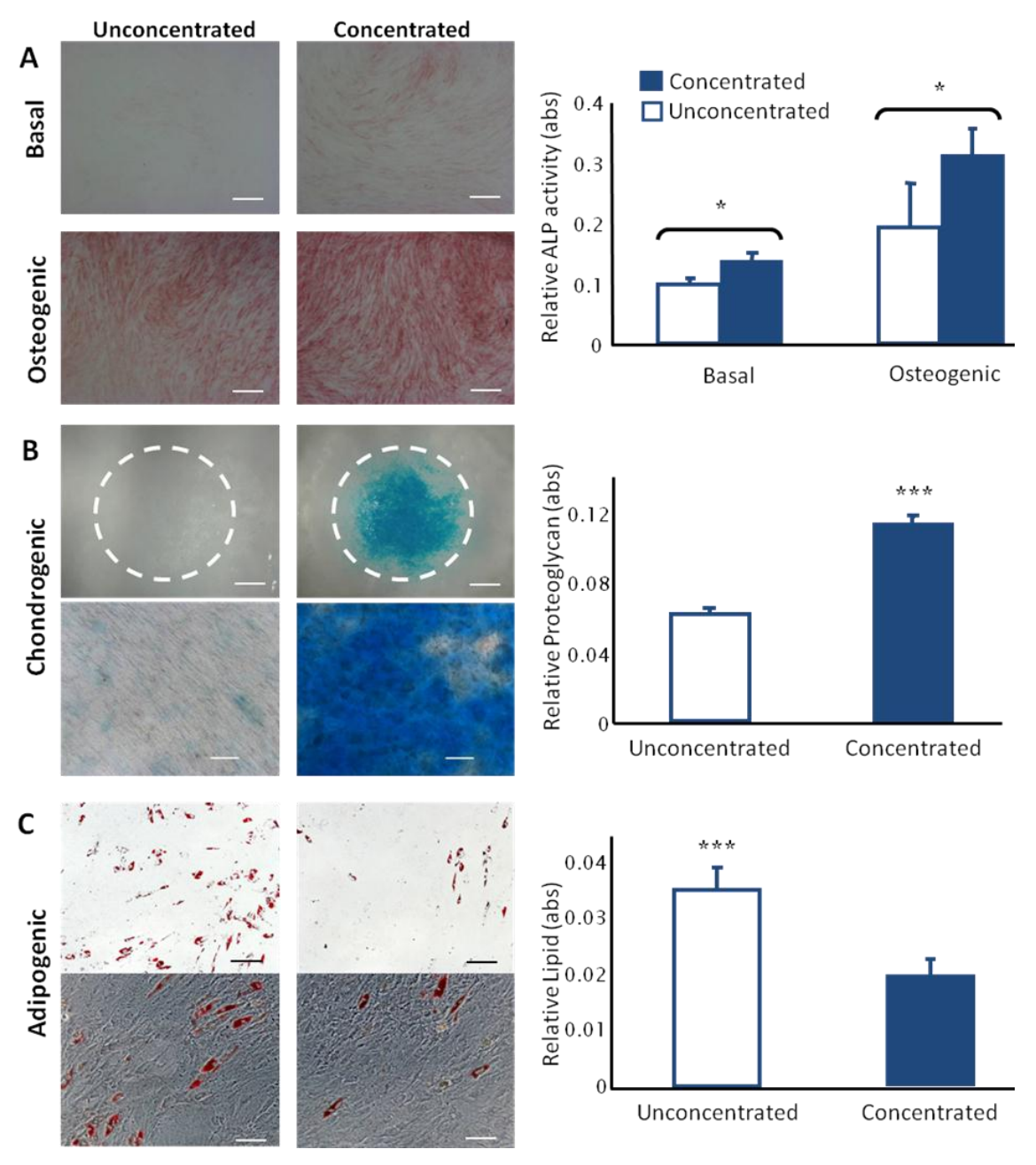


Fig. 2.10 Multilineage induction of human bone marrow stromal cell cultures derived from concentrated vs. unconcentrated BMA. Following a 2.54-fold concentration, aspirates were seeded at equal volumes and cells expanded before being transferred to differentiation conditions. Enhanced osteogenesis (A); ALP activity; p<0.05 (*)) and chondrogenesis (B); proteoglycan; p<0.001 (***)), but reduced adipogenesis (C); lipid; p<0.001 (***)) was observed in concentrated samples relative to unconcentrated samples (abs = absorbance). Scale bars: $100 \mu m$, except upper panel of B ($500 \mu m$) and upper panel of C ($200 \mu m$).

Furthermore, when cells obtained from concentrated *vs.* unconcentrated BMA were seeded at equivalent cell concentrations into chondrogenic high-density culture conditions, significantly higher proteoglycan synthesis (p<0.001) was observed in concentrated samples with negligible Alcian blue staining for proteoglycan being observed in cultures derived from, and seeded at densities equivalent to, unconcentrated BMA (Fig. 2.10B). In contrast, under adipogenic conditions, higher-density seeding facilitated by BMA concentration was observed to significantly reduce (p<0.001) the response to adipogenic induction compared with unconcentrated BMA (Fig. 2.10C).

2.5.3 Cell seeding onto decellularised human trabecular bone graft

To assess the effect of concentration of BMA on the seeding efficiency of adherent cells onto allogeneic bone graft, 25 ml of freshly obtained aspirate was filtered to achieve a 7.4-fold reduction in volume. Total nucleated cell counts revealed a 7.2-fold concentration of nucleated cells with 97.8% viability corresponding to 95.1% viable nucleated cell retention efficiency. Equal volumes of concentrated (Conc.vol.) and unconcentrated (Unconc.) BMA were seeded onto decellularised human trabecular bone and, following culture, assessed for relative seeding efficiency via imaging of viable cells and an assay for relative metabolic activity (Fig. 2.11A). To control for the various possible factors affecting seeding efficiency, two further control samples were prepared: concentrated BMA was added at 7.2-fold reduced volume to normalise for cell number and assess for the effect of concentration alone (Conc.cell), and a 7.2-fold reduced volume of concentrated BMA was re-diluted in PBS to normalise for volume and cell number and assess for the effect of nucleated cell concentration relative to erythrocytes alone (Conc.cell+vol.). In all cases, concentrated BMA demonstrated significantly higher seeding efficiency than the unconcentrated control (Fig. 2.11B and C). Conc.vol resulted in the highest seeding reflecting the increased number of nucleated cells present in these samples, however concentration resulted in significantly higher seeding even when normalised for cell number (Conc.cell and Conc.cell+vol.). That the increase in seeding efficiency was not lost when concentrated BMA was re-diluted (Conc.cell+vol.) indicates that the enhanced seeding observed in the samples normalised to the control by cell number can be attributed to concentration of nucleated cell number relative to erythrocytes.

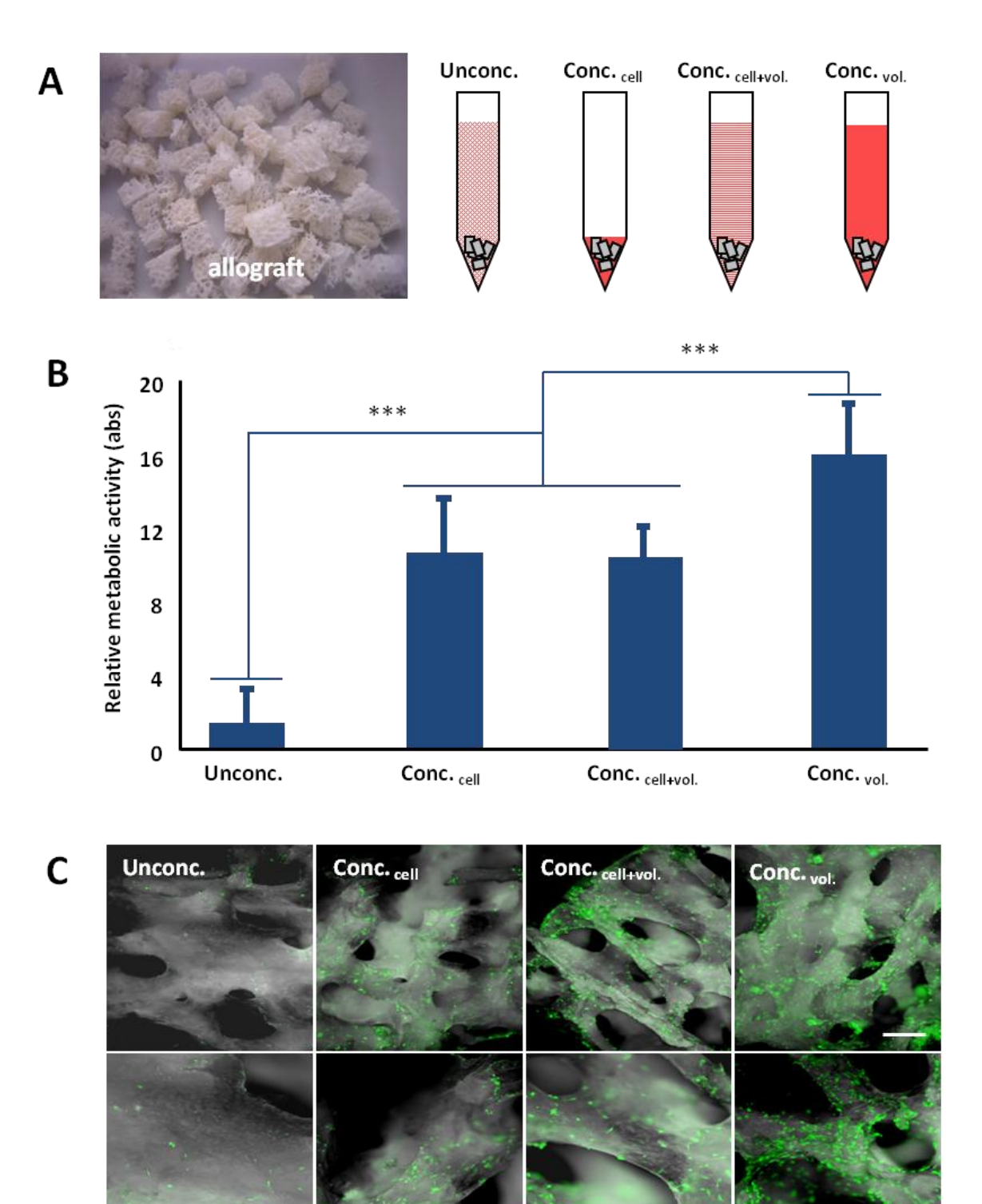


Fig. 2.11 Enhanced cell seeding efficiency via BMA enrichment. BMA was concentrated and seeded, at equal volumes, onto allograft (Conc. $_{vol.}$) to compare seeding efficiency relative to unconcentrated controls (Unconc.). In addition, concentrated BMA was normalised to the control by NC number (Conc. $_{cell}$) or normalised by cell number and volume by re-dilution (Conc. $_{cell+vol.}$) to assess the effect of concentration apart from cell number and concentration relative to erythrocytes respectively (A). In all cases seeding efficiency is significantly higher (p<0.001 (***)) when BMA is concentrated, as observed via WST-1 assays for gross metabolic activity (B) and CTG staining (C). Scale bars: 200 μ m, abs = absorbance.

2.6 <u>Discussion</u>

In the current study we assessed the potential of an acoustic-wave facilitated filtration technique to enrich BMA from an elderly patient cohort for the nucleated cell population, and tested the hypothesis that such cell enrichment enhances the regenerative efficacy of BMA.

This study demonstrated effective volume reduction in BMA from the femoral canal of a cohort of elderly patients. Following filtration to achieve a 4-fold reduction in volume, a corresponding 3.4-fold enrichment of viable nucleated cells and a 3.9-fold enrichment of CFU-Fs was observed (difference not significant), demonstrating this device to be effective for the intended function of SSC enrichment. Furthermore, the average filtration time of 18 minutes proved the viability and practicality for intra-operative clinical application of the device.

There was a wide variation of CFU-F/ml from the aspirated marrow of this cohort of patients (29-2108 CFU-F/ml), though interestingly, a wide range was also seen in a young cohort previously tested (710-1440 CFU-F/ml) (unpublished observations: JN Ridgway and SJ Curran, Smith & Nephew Ltd., 2010). These values are also consistent with a recent study comparing CFU-F numbers obtained from the iliac crest and the femoral canal (Cox *et al.* 2012). Furthermore dilution of marrow with peripheral blood during sampling is also likely to account for some variability (Horn *et al.* 2008, Cuthbert *et al.* 2012). This may explain the variable outcomes seen in clinical practice, and may account for the low CFU-F counts following concentration by centrifugation in the seven cases of non-union in Hernigou's series (Hernigou *et al.* 2005b). BMA from our cohort of elderly patients had a mean of 380 CFU-F/ml, significantly lower than the therapeutic threshold of 1000 CFU-F/ml suggested by Hernigou and colleagues.

A phenomenon of age-related decline in CFU-F number has been suggested by some authors (Muschler *et al.* 2001, Stolzing *et al.* 2008), although other studies have demonstrated maintenance of SSC number and function with ageing, including in osteoarthritic and osteoporotic bone (D'Ippolito *et al.* 1999, Stenderup *et al.* 2001, Oreffo *et al.* 1998). Nevertheless, the clinical indication for bone tissue engineering technology is most applicable to the elderly population, and the low CFU-F number found in this cohort of elderly patients highlights the pressing need for cell enrichment strategies in clinical practice. Enrichment of CFU-F by 3.7-fold over all samples filtered increased the mean value in concentrated aspirate to 1185 CFU-F/ml. There was a

close correspondence between volume reduction and concentration of viable nucleated cell count relative to both total volume and erythrocyte number indicating good specificity of filtration. Additionally, enriched aspirate contained significantly higher concentrations per ml aspirate of cells expressing three widely used SSC markers.

Following on from significant previous clinical and preclinical studies indicating the importance of SSC concentration for bone repair (Connolly *et al.* 1989, Connolly *et al.* 1991, Hernigou *et al.* 2005a and Hernigou *et al.* 2005b, Jäger *et al.* 2011, Pittenger *et al.* 1999), we designed two *in vitro* experiments to probe the regenerative significance of BMA cell concentration by assessing the effect of cell concentration on skeletal differentiation and seeding efficiency.

Following culture in osteo-, chondro- and adipogenic differentiation conditions, an enhanced osteogenic and chondrogenic response, but reduced adipogenic differentiation was observed in concentrated populations compared with populations derived from unconcentrated BMA. Interestingly, these significant differences, which reflect differences of initial cell-seeding density between treatments, were observed despite a relatively low small fold-difference in cell number (2.54) after the initial phase of expansion. These results thus underline the importance of cell concentration for the outcome of skeletal regeneration strategies. The importance of higher cell density for chondrogenic differentiation is well established, and provides the rationale for micromass culture approaches to chondrogenic differentiation (Pittenger et al. 1999, Johnstone et al. 1998). The influence of initial cell seeding density on osteogenic and adipogenic differentiation, however, remains controversial (Jaiswal et al. 1997, McBeath et al. 2004, Lu et al. 2009, Holy et al. 2000, Lode et al. 2008). The reduced adipogenic responsiveness observed in this study may be a function of the increased levels of ALP activity, indicating early osteogenesis, observed in basal cultures of concentrated BMA.

The seeding of cells onto 3D scaffolds and matrices is an important step in many tissue engineering approaches. Several recent studies have made use of allograft or allograft substitute materials seeded with BMA (Tilley *et al.* 2006, Jäger *et al.* 2011, Bolland *et al.* 2006), so the demonstration that cells enriched by the acoustic filtration method adhere in greater numbers onto allograft following enrichment is highly significant. In the current study we have demonstrated a significant enhancement of seeding efficiency in concentrated BMA over unconcentrated BMA. Furthermore the current studies show that the effect is not only a function of higher nucleated cell number within

a given plasma volume (though this is itself an important observation in a technique where volume is often a limiting factor), but that seeding efficacy is improved critically as a function of reduced erythrocytes. This is consistent with a previous study demonstrating the positive effect of erythrocyte lysis on CFU-F growth (Horn *et al.* 2008) and indicates that even in a situation where cell number is limiting, filtration of erythrocytes is itself of benefit for tissue engineering strategies utilising BMA. The negative impact of erythrocyte number on seeding efficiency may offer an insight into why concentration of SSCs is of regenerative significance independent of total number of SSCs delivered.

The current study provides evidence for the importance of BMA NC concentration for cell differentiation and seeding of scaffolds using an approach designed to be applicable intra-operatively. There of course remains substantial heterogeneity within this fraction with the CFU-F population constituting, in this cohort, a mean of only 0.012% (+/-0.013%) of total nucleated cells. Furthermore, well-documented functional heterogeneity exists within the CFU-F fraction itself (Sengers et al. 2010, Phinney 2012). There is thus considerable scope for further enrichment of SSCs and a large body of research is devoted to developing approaches to achieving this. It should be noted however that while this and previous studies (Connolly et al. 1989, Connolly et al. 1991, Hernigou et al. 2005a and b, Horn et al. 2008, Jäger et al. 2011) have indicated the importance of CFU-F concentration for regenerative outcome, the increments of benefit derived from further enrichment steps are yet to be defined experimentally in the current context of bone grafting and the relationship of concentration and efficacy is not necessarily straightforward (Cuomo et al. 2009, Jayakumar and Di Silvio 2010). Further work is therefore required to confirm the benefits of further enrichment in balance with the risks inherent in increasingly involved processes.

In conclusion, the null hypotheses that: 'negative pressure-assisted filtration does not significantly enhance the concentration of SSCs in human BMA' and 'enrichment of SSCs in human BMA by negative pressure-assisted filtration does not enhance osteogenic and chondrogenic cell differentiation and seeding efficiency onto allogeneic bone graft' can both be rejected.

This study provides evidence for the importance of BMA concentration for cell differentiation and seeding. We have presented an efficient and inexpensive alternative to the current clinical intra-operative strategies for administration of concentrated BMA. This solution to cell enrichment is amenable for development towards a single-use device that can be applied intra-operatively within the sterile field, thus offering considerable potential for clinical benefit.

Chapter III

Tantalum Trabecular Metal – Addition of human skeletal cells to an established orthopaedic implant to enhance bone-implant interface strength and clinical application

I gratefully acknowledge Dr Bram Sengers from the School of Biomedical Engineering, Southampton, for performing and analysing the mechanical testing component of this study. I thank Professor Anton Page for demonstrating and supervising my use of the electron microscope and Dr David Johnston for performing laser confocal microscopy. I also thank Mr Alex Aarvold and Mr Edward Tayton for many productive discussions which helped to direct this study, Miss Esther Ralph, Ms Stefanie Inglis and Miss Spandan Kalra for their laboratory support and the Orthopaedic Surgeons and theatre staff at University Hospital Southampton for assistance in acquiring bone marrow samples. Except where specified, all components of this study were performed by me.

A paper detailing this study has recently been published in the *Journal of Tissue Engineering* and Regenerative Medicine

A presentation based on this study was awarded first prize at the British Orthopaedic Research Society meeting, Cambridge, 2011

3.1 Introduction

3.1.1 Current clinical strategies for bone stock replacement

Autograft bone represents the current favoured standard clinical therapy for replacement of lost or damaged bone stock in a diverse range of musculoskeletal pathologies. However, despite excellent osteoconductive and inductive properties, the application of autograft is severely restricted due to pragmatic factors associated with donor site morbidity and dysfunction, thus only small defects can usually be treated (Giannoudis et al. 2005). As a result, allograft has been used as a substitute for over 30 years despite its reduced osteoinductivity – a consequence of processing to remove potential antigenicity. This results in a reparative structure that often heals by fibrosis and granulation, and is therefore frequently regarded as a 'void filler' rather than a true living construct (Ling et al. 1993; van der Donk et al. 2002; van Haaren et al. 2007). More recently, the addition of SSC populations to allograft has been demonstrated to improve the osteogenic and mechanical properties of allograft (Bolland et al. 2006; Bolland et al. 2007; Tilley et al. 2006), with in vivo incorporation and remodelling into the existing bone (Aarvold et al. 2011). However, there are major caveats to the use of allograft, including: i) cost, ii) structural variability, iii) potential for disease transmission, and iv) limited supply, driving the search for synthetic alternatives (Delloye et al. 2007).

3.1.2 The rationale for extending the clinical application of tantalum

Despite its current high cost, the clinical use of tantalum in orthopaedic implants has recently undergone an expansion, with increasing component options and configurations for widening applications (Bobyn *et al.* 2004, Levine *et al.* 2006, Patil *et al.* 2009). Tantalum, a transition metal element (symbol Ta, atomic number 73) is the 49th most abundant element on earth, making up around 1.7 ppm by weight (Singh 2009). (Fig. 3.1) Currently, it is mined primarily for the electronics industry, and the orthopaedic market makes up only a small percentage of tantalum consumption (Maccauro *et al.* 2009, Buckman 2000). Its main use today is in capacitors and high-fidelity electronic components, but its ductility, resistance to corrosion and inert nature are attractive in a variety of other applications. As such, it has been used safely in medical devices and implants for several years, and once it gains more routine clinical

use and is mined for the healthcare industry in its own right, the wholesale price of tantalum for orthopaedic components is only likely to decrease.

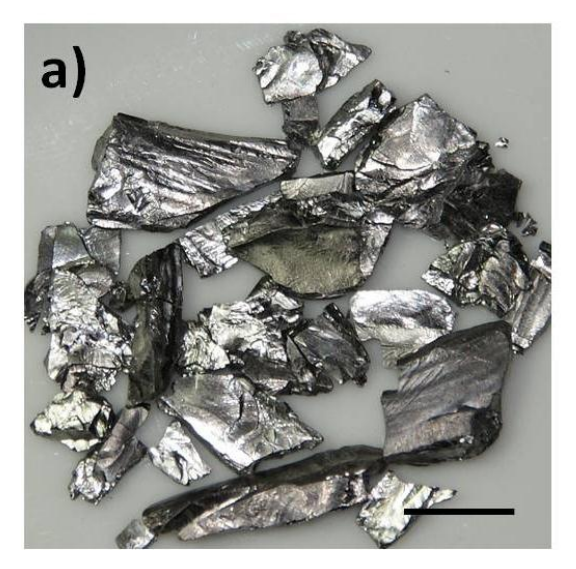


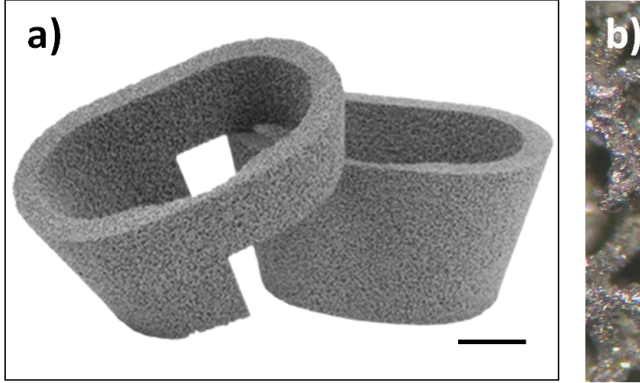


Fig. 3.1 Elemental tantalum a) after extraction from ore **b)** following isolation and purification. Scale bars: 10 mm. *Images from: a) http://images-of-elements.com/tantalum.php, b)* http://michael5000.blogspot.co.uk/2010/01/januarys-element-of-month-tantalum.html

Tantalum possesses characteristics that confer great advantages over traditional implant materials: it is chemically stable and biocompatible and can be manufactured to form a trabecular consistency similar to bone. The technology of chemical vapour infiltration and foam deposition onto a carbon skeleton, has allowed Tantalum Trabecular Metal (TTM) to be manufactured in a variety of different geometric net-shapes with a range of pore sizes to suit different applications (Bobyn *et al.* 1999a, Balla *et al.* 2010a) (Fig. 3.2). Furthermore, despite its high density, in a trabecular form tantalum possesses a favourable strength to weight ratio and has superior ductility to many alternative materials (Aubry *et al.* 2009, Shimko *et al.* 2005). These characteristics place it in an excellent position to combine it with regenerative medicine techniques for orthopaedic application.

The mechanical properties and established clinical safety of TTM already define this material as a useful orthopaedic implant particularly suited to scenarios where local bone density is low, or in applications where poor implant integration would be envisaged with non-porous alternative implants (Flecher *et al.* 2008, Gross and Goodman 2005, Lachiewicz and Soileau 2010). Excellent bone in-growth characteristics have been demonstrated in human and animal models (Bobyn *et al.*

1999b, Boscainos et al. 2007, Nehme et al. 2004) and it does not display some of the major disadvantages of allograft. However, current TTM implants rely on an interference fit into stable bone, and are not indicated to provide an immediate stable construct when bone stock is inadequate (Bobyn et al. 2004, Patil et al. 2009). In applications where there is poor initial implant stability, or when TTM is used in conjunction with bone grafting, loading may need to be limited until sound integration has occurred. Such scenarios will become increasingly common, particularly as the cohort of patients requiring revision or subsequent re-revision operations of hip and knee arthroplasty surgery is destined to increase dramatically over the coming years (McNamara IR 2010). Although TTM, which is neither degradable nor capable of remodelling, is not the consummate substitute for lost bone stock, it does possess several advantages over allograft that justify the use of pragmatic techniques to enhance its therapeutic properties. Development of enhanced bone-implant integration strategies will improve patient outcomes, dramatically extending the clinical applications of TTM as a substitute for allograft, particularly in elderly patients who have a limited biological reserve and need to be able to weight bear early.



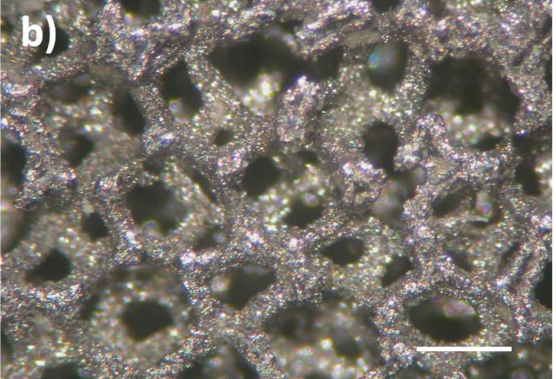


Fig. 3.2 Trabecular tantalum as supplied by manufacturer a) tibial augments for treating bone loss during revision total knee arthroplasty **b)** magnified image of cut surface of trabecular tantalum, demonstrating trabecular conformation and significant porosity. Scale bars: a) 10 mm, b) 1 mm. *Image a) from http://zimmer.com.*

3.2 Objectives

Although the interaction of tantalum with human SSCs has previously been reported (Findlay *et al.* 2004, Matsuno *et al.* 2001, Sagomonyants *et al.* 2011, Stiehler *et al.* 2008), a direct comparison of cell interaction between tantalum in trabecular conformation and current gold standards for skeletal tissue engineering, autograft and allograft, has never been undertaken.

This study examines the osteoconductive and inductive capacity of TTM in relation to allograft and autograft, to determine the potential of TTM with the addition of human skeletal stem cells in tissue engineering applications as an alternative to the current accepted standard treatments for loss of skeletal tissues.

3.3 Null hypothesis

- 1. TTM does not support skeletal cell growth and osteogenic differentiation comparable to allograft and autograft.
- 2. The addition of skeletal stem cells to TTM *in vitro* does not enhance early bone-TTM interface strength.

3.4 Materials and methods

3.4.1 Materials

Tissue culture reagents and all staining agents were purchased from Sigma, Aldrich, UK unless otherwise stated. CTG and EH-1 were purchased from Molecular Probes, Leiden, Netherlands. TTM was kindly donated by Zimmer Ltd., Swindon, UK.

3.4.2 Cell culture

Skeletal cell populations (primary passage) were obtained from the bone marrow of haematologically normal patients undergoing primary total hip replacement at University Hospital Southampton with the approval of the Local Research Ethics Committee (LREC 194/99) following informed patient consent, as previously described (Bolland et al. 2006). In brief, SSCs were harvested by repeatedly washing the marrow in aMEM and removing the washed cell population prior to centrifugation at 1100 rpm for 5 minutes at 4°C. The cell pellet was re-suspended in 10 ml αMEM and passed through a 70 µm filter. The cell fraction was plated into tissue culture flasks and incubated in basal medium (αMEM with 10% FCS) at 37°C in 5% CO₂. Cells immunoselected using the STRO-1 antibody were isolated by Magnetically Activated Cell Sorting (MACS) as described previously (Howard et al. 2002; Stewart et al. 1999). Cells were washed in sterile phosphate buffered saline (PBS) and media changes repeated every 3-4 days. Upon confluence the cells were released using 10% trypsin (Lonza, Wokingham, UK), centrifuged and re-suspended in basal medium, and the total cell count was determined using a haemocytometer. Specified cell concentrations were then seeded onto TTM, allograft or autograft constructs (as described in sections 3.4.6 and 3.4.8) and incubated in either basal (10% FCS) or osteogenic (basal medium supplemented with 100 µM ascorbate-2-phosphate and 10 nM dexamethasone) conditions. Control samples were incubated without cells in basal medium.

3.4.3 Tantalum preparation

TTM with a porosity of 75-85% was cut with a Buehler IsoMet Low Speed saw using a Series 15LC Diamond Wafering Blade (Buehler, Düsseldorf, Germany). Samples were then sterilised in 70% ethanol for 2 hours and washed in sterile PBS prior to use.

3.4.4 Allograft preparation

Allograft was cut into the specified size and shape from the calcar region of a single femoral head, removed during total hip arthroplasty for osteoarthritis. Samples were defatted in 2% hydrogen peroxide and washed five times consecutively in sterile PBS.

3.4.5 Autograft preparation

Autograft was taken from the calcar region of a second femoral head, removed during total hip arthroplasty for osteoarthritis. Samples were kept sterile, and were otherwise untreated.

3.4.6 Analysis of skeletal cell penetration and viability

Tantalum, allograft and autograft were cut into 3x2x2 mm cuboids and sizes were verified to +/- 0.03 mm using a digital calliper (RS Components Ltd, Corby, UK). Cuboids of each material were cultured in pairs (in either basal or osteogenic conditions) for 28 days on non-tissue culture plastic. Each culture group was seeded with either: 5x10⁵ unselected SSCs derived from the same patient as the autograft samples; 5x10⁵ STRO-1 positive cells in osteogenic conditions, from a third patient, or no cells (negative controls). After 28 days in culture, cuboids were taken from each group for live/dead immunostaining, cell proliferation assays, deoxyribonucleic acid (DNA) and ALP expression, and for molecular profiling.

3.4.6.1 Live/dead immunostaining

CTG was used to label viable cells (after 14, 28 and 63 days incubation) and EH-1 for necrotic cell nuclei. The samples were washed in PBS and then incubated for 90 minutes in 1 ml of standard CTG/ EH-1 solution (10 µg/ml CTG, 5 µg/ml EH-1). Samples were fixed in ethanol and stored in PBS prior to fluorescence microscopy using a standard fluorescein isothiocyanate (FITC) filter or for confocal microscopy using a Leica SP5 Laser Scanning Confocal Microscope and software (Leica Microsystems, Wetzlar, Germany).

3.4.6.2 Collagen type I and Bone Sialoprotein immunostaining

Following incubation, samples of TTM were fixed in 4% paraformaldehyde and immunostained with the anti-type I collagen (LF-67, rabbit polyclonal, 1:300 dil.) antibody provided by Dr L Fisher or anti-bone sialoprotein antibody (rabbit polyclonal, 1:100 dil.) antibody provided by Dr J Sodek. Following incubation with species-specific Alexa Fluor 594-labelled secondary antibodies and 4',6-diamidino-2-phenylindole (DAPI) nuclear counterstain, samples were visualised using a Zeiss Axiovert 200 inverted microscope (Carl Zeiss Ltd. Welwyn Garden City, UK). Negative controls (i.e. omission of the primary antibodies) were included in all immunostaining protocols.

3.4.6.3 WST-1 assay

Cell number and viability were quantified for 3 pairs of cuboids from each culture group using the WST-1 assay. After removal of the incubation medium and washing in PBS, 750 µl of 1:10 dilution WST-1 substrate (Roche Ltd, Welwyn Garden City, UK) was added to each pair. At 4 hours, three 100 µl aliquots of substrate were removed from each well and read in triplicate using a BioTek ELx-800 universal microplate spectrophotometer (BioTek, Potton, UK) at a wavelength of 450 nm. An increase in absorbance value (i.e. increase in optical density of the substrate) indicated increased cell number and viability. Mean and standard deviation were calculated for the optical densities of each group and compared to controls.

3.4.6.4 DNA assay

Cell number was determined using a standard DNA PicoGreen® assay, as previously described (Bolland *et al.*, 2006). In brief, scaffolds were washed in PBS and cells were released from the scaffold by incubation in collagenase IV (1 mg/ 5 ml medium) for 15 minutes, then 10% trypsin for 10 minutes, followed by repeated agitation and centrifugation at 1500 rpm for 10 minutes. After removal of supernatant, the material was fixed in 85% ethanol prior to air-drying. The cells were then rewashed in PBS and lysed in 1 ml of 0.5% Triton X-100 before undergoing three freeze-thaw cycles and mechanical lysis. Cell lysate was measured for DNA content using PicoGreen® (Molecular Probes, Paisley, UK) according to routine manufacturer protocol. 10 µl of lysate was run in triplicate for each well on a plate against calibrated standards, analysed using a BioTek FLx-800 microplate fluorescent reader.

3.4.6.5 Alkaline Phosphatase assay

ALP activity within the cell lysate was measured using p-nitrophenyl phosphate as the substrate in 2-amino-2-methyl-1-propanol alkaline buffer solution (Sigma, Poole, UK) according to manufacturer protocol. 10 µl of cell lysate was run in triplicate for each well on a plate against calibrated standards, analysed using a BioTek ELx-800 microplate reader.

3.4.6.6 Preparation for molecular analysis

Following incubation, samples were washed, incubated with collagenase, then trypsin and total RNA was extracted using Gibco's method with TRIzol reagent (Invitrogen, UK) for molecular analysis. Extracted RNA was subjected to DNase treatment (DNA-free RNA kit, Zymo Research, UK) and reverse-transcribed using the Super-Script First-strand system for RT-PCR (Reverse Transcription Polymerase Chain Reaction). Quantitative real-time RT-PCR (qRT-PCR) was performed using a 96-well optical reaction plate and a 7500 Real-Time PCR system (Applied Biosystems, Carlsbad, USA). Following complementary DNA (cDNA) synthesis, each sample underwent RT-PCR against a panel of osteogenic gene primers (Table 3.1). Values were calculated using the comparative threshold cycle (Ct) method and normalised to β -actin expression. Values were expressed as the mean \pm SD and expression was recorded relative to unselected SSCs incubated on allograft bone in basal medium.

Table 3.1 Osteogenic gene primer sequences used for RT-PCR

Primer		Sequence	
Beta actin (housekeeping gene)	β-actin	F: 5'-GGCATCCTCACCCTGAAGTA R: 5'-AGGTGTGGTGCCAGATTTTC	
Alkaline Phosphatase	ALP	F: 5'-GGAACTCCTGACCCTTGACC R: 5'-TCCTGTTCAGCTCGTACTGC	
Collagen type I alpha I	Col1A1	F: 5'-GAGTGCTGTCCCGTCTGC R: 5'-TTTCTTGTTCGGTGGGTG	
Runt-related transcription factor 2	RUNX-2	F: 5'-GTAGATGGACCTCGGGAACC R: 5'-GAGCTGGTCAGAACAAAC	
Sex determining region Y, box 9	SOX-9	F: 5'-CCCCAACAGATCGCCTACAG R: 5'-GAGTTCTGGTCGGTGTAGTC	

F = Forward, R = Reverse. Courtesy of Dr R. Tare, Bone and Joint Research Group, University of Southampton

3.4.7 Analysis of cellular morphology and penetration

3.4.7.1 Scanning Electron Microscopy

20x10x10 mm cuboids of TTM were cultured with or without 5x10⁵ SSCs for 21 days in osteogenic conditions, with regular medium changes. Following incubation, samples were fixed whole in 3% glutaraldehyde and 4% formaldehyde in 0.1M PIPES buffer (1,4-Piperazinediethanesulfonic acid) at pH 7.2. A post-fixative of 1% osmium tetroxide was applied before dehydrating in graded ethanols. Over 24 hours, the specimens were embedded in TAAB resin (TAAB Laboratories, Aldermaston, UK) after graded acetonitrile-resin steps and polymerised at 60°C. The embedded specimens were then sectioned using a Buehler 15LC Diamond Wafering Blade with copious irrigation (Fig. 3.3). Following dissolution of the resin with sodium ethoxide and 100% ethanol, the cut surface was silver-coated and visualised with a Quanta 200 Scanning Electron Microscope (SEM, FEI, Oregon, USA), to demonstrate the penetration of cells within the TTM.

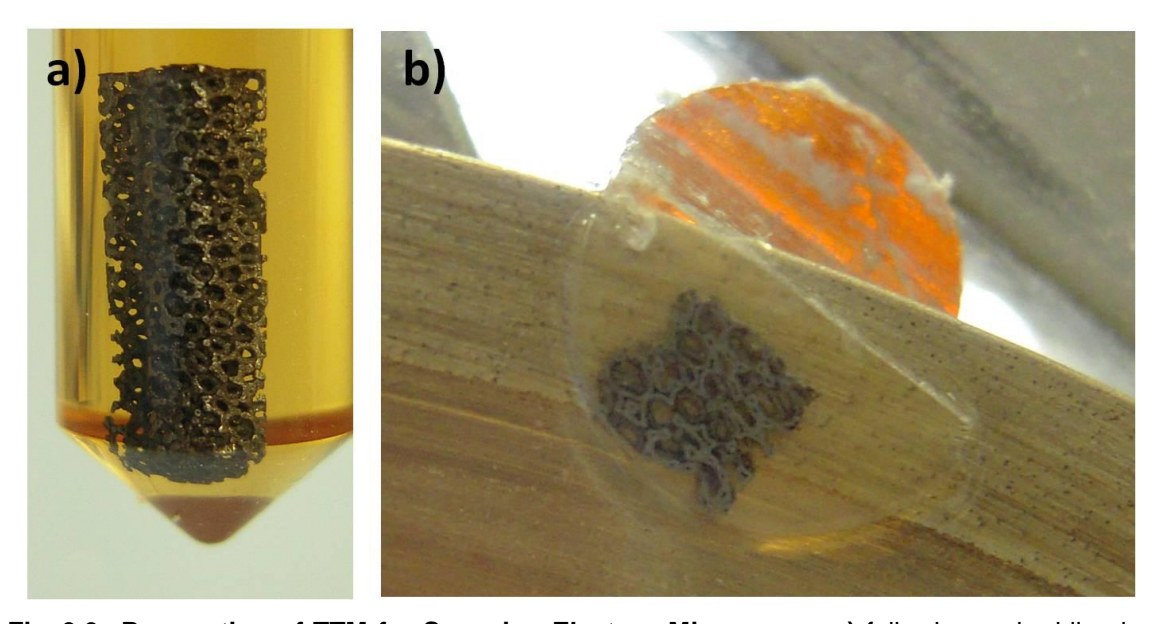


Fig. 3.3 Preparation of TTM for Scanning Electron Microscopy, a) following embedding in TAAB resin, b) during sectioning with a diamond wafering blade

3.4.8 Analysis of mechanical 'pull-apart' strength

Multiple (10x12x1 mm) sections of TTM and allograft were prepared and their dimensions verified as described, before sterilisation. Constructs of TTM/TTM, TTM/allograft or allograft/allograft were fabricated by sandwiching the two materials together in perpendicular directions with a custom-made polyethylene clip, to ensure a contact overlap area of precisely 10x10 mm. Test constructs were each seeded with 5x10⁵ SSCs (passage 2, from the same patient) and incubated for 9 weeks in osteogenic conditions before removing the clip and performing direct tensile 'pull-apart' strength assessment using a Bose EnduraTEC ELF3220 mechanical tester (Bose, Eden Prairie, Minnesota, USA), with a custom-made jig. Data were analysed using WinTest 2.58 data acquisition software and Matlab v 7.9.0 (Mathworks, Cambridge, UK).

3.4.9 Statistics

All experiments were run at least three times, with six replicates for mechanical tests, statistical analysis was performed using SPSS Ver. 18.0. Statistical comparison was made using Student's unpaired t-test with a p value less than 0.05 taken to be significant.

3.5 Results

3.5.1 Cellular proliferation, viability and immunostaining

Following culture of SSCs on TTM, adherent matrix was readily visible macroscopically within 14 days (Fig. 3.4 a) There was no substantial macroscopic difference in cell number or adherence between the two media types, and live-dead staining with CTG and EH-1 confirmed excellent adherence of viable cells throughout the trabecular matrix from an early stage of incubation, with cellular matrix coating the entire surface of tantalum (Fig. 3.4 b and c).

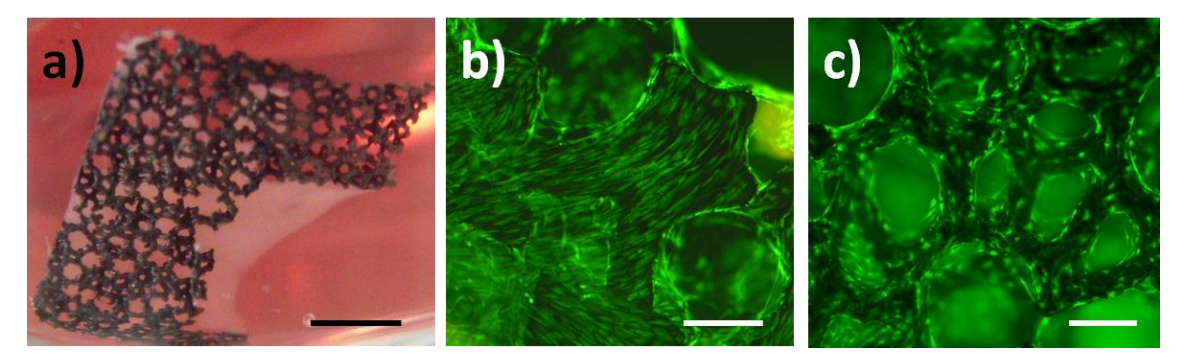


Fig. 3.4 Cellular proliferation and viability following culture with TTM: a) Macroscopic appearance of trabecular tantalum after culture with SSCs, abundant cellular matrix is visible adhering to the tantalum structure, **b)** and **c)** Live–dead staining after culture of: **b)** unselected SSCs in basal medium for 14 days; **c)** STRO-1 positive cells in osteogenic medium for 14 days; note the altered morphology of cells after incubation under osteogenic conditions. Scale bars: a) 5 mm, b) and c) 200 μm.

Cells maintained a flattened fibroblastic phenotype following culture in basal medium, however cells grown in osteogenic conditions displayed an enhanced osteoblastic morphology, with a pronounced cuboidal appearance (Fig. 3.5).

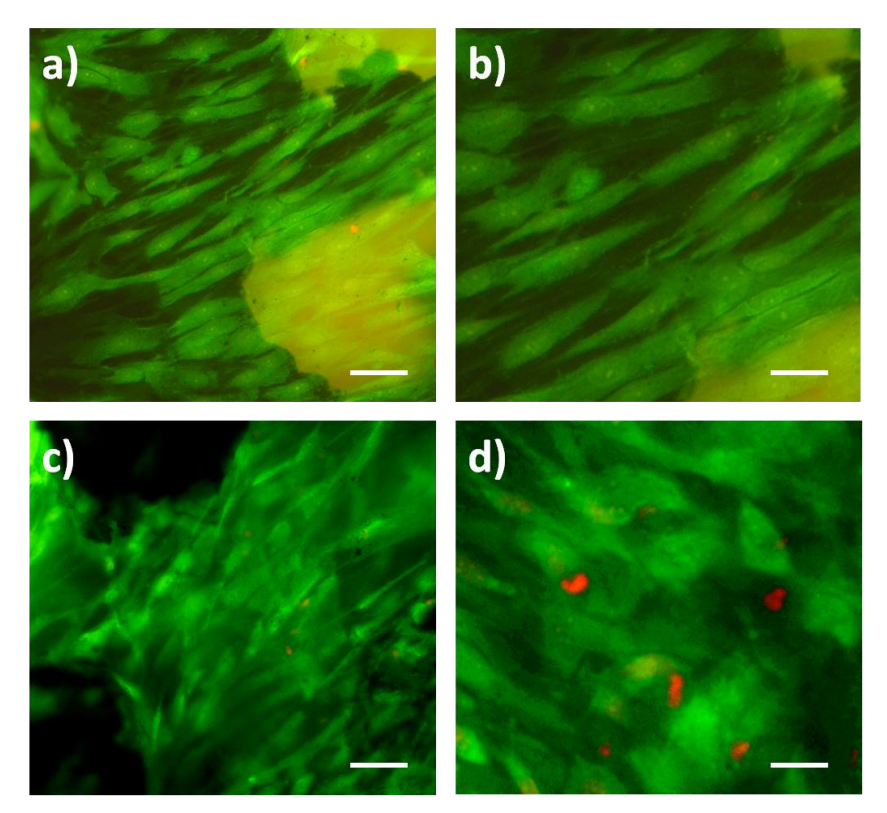


Fig. 3.5 Live/dead analysis of unselected SSCs grown on TTM: in basal (a) and b)) and osteogenic conditions (c) and d)); cells grown in basal conditions retained a fibroblastic phenotype, whereas osteogenic conditions stimulated phenotypic changes of SSCs to a more cuboidal osteoblastic morphology on TTM. Scale bars: a) and c) 200 μ m, b) and d) 500 μ m.

Confocal microscopy following extended culture periods demonstrated live SSCs surrounding a few dead cells (Fig. 3.6 a). Cross-sectional imaging achieved by confocal microscopy confirmed deep cellular in-growth between trabecula (Fig. 3.6 b).

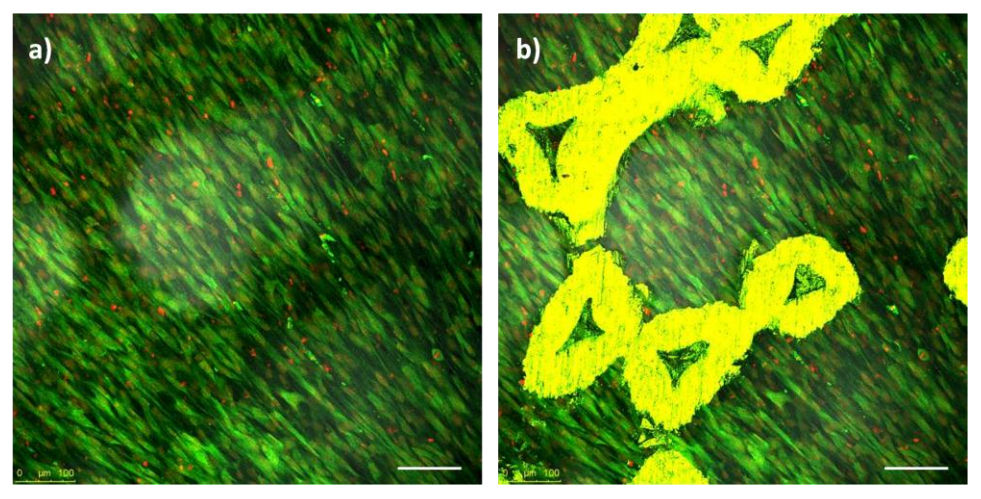


Fig. 3.6 Confocal microscopy of TTM cultured with SSCs in osteogenic medium: demonstrating live (green) and dead (red) cell staining; a) just superficial to the tantalum surface – the tantalum lattice is visible as a 'shadow' in the image; b) deeper within the trabecula of tantalum – the cut 'skeleton' surface is visible as bright yellow. Note the monopolar direction of the cells. Scale bars: $100 \ \mu m$.

Cells within the superficial layer, outside of the trabecular structure of tantalum were arranged in a haphazard fashion, but in deeper regions within the trabecula, cells were observed to be closely aligned (Fig. 3.7 a-c).

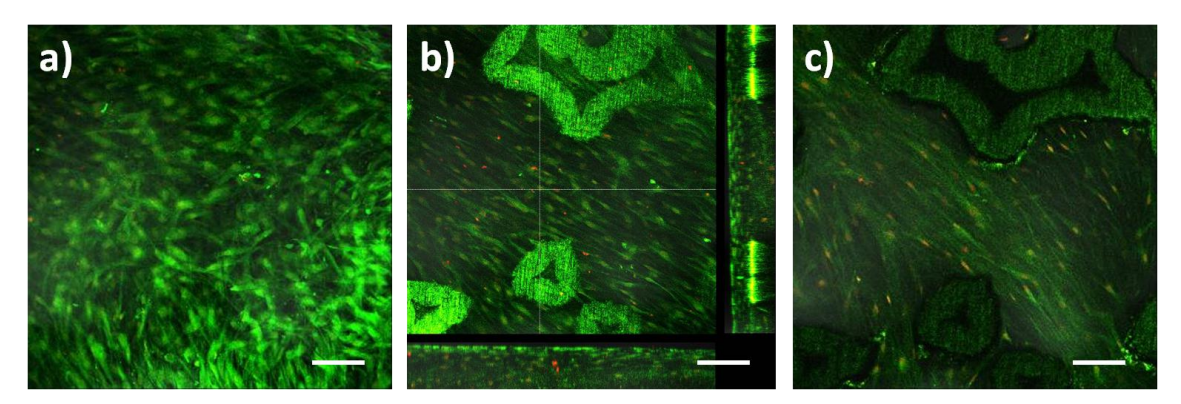


Fig. 3.7 Sequential 'slices' of SSCs growing on TTM: a) superficial to c) deep; b) demonstrates the cross-sectional profile of cellular growth on TTM to a depth of approximately 100 μ m, centred upon the cross-hairs; there was deep penetration of live cells into the structure with a consistent cytoplasmic alignment. Scale bars: 100 μ m

Immunostaining with collagen type I and BSP confirmed abundant ECM adherent to the surface and significantly, deep within the trabecular conformation, displaying high levels of collagen fibre organisation (Fig. 3.8).

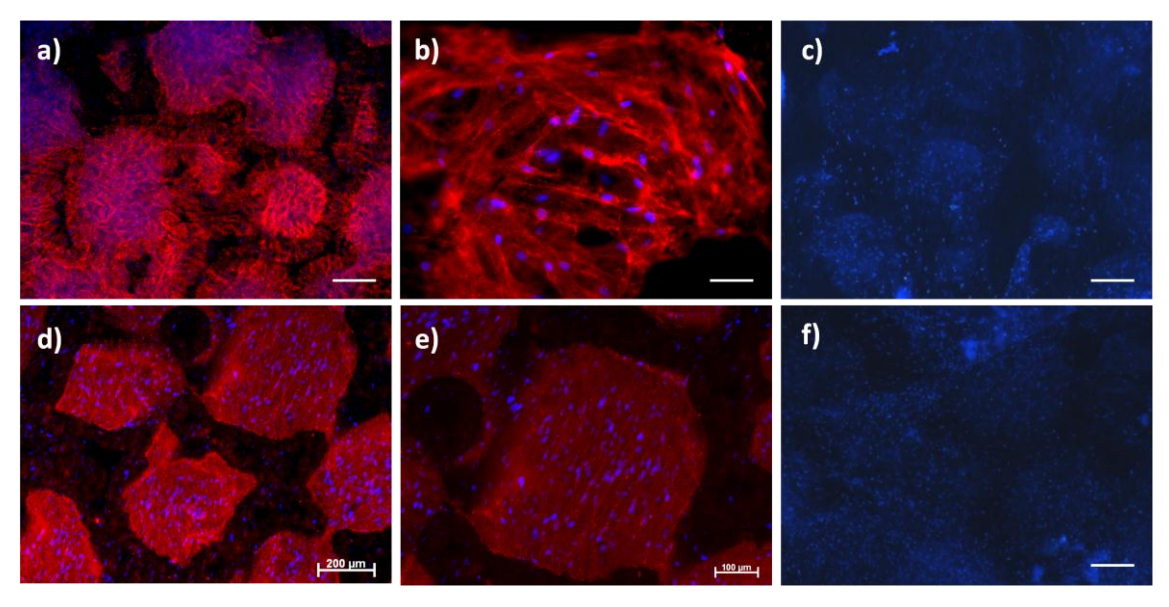


Fig. 3.8 Immunocytochemistry of cells cultured on TTM for 63 days: a) and b) Collagen type I, d) and e) BSP, c) and f) respective negative controls. Abundant ECM adherent to the surface fluoresces with Alexa Fluor 594 (red) and deep within the trabecular conformation, with high levels of collagen fibre organisation. Multiple cells are demonstrated by DAPI nuclear counterstain (blue) throughout the constructs. Scale bars: a, c, d and f = 200 μ m, b = 50 μ m, e = 100 μ m.

Live/dead analysis was also performed following culture of cells on allograft, TTM or autograft after 28 days in basal, osteogenic or selected STRO-1 positive cells in osteogenic conditions, to obtain a direct comparison between scaffolds (Fig. 3.9). In basal medium, cells were almost confluent on allograft (Fig. 3.9 b) but appeared fully confluent throughout both TTM and autograft (Fig. 3.9 f and j). When cultured in osteogenic conditions, fewer cells were visible on allograft compared to either TTM or autograft (Fig. 3.9 c, g and k). In addition, cells on allograft retained a fibroblastic morphology even when cultured in osteogenic conditions, whereas cells cultured with TTM or autograft had a cuboidal morphology. STRO-1 positive cells produced abundant ECM, particularly when cultured on TTM in osteogenic conditions (Fig. 3.9 d, h and l).

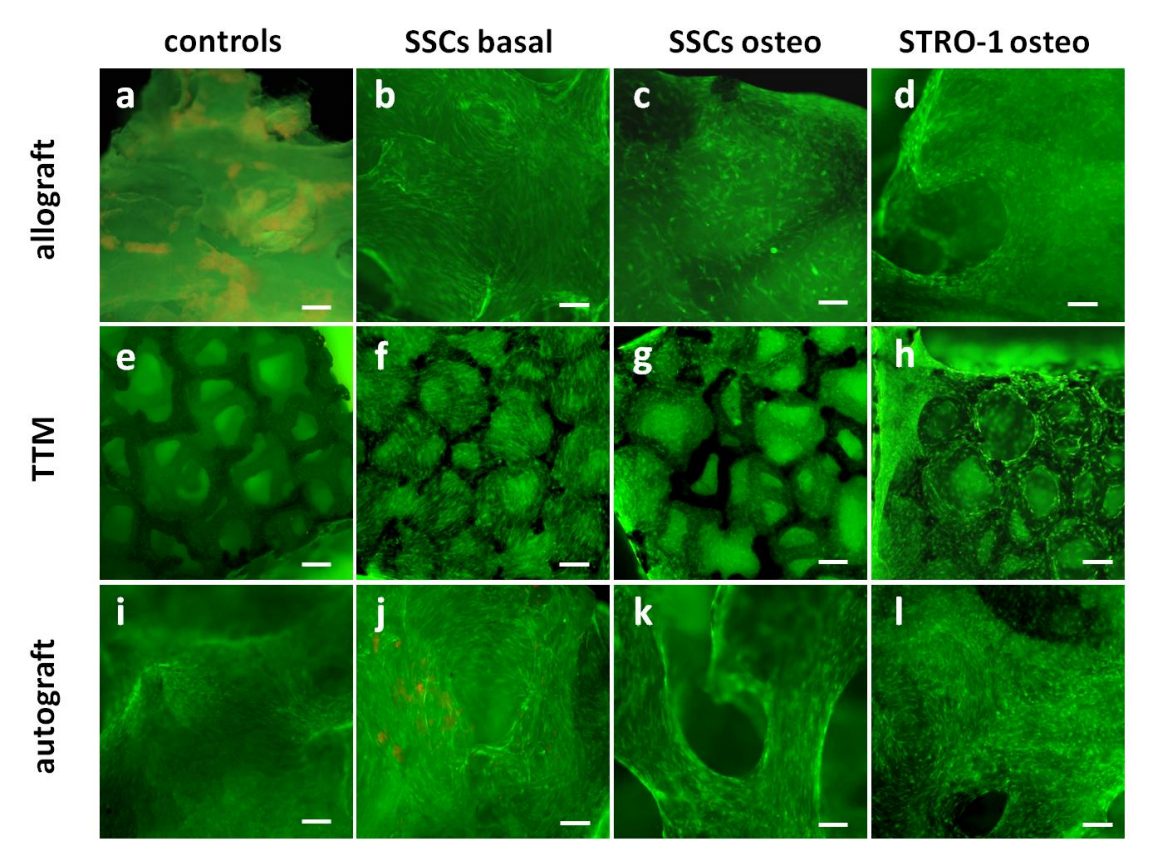


Fig. 3.9 Comparison of live/dead SSCs grown on allograft, TTM or autograft after 28 days in basal, osteogenic or selected STRO-1 positive cells under osteogenic conditions. Note that there were confluent cells on the control autograft (i), due to intrinsic cellular activity and proliferation over the culture period (in basal medium), but no live cells on control allograft (a) or TTM (e). In basal medium, cells were less dense on allograft (b) but appear entirely confluent throughout both TTM (f) and autograft (j). When cultured under osteogenic conditions, there were fewer cells visible on allograft (c) compared to the other constructs (g, k); in addition, cells on allograft retained a fibroblastic morphology under osteogenic conditions. STRO-1 positive cells produced abundant ECM, particularly when cultured on TTM (h). Scale bars: 200 μm

3.5.2 Analysis of cell proliferation

Following 28 days culture in basal or osteogenic conditions, proliferation of cells on TTM was compared with current clinical standard bone stock replacements, allograft and autograft using the WST-1 cell proliferation assay (Fig. 3.10). The autograft control showed relatively high proliferation in the absence of exogenous cells, given the intrinsic cellular activity of untreated autograft, confirmed also by live/dead images (Fig. 3.9 i). TTM supported an enhanced number of proliferating cells in comparison to allograft (p<0.001), and similar numbers to autograft irrespective of the culture conditions (p>0.05). In contrast, selected STRO-1 positive cells displayed significantly greater proliferation within TTM than either allograft or autograft in osteogenic conditions (p<0.001).

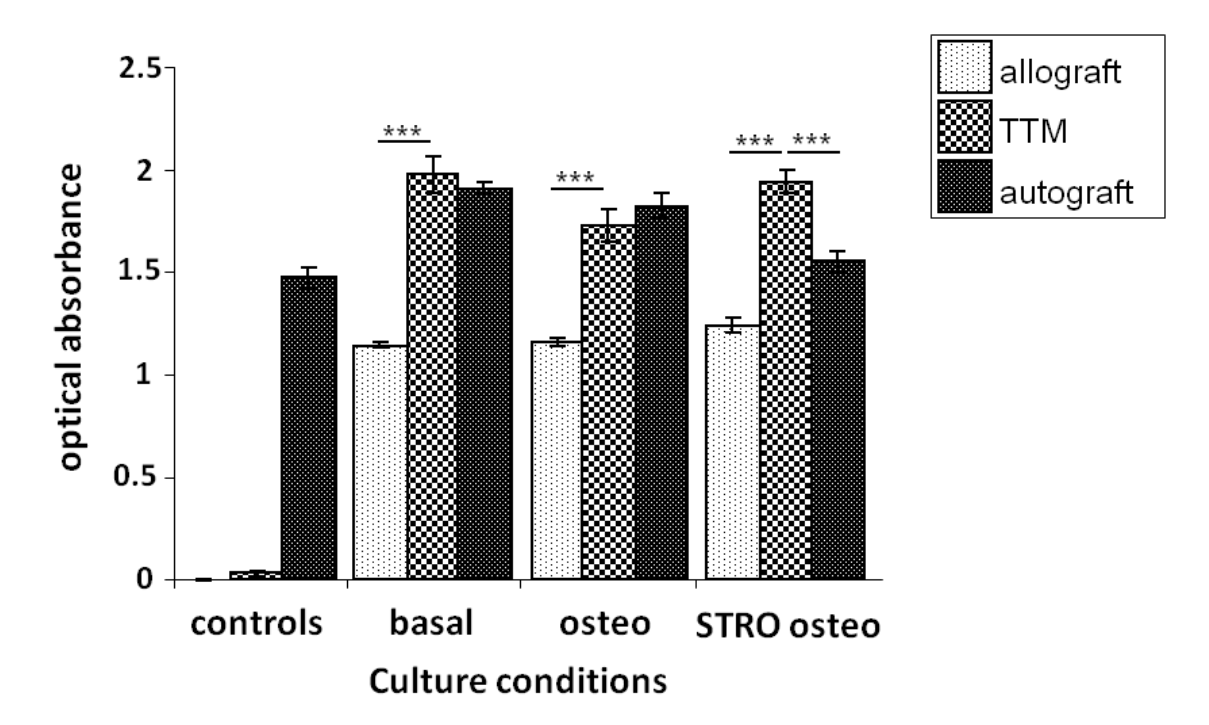


Fig. 3.10 Graph comparing cellular activity on allograft, TTM and autograft under basal and osteogenic conditions as measured by WST-1 cell proliferation assay. Control samples were cultured without additional cells in basal medium. High activity was present in control autograft due to intrinsic cellular activity. Error bars are SD, ***p<0.001.

3.5.3 Analysis of DNA, ALP and specific ALP Activity

Control autograft displayed significant intrinsic DNA activity, although ALP expression in this group was low suggesting minimal osteoinductive stimulus following incubation in basal medium (Fig. 3.11 and 3.12). When cultured with unselected SSCs in basal

medium, TTM demonstrated significantly greater DNA expression to allograft (p<0.05) but no significant difference to autograft (p>0.05). ALP activity on TTM was significantly lower than both allograft (p<0.01) and autograft (p<0.001) in these culture conditions, a trend reflected in specific ALP activity (Fig. 3.13). Following incubation with unselected SSCs in osteogenic conditions, there was no significant difference between allograft and TTM for DNA and ALP expression, however the clinical gold standard, autograft performed significantly better (p<0.001), supporting enhanced DNA and ALP activity. Consequently, specific cellular activity was similar for all groups cultured in osteogenic conditions (Fig. 3.13). Furthermore, when selected STRO-1 positive cells were cultured with each scaffold in osteogenic conditions, although the trends for DNA activity with unselected SSCs were replicated (Fig. 3.11), ALP activity was significantly higher on TTM than allograft (p<0.001) (Fig. 3.12), confirming that TTM specifically supports selected skeletal progenitor cell proliferation. In addition, STRO-1 positive cells cultured in osteogenic conditions displayed significantly enhanced specific ALP activity in the TTM group compared with both allograft (p<0.01) and autograft (p<0.05) (Fig. 3.13).

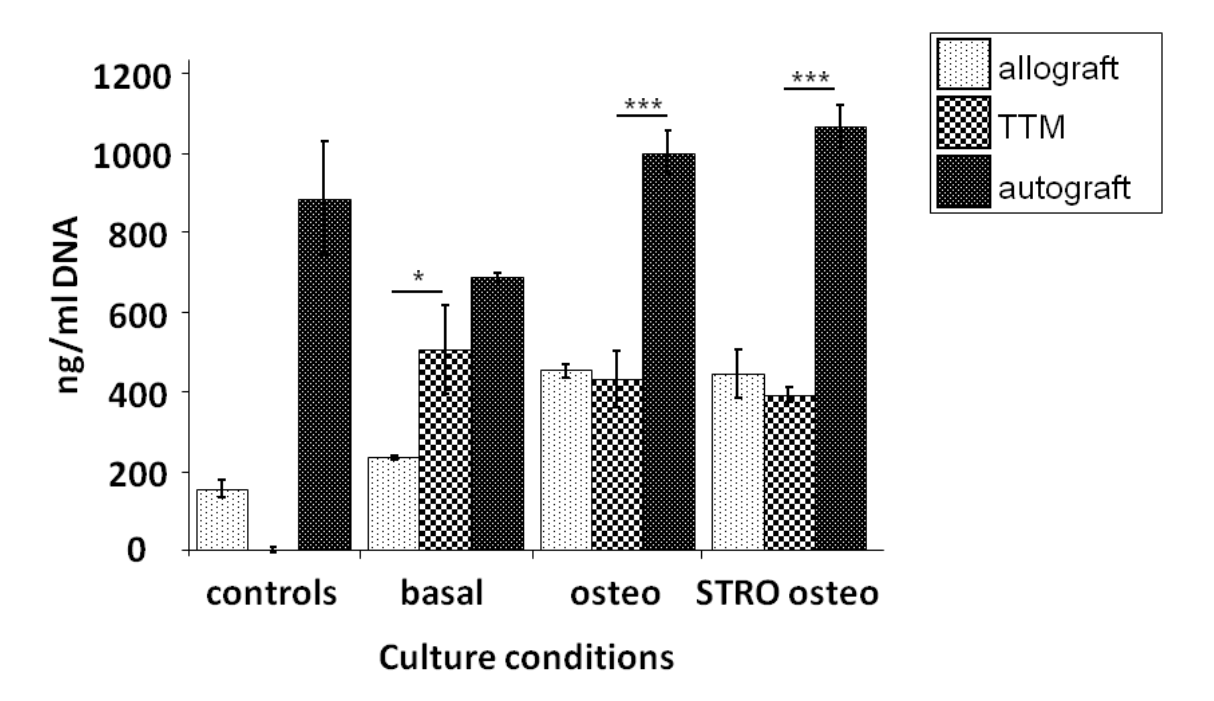


Fig. 3.11 Graph comparing cellular DNA activity on allograft, TTM and autograft under basal and osteogenic conditions. Control samples were cultured without additional cells in basal medium, although some activity was present in control allograft, due to residual cellular material following washing, and high activity was present in control autograft due to intrinsic cellular activity. Error bars are SD, $^*p < 0.05$, $^{***p} < 0.001$.

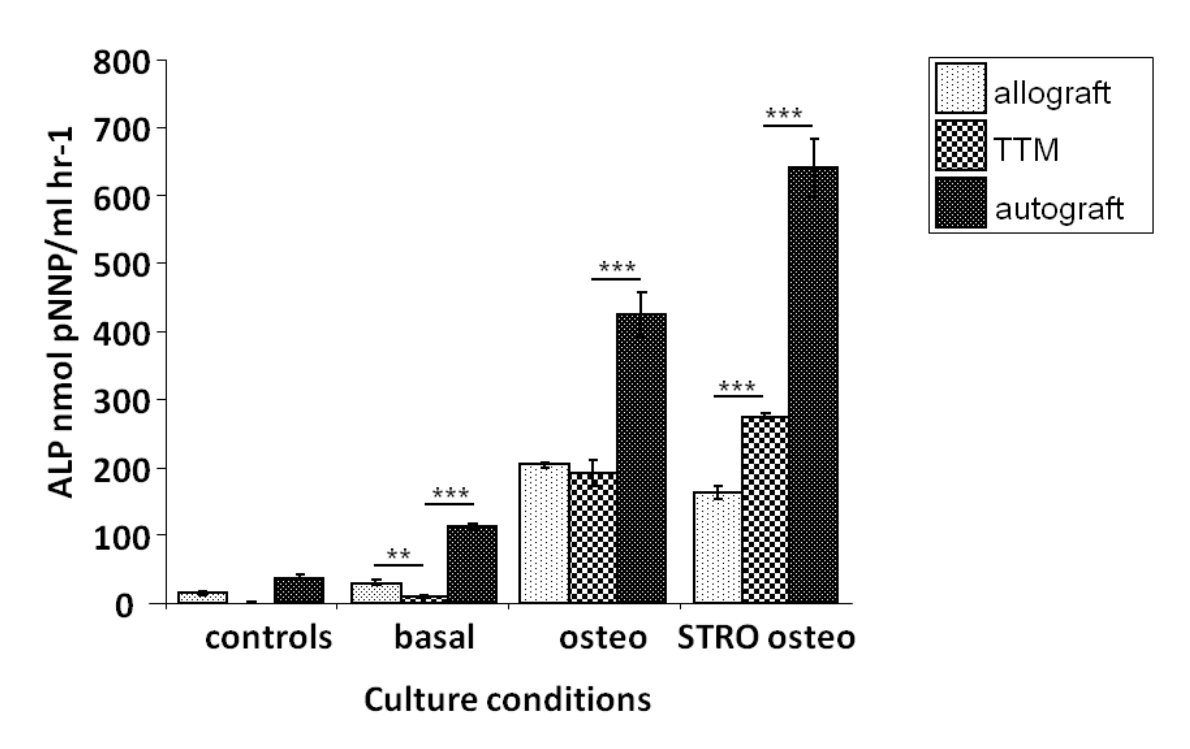


Fig. 3.12 Graph comparing cellular ALP activity on allograft, TTM and autograft under basal and osteogenic conditions. Control samples were cultured without additional cells in basal medium, although some activity was present in control allograft, due to residual cellular material following washing, and high activity was present in control autograft due to intrinsic cellular activity. Error bars are SD, **p < 0.01, ***p < 0.001.

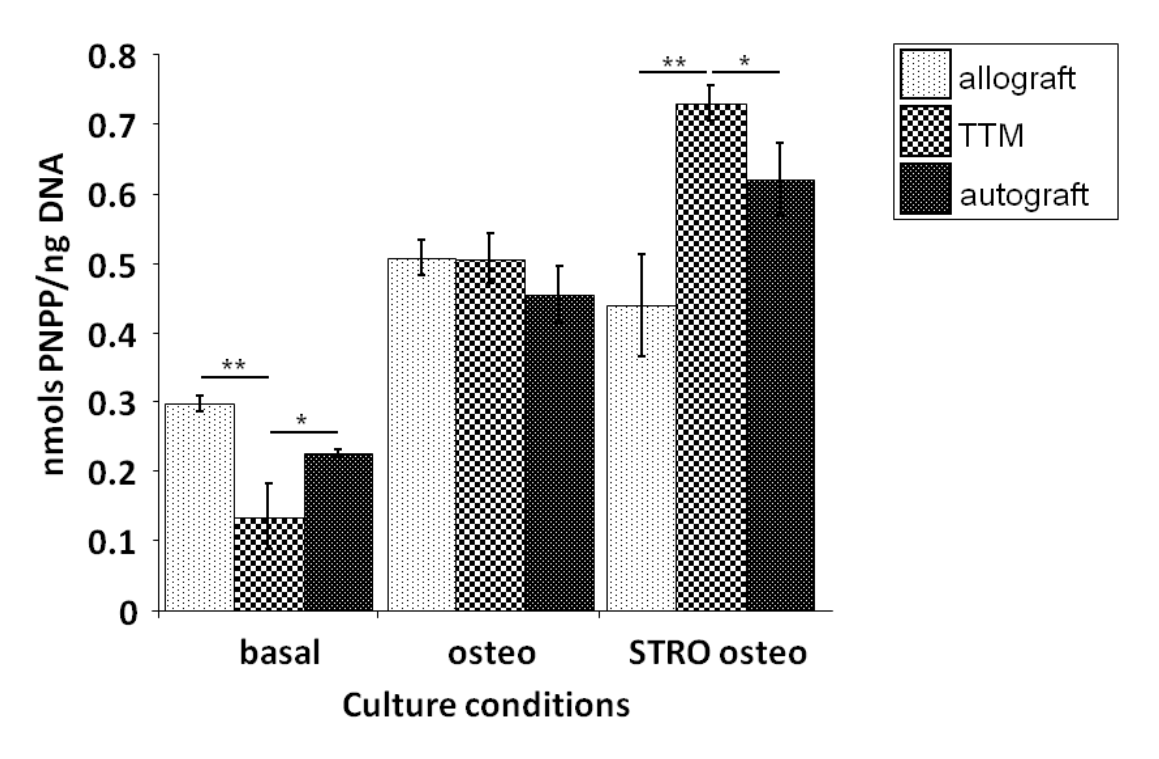


Fig. 3.13 Graph comparing specific cellular ALP activity on allograft, TTM and autograft under basal and osteogenic conditions. STRO-1 positive cells cultured in osteogenic conditions, displayed significantly enhanced specific ALP activity in the TTM group to both allograft (p<0.01) and autograft (p<0.05). Error bars are SD, *p < 0.05, **p < 0.01.

3.5.4 Molecular analysis

Molecular expression of allograft, autograft and TTM were compared for a panel of osteogenic genes following culture in basal and osteogenic conditions (Fig. 3.14).

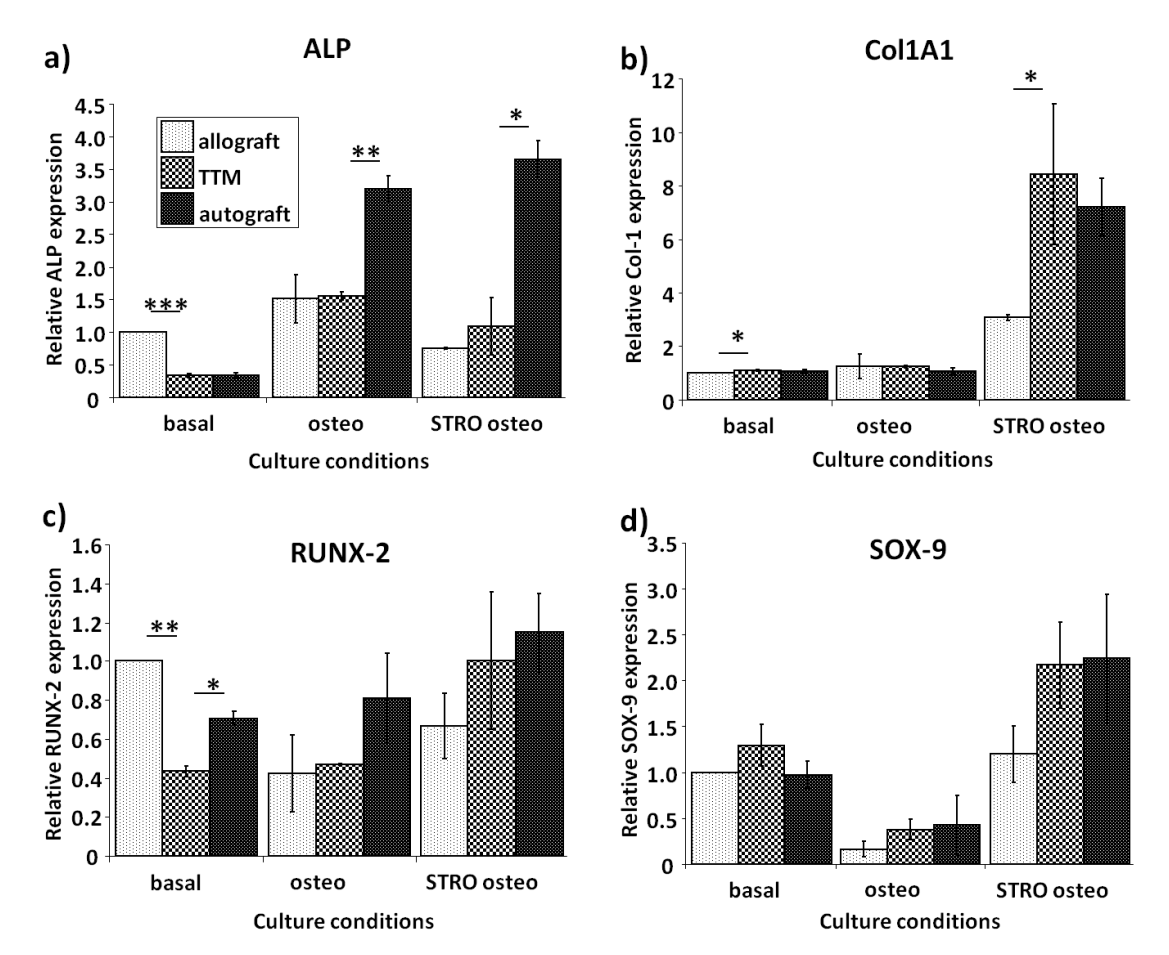


Fig. 3.14 Molecular expression of a panel of osteogenic genes of interest. All values are expressed relative to β-actin expression of unselected SSCs incubated on allograft in basal medium: **a)** ALP expression was highest in STRO-positive and unselected cells grown under osteogenic conditions on autograft. Although there was minimal ALP expression on both TTM and autograft in basal conditions, after osteogenic stimulation, TTM supported similar ALP expression to allograft; **b)** Col1A1 expression of unselected cells in TTM was similar to allograft and autograft in both basal and osteogenic conditions, although when cultured with STRO-positive cells, expression of Col1A1 on TTM was significantly higher than allograft and not significantly different to autograft. There was no significant difference in expression of RUNX-2 (c) or SOX-9 (d) on any scaffold under osteogenic conditions with either cell type; however, there was a trend under osteogenic conditions for TTM to support higher osteogenic gene expression than allograft. Error bars are SD, *p < 0.05, **p < 0.01, ***p < 0.001

ALP expression was highest in STRO-1 positive and unselected cells grown in osteogenic conditions on autograft. Although there was minimal ALP expression on both TTM and autograft in basal conditions, following osteogenic stimulation, TTM supported similar ALP expression to allograft (Fig. 3.14 a). Col1A1 expression of

unselected cells in TTM was comparable to allograft and autograft in both basal and osteogenic conditions, although following culture with STRO-1 positive cells, expression of Col1A1 on TTM was significantly higher than allograft, and not significantly different to autograft. There was no significant difference in expression of RUNX-2 or SOX-9 on any scaffold in osteogenic conditions with either cell type. Interestingly, there was a trend, in osteogenic culture conditions, for TTM to support higher osteogenic gene expression than allograft.

3.5.5 Analysis of cellular morphology and penetration

SEM of control (cultured in osteogenic media, processed and embedded but not seeded with cells) TTM revealed a regular trabecular structure (Fig. 3.15). The carbon framework was visible within the cut end-on trabecula, and high magnification revealed a crystalline deposition of tantalum (Fig. 3.15 c).

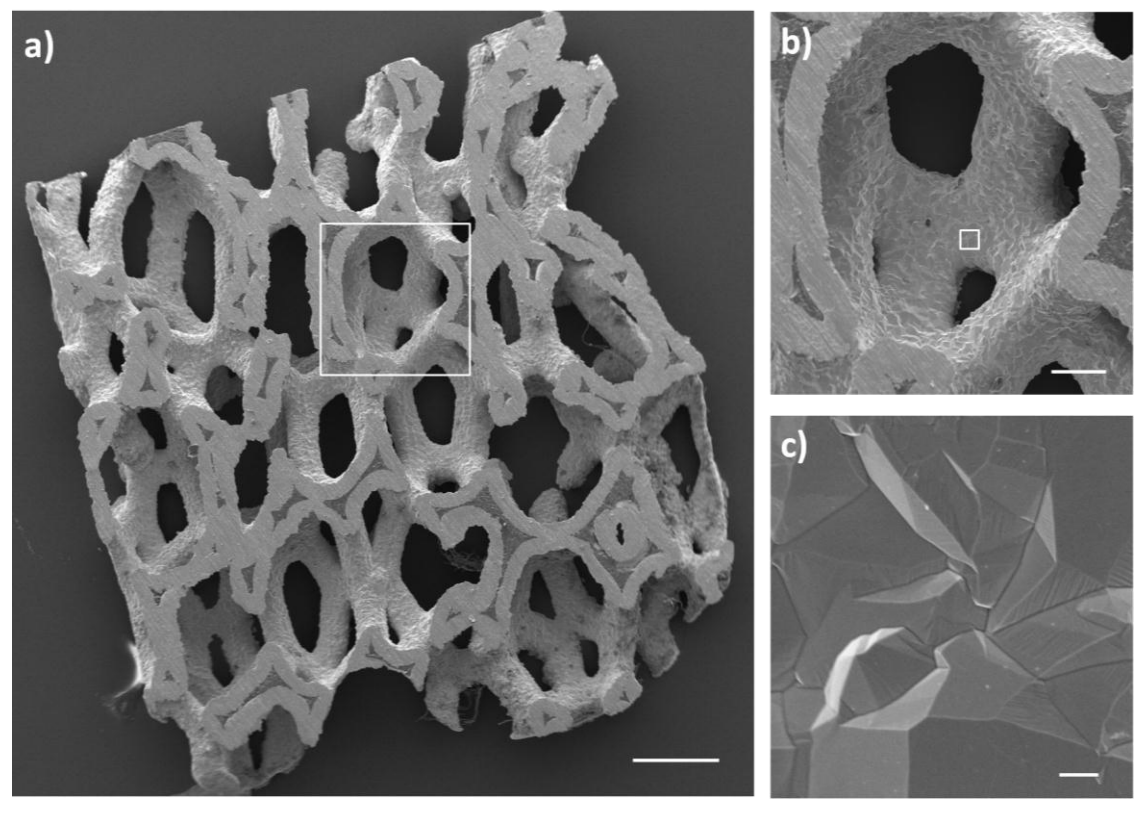


Fig. 3.15 SEM images of control TTM section, showing a) cut surface with intact trabecular structure, b) Magnified view of boxed area, c) Further magnified view (boxed area in b) demonstrating crystalline surface of tantalum. Scale bars: a) 500 μm, b) 100 μm, c) 2 μm.

Following culture for three weeks, SSCs were observed tightly adherent to the TTM surfaces, with projecting cell membranes and early matrix deposition (Fig. 3.16 a). SSCs were observed throughout the TTM, indicating sufficient nutrient delivery and osteogenic stimulation (Fig. 3.16 b and c). Furthermore, the cuboidal phenotype of cells was retained, even at depths of 1 cm (Fig. 3.16 c).

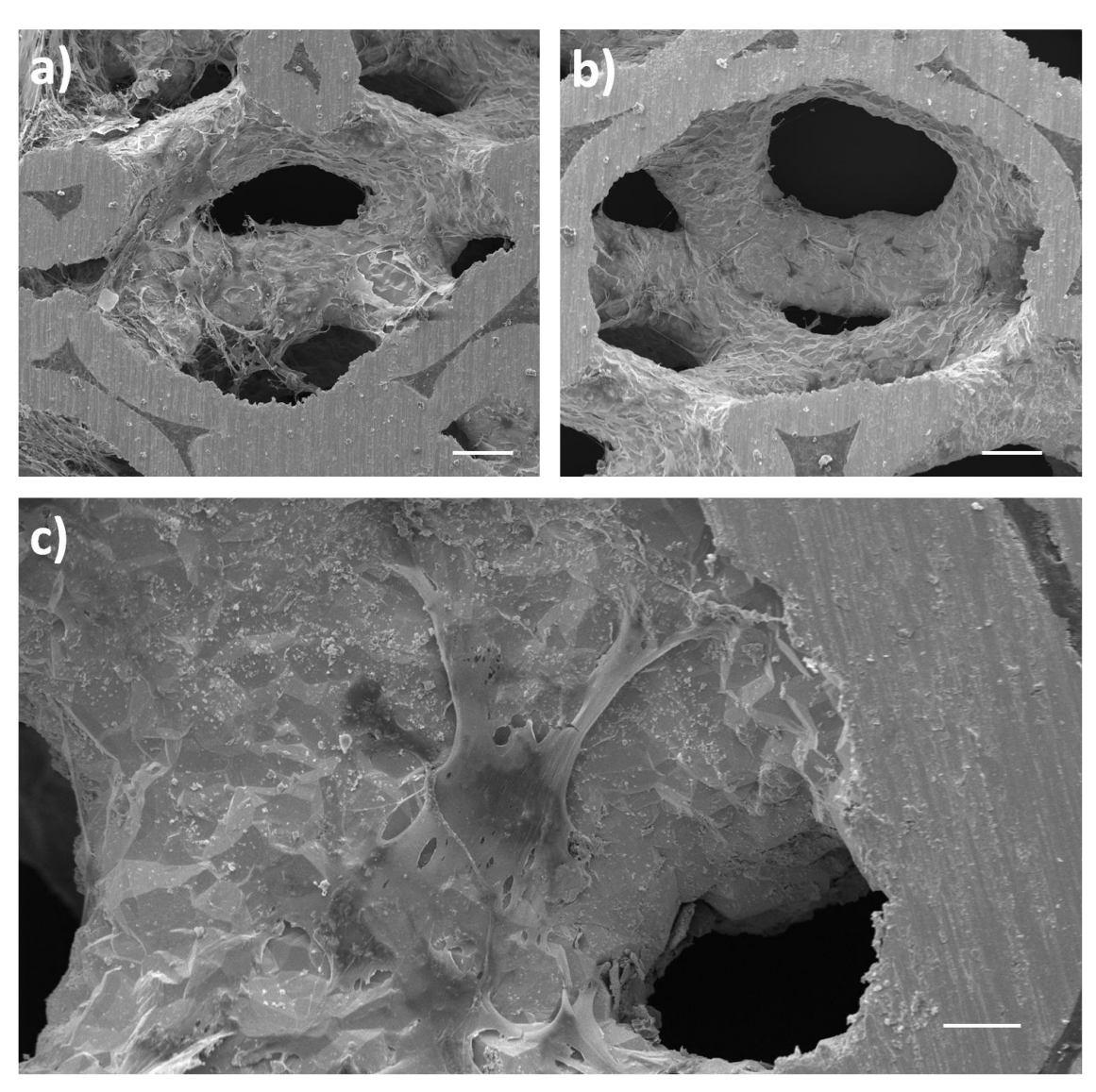


Fig. 3.16 SEM image of TTM cultured with SSCs for 3 weeks: a) demonstrates a section 5 mm deep, with multiple cells and matrix almost obscuring the underlying tantalum; $\bf b$ in the deeper zones (approximately 750 μ m), there are fewer cells, but they maintain interconnecting projections; $\bf c$) The cuboidal morphology of cells was maintained even at 1 cm depth, suggesting adequate nutrient delivery and osteogenic stimuli.

3.5.6 Mechanical 'pull-apart' strength

The three different acellular control constructs all displayed low tensile properties, and they did not differ significantly (maximum pull-apart stress of less than 0.02 N/m²). All constructs cultured with cells for 9 weeks displayed a significantly greater 'pull-apart' strength than acellular controls (p<0.05, 4.91x10³ N/m² for allograft/allograft (SD 1.79x10³), 7.52x10³ N/m² for TTM/allograft (SD 4.00x10³) and 1.02x10⁴ N/m² for TTM/TTM (SD 5.32x10³)). Although there was no significant difference between cellular allograft or TTM constructs, there was a trend to greater strength with TTM (an effect over and above any surface friction effects) (Fig. 3.17).

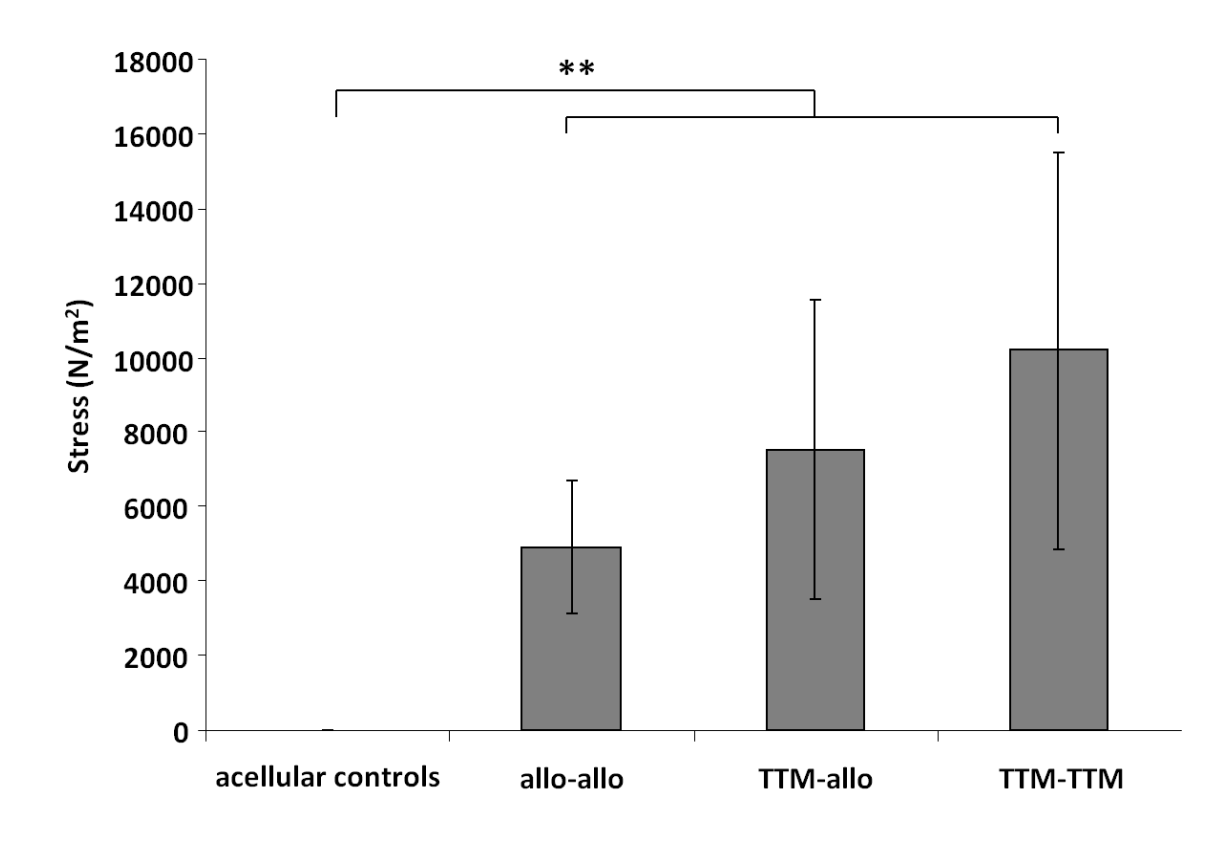


Fig. 3.17 Maximum mechanical 'pull-apart' stress for the different cellular constructs, cultured in osteogenic conditions for 9 weeks, in comparison to acellular controls. There is a significant increase in pull-apart strength for all cellular constructs (p<0.01) when compared to acellular controls. Although there is a trend towards increasing pull-apart strength in constructs containing TTM, this was not statistically significant. Error bars are SD, **p < 0.01.

3.6 Discussion

Recent research into skeletal tissue regeneration has centred upon the application of a structural, osteoconductive material combined with factors to enhance osteoinductive properties (Smith *et al.* 2011). However, the quest for suitable alternatives to biological materials for skeletal reconstruction has been complicated by the requirement for regulatory approval of any putative novel material before clinical implantation.

Following encouraging biocompatibility and osteogenesis assessments, the clinical use of tantalum in orthopaedic implants has recently undergone an expansion (Bobyn *et al.* 2004, Levine *et al.* 2006, Patil *et al.* 2009). Despite the high cost of tantalum, increasing component options and configurations are becoming available for widening applications. Particular advantages are conferred by the technology of chemical vapour infiltration and foam deposition onto a carbon skeleton, which has allowed TTM to be manufactured in a variety of different geometric net-shapes with a range of pore sizes to suit different applications (Balla *et al.* 2010; Bobyn *et al.* 1999a). The porosity of TTM used in this study was 75-85%, consistent with that of human cancellous bone (Shimko *et al.* 2005). Consequently, normalisation of each experimental group to volume resulted in approximately identical surface areas for cellular adherence and growth. The physical bulk and composition of TTM make it an attractive alternative to allograft, which has poor inherent structural properties amongst other drawbacks. Furthermore, tantalum forms a stable surface oxidation layer by self-passivation (Levine *et al.* 2006).

Our results confirmed excellent adherence and proliferation of SSCs on TTM in basal and osteogenic conditions, with deep penetration of viable cells visible on confocal and SEM beyond 5 mm depth, indicating the macro-porous three-dimensional structure is appropriate for cellular proliferation. Osteogenic stimulation resulted in a cuboidal cellular phenotype, consistent with increased expression of ALP both at a molecular and biochemical level. The ordered arrangement of cells grown on TTM, seen on confocal microscopy (Fig. 3.6 and 3.7 b and c) is not a feature of cells grown on allograft or a number of other scaffolds and only cells in close contact with the metal surface exhibited this arrangement. It is unclear whether the effect is mediated by chemical signals, surface nanotopography or macroporous effects, however, the presence of the metal in itself appears to act as a co-ordinating marker for cellular growth and positioning, and it may be possible in future to modulate the properties of TTM to enhance this property (Dalby et al. 2007; McMurray et al. 2011; McNamara LE et al. 2010). In addition to cellular proliferation, this study has demonstrated abundant,

organised ECM production (Fig. 3.4 a, 3.8, 3.9), which is a prerequisite for early shear and tensile strength in the clinical scenario.

Direct comparisons of SSC proliferation on TTM and those cultured on autograft and allograft, confirmed the potential of TTM to support cellular proliferation to levels comparable with allograft in all culture conditions, similar to autograft in osteogenic conditions. Although TTM did not enhance osteogenic differentiation of cells in basal conditions, ALP assays and molecular profiling demonstrated robust osteogenic differentiation when stimulated with osteogenic medium.

Mechanical testing confirmed that the addition of SSCs to TTM constructs significantly enhances the interface strength of the construct, and is in keeping with the exuberant production of ECM seen in cultured samples. It should be noted that this analysis is only a model of the clinical scenario and cannot replicate exactly the processes found *in vivo*. Clinical failure of a TTM component may be due to several factors, including different loading modes, such as shear, however we chose to measure only direct 'pull-apart' strength because no account was then needed of the frictional effects of TTM at the metal-bone interface. This provides an assessment of the direct cellular contribution to the construct's strength in the early stages after implantation, allowing a direct comparison to allograft. Moreover, the addition of appropriate temporally-controlled factors to the TTM construct to encourage angiogenesis and mineralisation may further enhance these properties.

In 1999, Bobyn *et al.* showed bone in-growth and enhanced osseointegration of TTM at intervals of up to 52 weeks in a transcortical canine model (Bobyn *et al.* 1999a). The authors also reported bone in-growth of 0.2 to 2 mm in canine acetabular tantalum components at 6 months (Bobyn *et al.* 1999b). Primary stability is always necessary in clinical orthopaedic use, and if an interference fit is not present at initial operation, additional techniques such as the use of cement, autograft or allograft, may be required (Flecher *et al.* 2010, Nabavi and Field 2009). Although the surface consistency of TTM displays a high coefficient of friction with bone, and its porosity promotes long-term tissue integration, any technique to expedite this process will be beneficial to the patient (Deglurkar *et al.* 2007; Hacking *et al.* 2000).

In 2004, Findlay *et al.* found no difference in osteoblast growth rates, gene expression, cell adherence or morphology between polished or textured tantalum discs *in vitro* versus tissue culture plastic (Findlay *et al.* 2004). They concluded that tantalum with

either a smooth or a microtextured surface treatment supports human osteoblast growth and differentiation in this two-dimensional model. In a further study, immortalised human mesenchymal stem cells cultured on smooth titanium, tantalum and chromium surfaces showed the same capacity for proliferation, and osteogenic differentiation (Stiehler et al. 2008). Welldon et al. compared the growth of human osteoblasts on three-dimensional TTM with tissue culture plastic, concluding that TTM is suitable for osteoblast growth and differentiation and may enhance mineralisation (Welldon et al. 2008). Further, TTM was superior to both tissue-culture plastic and titanium fibre mesh in stimulating bone formation in human osteoblast cultures of elderly patients, a particularly relevant finding in view of the ageing demographic (Sagomonyants et al. 2011). However, it is not yet understood whether this effect is brought about by the specific physicochemical properties of the material, its threedimensional structure, or both. The present study takes account of the threedimensional structure of TTM and its high porosity, which are important to encourage the appropriate fluid-flow characteristics for cellular infiltration and also provide a direct comparison with allograft and autograft (Sengers et al. 2009; Shimko et al. 2005).

In conclusion, the null hypotheses that: 'TTM does not support skeletal cell growth and osteogenic differentiation comparable to allograft and autograft' and 'the addition of skeletal stem cells to TTM *in vitro* does not enhance early bone-TTM interface strength', can both be rejected.

This study demonstrates the capacity of TTM to support skeletal cell growth and osteogenic differentiation and also the enhancement of the mechanical properties of TTM attributable to its interaction with SSCs.

These results support the use of TTM in clinical applications with the addition of SSCs as an alternative to allograft for tissue engineering osteo-regenerative strategies in the context of lost bone stock. Such clinical scenarios will become increasingly common given the ageing demographic, the projected rates of revision arthroplasty requiring bone stock replacement and the limitations of allograft. Early stage stability is important to reduce excessive implant motion and allow subsequent bone formation to provide long term integration (Bragdon *et al.* 1996), and this direct comparison with allogeneic and autogenous bone graft demonstrates that the addition of cells to TTM may extend the therapeutic options for TTM. Evaluation in animal models and preparation for clinical translation are planned.

Chapter IV

In vivo evaluation of novel ternary polymer blend scaffolds for skeletal tissue engineering strategies using a murine model

I am grateful to Dr Ferdous Khan at the University of Edinburgh for providing the polymer blend scaffolds and performing the initial high throughput characterisation (4.4.1 - 4.4.5). I also gratefully acknowledge the assistance of Dr Rahul Tare in providing a template for *in vitro* analysis, Dr Stuart Lanham for undertaking the CT scans and Dr Janos Kanczler for supervising the *in vivo* component and performing CT analysis, in addition to the technical expertise of Miss Esther Ralph and Mrs Carol Roberts who undertook some of the histological protocols. All other components of this study were performed by me.

A paper detailing this study has recently been published in *Advanced Functional Materials* under joint first authorship

4.1 Introduction

The current tissue engineering paradigm relies on the optimal characteristics and performance of several factors (cells, scaffolds and growth factors) that, when combined, interact to create a new living construct (Smith et al. 2011). Of these factors, the most modifiable are the biological and mechanical properties of the scaffold. As described in Chapter I (section 1.8), multiple possibilities of scaffold material exist, however the ideal scaffold for a mass-produced regenerative strategy would be synthetic, bioresorbable, with a controlled and highly reproducible resorption profile, producing non-toxic by-products, whilst maintaining sufficient structural integrity until the newly grown host tissue is able to replace or restore the function of the native tissue (Leong et al. 2003, Cancedda et al. 2007). In addition, for osteoregenerative applications, biomaterial scaffolds are required to mimic the 3D ECM environment, providing short-term mechanical stability along with increased surface area for cell migration, adhesion and differentiation as a prequel to new tissue growth (Schultz et al. 2000). In an ideal scenario, scaffolds should have a 3D porous interconnected network structure, with porosity over 60% (Mastrogiacomo et al. 2006) and individual pore sizes ranging from submicron to macroscopic (Ma et al. 2010, Moroni et al. 2008), which favours the maintenance of cellular activity (Deng et al. 2011), nutrient exchange (Laurencin et al. 1999) and bone function (Weiner and Traub 1992, Marotti 1993). Surface nanotopography and chemistry characteristics are also thought to be pivotal in promoting cellular attachment, proliferation and mineral deposition (McMurray et al. 2011). These requirements place extremely challenging demands on the scaffold design process, which aims to fulfil each criterion without compromising another (Oreffo et al. 2005).

Polymeric biomaterials are potential candidates for tissue engineering osteoregenerative strategies and are already commercially available for use in healthcare, in applications as diverse as drug delivery systems, sutures and orthopaedic fixation devices (Nair and Laurencin 2006, Gunatillake and Adhikari 2003) (Table 4.1). Certain specific polymeric formulations have the advantage of clinical approval (EMA (European Medicines Agency) in the EU, or FDA (Food and Drug Administration) in the US) and a track-record of clinical efficacy and safety. Consequently, these were prime candidates for initial assessments in regenerative medicine functions.

Highly variable chemical, mechanical and biological properties are displayed by polymer blends composed of varying combinations of base polymers and as the techniques of scaffold fabrication and manipulation have improved over recent years, the technology to manufacture and sample multiple formulations with only small chemical differences for cellular compatibility has become more commonplace.

Table 4.1 Biodegradable synthetic polymers approved for clinical use. Adapted from information in Gunatillake et al. 2003, Middleton and Tipton 2000, Zippel et al. 2010

Group	Polymer	Applications	
Polyesters	Poly(glycolic) acid – PGA	Suture (e.g Dexon by Covidien) Fracture fixation (e.g. PGA Smart Pins by Bionx)	
	Poly(L)lactic acid – PLLA	Fracture fixation (e.g. PLLA Smart Pins by Bionx) Interference screw (e.g. Bio-Interference by Arthrex) Suture anchor (e.g. Panalok by Mitek) Meniscus repair (e.g. Clearfix meniscal dart by Innovasive Devices)	
	Poly(DL)lactide - PDLLA	Pre-prosthetic maxillofacial augmentation (e.g. Sonic Pins Rx by Gebruder Martin GmbH)	
	Poly(lactide- <i>co</i> -glycolide) – PLGA	Suture (e.g. Vicryl by Ethicon) Fracture fixation (e.g. LactoSorb Screws and Plates by Biomet) Meniscus repair (e.g. SDsorb Meniscal staple by Surgical Dynamics)	
	Poly((DL)lactic-co- glycolic acid) – PDLLA co PGA	Interference screw (e.g. Biologically Quiet Interference Screw by Instrument Makar) Suture anchor (e.g. Biologically Quiet Biosphere/Mini-Screw by Instrument Makar) ACL reconstruction (e.g. Biologically Quiet Staple by Instrument Makar)	
Polylactone	Poly(caprolactone) - PCL	Suture (e.g. Monocryl by Ethicon)	
Polyether-ester	Poly(dioxanone) - PDO	Fracture fixation (e.g. Orthosorb pin by Johnson & Johnson) Suture (e.g. PDS by Ethicon)	
Polyglyconate	Poly(glycolic)acid-co- trimethylene carbonate – PGA co TMC	Suture (e.g. Maxon by US Surgical) Interference Screw (e.g. Endo-Fix screw by Smith & Nephew) Suture anchor (e.g. Suretak by Smith & Nephew)	

The exact mechanisms through which cells interact with polymers are incompletely understood, so the precise characteristics of each final scaffold cannot be predicted prior to manufacture (Shin *et al.* 2003). Consequently, the search for practical new biomaterials is characterised by a time-consuming iterative process, whereby each potential new polymer is studied for myriad desired properties, dictated by factors such as cell growth kinetics, scaffold degradation rates and rheological suitability. Subsequent structural modifications and re-evaluation are indicated until the desired material properties are reached (Oreffo *et al.* 2005).

One of the most promising techniques to overcome these challenges is the use of High Throughput (HT) chemical arrays, which allow rapid synthesis and screening of a large number of chemically diverse polymers by modifying specific parameters. These libraries can be interrogated for specific attributes including cell attachment, immobilisation and toxicity, allowing expedient identification of 'spotted' of 'hit' polymers with promising attributes (Tourniaire *et al.* 2006). This significantly enhances the process of tailoring precise scaffold characteristics for specific applications, facilitating further experimental and pre-clinical testing of candidate materials for suitability prior to regulatory approval. Similar processes can also be used for diagnostic or cell-sorting applications, or identification of polymeric substrates for surface modification of tissue engineering scaffolds to enhance skeletal cell growth and differentiation (Tare *et al.* 2009).

A recent study within the Bone and Joint Research Group, Southampton has successfully combined this HT approach with microarray techniques as the basis to identify and evaluate multiple promising polymers for a tissue engineering strategy (Khan *et al.* 2010). Candidate polymer blends were synthesised by combining two of seven rudimentary homopolymers in 135 unique permutations. The aim of the study was to produce a 'binary blend' polymer that displayed the positive biological and physical attributes of the two dissimilar contributory polymers, whilst suppressing the negative properties, resulting in an emergent blend with superior characteristics. In this study, the ability to function as a non-toxic matrix for cell attachment and growth was evaluated using HT strategies with: bone-marrow derived STRO-1 positive SSCs; fetal femur-derived skeletal cells; the early osteoblast-like MG63 cell line, and the mature osteoblast-like SaOs cell line. Following HT analysis, the 'hit' scaffold was fabricated in larger quantities and evaluated for its potential in a skeletal regeneration strategy using established *in vitro* and *in vivo* techniques (Khan *et al.* 2010).

New techniques of polymer blending have enabled the fabrication of a further generation of 'ternary blend' polymers, which aim to take advantage of the combined characteristics of *three* polymers for regenerative approaches (Grande and Carvalho 2011). Using similar techniques to those employed in the binary blend study, this chapter details the evaluation of these ternary blend polymers for their utility as scaffolds for skeletal tissue regeneration.

4.2 <u>Aims</u>

The aim of this work was to utilise an HT approach to identify, screen and characterise candidate ternary blend polymers, capable of stimulating and/ or modulating stem cell activity, for their ability to function as regenerative matrices. We aimed to use the results of this to select candidate polymers for further *in vitro* and *in vivo* analysis, following seeding of SSCs, to assess their suitability for skeletal regeneration applications.

4.3 Null hypotheses

- 1. Polymeric ternary blend biomaterials do not facilitate cell-attachment and lineage-differentiation suitable for skeletal regeneration strategies.
- 2. Polymeric ternary blend biomaterials do not function as suitable scaffolds for skeletal regeneration strategies.

4.4 Materials and methods

Polymeric ternary blends were formulated, fabricated and screened using HT analysis, by Dr Ferdous Khan at the University of Edinburgh.

4.4.1 Materials

Chitosan (CS), polyethylenimine (PEI), agarose (type 1-B), poly(L)lactic acid) (PLLA) and Silane-Prep™ microscope slides were from Sigma-Aldrich (Gillingham, UK). Polycaprolactone (PCL), poly(ethylene oxide) (PEO), poly(vinyl acetate) (PVAc) and poly(2-hydroxymethyl methacrylate) (PHEMA) were from Scientific Polymer Products (Ontario, USA). Analytical grade chloroform, glacial ethanoic acid, *N*-methyl-2-pyrrolidinone (NMP) and Hoechst-33342 Fluorescent stain were from Thermo Fisher Scientific (Loughborough, UK).

4.4.2 Ternary polymer blend microarray fabrication

Solvents were used to synthesise 1% w/v polymer solutions as shown in Table 4.2. These seven rudimentary homopolymer solutions were blended into 35 ternary combinations. Characterisation of the phase transition behaviour of these combinations isolated 19 polymers which formed stable miscible blends with at least three transition temperature phases, distinct from the original homopolymers. Each of these 19 ternary polymer blends was then fabricated in three different proportions (20:40:40, 50:25:25, 80:10:10) which were contact-printed onto the 1.2 µm-thick surface film of agarose-coated Silane-Prep™ slides using a QArray mini printer (Genetix, New Milton, UK) with 16 aQu solid pins. The printing conditions comprised of 5 stamps per spot, 200 ms inking time and 10 ms stamping time, resulting in a typical spot size of 300-400 µm in diameter, with a distance of approximately 750 µm between adjacent spots. Multiple slides were printed with identical polymer microarrays using this technique to allow six replicates, then the slides were dried for 24 hours under vacuum at 40°C and sterilised by UV irradiation for 30 minutes prior to cell seeding.

Table 4.2 Rudimentary homopolymers and applicable solvents used as the basis for fabrication of ternary polymer blends

Polymer	Chemical formula	Molecular weight (≈)	Solvent
Chitosan (CS)	HO OH OHO OH OHO OH	300000	2% C ₂ H ₄ O ₂
Polyethylenimine (PEI)		750000	NMP
Poly(L-lactic acid) (PLLA)	O CH ₃	152000	CHCl₃/NMP
Polycaprolactone (PCL)		120000	CHCl ₃ /NMP
Poly(ethylene oxide) (PEO)	$H = \begin{bmatrix} 0 & & \\ & & \end{bmatrix}_n O = H$	100000	CHCl ₃ /NMP
Poly(vinyl acetate) (PVAc)	H ₃ C O	260000	CHCl ₃ /NMP
Poly(2-hydroxymethyl methacrylate) (PHEMA)	O O OH	300000	NMP

 $C_2H_4O_2$ = ethanoic (acetic) acid, NMP = N-methyl-2-pyrrolidinone, CHCl₃ = chloroform

4.4.3 Cell acquisition and isolation

STRO-1 positive SSCs were isolated, using MACS, from the femoral bone marrow of haematologically normal individuals undergoing THR surgery, with the approval of the Southampton and South West Hampshire Local Regional Ethics Committee (LREC194/99) (as described in Chapter III, section 3.4.2). Human fetal SSCs were isolated from fetuses (8-11 weeks post-conception) following termination of pregnancy, according to guidelines issued by the Polkinghorne Report and with Local Regional

Ethics Committee approval. The cells were expanded prior to harvest by monolayer culture in basal medium for nine and 12 days respectively.

4.4.4 Selection of candidate ternary polymer blends for 3D fabrication

4.4.4.1 Scanning Electron Microscopy

A Philips XL30CPSEM Scanning Electron Microscope was used to investigate the surface morphology of the polymer microarrays. The glass slides containing the polymer arrays were attached to a specimen holder and sputter-coated with gold before image capture at 10 kV in a secondary electron imaging mode (Fig. 4.1).

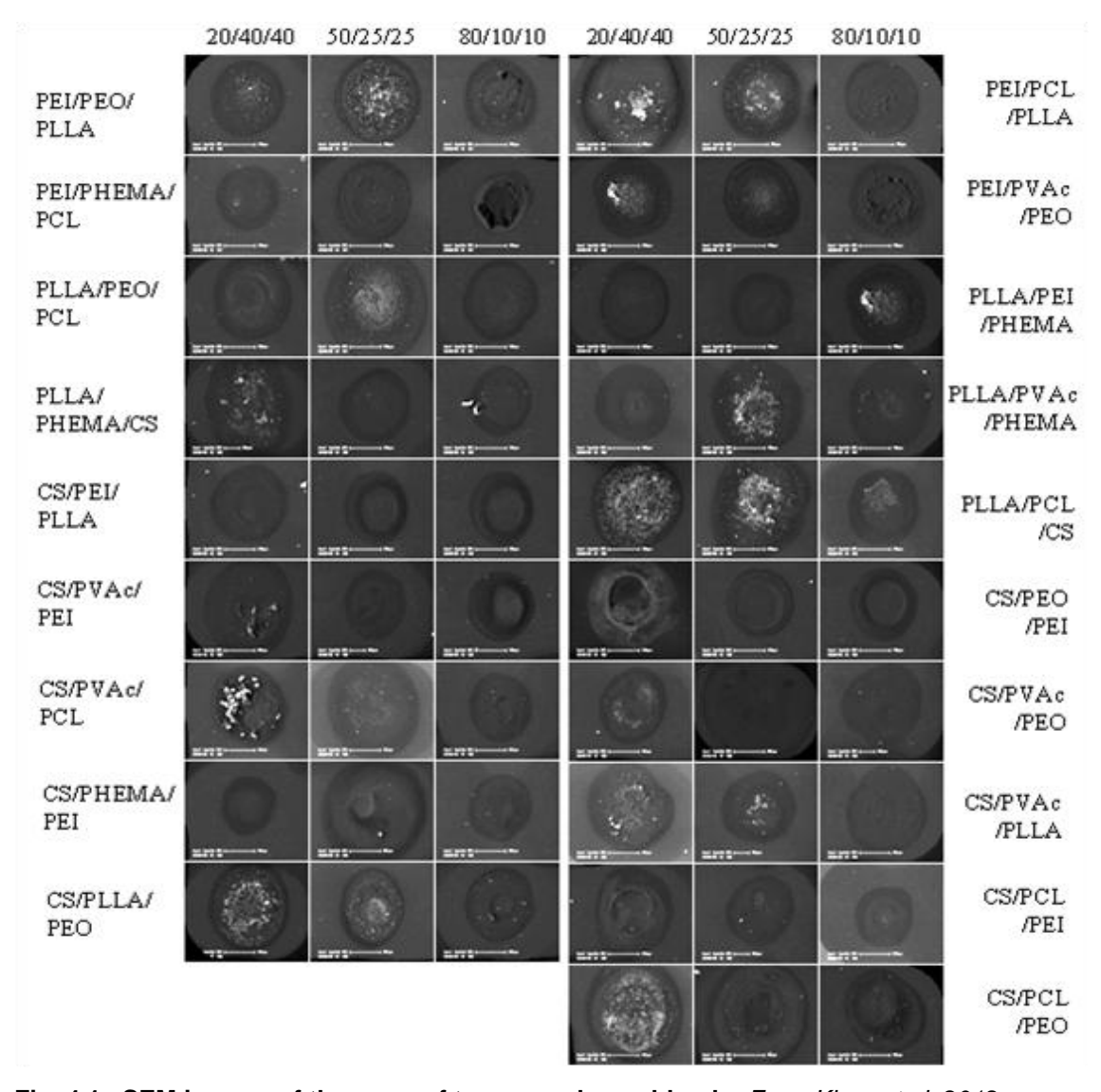
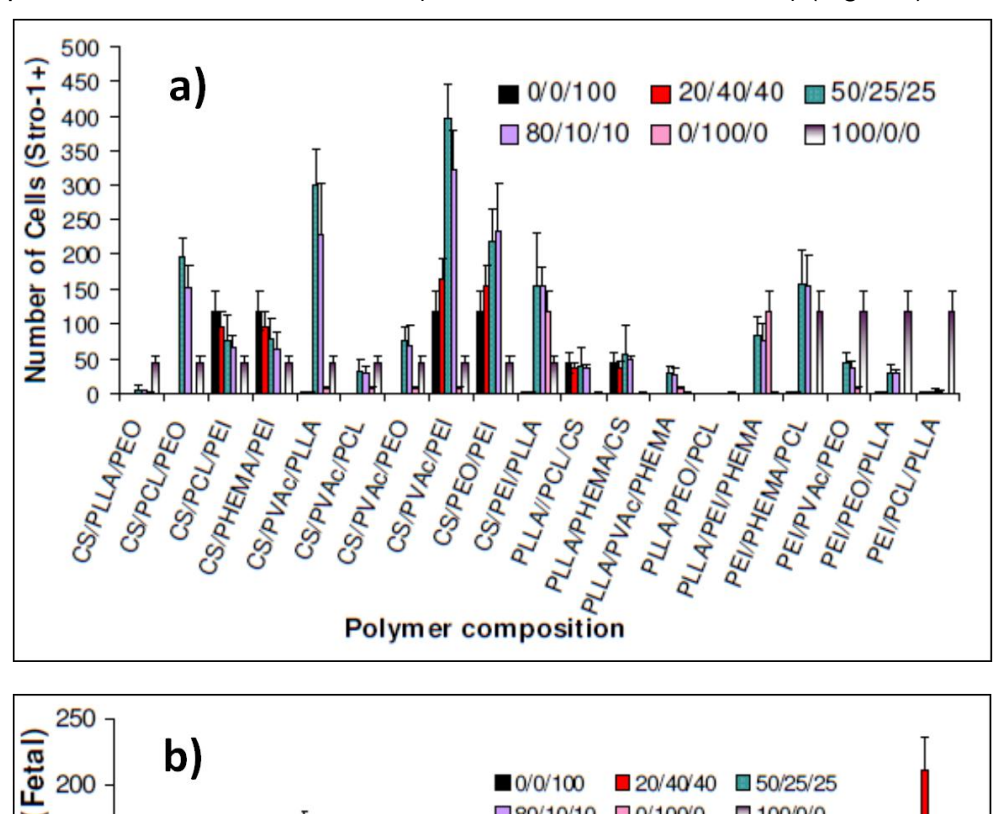


Fig. 4.1 SEM images of the array of ternary polymer blends. From Khan et al. 2012

4.4.4.2 Cell culture on polymer microarrays

Each microarray was sterilised prior to cell seeding under ultraviolet (UV) light for 30 minutes. 1x10⁶ STRO-1 positive or fetal SSCs were labelled with CellTracker[™] Green (as described in Chapter 2, section 2.4.12). Cell populations were incubated in 1.5 ml basal medium on each selected polymer microarray slide for 18 hours (3 microarray slides per cell type) at 37°C, 5% CO₂ in humidified atmosphere, followed by washing with PBS, fixing and nuclear counterstaining with Hoechst-33342 fluorescent stain. Quantitative analysis of cell adherence was achieved using an automated microscope equipped with Pathfinder[™] software (IMSTAR S.A., Paris, France) (Fig. 4.2).



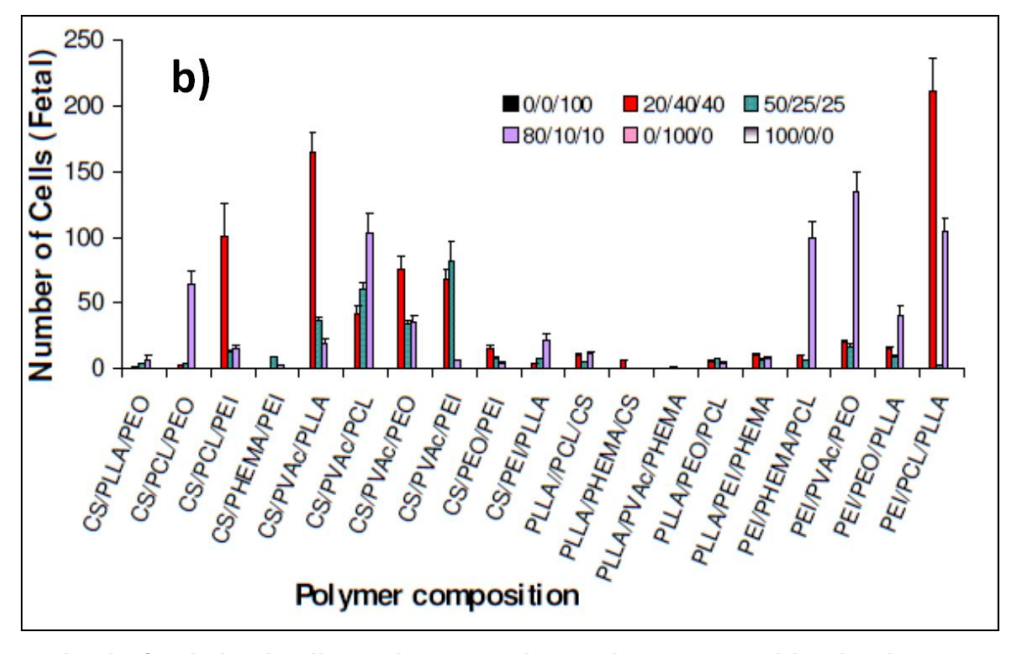


Fig. 4.2 Analysis skeletal cell attachment and growth on ternary blend polymer spots: a) STRO-1 positive, b) fetal skeletal cells, evaluated as mean number (+/- SD, *n*=3 for each spot) of cells on each polymer spot. *From Khan et al. 2012*

Cell compatibility and binding was then confirmed for each cell type by counting viable cells and cell nuclei bound to each polymer spot using the FITC and DAPI channels on a Zeiss Axiovert 200 inverted microscope (Fig. 4.3).

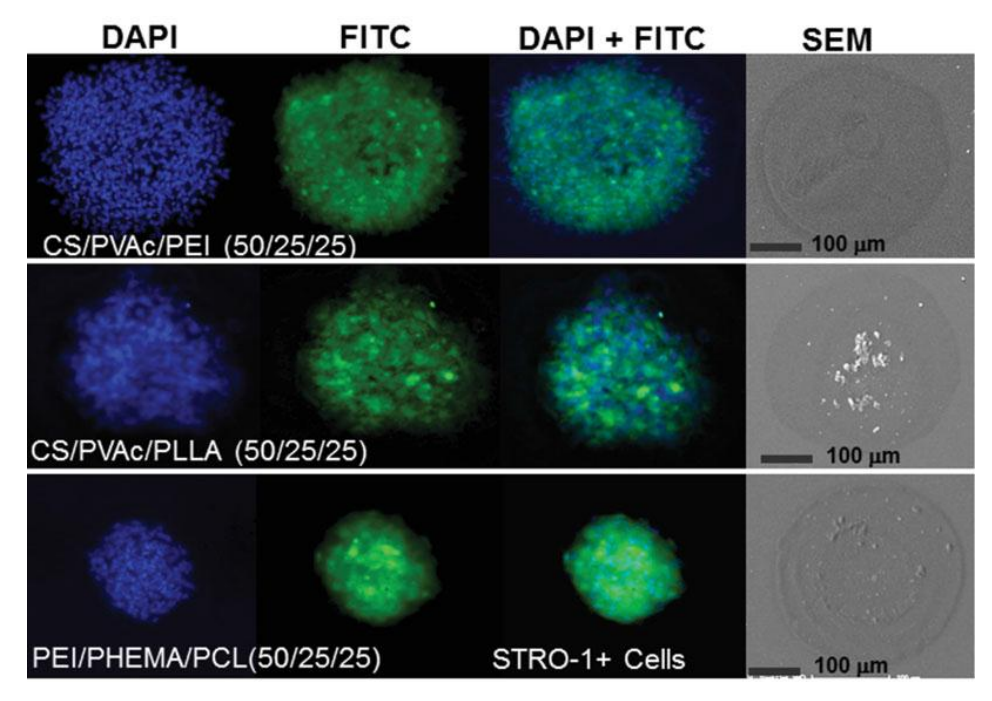


Fig. 4.3 Example of affinity analysis for STRO-1 positive cell adhesion (FITC) and nuclear counterstain (DAPI) for three ternary polymer blends: CS/PVAc/PEI (50/25/25), CS/PVAc/PLLA (50/25/25) and PEI/PHEMA/PCL (50/25/25), with corresponding SEM images (right). From Khan et al. 2012

Using the SEM and the cell adherence data, a shortlist of four ternary blend polymers was compiled (in order of preference) with the aim of targeting blends that displayed a homogeneous porous consistency with good cellular attachment with both cell types:

- 1. CS/PVAc/PEI 50/25/25
- 2. PEI/PHEMA/PCL 50/25/25
- 3. CS/PEI/PLLA 50/25/25
- 4. CS/PVAc/PLLA 50/25/25

4.4.5 Manufacture of selected 3D polymer blend scaffolds

The chosen scaffolds were fabricated using solutions of the homopolymers, each in its appropriate solvent (see Table 4.2), by Dr F Khan at the University of Edinburgh. The resulting blends were vortexed for 15 minutes before freezing in liquid nitrogen and undergoing a freeze-drying process in glass vials until no solvent remained, yielding

scaffold cylinders (approximately 23 mm diameter x 40 mm height). Unfortunately, despite modifications to the solvent evaporation technique, blend 2 (PEI/PHEMA/PCL 50/25/25) was not mechanically stable in a 3D configuration and could not be synthesised in appropriate quantities to yield a homogeneous polymer scaffold, so only blends 1,3 and 4 underwent further analysis *in vitro*.

4.4.6 Assessment of 3D scaffold characteristics

Macroscopic and microscopic analysis was undertaken to ascertain the physical properties of each 3D scaffold. Multiple discs (4mm diameter x 1.5mm height) were cut from the scaffold cylinders using sterile tissue biopsy punches (NHS Supply Chain, Alfreton, UK) and placed into the standard solutions used for processing and analysis to ensure insolubility and maintenance of a robust structure following these processes (as detailed in section 4.4.8).

4.4.7 *In vitro* pilot culture

Blends 1, 3 and 4 underwent pilot cell culture for seven days to validate the experimental technique, to confirm results of the microarray analysis of initial cell adherence and viability, and to ensure maintenance of appropriate scaffold structural properties following culture. Following sterilisation overnight by exposure to UV irradiation, two discs of each polymer blend were mounted onto 21 gauge needles and seeded with 10⁷ STRO-1 positive cells in 2 ml of basal medium and gently agitated for 12 hours. Subsequently, one disc of each polymer was incubated at 37°C in 5% humidified atmosphere in either basal medium (supplemented with 10% FCS) or osteogenic medium (basal medium supplemented with 100 ng/ml rhBMP-2, 100 μM ascorbate-2-phosphate and 10 nM dexamethasone) for 7 days with medium changes every third day. 5ml of medium was removed from each sample and pH was tested using a digital Bench pH meter (Hanna Instruments, Bedfordshire, UK) to detect potentially harmful acidic breakdown product from the scaffolds.

4.4.7.1 Characterisation of cell activity following in vitro pilot culture

Following culture, each polymer scaffold was washed in PBS and processed for cell viability analysis and ALP staining (described in Chapter 3, sections 3.4.6.1 and 3.4.6.5 respectively), to assess early cell survival, proliferation and osteogenic activity.

4.4.8 Structural analysis of the chosen scaffold

Following the above assessments, polymer blend 4 (CS/PVAc/PLLA 50/25/25) was chosen to be fabricated in larger quantities for further *in vitro* and *in vivo* analysis. Structural assessment of overall scaffold porosity, pore size and mechanical properties was undertaken by Dr F Khan using liquid displacement, SEM and mechanical testing respectively (Table 4.3)

Table 4.3 Structural properties of the selected polymer blend scaffold (CS/PVAc/PLLA 50/25/25)

Density (+/-SD) g mm ⁻³	Porosity (+/-SD) %	Pore diameter (range) µm	Maximum load N	Tensile strength Pa	Elongation at failure %	Stiffness N/mm
43.8 (1.4)	73.6 (5.7)	50-600	1.65	330	9.68	0.83

4.4.9 In vitro culture and analysis of single selected scaffold

Sterile discs of the single best-performing polymer blend (as indicated by the results of prior experiments described above), were mounted onto 21 gauge needles and seeded in batches of 5 discs with 5x10⁶ STRO-1 positive cells per ml, as previously described (section 4.4.7). For this main *in vitro* experiment, 20 discs were then incubated in basal conditions and 20 discs in osteogenic conditions for 28 days, with medium changes every third day. A single disc was removed from each group at day seven and day 28 for cell viability and ALP analysis. The remaining discs were removed on day 28 and were either fixed in 4% paraformaldehyde for immunohistochemical analysis, or prepared for molecular extraction by rinsing in PBS and placing on ice.

4.4.9.1 Immunohistochemical analysis

Each fixed disc was cut into quarters and the resulting samples were combined and split into five groups for immunohistochemical analysis of osteogenic expression with five discrete markers. Initial attempts to section the samples and mount them onto slides proved unreliable as some sections did not adhere to the slides and the microarchitecture of untreated scaffold was distorted by the sectioning process. Therefore the fixed samples were carefully dissected into four approximately equal sizes and

immersed directly within aliquots of the appropriate solutions containing the respective antibody. Only samples incubated in osteogenic conditions underwent this analysis as the basal samples were spoiled during the previous process. 1% BSA in PBS was used as the blocking buffer for 5 minutes, before application of the appropriate primary antibody, diluted in 1% BSA in PBS: anti-type I collagen (LF-67, rabbit polyclonal, 1:300 dilution) and anti-osteonectin (LF-8, rabbit polyclonal, 1:100 dilution) were provided by Dr L Fisher; anti-bone sialoprotein (rabbit polyclonal 1:100 dilution) was provided by Dr J Sodek, and anti-osteopontin (rabbit polyclonal, 1:100 dilution) and anti-osteocalcin (mouse monoclonal, 1:100 dilution) were from GeneTex Inc. (Irvine, California, USA). Samples were incubated overnight at 4°C prior to rinsing in running water and immersion for 5 minutes in each of three wash buffers containing: Trizma wash (12.1 g 50 mM tris[hydroxymethyl]aminomethane (Trizma base, Sigma), 1 ml 0.05% polyoxyethylene-sorbitan monolaurate (Tween 20, Sigma), 2 I H₂O) and (a) high salt (46.7 g NaCl), (b) low salt (17.4 g NaCl) and (c) double concentration Trizma wash (0.1 M), adjusted to pH 8.5. Following complete removal of the final wash buffer, 100 μl of appropriate Alexa 594 fluorochrome-conjugated secondary antibody (monoclonal (anti-mouse) diluted 1:50, polyclonal (anti-rabbit) diluted 1:30 in 1% BSA in PBS) was applied at room temperature for one hour, before rinsing and incubating with 300 nM DAPI nuclear counterstain (Invitrogen, 1:100 dilution with PBS) for 5 minutes. Samples were stored in dark conditions at 4°C before visualisation with confocal microscopy, using a Leica SP5 laser scanning confocal microscope and software (Leica Microsystems, Wetzlar, Germany). Negative controls (i.e. omission of the primary antibodies) were included in all immunostaining protocols.

4.4.9.2 Preparation for molecular analysis

The remaining discs from each culture group were prepared for molecular extraction. Gibco's TRIzol method was initially employed: following rinsing in PBS, the samples were incubated in dilute collagenase IV (100 U/ml in α MEM) for 30 minutes at 37°C and then released with 10% trypsin for five minutes (Lonza, Wokingham, UK). The fluid removed was centrifuged at 1000 rpm for 10 minutes and the supernatant was vortexed briefly and mechanically lysed with TRIzol reagent before snap-freezing at -80°C. During this time, the scaffolds were kept on ice and following addition of TRIzol onto the scaffolds, any remaining cells were sonicated directly from the scaffolds using a sonicator at 100 J for 30 seconds. These samples were snap-frozen alongside the initial samples. An alternative method of RNA extraction was also attempted using the Qiagen AllPrep DNA/RNA Micro kit (Qiagen, Crawley, UK) following the manufacturer's protocol.

Upon defrosting, RNA was isolated by phase separation in chloroform with centrifugation at 13000 rpm. The uppermost layer of isolated RNA was precipitated using isopropanol with centrifugation at 12000 rpm before extraction of the pellet and washing with 75% ethanol with centrifugation at 7500 rpm. The RNA was re-dissolved in ultra-pure H₂O and nucleic acid concentration and purity were assessed using a spectrophotometer (NanoDrop 3300, Wilmington, Delaware, USA). Because the purity of RNA was universally assessed as low, RNA cleanup steps were employed as per manufacturer's instructions, using the DNA-free RNA kit by Zymo Research (Cambridge Bioscience, Cambridge, UK). These steps comprised application of a binding buffer and multiple passes through the zymo-spin column, following addition of Following a further preparation and RNA wash buffer solutions. spectrophotometric assessment of RNA yield and purity, cDNA was synthesised using the Superscript First-Strand cDNA kit (Invitrogen) and Real Time PCR was set up using a SYBR® Green mastermix. qRT-PCR was performed using a 96-well optical reaction plate and a 7500 Real Time PCR system (Applied Biosystems, Carlsbad, USA). Following cDNA synthesis, each sample underwent RT-PCR against a panel of osteogenic gene primers (Table 4.4). Values were calculated using the comparative threshold cycle (Ct) method and normalised to β-actin expression.

Table 4.4 Osteogenic gene primer sequences used for RT-PCR

Primer		Sequence		
Beta actin (housekeeping gene)	b-actin	F: 5'-GGCATCCTCACCCTGAAGTA R: 5'-AGGTGTGGTGCCAGATTTTC		
Alkaline Phosphatase	ALP	F: 5'-GGAACTCCTGACCCTTGACC R: 5'-TCCTGTTCAGCTCGTACTGC		
Collagen type I alpha I	Col1A1	F: 5'-GAGTGCTGTCCCGTCTGC R: 5'-TTTCTTGTTCGGTGGGTG		
Runt-related transcription factor 2	RUNX-2	F: 5'-GTAGATGGACCTCGGGAACC R: 5'-GAGCTGGTCAGAACAAAC		
Sex determining region Y, box 9	SOX-9	F: 5'-CCCCAACAGATCGCCTACAG R: 5'-GAGTTCTGGTCGGTGTAGTC		

F = Forward, R = Reverse. Courtesy of Dr R. Tare, Bone and Joint Research Group, University of Southampton

4.4.10 In vivo studies

4.4.10.1 Scaffold preparation prior to implantation

Discs of the single best-performing polymer blend were mounted onto 21 gauge needles, sterilised in antibiotic/antimycotic solution overnight, washed in PBS and exposed to UV irradiation for a further 12 hours, before degassing and soaking in basal medium overnight. These scaffolds were then seeded overnight in batches of 5 discs with 10⁷ STRO-1 positive cells per 2 ml of basal medium, as previously described (section 4.4.7). Similar samples of control scaffold were treated in an identical manner, but were incubated without stem cells. In addition, silicone cylinders of identical dimensions to the polymer discs were prepared and sterilised as above, to act as inert spacers and therefore negative controls.

4.4.10.2 Implantation into the murine femoral segmental defect

This segmental bone defect allows evaluation of new bone formation in a clinically relevant model. A standard mouse femoral bone defect model was used, with a 5 mm femoral diaphyseal segmental osteotomy. This part of the study was carried out in accordance with the protocol described previously by Kanczler *et al.* (Kanczler *et al.* 2010)

Four mice in three study groups underwent the procedure: for the control group, a critical diaphyseal defect was made in the femur, and stabilised with intramedullary fixation, using a silicone disc as a control spacer. The second group underwent the same procedure, except with interposition of the polymer scaffold alone within the defect. The third group received the polymer scaffold that had been seeded with 5x10⁶ STRO positive cells.

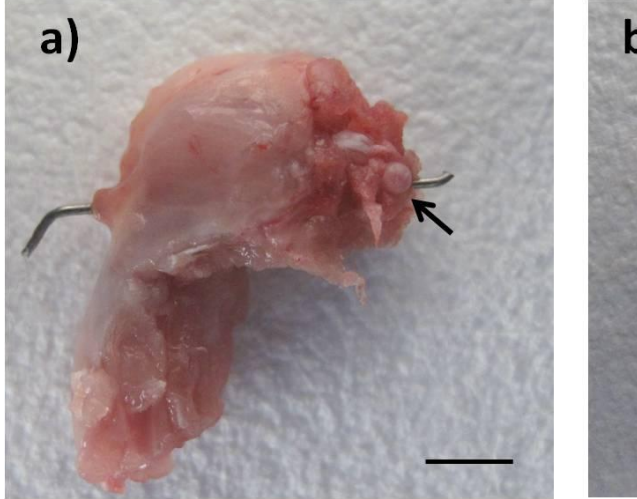
MF-1 nu/nu immunodeficient mice were anaesthetised intraperitoneally using a 1:1 ratio of Hypnorm (fentanyl/fluanisone) to Hypnovel (midazolam), with dosage adjusted to weight. The animals were placed on a thermostatically-controlled blanket and full aseptic technique was employed throughout each procedure. Following skin preparation with chlorhexidine-alcohol solution, an incision was made directly over the palpable right femoral shaft and brought proximally over the posterior aspect of the right thigh. Careful blunt muscular dissection was used to expose the femoral shaft and tendon insertions at the trochanter proximally. The femoral shaft was supported with forceps whilst a 23 gauge hypodermic needle was introduced through the trochanter into the femoral intramedullary canal and advanced through the supracondylar

metaphysis until the tip was visible at the knee. The needle was then gently retracted into the proximal femur and a 5 mm mid-femoral shaft osteotomy was created using a micro-sagittal saw, before re-inserting the needle through 3 discs of test scaffold (incubated *a priori* in osteogenic conditions with or without SSCs, as described in section 4.4.10.1) or a silicone spacer. Correct needle placement was confirmed by Faxitron specimen X-ray imaging (MX-20, Qados Ltd, Sandhurst, UK), and careful attention was paid to remove loose bone fragments within or around the osteotomy site. The ends of each needle were bent, cut and positioned subcutaneously to prevent injury or irritation to the animals. Sufficient angulatory and rotational stability was achieved through the interference fit at the dense trochanteric and supracondylar bone to allow post-operative weight-bearing. The skin was closed with non-absorbable monofilament sutures and the wound site protected with a permeable spray film dressing (Opsite spray, Smith & Nephew, London, UK).

After recovery, the animals were monitored on a daily basis for potential complications and killed by a Schedule 1 method (carbon dioxide inhalation) at 28 days.

4.4.10.3 Preparation of murine femoral samples

The entire right femur was disarticulated at the hip and sectioned through the tibia of each mouse before careful dissection of superficial tissue layers over the defect site (Fig. 4.4)



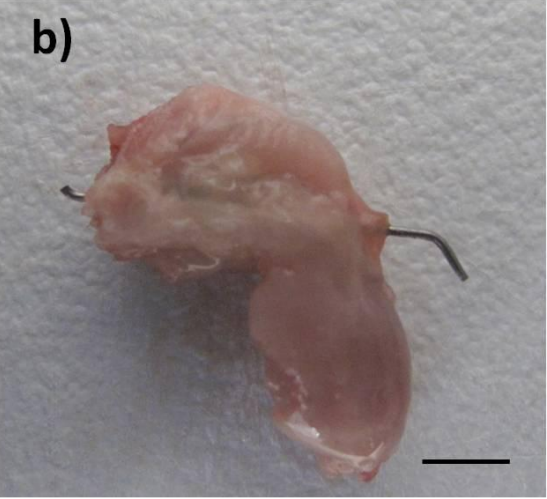


Fig. 4.4 Femoral specimens following harvesting: a) medial and **b)** lateral views. The intramedullary device is visible; it inserts into the greater trochanter, through the defect site and exits through the knee. The disarticulated femoral head is visible in a) (arrow). Scale bar: 1 cm

4.4.10.4 Radiographic analysis of bone formation

Plain radiographic analysis was performed by Faxitron imaging prior to fixation of each sample in periodate-lysine-paraformaldehyde (PLP) fixative for 48 hours within a 5 ml bijou tube. Quantitative 3D analysis was performed using the X-TEK benchtop 160Xi CT scanner for Micro computed tomography (µCT, X-TEK Systems Ltd, Tring, UK), equipped with a Hamamatsu C7943 X-ray flat panel sensor (Hamamatsu Photonics, Welwyn Garden City, UK). Samples were scanned using a molybdenum target at 100 kV, 70 μA, with an exposure time of 2134 ms and 1x digital gain. Following successful data acquisition and initial image reconstruction of each entire femur with a 15 µm voxel resolution. the femora were decalcified in Tris-EDTA (0.1)M tris(hydroxymethyl)aminomethane- 5% ethylenediaminetetraacetic acid) at pH 7.3, for 4 weeks, with regular changes of solution and constant agitation. Faxitron imaging was undertaken between the third and fourth week to identify adequate decalcification and guide the timing of histological processing.

4.4.10.5 CT image analysis

Following image reconstruction, a constant region of interest with dimensions 5 mm x 5 mm x length of original defect, was assigned within each femur with reference to the Faxitron images acquired at day 0 and 28. The reconstructed images were visualised and analysed using Studio Max 1.2.1 software (Volume Graphics GmbH, Heidelberg, Germany). Manual thresholds were selected to exclude soft tissue and scaffold, and the metal intramedullary needles were digitally subtracted to quantify bone volume, bone surface/ bone volume, bone volume/ total volume, trabecular number, trabecular thickness and trabecular spacing. GraphPad Prism software was used for statistical analysis. Differences between groups were determined by one-way ANOVA with a *post hoc* Tukey test and were considered to be significantly different if p<0.05.

4.4.10.6 Histological and Immunohistochemical analysis

Following decalcification, samples were dehydrated through graded ethanol concentrations (50%, 1 hour; 90%, 1 hour; 100%, 1 hour, and 100%, 1 hour), prepared with histoclear and embedded in low-melting point paraffin wax using an automated Shandon Citadel 2000 tissue processor. The use of chloroform was avoided because pilot experiments indicated dissolution of the polymers occurred during prolonged exposure. A microtome was used to cut each sample into twenty semi-sequential 6 μ m sections before mounting onto glass microscope slides.

4.4.10.6.1 Histochemical staining

Sections were brought to room temperature, de-waxed in Histoclear and hydrated with graded methanol concentrations (2 x 100% for 2 minutes, 90% for 2 minutes, 70% for 2 minutes, 50% for 2 minutes) and finally 100% H_2O for 5 minutes before each procedure:

- Weigert's haematoxylin/Alcian blue/ Sirius red (A/S) staining

Weigert's haematoxylin (10 g haematoxylin in 1 L methanol left to ripen for four weeks, 6 g ferric chloride, 500 ml H₂O, 5 ml conc. HCl) was applied for 10 minutes prior to immersing briefly in acid/alcohol (2% HCl in 50% methanol). Sections were stained in Alcian blue (1.5 g Alcian blue 8GX, 300 ml distilled H₂O, 3 ml concentrated ethanoic (acetic) acid) for 10 minutes, 1% fresh molybdophosphoric acid for 20 minutes, and Sirius red (0.3 g Sirius red F3B, 100 ml saturated picric acid, 200 ml distilled H₂O) for 60 minutes. Sections were rinsed thoroughly in water between each stain. Slides were dehydrated in methanol and mounted in DPX (Distyrene, Plasticer and Xylene; BDH Laboratory Supplies, Poole, UK).

- Goldner's Trichrome

Weigert's haematoxylin was applied for 10 minutes, immersed in acid/alcohol briefly and rinsed in water before staining in Ponceau-fuchsin-azophloxin solution for 5 minutes (composed of 10 ml Ponceau-fuchsin solution (0.75 g Ponceau 2R, 0.25 g acid fuchsin with 100 ml dilute ethanoic acid) added to 0.5 g azophloxin with 100 ml dilute ethanoic acid) and rinsing in 1% ethanoic acid. Slides were then stained in phosphomolybdic acid/ orange G solution for 20 minutes (composed of 5 g phosphomolybdic acid, 2 g Orange G, a single crystal of thymol (2-isopropyl-5-methylphenol) dissolved in 500 ml H₂O), rinsed in 1% ethanoic acid, before staining with light green for 5 minutes and mounting in DPX.

4.4.10.6.2 Immunohistochemical staining

Immunohistochemical staining for collagen type I and von Willebrand's Factor (vWF) was performed as described previously in section 4.4.9.1, however due to unavailability of the appropriate confocal laser required for fluorescent analysis, visualisation was achieved using the avidin/biotin method with peroxidise and 3-amino-9-ethylcarbazole (AEC), which yielded a brown reaction product. Negative control samples were included in each staining run, which yielded no evidence of staining.

4.5 Results

4.5.1 Physical characteristics of selected blends

Assessment of cell adherence to the polymer blend microarrays was used to select candidate scaffolds for larger scale fabrication and the physical characteristics of these scaffolds were assessed for suitability as a potential tissue engineering construct:

Blend 1 (CS/PVAc/PEI 50/25/25) – A porous cylinder, approximately 15 mm diameter, cream in colour with a heterogeneous structure, dense centrally and less dense circumferentially, with a fibrous consistency.

Blend 2 (PEI/PHEMA/PCL 50/25/25) – This blend could not be fabricated in sufficient quantities and was therefore not assessed further.

Blend 3 (CS/PEI/PLLA 50/25/25) – Fragile, porous incomplete cylinders, with a dark cream colour. The material readily disintegrated to form a powder.

Blend 4 (CS/PVAc/PLLA 50/25/25) – Rigid, malleable bright white cylinders (approximately 17 mm diameter). Small pores (approximately 50-500 μm diameter), but a homogeneous structure throughout.

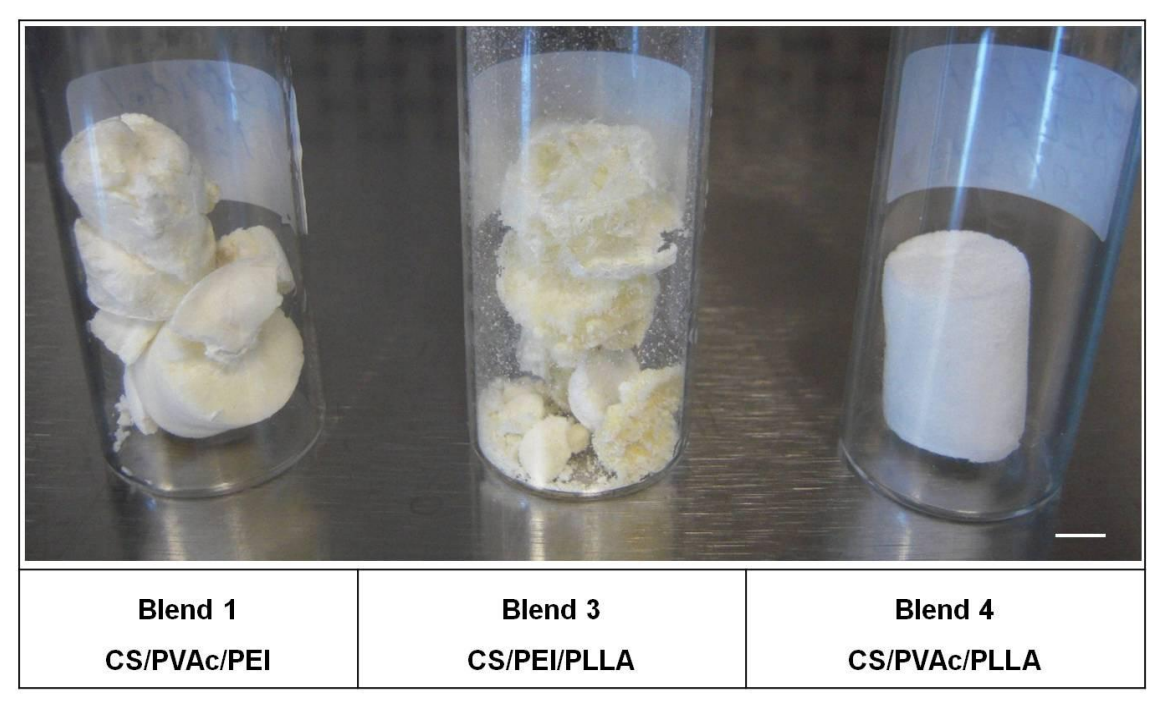


Fig. 4.5 Characteristics of polymer ternary blends as received. Scale bar: 1 cm

4.5.2 Solubility/ stability assessment

Characteristics were assessed following immersion of 4 mm diameter discs of each ternary blend in various standard solvents/solutions used for processing/ analysis (Table 4.5).

Table 4.5 Assessment of solubility and stability of each polymer blend. 4 mm diameter discs were immersed in standard solvents for 24 hours and 7 days to assess their physical stability.

Blend		7 days			
Diena	PBS	90% Ethanol	Histoclear	Chloroform	Basal media
1 CS/PVAc/PEI	No change	Expanded by ~ 25%	No change	No change	Expanded by ~ 10%, fragile
3 CS/PEI/PLLA	Expanded by ~ 50%	Dissolved	No change	Dissolved slightly	Disintegrated
4 CS/PVAc/PLLA	No change	No change	No change	Dissolved entirely	No change

4.5.3 Seven day in vitro pilot culture

At the end of the pilot culture period, cell viability analysis and ALP staining was performed (Table 4.6, Figs. 4.6-4.8). Analysis of live cells was impeded by intense green auto-fluorescence of the polymers and multi-dimensional acquisition (overlaying images acquired with different filters) was used in some cases to differentiate polymer auto-fluorescence from true cellular activity (Fig. $4.8 \, f$ and h). Blend 4 (CS/PVAc/PLLA 50/25/25) possessed better structural properties than the other two blends tested, and was less susceptible to degradation following exposure to solvents (Table 4.5). It did however dissolve entirely in chloroform, so alternative methods were employed to embed the polymer for histological analyses. Furthermore, blend 4 supported substantially greater numbers of live cells in both basal and osteogenic conditions in the day 7 *in vitro* culture tests (Fig. 4.6-4.8). Therefore, blend 4 was used for further *in vitro* and *in vivo* analysis.

Table 4.6 Analysis of cell viability, ALP staining and pH following pilot 7 day *in vitro* culture of SSCs on each polymer blend

Blend	Medium	рН	Live/dead result	ALP stain result
1	Basal	7.88	Occasional live cells centrally	Light patchy staining throughout
CS/PVAc/PEI	Osteo	7.94	Multiple live cells	Light staining
CON VACIL	Control	7.95	No cells	No staining
3	Basal	7.83	Live cells throughout remaining fragment	Intense staining throughout
CS/PEI/PLLA	Osteo	7.92	Dissolved	Dissolved
00/1 21/1 22/1	Control	7.95	Dissolved	No staining
4	Basal	7.91	Live cells throughout, some apoptotic cells centrally	Consistent light staining throughout
CS/PVAc/PLLA	Osteo	7.89	Multiple live cells throughout	Light staining with patches of intense staining
	Control	7.94	No cells	No staining

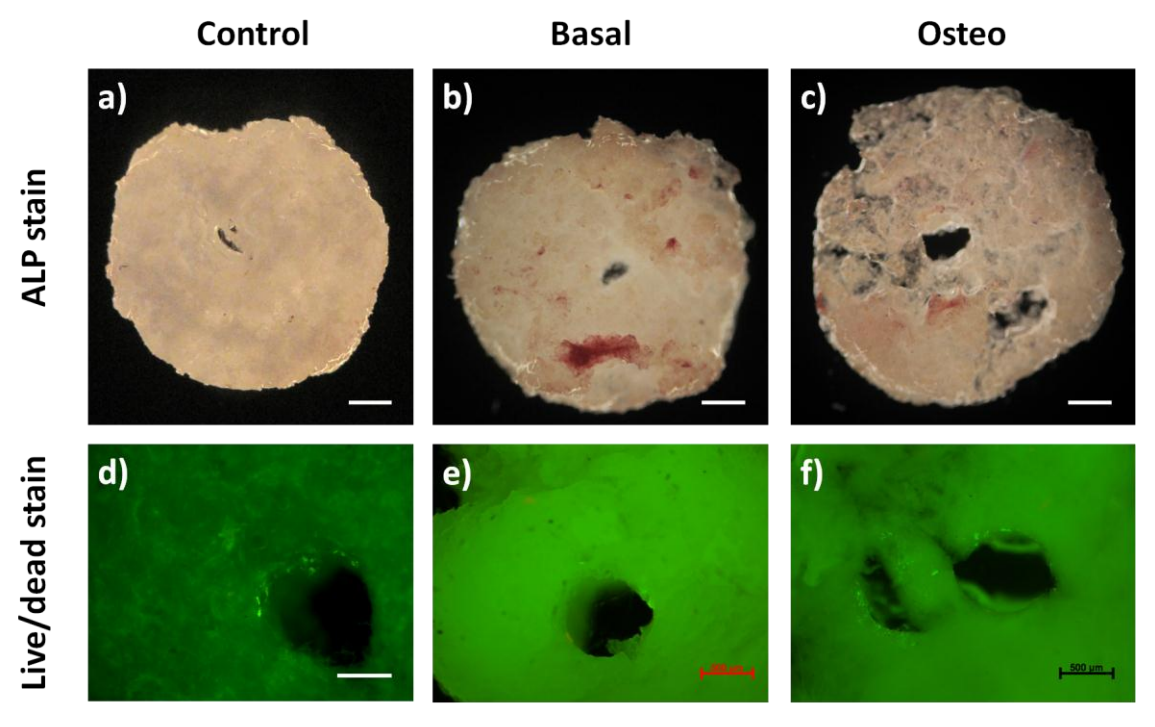


Fig. 4.6 Analysis of ALP staining and cell viability for discs of ternary blend 1 (CS/PVAc/PEI 50/25/25). a) – c) ALP stain and d) – f) Live/dead stain, of polymer incubated with no cells (control) and with cells in basal and osteogenic medium respectively. Scale bars: $500 \ \mu m$

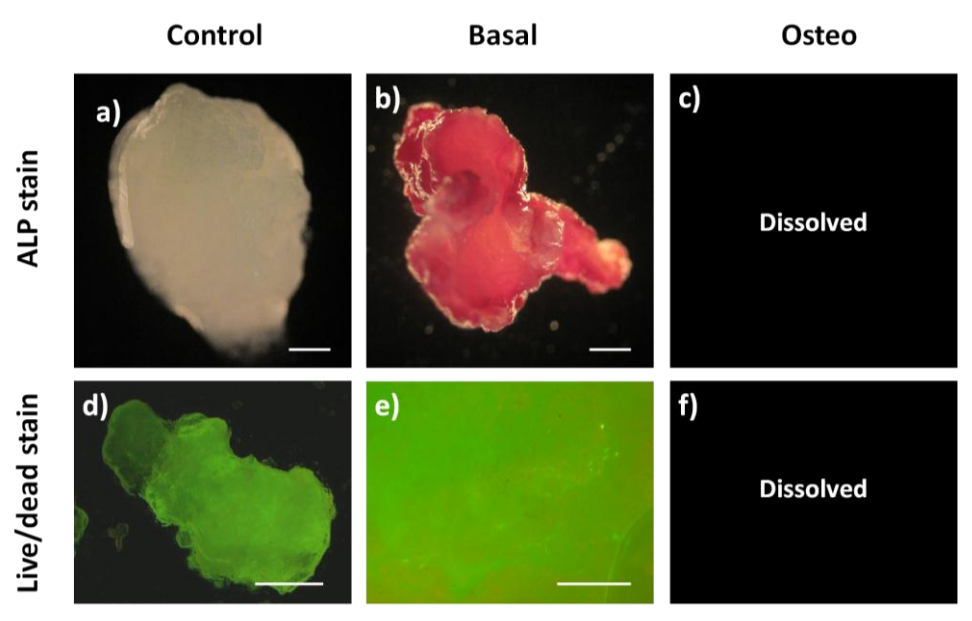


Fig. 4.7 Analysis of ALP staining and cell viability for discs of ternary blend 3 (CS/PEI/PLLA 50/25/25). a) - c) ALP stain, d) - f) Live/dead stain, of polymer incubated with no cells (control) and with cells in basal and osteogenic medium respectively. Scale bars: 500 µm

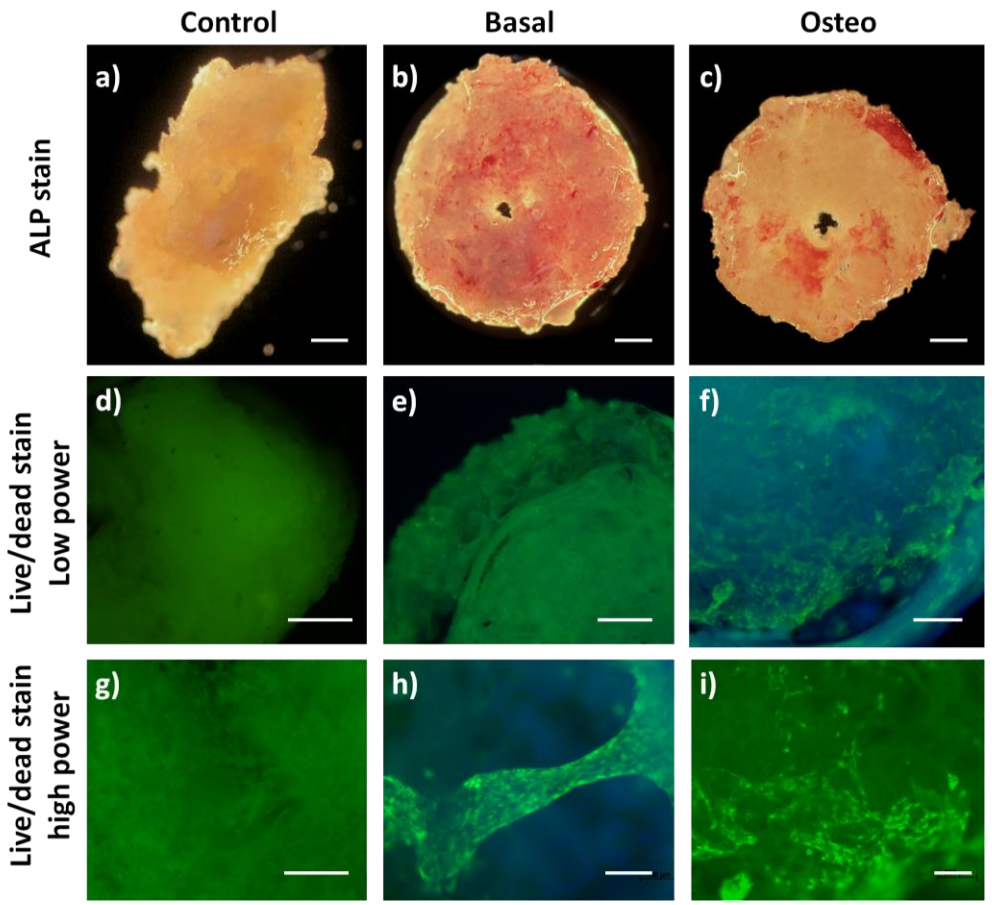


Fig. 4.8 Analysis of ALP staining and cell viability for discs of ternary blend 4 (CS/PVAc/PLLA 50/25/25). a) – c) ALP stain, d) – i) low and high magnification images of live/dead stain, of polymer incubated with no cells (control) and with cells in basal and osteogenic medium respectively, f) and h) are multidimensional acquisition images, where polymer fluoresces blue with the DAPI filter and live cells are green with the FITC filter. Scale bars: a) – f) 500 μ m, g) – i) 200 μ m

4.5.4 *In vitro* analysis of selected polymer scaffold – Blend 4 (CS/PVAc/PLLA 50/25/25)

4.5.4.1 Analysis of ALP production and cell viability

Following culture in both basal and osteogenic conditions, there was evidence of prolific cell growth on the scaffold as demonstrated by confocal microscopy, with early osteogenic differentiation on ALP stain, which was enhanced by osteogenic conditions. Cell viability analysis demonstrated live cells throughout the scaffold matrix in both basal and osteogenic conditions, and this was confirmed using confocal microscopy.

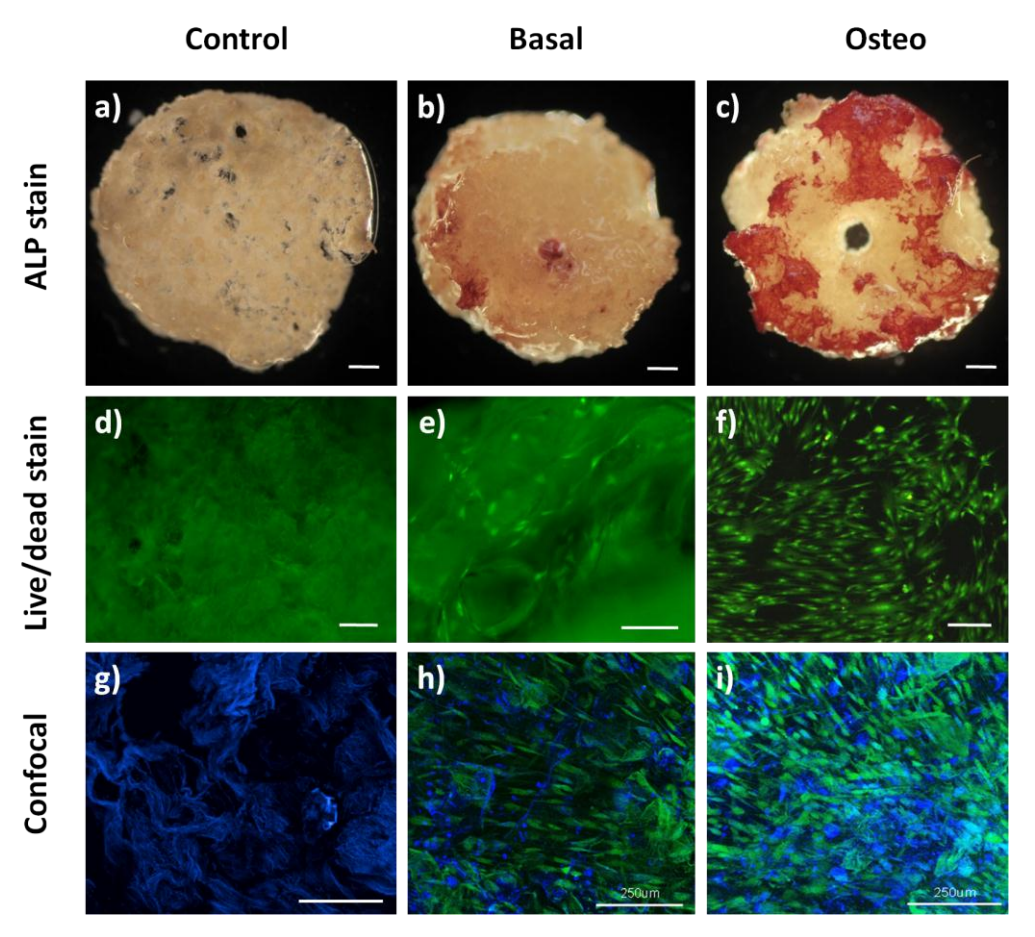


Fig. 4.9 Analysis of ALP staining and cell viability for discs of ternary blend 4 (CS/PVAc/PLLA 50/25/25) following 28 days *in vitro* culture. a) – c) ALP stain indicates early osteogenic differentiation, particularly in c); d) – f) live/dead analysis demonstrates multiple live cells (green) and no dead cells (red); g) – i) Confocal images confirm viable STRO-1 positive cells stained with CellTrackerTM Green, with the superimposed auto-fluorescence of the polymer matrix using the DAPI filter (blue). Scale bars: a) – c) 500 μ m, d) – f) 200 μ m, g) – i) 250 μ m

4.5.4.2 Immunostaining for osteogenic bone-matrix proteins

Immunostaining confirmed the expression of osteogenic collagenous and non-collagenous bone-matrix proteins (Fig. 4.10). Patterns of expression differed between antibodies, with collagen type I staining closely following the ECM of the cells, although

other antibodies stained specific (sometimes punctate) regions around the cells. Apart from osteocalcin, the cells produced all the osteogenic proteins tested. This was verified by the absence of staining in all negative controls, visualised using the same threshold values (Fig. 4.10 k) and I)).

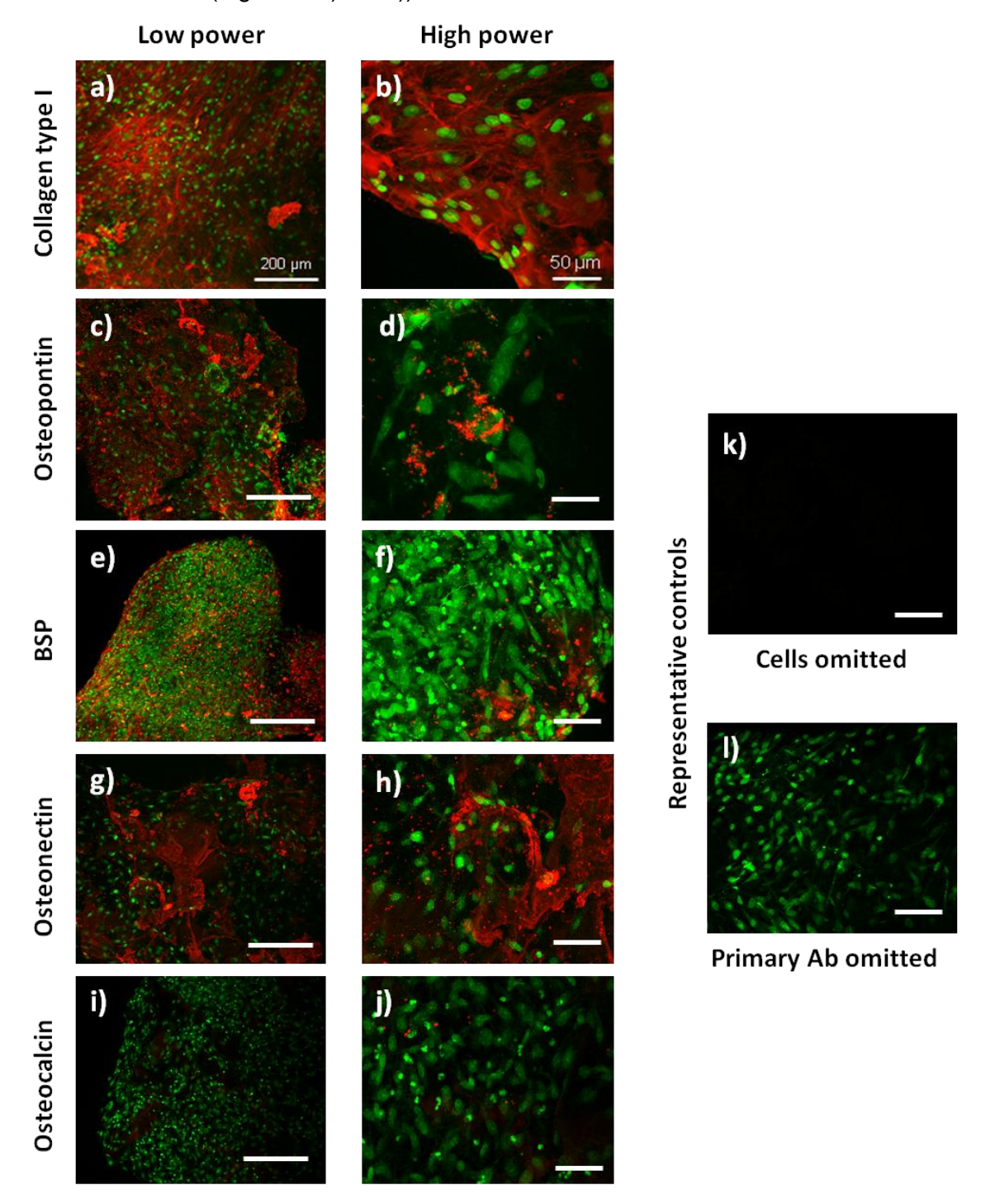


Fig. 4.10 Immunostaining for osteogenic bone-matrix proteins produced by STRO-1 positive cells cultured on ternary blend 4 (CS/PVAc/PLLA 50/25/25) scaffold. Cell nuclei are stained with DAPI (green) and each bone-matrix protein is demonstrated by the Alexa 594 fluorochrome-conjugated secondary antibody (red). Controls are k) no cells but full immunostaining protocol, I) polymer cultured with cells but with primary antibody omitted. Scale bars: low power 200 μ m, high power and controls 500 μ m

5.4.4.3 Molecular profiling

RNA extraction proved unsuccessful despite use of Gibco's TRIzol extraction method with collagenase IV, trypsin, sonication and also a proprietary RNA extraction kit (Qiagen AllPrep Micro Kit). Spectrophotometric assessment yielded universally poor RNA yields and purity ratios even after RNA cleanup steps. cDNA synthesis and RT-PCR produced amplification plots and Ct values that were not deemed representative of the cellular activity demonstrated on the other experimental modalities. Consequently, these results have not been presented here, and the reasons for failure of molecular profiling on this occasion will be detailed in the discussion.

4.5.5 In vivo analysis of Blend 4 (CS/PVAc/PLLA 50/25/25)

4.5.5.1 Radiographic analysis

The load-bearing murine critical-sized femoral defect model was employed to investigate the osteogenic potential of human STRO-1 positive cells seeded on the polymer scaffold.

Two-dimensional *in vivo* digital x-ray images were used to assess the positioning of the diaphyseal defect, intramedullary device and scaffold, and to visualise bone formation over the study period. In addition, 3D images of the entire femora were generated by μ CT analysis following 28 days implantation, to evaluate the extent of bone healing in femoral defects implanted with cell-seeded scaffolds, scaffolds without cells, or spacers (Figs. 4.11 – 4.13). No intra-operative or post-operative deaths occurred during the study period. A single intra-operative complication was noted in mouse 6, where the intramedullary device was placed outside of the femur distal to the osteotomy site (as described in section 4.5.5.1.2). Despite resulting in an unstable construct, the mouse showed no signs of discomfort and mobilised adequately post-operatively, and the results were included in the final analysis. No post-operative infections or abrupt weight loss occurred during the study period.

4.5.5.1.1 Control samples

The control samples showed negligible bone regeneration (Fig. 4.11). Bone that was present at day 28 also appeared in the day 0 samples as remaining fragments left following creation of the osteotomy. The only exception was sample 4, where a bridge of new bone does appear to have formed over the incubation period, although even in this sample no bone continuity is present. No samples were excluded in further

quantitative analysis, although for subsequent μ CT analysis, remaining fragments of bone seen within the osteotomy site at day 0 were digitally excluded from the analysis of all samples.

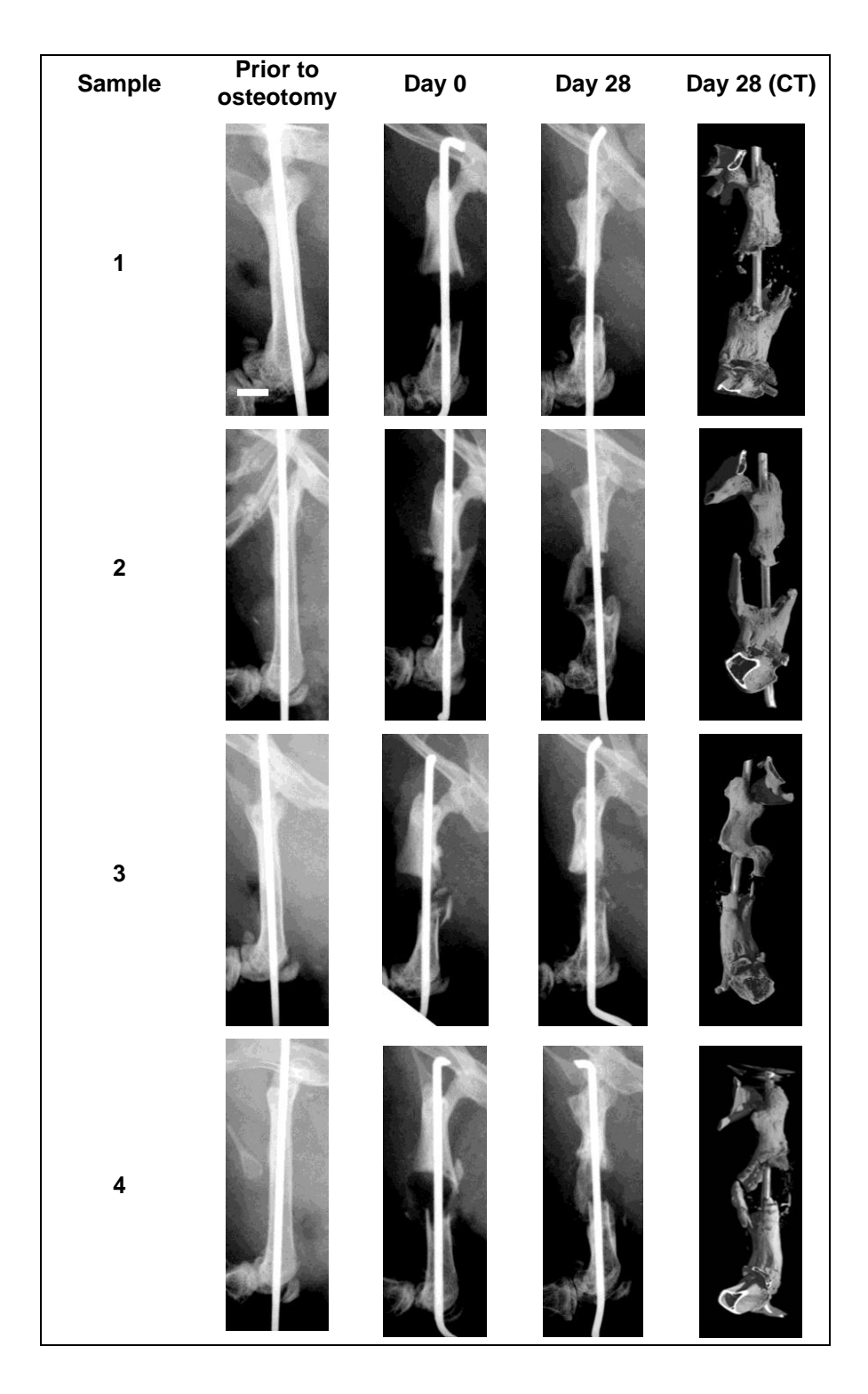


Fig. 4.11 Radiographic analysis of the murine femoral defects at day 0 and day 28 – Control samples 1-4, containing a defect with silicone spacer. Scale bar: 3 mm for all images

4.5.5.1.2 Polymer alone samples

Samples containing the polymer scaffold demonstrated more new bone formation when compared to control samples. New calcification was appropriately positioned in relation to the segmental defect site, with the impression of robust bone formation (Fig. 4.12).

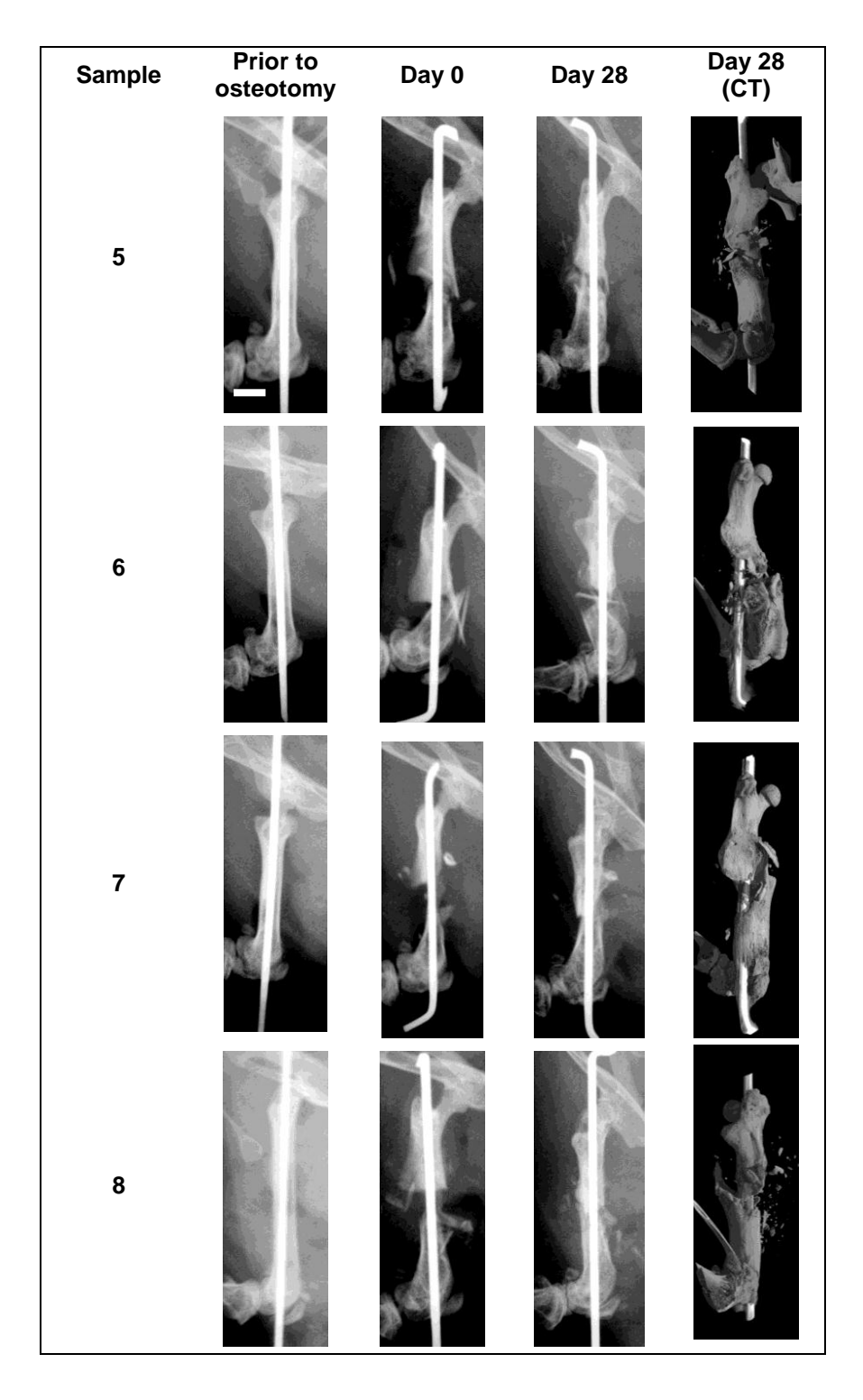


Fig. 4.12 Radiographic analysis of the murine femoral defects at day 0 and day 28 – Polymer alone samples 5-8, containing a defect with ternary blend polymer 4. Scale bar: 3 mm

Sample 6 displays a technical error in intramedullary device insertion: following reinsertion of the pin (day 0 Faxitron), it is seen to bypass the distal femur entirely, resulting in an unstable construct. The action of weight-bearing appears to have improved the initial poor angulation; however the macro-movement induced by such an unstable construct is likely to have had a negative impact on bone healing at this site. Despite this shortcoming, it was included in the final quantitative analysis of bone formation as omission would have resulted in a significantly smaller sample group.

4.5.5.1.3 Polymer + SSCs samples

Radiographic images of the polymer + SSCs group showed robust new bone tissue formation at day 28, with calcified tissue filling the osteotomy site and in several cases extending well beyond this region. All samples in this group showed complete bone bridging within or around the osteotomy site. In all samples there was also evidence of surrounding callus formation and in several specimens there was bone formation at ectopic sites not seen in either of the other groups (Fig. 4.13, samples 10 and 11). This ectopic bone formation correlates with the position of the scaffold and was interfaced to the new bone within the osteotomy site.

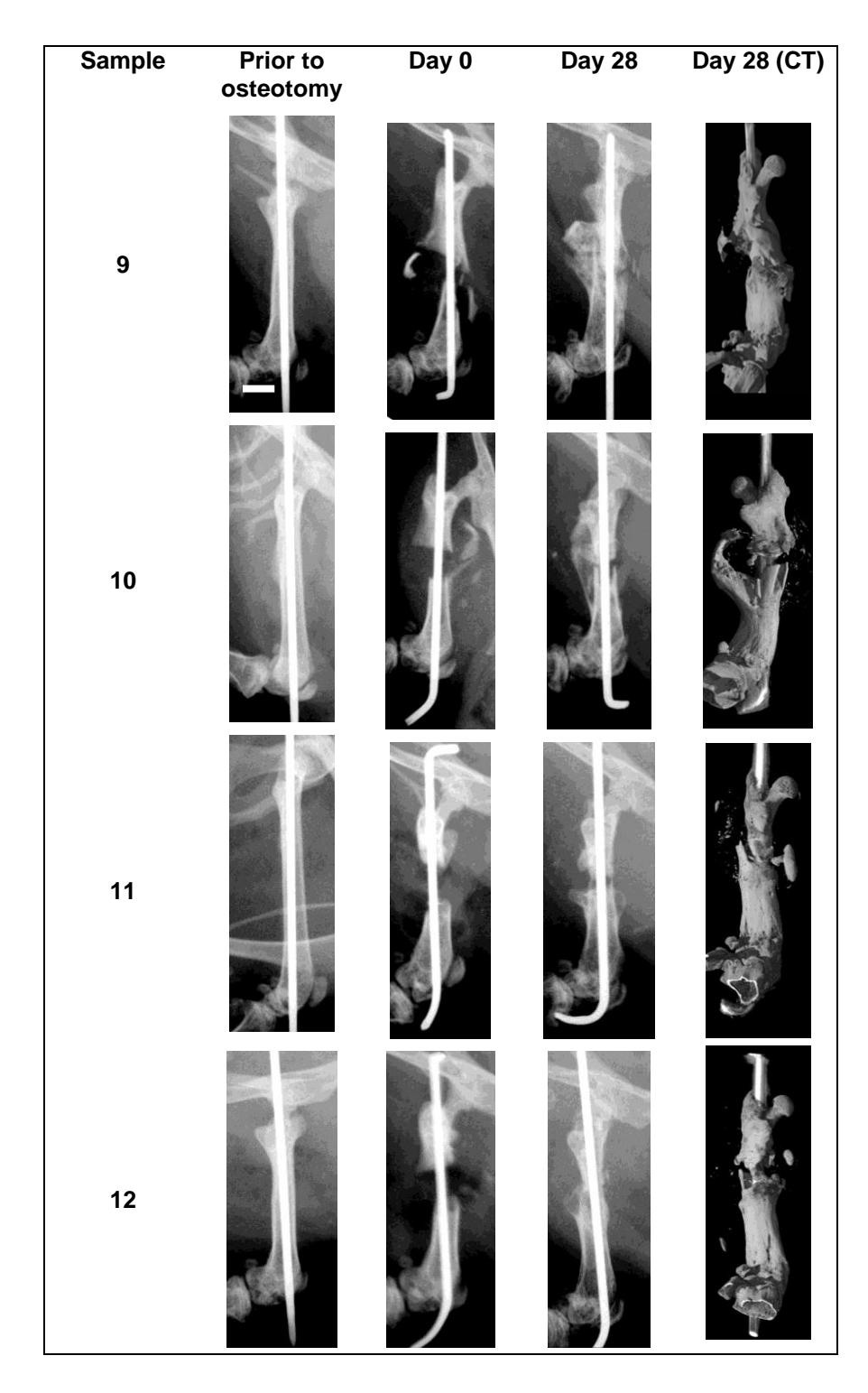


Fig 4.13 Radiographic analysis of the murine femoral defects at day 0 and day 28 – Polymer + SSC samples 9-12, containing a defect with ternary blend polymer incubated with SSCs. Scale bar: 3 mm for all images

4.5.5.2 Analysis of change in femoral length

Using the faxitron images, the intramedullary device length was measured for each specimen (distance between trochanteric insertion point and distal exit point) to compare lengths at day 0 with day 28, this enabled quantification of any compression that may have occurred during the incubation period (Fig. 4.14).

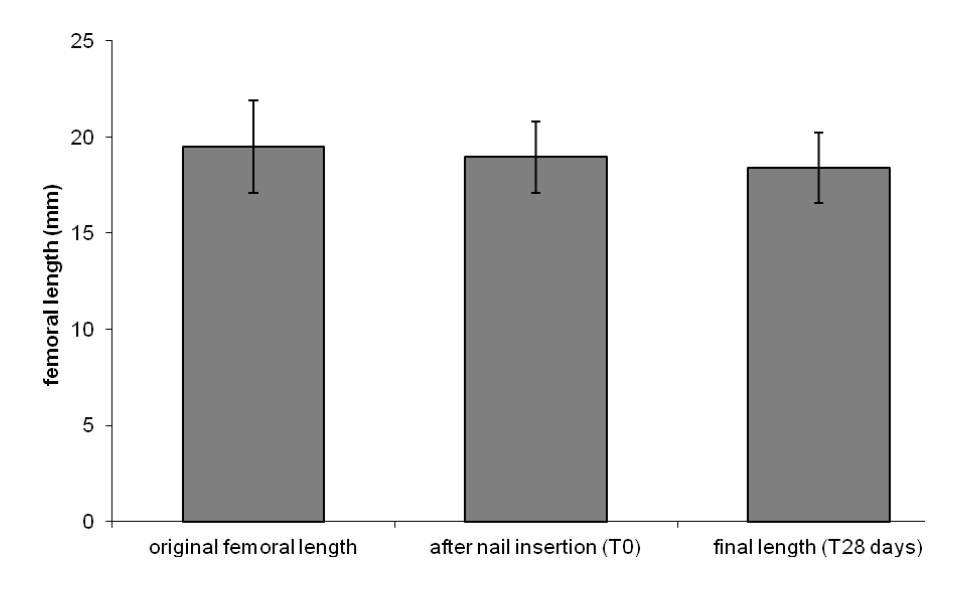


Fig. 4.14 Changes in femoral length, measured before nail insertion, immediately following nail insertion (T0), and at day 28 (T28) after the experimental period. Mean values +/- SD are indicated. There was no statistically significant difference in nail length throughout the experiment.

A mean value was taken for each group, and standard deviations were calculated. The mean femoral length before osteotomy was 19.49 mm (SD 2.40), immediately following osteotomy was 18.94 mm (SD 1.86) and at the end of the 28 day experimental period was 18.41 mm (SD 1.83). Using one way repeated measures ANOVA (Analysis of Variance), Mauchley's test of sphericity was calculated at 0.277, with an F-ratio of 1.675, indicating a very low probability of significant difference.

4.5.5.3 Quantitative μCT analysis

High resolution CT scans of the defect regions implanted with the polymer blend 4 scaffold at day 28 clearly demonstrated increased bone healing in both scaffold groups compared to control samples. The difference between the two scaffold groups was less marked, however the visibility of the intramedullary device was reduced in the scaffold + SSCs groups when compared to the polymer alone samples, indicating greater bone formation in the former group, obscuring the nail (Fig. 4.15).

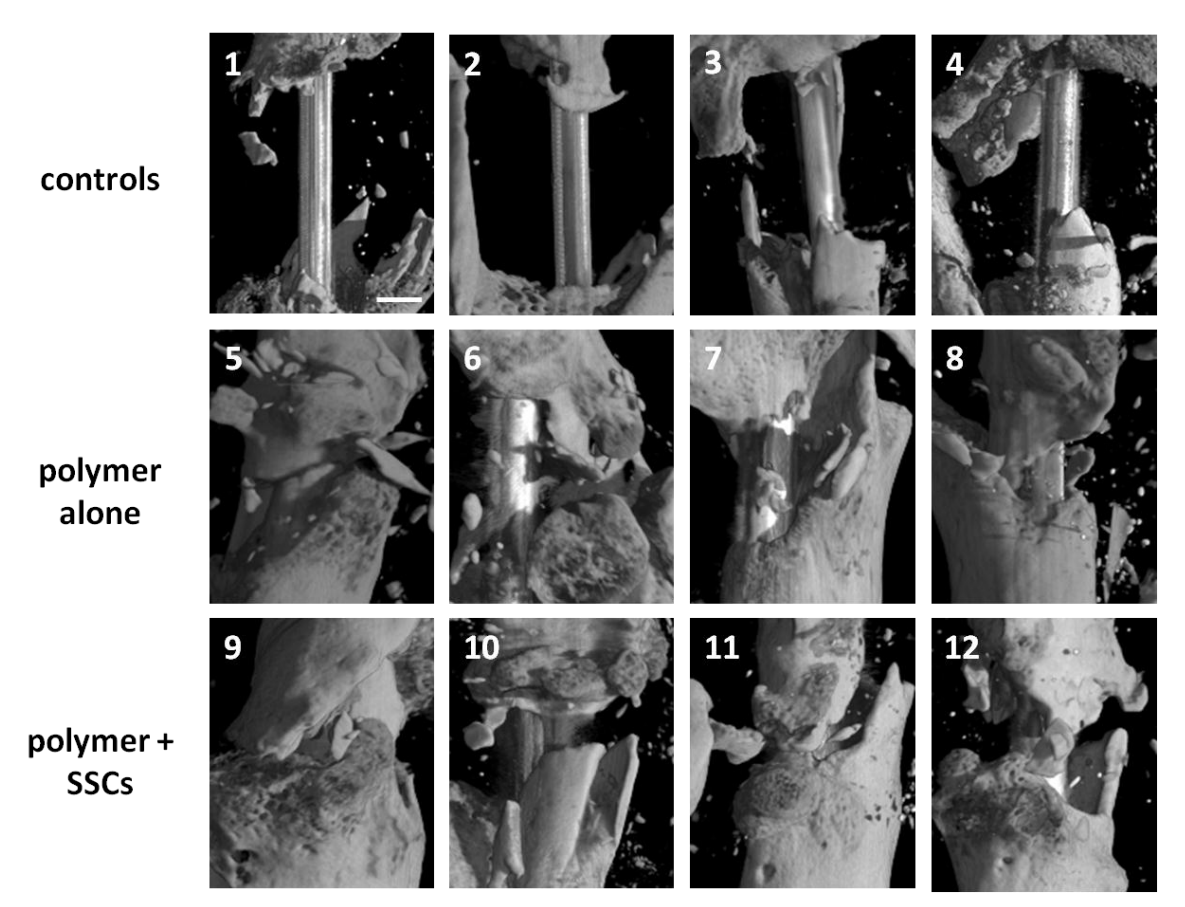


Fig 4.15 Selected regions of interest within the osteotomy defect analysed by quantitative μCT after 28 days. The intramedullary device is visible in these specimens, but was digitally subtracted prior to quantitative analysis of bone formation. Scale bar: 1 mm, all images

To assess bone remodelling, indices of bone histomorphometry were measured from the 3D µCT data (Fig. 4.16). A trend towards increased bone volume was observed in the defect regions implanted with scaffold alone and with scaffold and SSCs, although neither was statistically significantly different from the control. Quantitative analysis of bone volume (BV) was much lower in sample 12 than any of the other polymer samples, and this in part, accounts for the wide error bars. The ratio of BV/ total volume (TV) showed a significant increase in the defect regions implanted with scaffolds alone (8.9 +/- 2.3) compared to controls (3.9 +/- 1.3), although the addition of SSCs to the scaffold did not enhance this significantly (10.2 +/- 1.6). Examination of trabecular number showed a significantly increased density within defect regions associated with the scaffold + SSCs group (4.2 +/- 0.4) and scaffold only group (3.5 +/- 0.8) when compared to the control group (1.9 +/- 0.6) and trabecular spacing was significantly reduced in the scaffold + SSCs group (0.112 +/- 0.015) when compared to both scaffold alone (0.119 +/- 0.026) and control (0.151 +/- 0.007). There was no significant difference between the groups for bone surface/bone volume ratio or trabecular thickness.

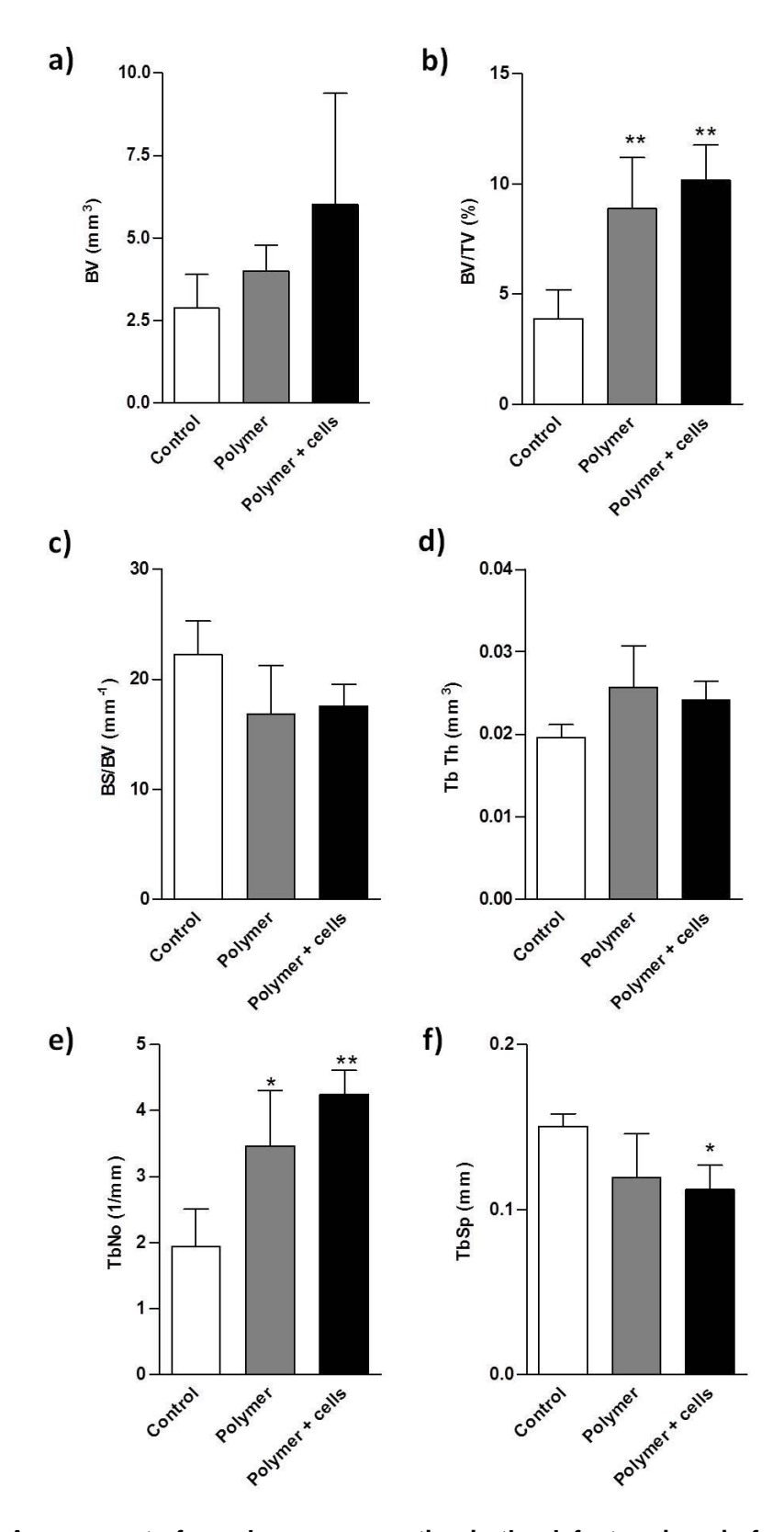


Fig. 4.16 Assessment of new bone regeneration in the defect regions in femora of mice at 28 days following implantation, using indices of a) bone volume (BV), b) bone volume/ total volume (BV/TV), c) bone surface/ bone volume (BS/BV), d) trabecular thickness (TbTh), e) trabecular number (TbNo) and f) trabecular spacing (TbSp). Results are expressed as mean +/-SD, n=4 per group, *=p<0.05, *=p<0.005.

4.5.5.4 Histological analysis

For each specimen, transverse sections of the entire femur were constructed at low magnification to enable identification of regions of interest:

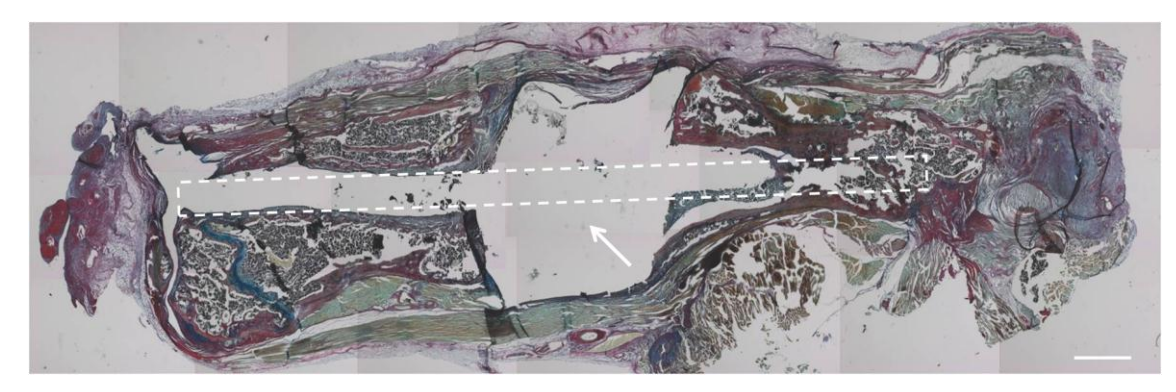


Fig. 4.17 Whole femur stained with A/S. Note the empty control diaphyseal defect (arrow), and the intramedullary defect made by the nail (outline). Scale bar: 1cm

4.5.5.4.1 Empty defect control samples

Control samples typically showed negligible or no bone formation within or around the defect site. The cortical bone of the mouse femora were stained red with Sirius red, and the physeal zones that contain proteoglycans stained blue with Alcian blue, however there was universally negligible stain around the defect site with A/S stain (Fig. 4.17 and 4.18). Although cells could be appreciated on higher magnification views within the medullary canal and trabecula (Fig. 4.18 b), these did not infiltrate the defect itself in any of the control samples.

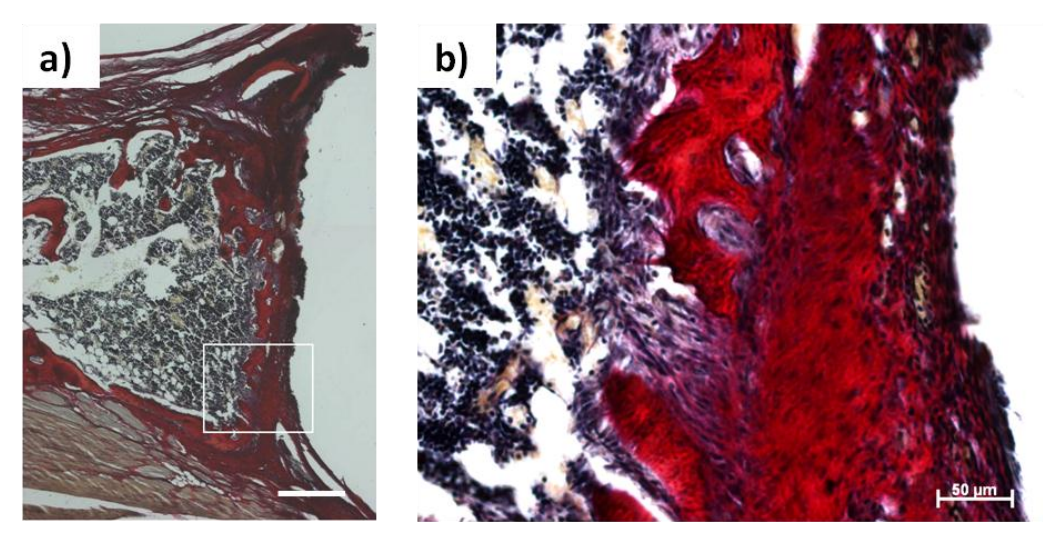


Fig 4.18 Images of proximal femur and defect region of an empty control sample, stained with A/S. Low a) and high b) magnification images. There is red staining around the edges of the defect suggestive of new collagen formation; however this has not extended into the defect site. Scale bars: a) 250 μm, b) 50 μm

Goldner's Trichrome stain also confirmed trabecula within the metaphysis, containing multiple cells, however few cells were present within or around the defect, and no osteoid was laid down, as demonstrated by an absence of red staining (Fig. 4.19).



Fig. 4.19 Goldner's Trichrome stain – empty defect control. Minimal osteoid has been laid down around the defect region (arrow), as demonstrated by an absence of red staining. Scale bar: $500 \ \mu m$

Collagen I immunohistochemistry stained positive in areas of existing cortical bone and also around the edges of the defect site, however there was limited collagen I activity around the defect (Fig. 4.20 a).

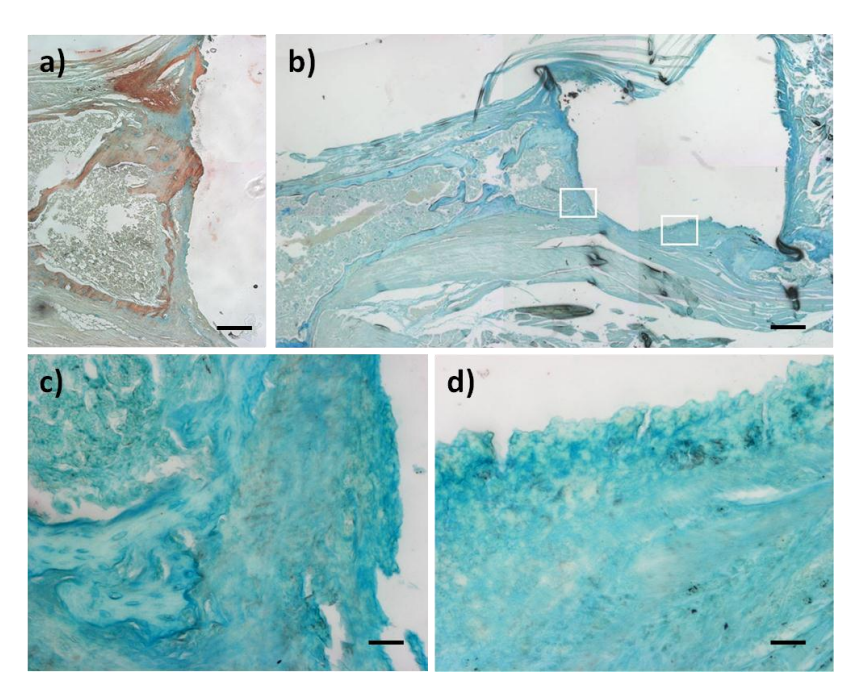


Fig. 4.20 Immunohistochemistry of part of an empty defect control sample. a) Collagen type I staining confirmed expression in areas of existing cortical bone, but limited staining around the defect itself. Low **(b)** and higher magnification areas **(c, d)** of a section stained for vWF show little staining around the defect site, although there was evidence of expression within the medullary canal. Scale bars: a) and c) 500 μm, b) 250 μm, d-e) 50 μm

Minimal staining for vWF was encountered around the defect sites of these control samples, although some staining of the cells within the medullary canal occurred, consistent normal endothelial cell activity within this region (Fig. 4.20 b-d).

4.5.5.4.2 Polymer alone samples

These samples exhibited significantly more cellular activity within and around the defect region (Fig. 4.21). A/S staining revealed the cut ends of the bone at the osteotomy sites closed over with new bone matrix, similar to the empty defect controls. In contrast however, the site occupied by the polymer had significant cellular infiltration (seen particularly in Fig. 4.21 c-e).

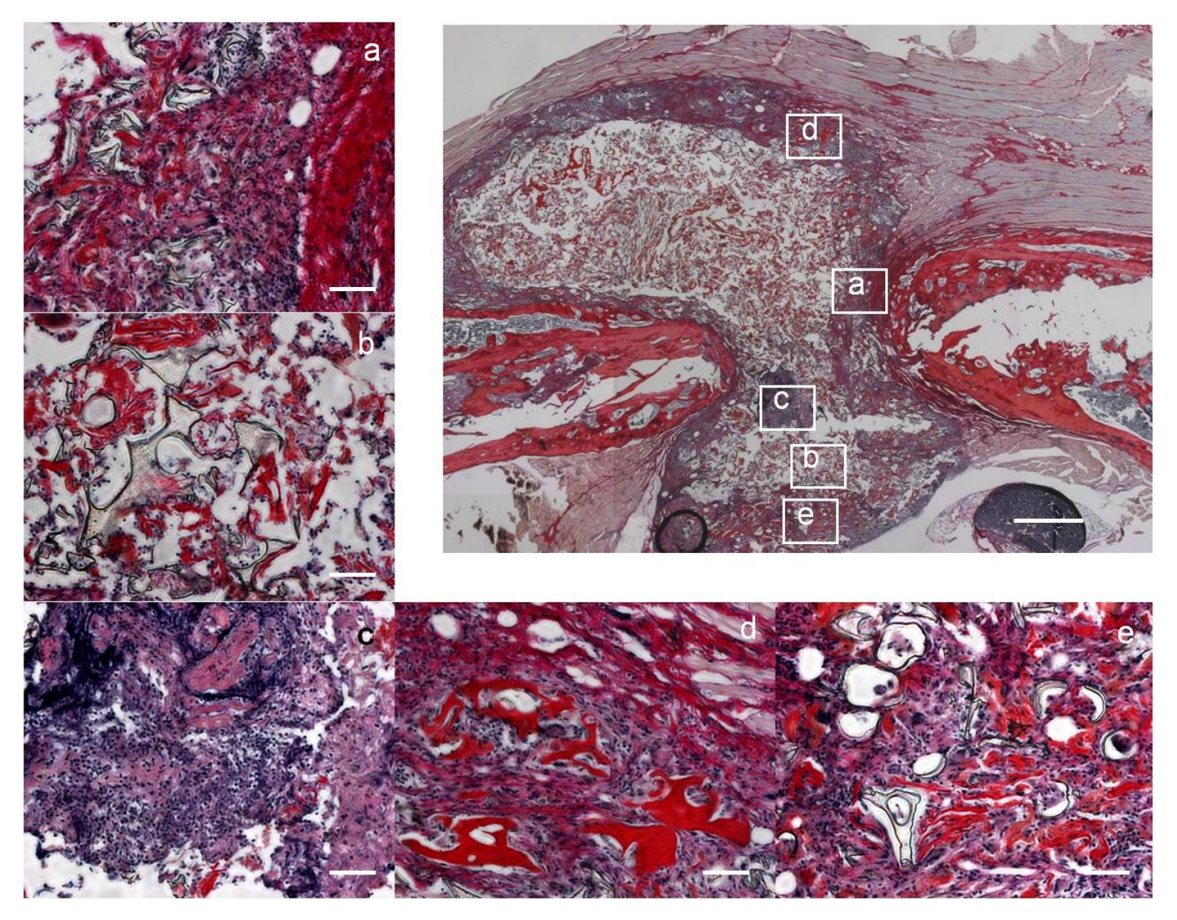


Fig. 4.21 Low magnification image of femoral segmental defect treated with polymer alone (inset) along with 5 regions of interest (a-e) stained with A/S. Note the significant cellular infiltration and new osteoid seen within a distinct 'pseudo-capsule' between the two bone ends. a) The cut end of the bone has sealed with new osteoid and significant trabecular bone formation is seen around this area. b) A peripheral area demonstrating fragmented remains of the translucent polymer scaffold surrounded closely by new osteoid (red) and cells (cell nuclei stained with Weigert's Haematoxylin). c) A central region directly between the bone ends with significant cell infiltration and evidence of osteoid formation. d and e) Peripheral zones, both distant from the defect region showing abundant cells and bone formation, consistent with callus formation. Scale bars: inset 500 μm, a-e) 50 μm

Fragmented remains of the polymer were clearly visible on high power images, with new trabecula forming around these pieces (Fig 4.21 a, b, e). These new trabecula formed at sites distant to the osteotomy (d and e), although the whole process was well-defined within a 'pseudo-capsule', bounded by the muscle around the femur. Fig. 4.21 c shows an area directly between the two bone-ends within the defect region with a particularly high concentration of infiltrated cells.

Collagen I immunohistochemistry revealed positive expression throughout the femoral cortex as seen previously, but staining was also observed within the defect region, and throughout those areas infiltrated with cells (Fig 4.22).

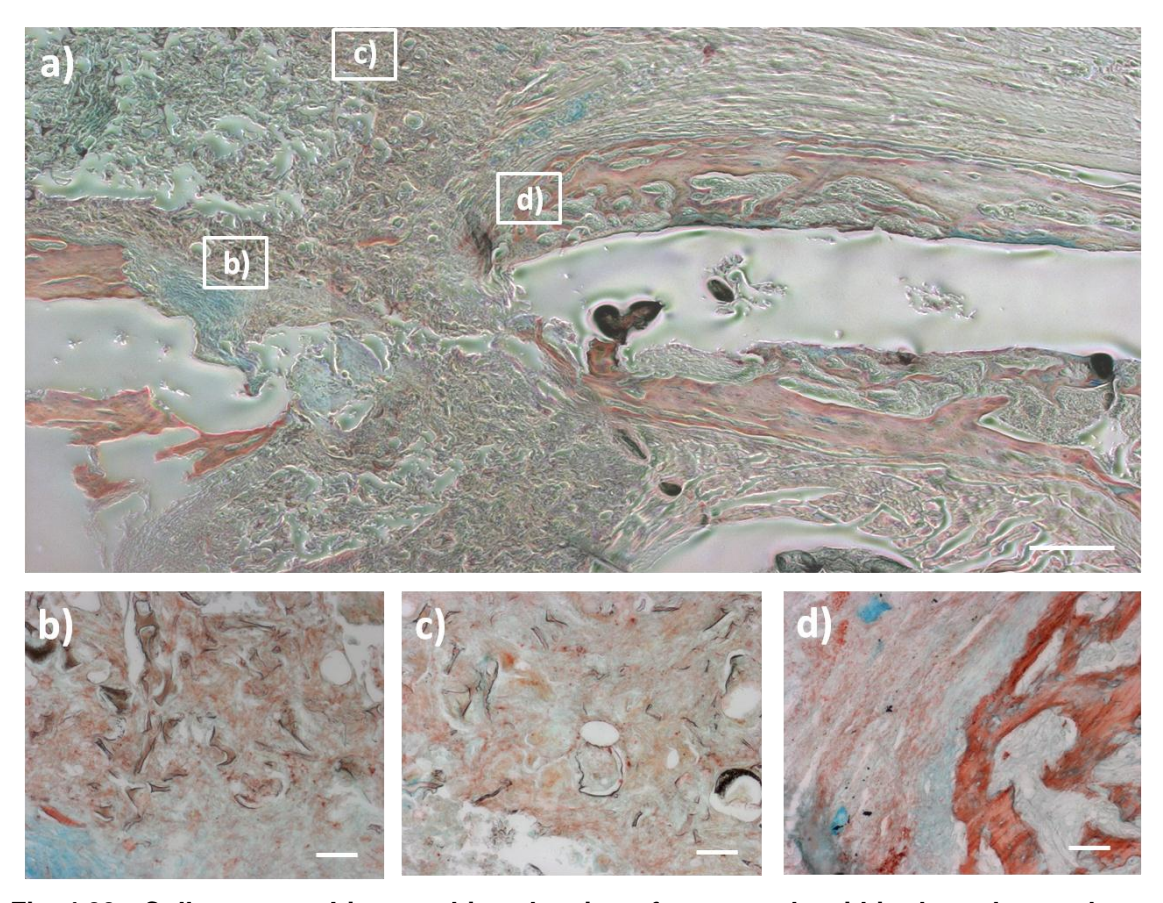


Fig. 4.22 Collagen type I immunohistochemistry for a sample within the polymer alone group. Note increased expression throughout the defect region as compared to control samples (Fig. 4.20 a), with localisation to the new osteoid. Scale bars: a) 500 μ m, b-d) 50 μ m

vWF staining for endothelial cells showed limited expression within the defect region itself (Fig. 4.23 b-d), however the area characterised by cellular infiltration was surrounded by tissue that stained positive for vWF (Fig 4.23 a). The remaining fragments of polymer also took up some of the brown oxidation product. This is unlikely

to reflect true endothelial cells expression, but is distinguished from other regions of true expression, particularly in higher power images.

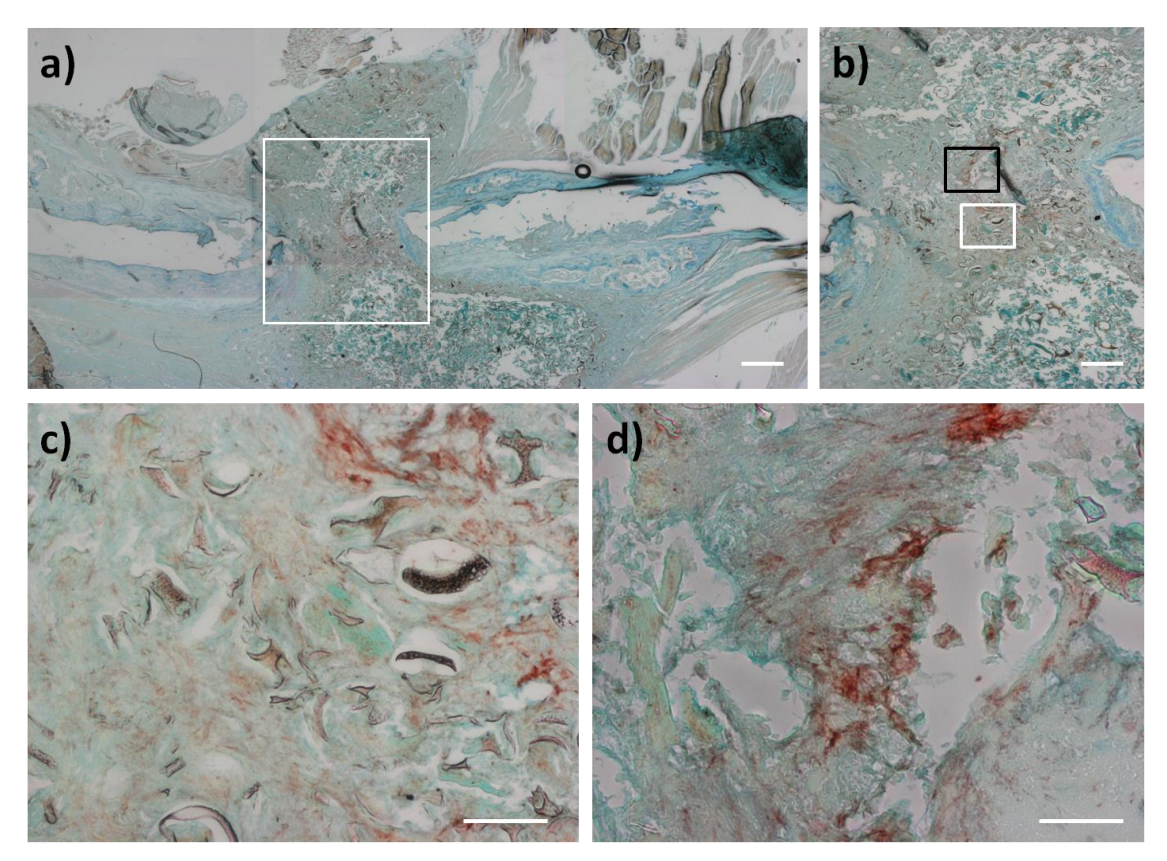


Fig. 4.23 vWF immunohistochemistry of a polymer alone sample, confirming expression within the tissues surrounding the defect, and also to a limited degree within the defect region itself (white box in a), magnified in b)). Note the brown uptake of the remaining polymer fragments which is easily distinguished from true expression in the higher magnification images (c) and d), magnified sections from white and black boxes of b) respectively). Scale bars: a) 1 mm, b) $200 \, \mu m$, c) – d) $50 \, \mu m$

4.5.5.4.3 Polymer + SSCs samples

A/S staining of the entire femoral sections revealed abundant osteoid formation with the development of morphologically normal trabecula and cellular infiltration. Furthermore, there was evidence of mature chondrocytic differentiation particularly at the intersection of the newly laid down matrix, with evidence of an endochondral ossification process, seen only in this group of samples (Fig. 4.24).

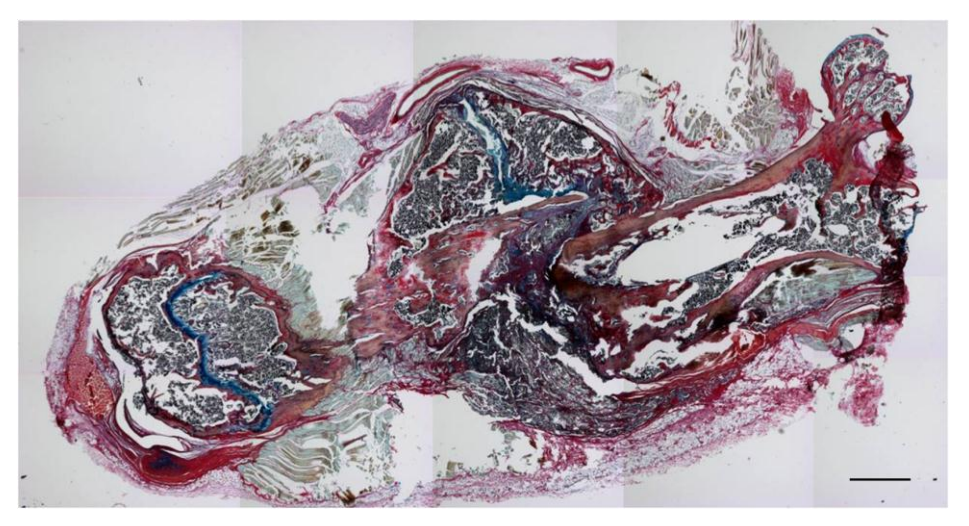


Fig. 4.24 Cross-sectional overview of an entire femur from the polymer + SSCs group, demonstrating abundant new bone matrix within the osteotomy site and throughout the defect region. There is evidence of organised bone healing within a well-defined region around the osteotomy site, with mature trabecular formation and a 'watershed' area of chondrocytes suggesting a process of endochondral ossification. Scale bar: 2 mm

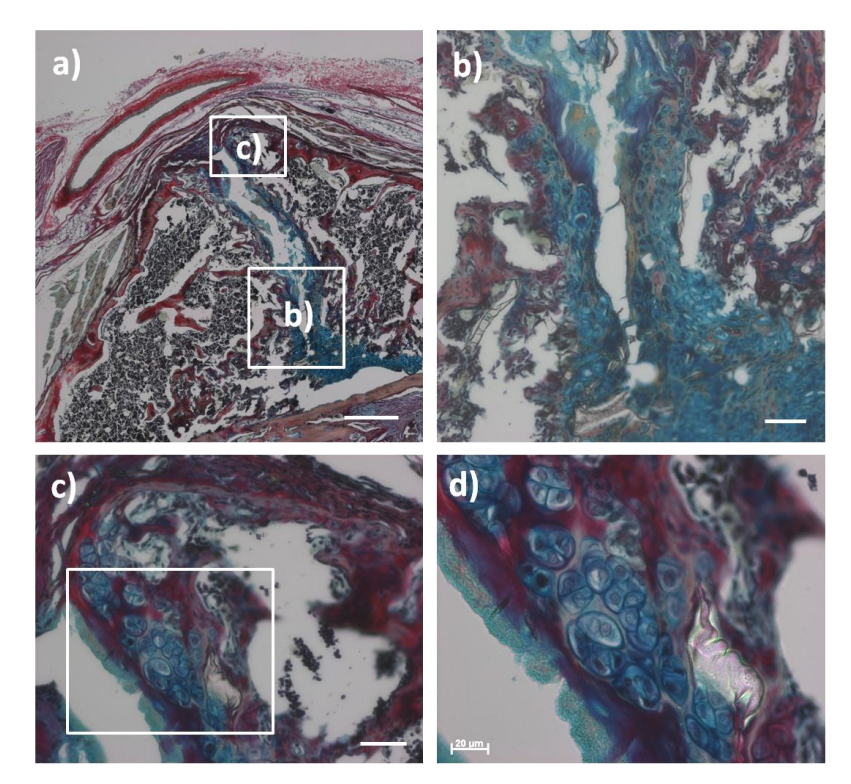


Fig. 4.25 Regions of interest from Fig. 4.24: a) Well-defined trabecula are clearly seen with surrounding cellular infiltration. A distinct zone of chondrocytic differentiation is demonstrated at the interface between the two advancing bone matrix zones. An endothelial lined cyst is visible superficial to the regenerated bone area, which may represent a bursa, formed as a reaction to the intense bone-formation. b) 10x magnification image of the central regenerated area, demonstrating a distinct zone of chondrocytes. c) 20x magnification of the most superficial part of this zone; the chondrocytes are situated within the trabecula of newly-formed bone matrix. With increasing distance from this area, chondrocytes become progressively sparser, with increasing numbers of undifferentiated cells. d) 40x magnification of a region in c). Clonal chondrocytic clusters are visible, suggestive of intense cellular activity and turnover in this region. Scale bars: a) 1 mm, b) 150 μm, c) 50 μm, d) 20 μm

Collagen type I immunohistochemistry of the polymer + SSCs group confirmed expression throughout the trabecula of the newly-formed bone within the defect site. Expression is very similar to that of native bone, as seen in Fig. 4.26 of the polymer alone sample, stained for collagen type I.

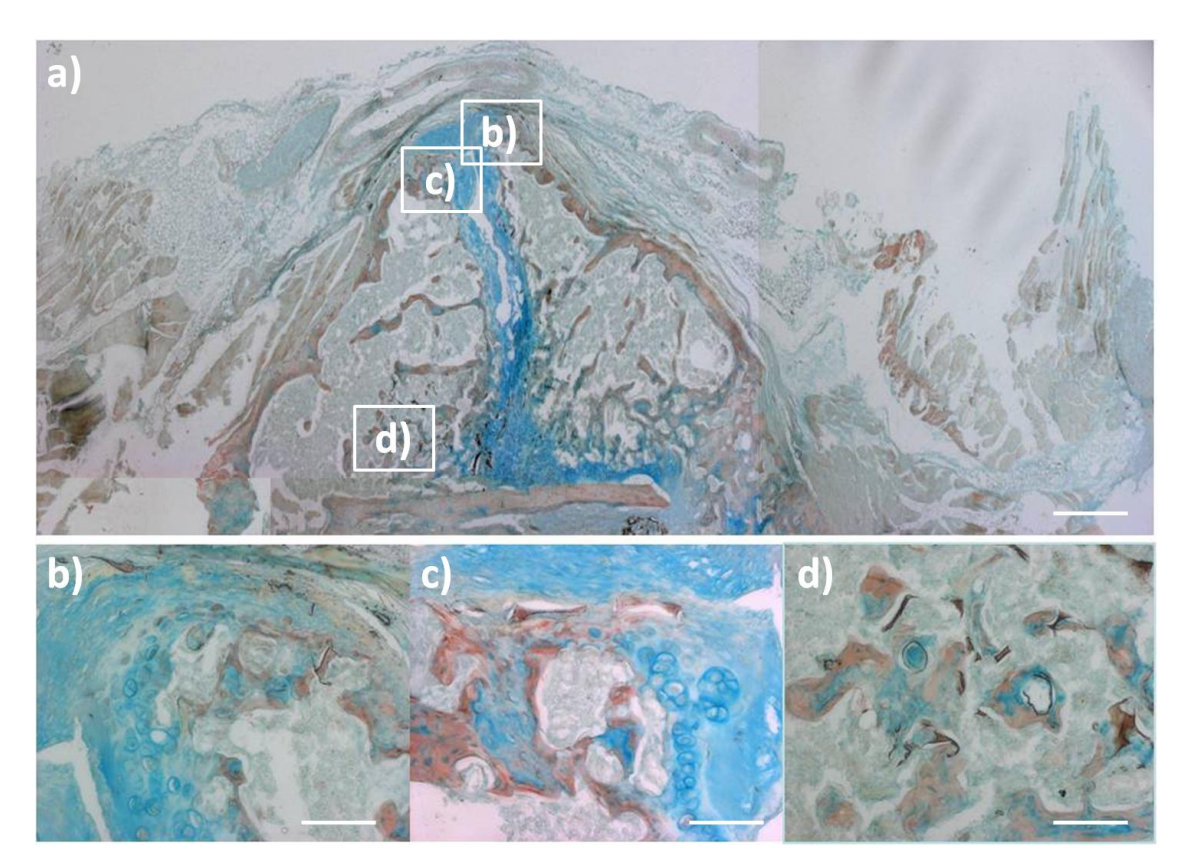


Fig. 4.26 Collagen type I immunohistochemistry of a sample containing polymer + SSCs. a) Overview of the same region seen in Fig. 4.2. Expression is seen throughout the newly-formed trabecula. b-d) Higher magnification images of regions of interest; b) Collagen expression is seen just behind the advancing zone of chondrocytes at the transition area; c) Expression is observed within some chondrocytes adjacent to the new bone; d) Fragments of polymer remain, these take up the brown stain, but are seen quite distinctly from the new bone formation on higher magnification sections. Scale bars: a) 1 mm, b-d) 200 μm

vWF immunohistochemistry of the polymer + SSC samples demonstrated expression around the undifferentiated cells behind the advancing area of chondrocytes within the osteotomy site (Fig. 4.27). There was also a discrete layer of expression within the space at the interface. vWF was expressed within the osteoid in the central defect area, and although there was artefactual uptake of oxidation product by the fragmented polymer, this was easily distinguishable from true cellular expression on higher magnification images.

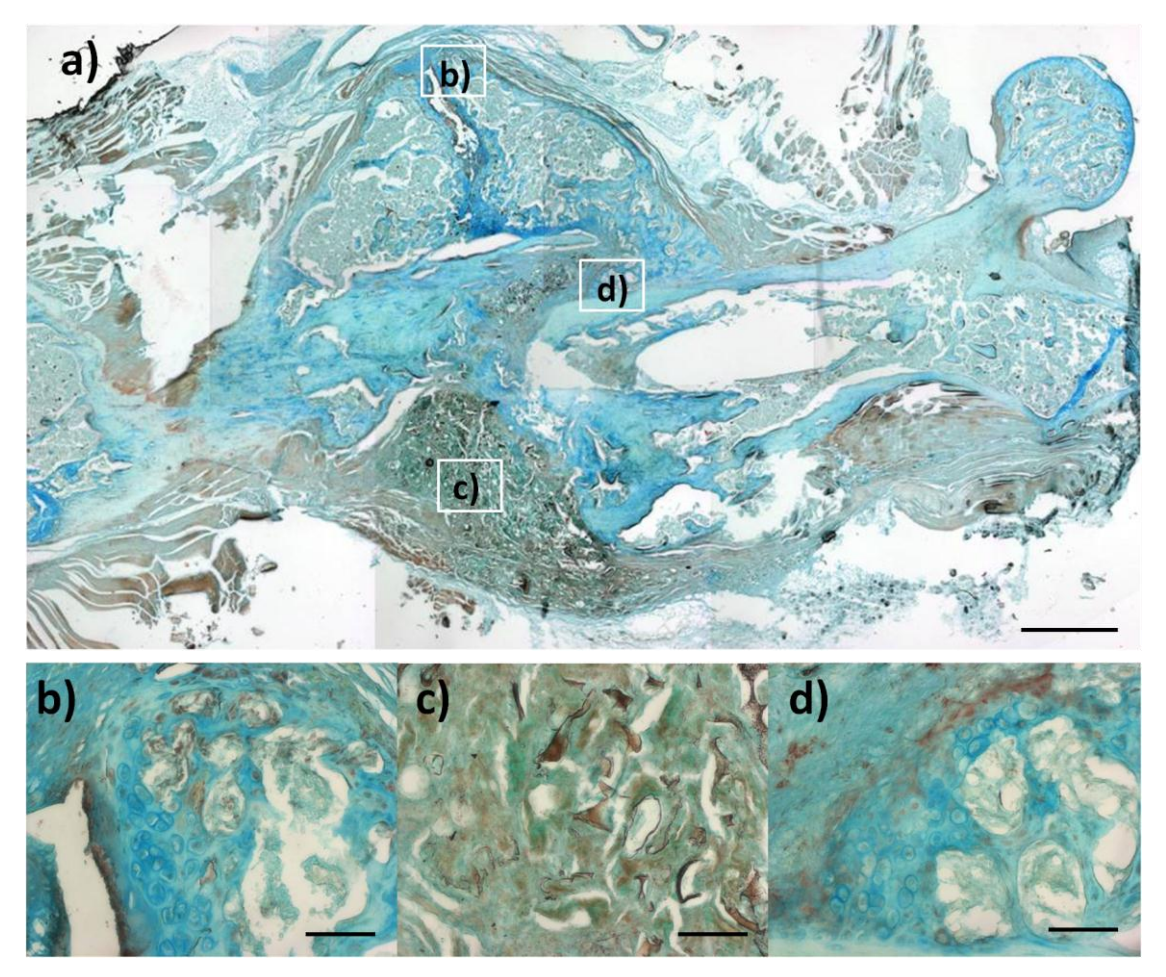


Fig. 4.27 vWF immunohistochemistry of a sample from the polymer + SSCs group. a) Overview of entire femoral section. b-d) Higher magnification images of regions of interest; b) vWF expression is seen mainly around the undifferentiated cells behind the advancing area of chondrocytes, but there is also a discrete layer of expression within the space at the interface. c) vWF is expressed within the osteoid in the central defect area, it is seen distinctly from the staining of fragmented polymer. d) Several zones of vWF expression are seen, such as this layer demonstrating expression near the central area of the osteotomy defect. Scale bars: a) 2 mm, b-d) 200 μ m

4.6 Discussion

The aim of these studies was to investigate the potential of polymeric ternary blend biomaterials to facilitate cell-attachment and differentiation suitable for skeletal regeneration strategies. By combining a high throughput approach - which allowed rapid synthesis of a large number of chemically diverse polymeric materials, with the multiplexing potential of a microarray platform - large libraries of synthetic but biodegradable polymer blends were screened for characteristics including the ability to support skeletal progenitor cell growth and differentiation. Three candidate polymeric blends that could be fabricated in sufficient quantities for macroscopic analysis were then examined individually in vitro for their efficacy in supporting the generation of a differentiated osteoblast population of STRO-1 positive stem cells. To minimise the use of animals, only the most efficacious blend underwent further analysis for its ability to provide a robust 3D scaffold for skeletal tissue regeneration in immunocompromised mice. The current data show that certain polymeric ternary blends, in particular CS/PVAc/PLLA, are capable of enhancing skeletal regeneration, both in vitro and in a small animal model, although these data remain inconclusive regarding the additional ability of incorporated exogenous SSCs as a true tissue engineering construct.

Polymer blend 1 (CS/PVAc/PEI) consisted of a heterogeneous structure that was denser in the central portion of each cylinder. Although this may produce a relatively strong scaffold under compression, it would not permit predictable cellular infiltration and would be unlikely to undergo complete or consistent bio-absorption. Furthermore, this blend supported SSCs poorly *in vitro*. Blend 3 (CS/PEI/PLLA) showed good cell adherence and ALP positivity on pilot *in vitro* culture, although its delicate structural characteristics and high solubility made it unsuitable as a test polymer. Despite strong ALP staining on the basal cultured sample, it dissolved readily even within the culture medium. If a similar blend could be fabricated with improved structural properties, this would be a good candidate for future assessment.

Blend 4 (CS/PVAc/PLLA) was homogeneous with a uniform pore-size, ideal for cellular infiltration (50-500 µm diameter). It did not dissolve or disintegrate readily in the test solutions and consistently bound to, and supported SSCs *in vitro*, at 7 and 28 days culture. However, it did require the presence of exogenous osteoinductive factors (BMP-2, ascorbate and dexamethasone) to stimulate the production of a mature osteoblast population *in vitro*, as demonstrated by positive ALP staining (Fig. 4.9).

Other osteogenic bone-matrix proteins were expressed following osteoinduction of cells grown on blend 4, with strong consistent staining for collagen type I, osteopontin, osteonectin and bone sialoprotein. However osteocalcin was not expressed, perhaps because this is a late marker of osteogenesis (Sharma *et al.* 2006), and may not yet have been produced in sufficient quantities. The staining pattern was variable when using immunofluorescent staining with these antibodies: collagen type I produced typical strand-like staining, whereas the localisation of osteopontin and BSP was more sporadic with punctate fluorescence. The true nature of this fluorescence was verified though, by using positive and negative control samples for each specimen without adjusting threshold sensitivity values between specimens.

Molecular profiling was attempted using differing methods without success. Several causes for this are likely: only 4 discs were available from each group for molecular assessment, so cellular yield was relatively low. Additionally, cells were found to adhere strongly to the polymer and all methods of removal caused fragmentation of the polymer. The resulting mixture of fragmented and partially dissolved scaffold, combined with whole and lysed cells became difficult to separate, resulting in impure RNA, which impeded subsequent extraction and analysis using PCR. Future molecular analysis may require culture of cells on a larger scale to gain a significant yield. Separation of the polymer from the cells could be achieved in future by trialling different solvents to identify one that would dissolve the polymer into solution without damaging the cells, allowing the latter to be readily separated by mechanical filtration.

Multiple, well-validated small *in vivo* models are available for the analysis of putative scaffold materials for skeletal regeneration (Coraca *et al.* 2008, Matsushima *et al.* 2009, Kanczler *et al.* 2008, Kanczler *et al.* 2010, Khan *et al.* 2010). Our group has considerable expertise using the load-bearing murine critical-sized femoral defect model employed in this study, and the results confirm this model to have been an appropriate choice. All mice survived the study protocol with little morbidity. A single complication occurred, where the distal portion of the intramedullary pin was placed outside of the femur. Although this is clearly visible on the CT reconstruction following the study period, this was not appreciated on initial plain radiographic analysis. Several methods of securing the murine femoral osteotomy are available, including external fixators, locking plates and intramedullary locking nails (Cheung *et al.* 2003, Histing *et al.* 2010, Garcia *et al.* 2010). Each system has its advantages and disadvantages, in particular: external fixation ensures the stabilising construct is distant from, and therefore cannot interfere with the bone regenerative site. This potentially allows for

easier analysis, but carries the disadvantage of higher infection rate through the pin tracts; plates can provide good stability, but because they provide stability from a single cortex, construct failure is a risk and the minute screws can be demanding to apply in a mouse model; locked intramedullary devices require the use of a jig to locate the proximal and distal interlocking holes, leading to technical difficulties when performed on an extremely small scale, they also carry the disadvantage of passing directly through the test osteotomy site. The non-interlocked intramedullary pin was selected for this study following successful use in previous similar studies Kanczler et al. 2008, Kanczler et al. 2010, Khan et al. 2010. Despite a lack of rotational stability, the interference fit within the bone ends resulted in no significant shortening of the construct throughout the study period (see Fig. 4.14). In addition, comparison of the radiographic images confirmed little rotational movement between day 0 and day 28 of the study period, therefore it can be concluded that our model is adequate for the current study. Furthermore, absolute stability would have resulted in healing by intramembranous ossification, whereas relative stability (as in our model) results in slower endochondral ossification by fracture callus (Histing et al. 2010). The latter emulates the clinical scenario more closely, and is therefore more applicable to this study. In addition, we were confident that removal of the intramedullary device, either physically or digitally following the test period would facilitate analysis of bone regeneration.

Review of the radiographic images (including μ CT reconstructions) demonstrates greater bone formation within the osteotomy site of the femora treated with the polymer blend when compared with controls and this was further enhanced by the addition of SSCs to the construct. Statistical analysis did not prove the latter enhancement to be significant by most measures of bone formation, although a definite trend is demonstrated. Histological analysis corroborates this trend, demonstrating greater cellular infiltration within the polymer samples, which was further enhanced in the polymer + SSCs group. Hydrolytic degradation of the polymer appeared to match new bone in-growth, and new trabecula were seen in both the polymer groups with coincident, appropriate collagen type I expression.

Histological differences were encountered between the polymer groups – samples in the polymer alone group showed mainly woven bone generation within the osteotomy gap, although samples in the polymer + SSCs group demonstrated endochondral ossification, with a widespread callus reaction and mature chondrocyte development, prior to the formation of well-organised trabecula. Endothelial tissue infiltration into and

around the osteotomy site (as demonstrated by positive vWF staining) was confirmed in both polymer groups, suggesting vascularisation was taking place – a pivotal prerequisite for osteogenesis.

Although some of the statistical analyses of bone formation did not reach statistical significance, histological and radiographic evidence confirms enhanced osteogenesis in both polymer groups. Regeneration appears further enhanced by the addition of SSCs, although characteristics of the polymer scaffold alone appear to have been beneficial in providing an appropriate spatial and biologically favourable environment for osteogenesis. It should be noted that digital subtraction of the intramedullary device was more difficult than anticipated, and this is likely to have led to an underestimation of bone formation in the test groups, particularly with the few samples analysed. However the ability of polymeric scaffolds functionalised with biological cues to stimulate tissue formation without the application of progenitor cells is not a novel concept - Lee et al. have shown regeneration of rabbit humeral head cartilage by implantation of polycaprolactone and hydroxyapatite bioscaffolds spatially infused with TGF-β3-adsorbed hydrogel (Lee CH et al. 2010). Future experiments would be required with larger numbers over a longer time period to differentiate the effect of addition of SSCs to the polymer, and to deduce whether there is a true requirement for exogenous SSCs with the polymer to produce adequate bone healing, as this study suggests the polymer alone has a very beneficial therapeutic effect. This could be combined with functionalisation of the ternary blend with osteoinductive factors, such as BMP or VEGF for temporal release, to further enhance osteogenic properties (Kanczler et al. 2010). Furthermore, the translation of this technology to larger scale models would be required to validate ternary blend biomaterials for their functionality with respect to weight-bearing and remodelling capacity prior to clinical application.

In conclusion, the null hypotheses that: 'polymeric ternary blend biomaterials do not facilitate cell-attachment and lineage-differentiation suitable for skeletal regeneration strategies', and 'polymeric ternary blend biomaterials do not function as suitable scaffolds for skeletal regeneration strategies' can both be rejected, however it is still unclear if the proven osteoregenerative capacity of the ternary blend polymer under test *in vivo* is further enhanced by the addition of SSCs.

Chapter V

In vivo evaluation of a candidate binary polymer blend scaffold for skeletal tissue engineering strategies using an ovine model

I am grateful to Dr Ferdous Khan at the University of Edinburgh for providing the polymer blend scaffolds and for the prior work of Dr Rahul Tare and Dr Janos Kanczler in characterising these polymers *in vitro* and in a small animal model. This study was performed with Mr Edward Tayton and Mr Alexander Aarvold under the supervision of Professor Allen Goodship, using the extensive knowledge and facilities at the Royal Veterinary College, Hertfordshire. In addition, I am grateful for many useful discussions gained from visits to the laboratories of Professor John Field, Adelaide and Professor Dietmar Hutmacher, Brisbane, Australia. I also gratefully acknowledge Dr Stuart Lanham for performing CT analysis, Dr Richard Cook for undertaking mechanical testing, in addition to the technical expertise of Ms Gillian Hughes, Miss Esther Ralph and Mrs Carol Roberts. All experimental, operative and analytical components of this study were conducted by Mr Tayton and me.

5.1 Introduction

5.1.1 The requirement for large animal studies

Although many successful *in vitro* and *in vivo* laboratory studies have shown potential application for a variety of tissue regenerative strategies, to date, there has been limited translation to clinical practice. There exists a considerable translational gap due to the paucity of potential strategies that undergo 'up-scaling' prior to pre-clinical trials, primarily due to considerations of cost, regulation, logistics and expertise (see chapter VII). Currently, no synthetic system is able to replicate the diverse biomechanical conditions present within a large organism, so in order to fully evaluate a candidate biomaterial for skeletal regeneration strategies prior to clinical application, a large animal study is required to bridge this gap.

5.1.2 Selection of appropriate large animal model

The performance of any biomaterial must be evaluated for safety, efficacy and practicality in a suitable model to simulate human *in vivo* conditions as closely as possible. Myriad variables must be defined and controlled to ensure the model used will assess the most relevant attributes to the clinical domain of interest, whilst minimising variations in outcome and also the number of animals required to achieve statistical power (Table 5.1) (Muschler *et al.* 2010).

Table 5.1 Variables within a large animal model, which need to be defined and controlled

Inherent variables	Modifiable variables	Experimental variables
Subspecies	Diet/ Nutritional status	Anaesthetic/ pain management
Gender	Exercise/ activity regime	Surgical procedure
Partum	Gonadal/ lactation status	Anatomic location
Age	Temperament	Fixation technique
Animal to animal variation	Environment	Assessment outcomes

Adapted from Muschler et al. 2010

In comparison to humans, the chosen animal model must demonstrate corresponding physiological and pathophysiological mechanisms with respect to the intervention being considered. This includes tissue repair and regeneration, but also consideration of size and proportions as well as static and dynamic forces to which the construct and associated tissues will be subjected. Although dogs, primates, horses, goats, pigs and sheep have been used in pre-clinical analysis of skeletal defect healing, the latter group has become increasingly popular as test subjects. Allowances are generally accepted for the quadrupedal gait of most large mammals used in research and the resultant variation in subjected mechanical forces when compared to the bipedal human gait. The chosen animal should ideally be in sufficient supply, domesticated with a placid nature, of equivalent weight to an adult human, with similar skeletal architecture and dimensions. Further criteria include costs of acquisition and care, local availability, acceptability to society, tolerance to captivity and ease of housing (Pearce et al. 2007). Several previous studies have made use of dogs as models for orthopaedic research (Martini et al. 2001). Larger breeds closely resemble humans with regard to bone weight, density, mineral composition and protein constituents, although significant differences in their bone microstructure and remodelling have been described due to their characteristics as fast-growing animals (Aerssens et al. 1998). In particular, dog bones have higher rates of trabecular and cortical bone turnover with only a limited cortical osteonal structure when compared to human bone. Recently, the use of dogs as experimental models has significantly decreased, mainly due to ethical concerns, although canine studies still account for approximately 9% of large animal musculoskeletal studies published in prominent journals (O'Loughlin et al. 2008).

Ovine models have recently become more popular, due partly to their abundant availability and relatively low cost but also because they share several biological attributes with humans: mature sheep have a body mass similar to adult humans and similar long bone dimensions, enabling the use of implants designed for humans with little modification (Newman et al. 1995). The mechanical loading environment in sheep has been characterised, with forces and moments of approximately half of those found in humans during normal ambulation (Taylor et al. 2004, Taylor et al. 2006), probably because they are quadrupedal. Furthermore, ovine bone mineral composition, metabolic and remodelling rates are roughly equivalent to those of humans (Ravaglioli et al. 1996) however some researchers maintain that significant histological differences exist, particularly in younger sheep (less than 7 years old) prior to secondary osteonal remodelling (Newman et al. 1995, Reichert et al. 2010). The differentiation potential of ovine derived SSCs has also recently been characterised, enabling laboratory

protocols to be defined to induce osteogenic differentiation in ovine cells (McCarty *et al.* 2009). Sheep are generally favoured over goats because sheep are calmer, with a more docile disposition. Although the pig has been described as a highly representative morphological and biomechanical model of human bone regeneration, their appendicular bones are considerably shorter than those of sheep and humans, and their obstinate, and sometimes vicious temperament can make handling and safe perioperative care a particular challenge (Newman *et al.* 1995). Perhaps the most compelling factors determining final choice will include previous local experience along with appropriate facilities and expertise in using a particular species.

5.1.3 Selection of appropriate defect and bone site

Although the humerus is the largest bone in quadrupeds (Muschler *et al.* 2010), animal studies of skeletal regeneration using tissue engineered constructs often make use of tibial segmental defects to more closely mimic the clinical circumstance. The tibial diaphysis is the most common site in humans for problematic post-traumatic skeletal defects, because of poor soft tissue coverage, which often complicates treatment (DeCoster *et al.* 2004). This potential complication can be examined in sheep tibiae which have a similar soft tissue envelope to human tibiae. Furthermore, the suitability of the tibia in these models is reinforced by facile surgical exposure and a choice of fixation systems analogous to the clinical scenario.

5.1.4 Critical segmental defect

In order to investigate the effects of various skeletal regenerative approaches and bone repair mechanisms, a variety of critical sized tibial defect models have been created. A critical sized defect is defined as the smallest intra-osseous defect in a particular bone and species of animal that will not spontaneously unite within its lifetime, or as a defect which demonstrates less than 10% regeneration (Gugala *et al.* 2007, Reichert *et al.* 2009). This size is often quantified by multiplying the diaphyseal diameter by 2.5 (Lindsey *et al.* 2006), but is in fact highly variable, and dependent on multiple inherent and procedural factors (Table 5.2).

Table 5.2 Inherent and procedural factors that affect the size of a critical segmental defect

Inherent	Procedural
Age	Site, size and method of ostectomy
Species	Nutrition
Bone structure	Presence of periosteum
Mechanical loads/stresses	Fixation method - absolute or relative stability

It has been shown that unfilled defects of significantly smaller than 2.5 times the diaphyseal diameter do not undergo spontaneous healing when the construct is significantly devascularised, periosteum is stripped or removed, heat damage is allowed during creation of the ostectomy, or if the construct fixation method only allows primary bone healing, such as in absolute stability (Wallace *et al.* 1991, Kuttenberger *et al.* 2010, Goodship *et al.* 1993, Epari *et al.* 2006, Epari *et al.* 2008). Consequently, the best designed studies include a control group where the defect has not been filled with scaffold, in order to demonstrate an absence of regeneration in these samples.

5.1.5 Methods of fixation

Several methods can be employed to achieve fixation of a segmental skeletal defect. Clinically, diaphyseal tibial fractures are now most commonly stabilised with intramedullary nailing (Giannoudis *et al.* 2006). Although close correlation to the human clinical scenario is beneficial, additional factors have to be considered when selecting the most appropriate system for large animal studies. Table 5.3 summarises previous ovine segmental defect studies, including fixation technique.

Table 5.3 Previous ovine segmental defect studies

Author, year	Fixation	Approach	Defect	Bone	Age of	Empty	Filler/ scaffold
Wallace et al.			size		sheep	control	
1991 Goodship <i>et al.</i>	Ex-fix	AM	2 mm	Tibia	3 yrs	Υ	Nil
1993	Ex-fix	AM	fracture	Tibia	adult	Υ	Nil
Wallace et al. 1995	Ex-fix	AM	2 mm	Tibia	adult	Υ	Nil
Augat <i>et al.</i> 1997	Ex-fix	NS	3 mm	Tibia	2-3 yrs	N	Nil
Gao <i>et al.</i> 1997	Plates	NS	16 mm	Tibia	adult	N	Biocoral vs. TCP
Hente <i>et al.</i> 1999	Ex-fix	AM	3 mm	Tibia	6-11 yrs	Υ	Nil. Dynamic vs. static fixation
den Boer et al. 1999	IM nail	AM	30 mm	Tibia	adult	Υ	Empty vs. cancellous bone
Gugala <i>et al.</i> 1999	Ex-fix	NS	40 mm	Tibia	6-7 yrs	N	PLDLLA membrane +/- cancellous bone autograft
Marcacci et al. 1999	Ex-fix	AM	35 mm	Tibia	2 yrs	N	HA block
Petite <i>et al.</i> 2000	Plate	lateral	6, 12, 25 mm	Meta- tarsus	2 yrs	N	Coral +/- BMA or Coral +/- SSCs
Blokhuis <i>et al.</i> 2000	IM nail	AM	30 mm	Tibia	≥ 2 yrs	Υ	TCP +/- BMA vs. autologous bone
Kon <i>et al.</i> 2000	Ex-fix	AM	35 mm	Tibia	2 yrs	N	Porous HA cylinder +/- autologous SSCs
Gugala & Gogolewski 2002	Ex-fix	NS	40 mm	Tibia	6-7 yrs	N	PLDLLA membrane +/- cancellous bone autograft
den Boer et al. 2003	IM nail	AM	30 mm	Tibia	adult	Υ	Porous HA +/- OP-1 +/- BMA +/- corticocancellous autograft
Augat et al. 2003	Ex-fix	AM	3 mm	Tibia	4-5 yrs	N	Nil. Axial vs. shear movements allowed
Bloemers et al. 2003	IM nail	AM	30 mm	Tibia	≥ 2 yrs	N	CaPO ₄ vs. autologous bone
Regauer et al. 2005	IM nail	NS	50 mm	Tibia	adult	N	DBM +/- OP-1 +/- BMA vs. bone autograft
Schell et al. 2005	Ex-fix	AM	3 mm	Tibia	2.5-3.5 yrs	Υ	Nil. Rigid vs. semi-rigid ex-fix
Epari <i>et al.</i> 2006	Ex-fix	AM	3 mm	Tibia	2.5-3.5 yrs	Υ	Nil. Rigid vs. dynamic ex-fix
Maissen <i>et al.</i> 2006	Ex-fix	NS	18mm	Tibia	4-5 yrs	Υ	PLDLLA +/- TGF-β vs. bone autograft
Mastrogiacomo <i>et al.</i> 2006	Plate	NS	48 mm	Tibia	2 yrs	N	Si-TCP and HA-TCP mix +/- SSCs
Sarkar <i>et al.</i> 2006	IM nail	NS	25 mm	Tibia	5.5-7.5 yrs	N	PRP-loaded collagen
Teixeira et al. 2007	Plate + cage	NS	35 mm	Tibia	4-5 mths	N	Autograft bone vs. HA + collagen + BMP + DBM
Mastrogiacomo et al. 2007	Plate	NS	40 mm	Tibia	2-4yrs	N	Si-TCP and HA-TCP mix +/- SSCs
Tyllianakis <i>et al.</i> 2007	IM nail	AM	0-30 mm	Tibia	16-20 mths	Υ	Nil
Epari <i>et al.</i> 2008	Ex-fix	AM	3 mm	Tibia	2-3 yrs	N	Nil
Field et al. 2009	IM nail	lateral	50 mm	Femur	3 yrs	Υ	TCP/ PLDLLA mesh vs. milled allograft vs. cortical strut graft
Rozen <i>et al.</i> 2009	Plate	PL	32 mm	Tibia	2 yrs	Υ	EPCs
Schneiders et al. 2009	IM nail	AM	30 mm	Tibia	NS	N	HA/Collagen +/- chondroitin sulphate
	•	•	•		•	•	· · · · · · · · · · · · · · · · · · ·

5.1.5.1 Intramedullary nails

Nails can be either reamed or unreamed, each with its own advantages and disadvantages: reaming can significantly alter endosteal blood circulation and cause thermal necrosis (Schroeder et al. 2010). Subsequent nail insertion can increase intramedullary pressure, potentially leading to pulmonary microvascular damage, air or fat embolism (Pape et al. 2006). Unreamed nails are generally of smaller diameter and often possess minimal interference fit, relying solely on the integrity of interlocking screws for stability. Such nails may therefore produce relative, rather than absolute stability at the fracture/osteotomy site and are more prone to failure (Duan et al. 2012). Successful skeletal regeneration studies have been undertaken using intramedullary nailing to stabilise segmental defects in ovine tibiae (den Boer et al. 1999, Bloemers et al. 2003, Teixeira et al. 2007, Tyllianakis et al. 2007) and femora (Field et al. 2009), however the nail becomes an intrinsic part of the osteotomy gap and its presence could affect regeneration, and complicate its subsequent radiological and histological analysis.

5.1.5.2 Internal plate fixation

Although in the clinical situation, internal plate and screw fixation techniques are most commonly used for metaphyseal fractures, plates are also indicated in diaphyseal tibial fracture fixation, particularly in the immature skeleton, when damage to physeal growth zones should be avoided. Several researchers have used plating systems in ovine models with varying success. Optimal reduction can be achieved under direct vision, using the same exposure as for the insertion of a putative biomaterial, and the fixation can easily be removed *post mortem* with little impact on the osteotomy site or its subsequent analysis. However, many previous studies used conventional plate systems resulting in significant rates of construct failure. Modern limiting-contact locking dynamic compression plates (LC DCPs) prevent high contact pressures between the plate and cortical bone, avoiding the reduction of periosteal blood flow and localised osteoporosis through stress shielding, and potentially reducing implant failure rates (Reichert *et al.* 2010).

5.1.5.3 External fixation

Clinically, external fixation is most often employed as a temporary measure to stabilise open or grossly contaminated fractures, however they are also frequently used in limb lengthening, deformity correction, arthrodesis and salvage procedures. The versatility and ease of use of external fixation systems have made them a frequent implant of choice for ovine studies. Furthermore, the Schanz screws which stabilise the bone can

be inserted with minimal trauma at some distance proximally and distally, leaving no hardware whatsoever at or near the experimental site.

Healing periods following external fixator application have been reported to be significantly longer when compared to other fixation devices, and this may be a function of the possibility of obtaining an extremely stiff construct, leading to absolute stability with very little movement at the osteotomy site and stress protection (O'Doherty *et al.* 1995). Furthermore, the risk of pin site infection and loosening is a concern, and the external structure itself may affect the gait of sheep, or cause injury or difficulty with wound dressings.

5.1.6 Binary blend polymer scaffold

The design, fabrication and assessment of putative biomaterials for potential clinical application require the input of many coordinated agencies for success (see Chapter VI). Consequently, multiple strategies will often be under simultaneous consideration within a single research group. Since each potential biomaterial undergoes a similar iteration during analysis, an 'evolution' of strategies is seen over time, where one candidate material will be undergoing large scale *in vivo* analysis, while a more refined material developed using results from testing of the first material will still be undergoing preliminary *in vitro* assessment.

In a prior study, performed within the Bone and Joint Research Group Southampton, the biocompatibility and applicability for skeletal regeneration of candidate *binary* polymer blend scaffolds was assessed *in vitro* as well as in a murine skeletal defect model (Khan *et al.* 2010). These scaffolds are similar to those analysed in the small *in vivo* model in chapter V of this thesis, although these materials were synthesised using a combination of just two (rather than three) polymers. The study found the binary blend PLLA/PCL (20/80) displayed a bone-like architecture as well as providing a robust template for STRO-1 positive SSC attachment and bone regeneration *in vitro* and in a murine segmental femoral defect model. This polymer blend was therefore chosen as the scaffold for up-scaling to our ovine tibial segmental defect model, with the hypothesis that the polymer scaffold would also provide a suitable template for ovine SSC attachment and bone regeneration on a larger scale. In addition, an aim of this study was to establish a reproducible technique for analysis of candidate biomaterials in a large animal skeletal defect model.

5.2 Objectives

- To establish a consistent and reproducible technique for stabilisation of a 35 mm tibial critical defect in sheep, for subsequent trialling of tissue regeneration strategies.
- To demonstrate a living cell composite using cultured skeletal stem cells on synthetic scaffold to augment bone formation in a large animal segmental defect model.

5.3 Null hypothesis

 The polymeric binary blend biomaterial PLLA/PCL (20/80) does not function as a suitable scaffold for skeletal regeneration strategies in an ovine tibial segmental defect model.

5.4 Materials and methods

5.4.1 Polymer fabrication

Polymeric binary blend (PLLA/PCL (80/20)) scaffolds were formulated and fabricated by Dr F Khan at the University of Edinburgh using solvent mixing techniques as previously described (Chapter IV). 10 identical scaffolds were produced (diameter 23 mm, length 40 mm) (Fig. 5.1 a).

5.4.2 Initial processing of polymer scaffolds

The received polymers required preliminary processing before they were suitable for application in the ovine study. Although the polymer is fabricated as a macroporous scaffold, during manufacture, each scaffold becomes coated in an impermeable thin film of polymer. This was carefully removed by peeling the film off to reveal the underlying structure. The scaffolds were cut to precisely 35 mm in length using a scalpel blade, as measured by digital callipers. Additionally, to recreate the medullary canal of the ovine tibia and further improve diffusion of medium and cells in culture, a central canal was drilled down of each scaffold using an 8 mm High Speed Steel (HSS) drill bit at a slow speed to prevent thermal damage to the polymer. The final scaffolds were identical in size, shape and surface consistency (Fig. 5.1 b).

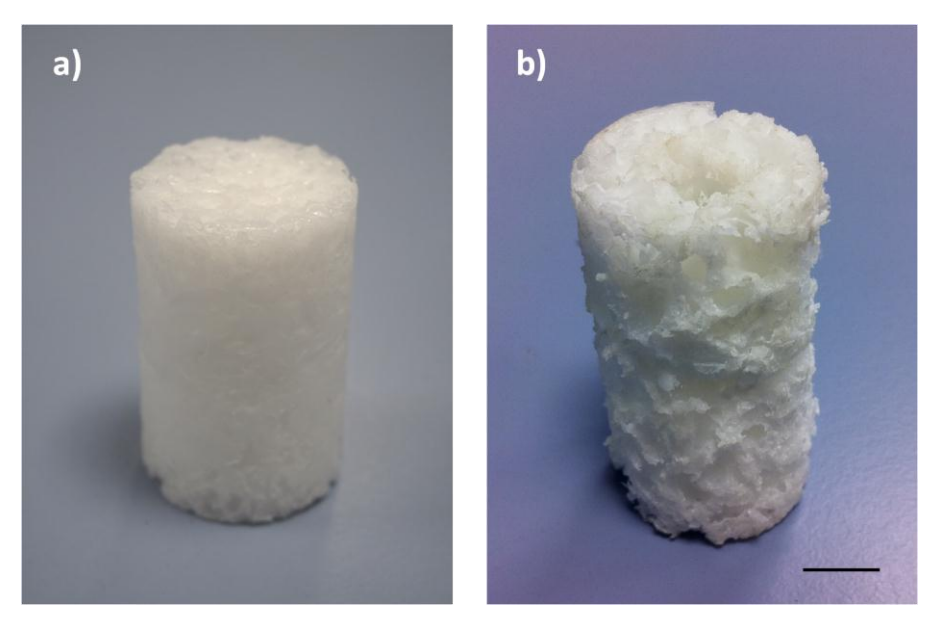


Fig. 5.1 Binary polymer scaffold, a) as initially received, **b)** following processing. Scale bar: 10 mm

The scaffolds and off-cuts produced during initial processing were sterilised by immersion in 5 x antibiotic/antimycotic solution and degassing using negative pressure. Scaffolds remained in this solution for 24 hours before transfer to basal medium and subsequent UV irradiation overnight.

5.4.3 Preliminary experiments

Although the previous study (Khan *et al.* 2010) confirmed good adherence of human SSCs onto the test polymer with appropriate osteoinduction on a small scale, no study has shown similar effects for ovine cells on larger scaffolds. Additionally, although our laboratory has considerable experience isolating and culturing human SSCs, no practical experience existed in culturing ovine cells. Therefore, a series of experiments was devised to confirm appropriate scaffold characteristics for ovine cell adherence and growth and to define the most appropriate protocols for ovine cell seeding and initial incubation prior to implantation.

5.4.3.1 Confirmation of scaffold porosity and interconnectivity

5.4.3.1.1 Scanning Electron Microscopy

SEM was performed on cut sections of the scaffold by Dr F Khan to confirm porosity and define pore sizes.

5.4.3.1.2 Alcian blue penetration test

A cuboid of polymer scaffold was prepared (5x5x40 mm) and supported upright in a specimen pot. The superior aspect was sealed circumferentially using histology embedding wax and Alcian blue dye was infiltrated from the top so that no dye could pass around the outside of the scaffold. Following 12 hours, the scaffold below the wax seal was sectioned and examined for the presence of the dye within the pores.

5.4.3.2 Acquisition of ovine iliac crest BMA

Iliac crest aspirates were obtained from mature 'cull' ewe sheep (Northern Mule, weight approximately 70-80 kg) undergoing experimental surgery as approved by the relevant Home Office Animals (Scientific Procedures) Act 1986 Project Licence. All operators

were in possession of a current and valid Personal Licence and all sheep used in this study were appropriately assessed, screened and quarantined prior to any intervention.

Following appropriate sedation and anaesthesia (see appendix for protocol), the sheep were placed in right lateral recumbency. The aspiration site in the left posterior superior iliac crest was identified and wool was shaved to a diameter of approximately 5 cm around this area. The hide was prepared with two applications of aqueous iodine scrub solution and draped appropriately. Sterile technique was maintained henceforth. A scalpel blade was used to make a small incision over the aspiration site, directly onto bone. The trocar, 11 gauge aspiration needle (Rocket Medical) and 20 ml Luer lock syringe were pre-heparinised with 0.5 ml of 1000 units/ml heparin. The trocar and aspiration needle were passed through the incision, directly into the iliac crest and in an antero-caudal direction. Care was taken to ensure the needle remained within the cancellous bone of the iliac crest. The trocar was removed and the syringe screwed onto the aspiration needle tightly to ensure a tight seal. Aspiration was achieved by gentle pressure on the syringe. Once the required quantity of bone marrow (approx 5 ml) had been aspirated, the needle was withdrawn and gentle pressure was applied to the aspiration site until haemostasis was achieved. The aspiration site was closed with a single nylon suture (Ethilon, Ethicon, Livingstone, UK). The aspirate was gently agitated to mix with heparin inside the syringe before storage at 5°C.





Fig 5.2 a) Mature Northern Mule 'cull' sheep used for the study. b) Aspiration technique from iliac crest using needle and trocar. The gloved thumb and forefinger mark either side of the iliac crest. The same technique was used throughout the main experimental procedure, although a wider surrounding area was sheared, prepared and draped to maintain full asepsis.

5.4.3.3 Isolation and culture of ovine SSCs

BMAs were transported to the laboratory and cultured expediently. Aspirates were centrifuged at 11000 rpm for 4 minutes and the supernatant removed before resuspending and seeding the cells onto tissue culture plastic in osteogenic conditions at a density of $1x10^6$ cells per T175 flask. An initial ovine BMA sample was used to ensure these standard isolation and monolayer culturing techniques would be suitable for ovine cells, and this sample was split, with half the cells cultured in basal and half in osteogenic conditions. Medium changes were performed every three days until cells achieved approximately 75 – 80% confluence (approximately one week).

5.4.3.4 In vitro incubation of ovine SSCs with test scaffold

Cells were released from the tissue culture plastic flasks with trypsin and prepared as four varying concentrations of cells in basal medium: $1x10^4$; $1x10^5$; $2.5x10^5$, and $5x10^5$ cells/ml. One ml of each concentration was then seeded onto prepared 10 mm cubes of polymer scaffold (n=3) for three hours before static incubation in either basal or osteogenic conditions for 28 days. Following culture, the scaffolds were prepared for fluorescent viable cell analysis (using Vybrant[®] Green), and quantitative ALP and DNA analysis as previously described (Chapter III).

5.4.4 Ovine tibial segmental defect model

In order to adequately assess the utility of the candidate polymer scaffold in an ovine tibial segmental defect model, this study required a complete set of results from three groups of four study animals. It was therefore decided that any failure of an animal to recover, or death before the completion of the protocol would result in that particular test being repeated to ensure a complete set of results.

Northern Mule sheep with a body weight of approximately 70 - 80 kg at the start of the study period were all subjected to pre-operative iliac crest bone marrow harvest and underwent equivalent standard anaesthetic, analgesic and skeletal fixation regimes, with similar management post-operatively. Apart from varying management at the tibial defect site, all other pre-, peri- and post-operative variables were minimised to ensure comparability between study groups.

This study was performed under Home Office Animal Licence Approval with Professor Goodship as Project Licence holder and Research Fellows from Southampton operating under secondary availability within the authority of their Personal Licences. All the procedures were designed to comply with Home Office stipulations and to adhere to the principles of animal experimentation (Russell *et al.* 1959).

5.4.4.1 Fixation design and selection

A thorough literature review was undertaken and the potential benefits of using internal plate and screw, intramedullary nail, or external fixation systems was assessed prior to making a final decision (see Section 5.15). In addition to local laboratory scientist and veterinary expertise, advice was sought from centres with experienced personnel who are conducting similar ovine studies. This included visits to the laboratories of: Prof John Field (Adelaide, Australia), an advocate of intramedullary fixation; Prof Dietmar Hutmacher (Brisbane, Australia), who uses internal plate fixation, and Prof Allen Goodship (Royal Veterinary College, Hertfordshire), who prefers external fixation. The opportunity to assist in some operative procedures at all centres, helped to inform the preferred fixation method chosen for the present study.

5.4.4.2 Cadaveric procedures

We obtained several disarticulated fresh sheep tibiae (Uptons Butchers of Bassett, Southampton, UK) and trialled these with both a custom-made intramedullary nail and external fixator. The external fixator method was preferred as it provided improved stability of fixation over the intramedullary device. In addition, the procedure could be tailored to account for an array of bone lengths and diameter, and external fixation did not cause collateral damage to the knee joint which may have hampered post-operative mobilisation and weight bearing. Additionally, Prof Goodship had most experience with external fixation models in ovine segmental defects and rarely suffered post-operative complications. Further cadaveric procedures using whole sheep hind limbs were therefore undertaken using the external fixator. These cadaveric 'dry run' procedures were performed to ensure familiarity with the equipment and processes involved and reduce unexpected live animal morbidity (Fig. 5.3).

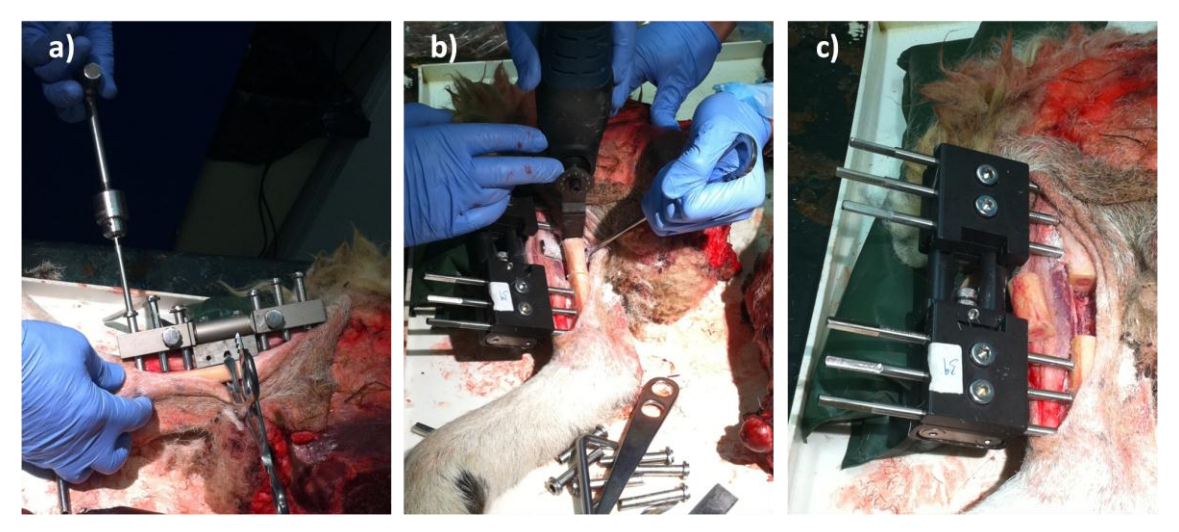


Fig. 5.3 Cadaveric 'dry run' procedure using a whole sheep hind limb. a) The tibial diaphysis has been exposed and the jig applied using forceps. A Schanz screw is inserted by hand to prevent thermal necrosis. b) The external fixator has been tightened onto the six Schanz screws and the segmental defect is removed using a sagittal saw. c) The final construct following removal of the defect

5.4.4.3 Study cohorts

12 sheep were randomly assigned to one of three treatment groups:

Group 1 – negative controls (4 sheep)

Empty 35 mm tibial defect with skeletal fixation only

• Group 2 – positive controls (4 sheep)

35 mm tibial defect with polymer scaffold and fixation

• Group 3 – treatment group (4 sheep)

35 mm tibial defect with polymer scaffold, autologous SSCs and fixation

5.4.4.4 Bone marrow harvesting

All live sheep underwent bone marrow aspiration from the iliac crest as a separate procedure (see Section 5.4.3.2) approximately two weeks prior to the segmental defect operation. Marrow from sheep assigned to group 1 and 2 that was not required for reimplantation, was used for *in vitro* preliminary experimentation. Marrow from sheep in group 3 was transported to the laboratory for isolation, culture and seeding onto the polymer scaffold.

5.4.4.5 Scaffold preparation and cell seeding prior to implantation

Polymer scaffolds were prepared and sterilised as previously described (Section 5.4.2). For scaffolds in group 3, autologous ovine SSCs that had been grown in monolayer culture to approximately 75% confluence were released and seeded onto the scaffolds at a concentration of 5x10⁵ cells/ml (20 ml total). The seeded scaffolds were gently rotated in osteogenic medium for 7 days prior to implantation into the tibial segmental defect model. Scaffolds from group 2 underwent the identical processes, except no cell seeding took place. On the day of implantation, the scaffolds were assessed microscopically to confirm absence of infection before undergoing a change of medium, and transportation at 37°C to the operating facility.

5.4.4.6 Surgical procedure

5.4.4.6.1 Premedication, anaesthesia and preparation

Sheep were allocated individual pens and food was withheld prior to surgery (Fig. 5.4 a). A fentanyl transdermal patch (Durogesic, Jannsen Cilag, High Wycombe, UK) was applied 12 hours pre-operatively.

Prior to anaesthesia, xylazine (Rompun, Bayer Healthcare, Newbury, UK) premedication was administered and each sheep was weighed (Fig. 5.4 c). Following venous cannulation, anaesthesia was induced using intravenous ketamine (Ketaset, Fort Dodge Animal Health, Southampton, UK) and maintained on the inhalational agent isoflurane (Isoflo, Abbott, Maidenhead, UK).

Once unconscious, the sheep were intubated with a cuffed endotracheal tube (Fig. 5.4 d), and connected to an anaesthetic machine for maintenance and close monitoring for the duration of surgery. Cefalexin (Ceporex, MSD Animal Health, Hoddesdon, Hertfordshire, UK) and maintenance fluids were administered intravenously. The sheep were secured in right lateral recumbency and wool was shaved from the entire limb and hindquarter. The hide was prepared with two applications of aqueous iodine scrub solution and draped appropriately. Sterile technique was maintained henceforth (Fig. 5.4 e).



Fig. 5.4 Premedication, anaesthesia and preparation: a) Sheep were housed in individual pens both pre- and post-operatively **b)** Operating theatre prepared for sheep surgery, note the anaesthetic machine, cardio-respiratory monitoring, suction, lighting, diathermy machine, warming blanket and bucket for collecting rumen fluid intra-operatively. **c)** All sheep were weighed immediately prior to induction. **d)** Intubation using a long straight-bladed laryngoscope, standard human adult endotracheal tube and bougie. **e)** Once anaesthetised, sheep were secured in lateral recumbency before shaving, antiseptic hide preparation and draping.

5.4.4.6.2 Operative procedure

5.4.4.6.2.1 Incision and approach

An anteromedial approach was used to access the diaphyseal portion of the right tibia through an approximately 12 cm incision. The periosteum was carefully and entirely removed around the site of the proposed ostectomy.

5.4.4.6.2.2 Fixation and creation of defect

The proprietary jig was secured against the bone in the required position ensuring all the guides for the Schanz screws corresponded with the centre of the tibial shaft. The 35 mm ostectomy was marked on the tibia using diathermy. Six 4 mm diameter holes

were drilled through the jig guides and a Schanz screw was carefully inserted into each hole by hand to avoid thermal necrosis or splitting of the bone. Because ovine tibiae widen significantly distal to the proximal metaphyseal flare, we used two Schanz screws with a 30 mm long threaded section proximally and four Schanz screws with a 20 mm long threaded section distally. This was replicated for each sheep, and ensured sound bicortical fixation for every screw. Furthermore, the order of insertion of the Schanz screws was also standardised (Table 5.4). The jig was removed and the custom-made modular external fixator (Orthofix, Maidenhead, UK) was applied to the Schanz screws and secured in place at a distance of precisely 30 mm from the near tibial cortex. The 35 mm ostectomy was made at the pre-marked site using an electric reciprocating sagittal saw (Bosch, Uxbridge, UK) with the external fixator in place. Care was taken to ensure perpendicular cuts and normal saline was instilled throughout sawing to provide lubrication and prevent thermal necrosis. The segment of bone was removed along with any remaining periosteum.

Table 5.4 Insertion order of Schanz screws into the ovine tibiae. Note screws at position A and B had a 30 mm threaded section (20 mm for all other screws).

Schanz screw	Order of insertion (1 to 6)	PROXIMAL
	Proximal	
Α	6	A
В	2	- B
С	4	C
	Defect	DEFECT REGION
D	3	
E	5	E
F	1	
	Distal	DISTAL

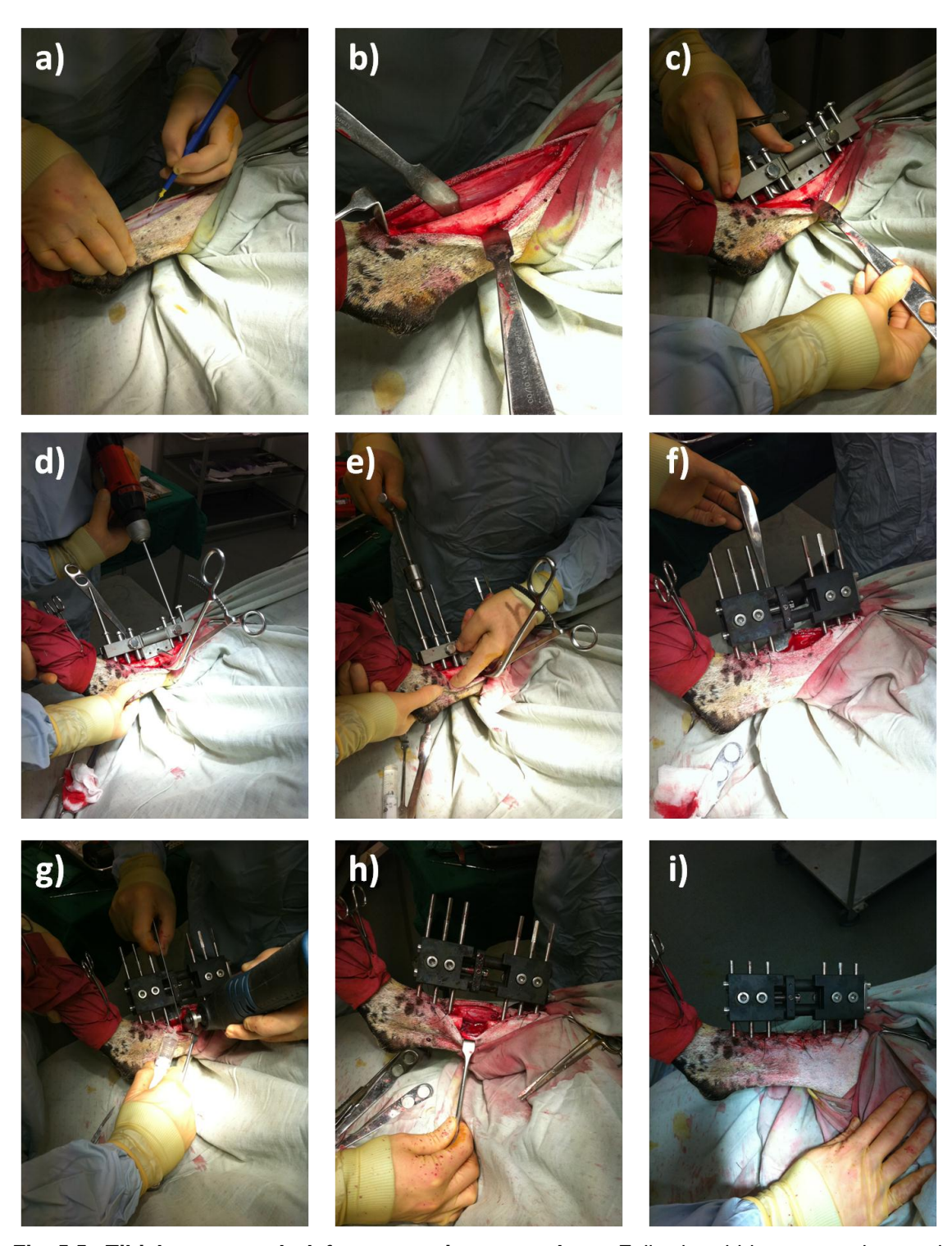
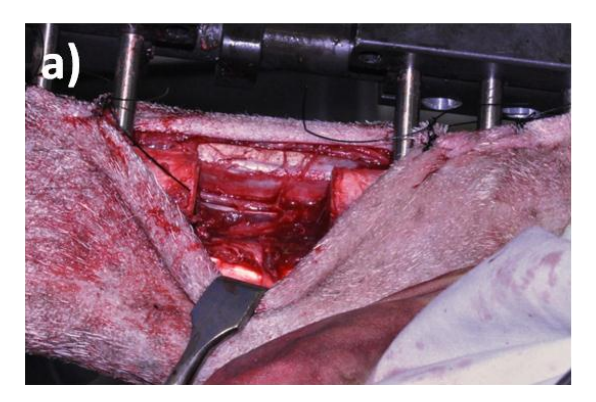


Fig. 5.5 Tibial segmental defect operative procedure. Following hide preparation and draping: a) an anteromedial approach was used to access the diaphyseal portion of the right tibia, b) The periosteum was carefully and entirely removed around the site of the proposed ostectomy, c) The proprietary jig was secured against the bone and the 35 mm ostectomy was marked on the tibia using diathermy, d) Six 4 mm diameter holes were drilled through the jig guides and e) Schanz screws were inserted in a standardised order. f) The jig was removed and the external fixator was secured in place. g) The ostectomy was made at the pre-marked site using an electric reciprocating sagittal saw. h) The segment of bone was removed along with any remaining periosteum. i) Appearance following closure.

5.4.4.6.2.3 Scaffold insertion and stabilisation

The defect was gently washed with saline to remove excess bone debris. For animals assigned to group 1 (negative controls), 5 ml of 0.25% bupivacaine (Marcain, AstraZenica UK Ltd, Luton, UK) was infiltrated around the wound for post-operative analgesia prior to closure. Animals in groups 2 and 3 (positive controls and treatment group) received the polymer without and with autologous ovine SSCs respectively (Fig. 5.6), prior to infiltration of 5 ml of 0.25% bupivacaine.



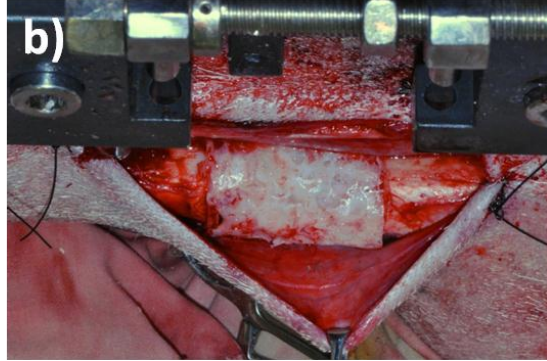


Fig. 5.6 a) Empty defect and b) scaffold in situ, immediately prior to closure

A calibration screw on the external fixator allowed incremental modifications in the defect size, enabling compression fitting of the scaffold between the two cut bone ends. Furthermore, this allowed final adjustments to be made to the size of the ostectomy gap, to ensure the gap was exactly 35 mm.

5.4.4.6.2.4 Closure and dressings

The fascia was closed with continuous 0 polyglactin (Vicryl, Ethicon) sutures and the hide closed with interrupted 3/0 nylon (Ethilon, Ethicon) mattress sutures. OpSite spray (Smith & Nephew, Hull, UK) and gauze dressings were applied to the operative site. All nuts and bolts on the external fixator where checked to ensure tightness and the protruding ends of the Schanz screws were cut short using bolt cutters. The entire construct was dressed with wool and crepe bandages and secured using adhesive tape.

5.4.4.6.3 Peri-operative radiography

Anteroposterior and lateral radiographs were made of the entire tibia before anaesthetic reversal, each including a radiographic aluminium step wedge (CNMC, Nashville, USA) for densitometric analysis (fig. 5.7 a).

5.4.4.6.4 Post-operative procedure

Following extubation, the sheep were sat up and rested against the side of their individual enclosures. Careful observations were taken with reducing frequency over the initial 24 hour post-operative period. Five cefalexin doses, once daily were administered and post-operative analgesia consisted of a Fentanyl patches for 48 hours followed by buprenorphine (Vetergesic, Alstoe Animal Health, Melton Mowbray, UK) intramuscular injection once daily as required. Sheep were allowed to mobilise full weight bearing immediately as tolerated with unhindered access to food and water for the remainder of the study period (Fig. 5.7 b). Weekly checks were made of the wounds and fixators to ensure there was no loosening, and sutures were removed after 14 days.

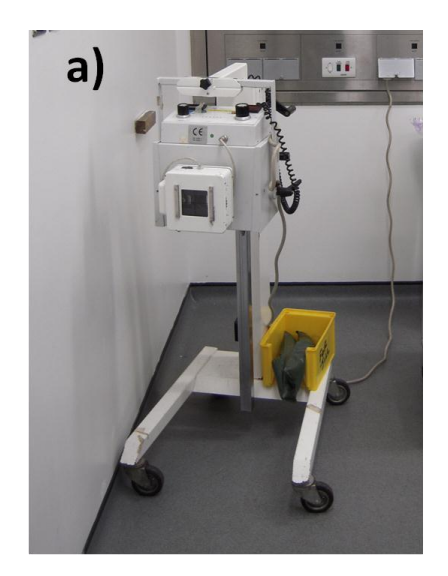




Fig. 5.7 Post-operative procedure: a) Portable x-ray machine used to make radiographs post-operatively. **b)** A sheep within two hours post-operatively standing fully weight-bearing. Note the dressings securely covering the external fixator and operative site.

5.4.4.7 Post-operative analysis

Sheep underwent sedation (as previously described) for further radiography of the tibia at two and six weeks post-operatively.

5.4.4.8 Euthanasia and specimen harvest

Euthanasia was performed 12 weeks after the operative day with pentobarbital solution 20% (Pharmasol Ltd, Andover, UK). The tibiae were disarticulated with fixators *in situ*, surrounding musculature and soft tissue were carefully removed without disturbing the constructs and final radiographs were made. The contralateral tibiae were also harvested and prepared similarly to act as controls for mechanical testing. Specimens were frozen at -80°C prior to analysis.

5.4.4.9 *Post-mortem* specimen analysis

In addition to post-operative radiographs, each specimen underwent the following analysis:

5.4.4.9.1 μ CT analysis

External fixators were removed from the frozen specimens, however the Schanz pins were left *in situ* and used to support specimens during CT scanning. All samples were scanned using an Xtek Benchtop 160Xi scanner (Xtek Systems Ltd, Tring, UK) equipped with a Hamamatsu C7943 X-ray flat panel sensor (Hamamatsu Photonics, Welwyn Garden City, UK). Scan resolution was up to 31 μm at 150 kV and 60 μA, using a molybdenum target with an exposure time of 534 ms and four-fold digital gain. Reconstructed volume images were analysed using VGStudio Max 1.2.1 software (Volume Graphics GmbH, Heidelberg, Germany). Initial scans were used as an overview of new tissue formation, and captured a 60 mm length, centred upon the segmental defect. Further high-resolution scans were made of regions of interest.

5.4.4.9.2 Mechanical testing

Following CT visualisation, the specimens were defrosted entirely and the constructs were assessed for maximum strength under torque loading. This was deemed the most suitable method as the mode of failure of long bones of the lower limbs is most frequently through compressive torque. Test constructs were compared with whole tibiae from the contralateral side. The soft tissue at the ends of the tibiae was removed before being potted in quick-set cement (Polycell, ICI, London, UK) in a custom designed rig. The gauge length was measured as the distance between the potted ends of the tibia. The tibiae were tested at a rate of 1° per second in an Instron 8874 (Instron Corp., MA, USA) to 90° of rotation (Fig. 5.8).

Dimensions of the bones were obtained from the intact tibiae after failure. The control tibiae were assumed to be hollow cylinders, with the dimensions based on an average of three measurements of the diameter and wall thickness. Values for the tibiae containing scaffolds were calculated using the scaffold dimensions. The shear modulus (GPa), bone stiffness (Nm/degree and Nm/radians), maximum torque (Nm), maximum shear stress (MPa) and the maximal angular deformation at failure (degrees) was calculated for each sample where a definite failure occurred.



Fig. 5.8 Constructs and intact tibiae (shown here) were assessed for maximum strength under torque loading using an Instron testing rig

5.4.4.9.3 Macroscopic analysis

Preparation of the specimens for analysis also enabled a thorough macroscopic evaluation of the integrity of scaffold material as well as an assessment of scaffold integration and mode and site of failure.

5.4.4.9.4 Histology

Following mechanical testing, several samples, each measuring approximately 10 mm³ and representing a region of interest (ROI), were removed from each construct. ROI were as follows (Fig. 5.9):

A – the interface between the proximal cut end of tibia and polymer scaffold; to demonstrate any integration that may strengthen the construct.

B- an area on the surface of the mid-section of scaffold; to demonstrate any new tissue at the furthest distance from native bone ends, but closely exposed to the host vasculature.

C – an area on the inner face of the scaffold mid-section; to demonstrate new tissue at the furthest distance from the bone ends, and also distant from host vasculature, thus relying upon diffusion and new vessel in-growth for regeneration to take place.

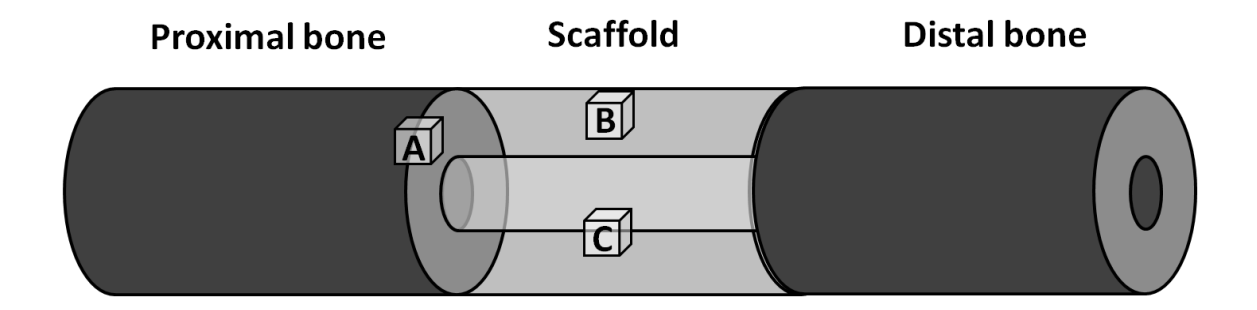


Fig. 5.9 Cubes of tissue/polymer were taken from the indicated regions for histological analysis: a) the interface between the proximal cut end of tibia and polymer scaffold, b) an area on the surface of the mid-section of scaffold, c) an area on the inner face of the scaffold mid-section

Each ROI specimen was decalcified over a period of approximately four weeks using Tris-EDTA (using Faxitron analysis to confirm complete decalcification), before embedding in wax and cutting into 5 µm semi-sequential sections and mounting on slides (as previously described in Chapter IV). Slides were stained with A/S (see Chapter IV) before visualisation using a Zeiss Axiovert 200 inverted microscope (Carl Zeiss Ltd. Welwyn Garden City, UK).

5.5 Results

5.5.1 Preliminary experiments

5.5.1.1 Confirmation of scaffold porosity

Although this polymeric scaffold had previously been produced on a small scale and assessed for its utility in a murine *in vivo* model (Khan *et al.* 2010), it was necessary to verify that scaffolds manufactured to a scale suitable for clinical implantation would possess the same architecture and overall structure. SEM confirmed a range of pore diameters from 300 µm to 1.5 mm, with significant pore interconnectivity (Fig. 5.10).

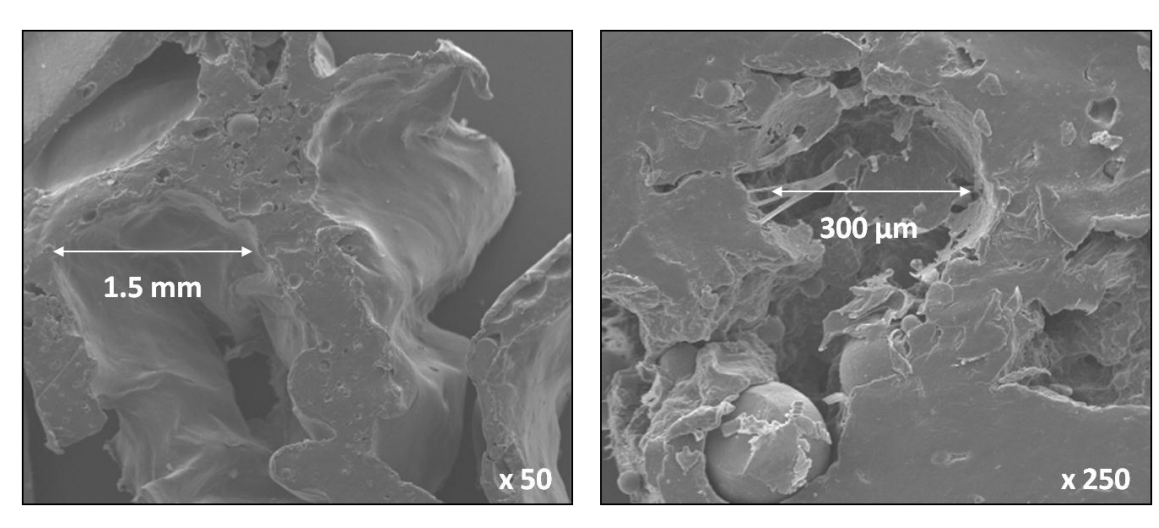


Fig. 5.10 SEM images of polymer scaffold demonstrating multiple pores of varying dimensions necessary for rapid cellular infiltration

The Alcian blue penetration test showed considerable permeation of the dye through the scaffold structure, which was confirmed to exist throughout the scaffold by cutting sections through it (Fig. 5.11). This further confirmed pore interconnectivity sufficient for diffusion of nutrients and metabolic waste products from cells within the polymer matrix. These properties are critical to allow cellular adhesion, penetration and infiltration.

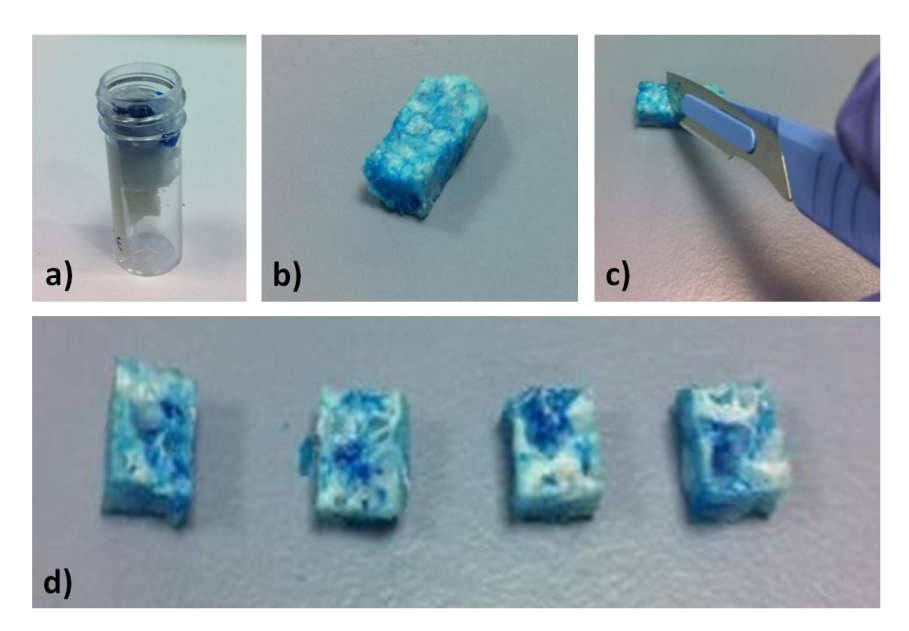


Fig. 5.11 Alcian blue penetration test: a) experimental set-up, the polymer is suspended in a perforated specimen container and the proximal end 'sealed' with histology wax before addition of Alcian blue. b) Polymer scaffold following experiment and removal of wax, note the blue dye is visible throughout the sample. c) The scaffold was dissected into four pieces. d) Cross sections of the scaffold from proximal (left) to distal (right), demonstrating even penetration of the dye throughout the specimen, with particular staining around the larger pores. Note the absence of a diffusion gradient.

5.5.1.2 Isolation and culture of ovine SSCs

Following standard isolation and monolayer culture techniques on tissue culture plastic, ovine cells grew to full confluence in both basal and osteogenic medium (Fig. 5.12). No major differences in morphology or speed of growth were observed between the two groups and therefore the decision was made to seed the ovine SSCs for group 3 of the segmental defect model in osteogenic conditions.

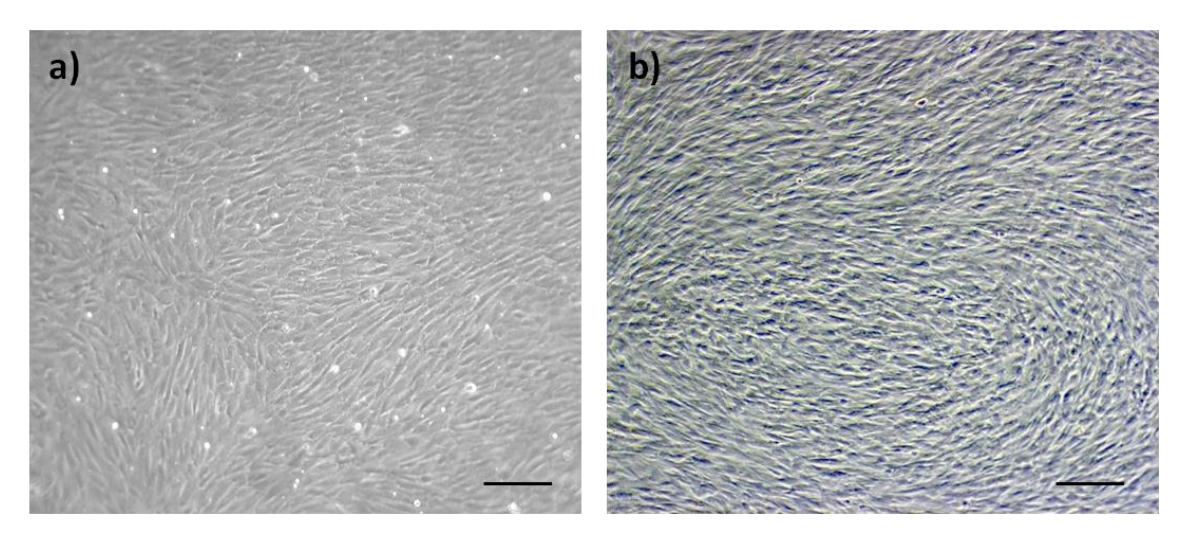


Fig. 5.12 Ovine BMA cells grown to confluence on monolayer tissue culture plastic in a) basal and b) osteogenic conditions. Scale bar: 200 µm

5.5.1.3 In vitro incubation of ovine SSCs with test scaffold

Analysis of DNA concentration (Fig. 5.13 a) showed the scaffolds with cells incubated in osteogenic conditions contained substantially more DNA after 28 days incubation, indicating improved cell survival and proliferation over those incubated in basal conditions. Seeding density did not appear to be such an important factor. ALP concentration (Fig. 5.13 b) was similar amongst all seeding densities and culture conditions, with substantial ALP production even in cells cultured in basal medium. Note that even though basal samples were seeded at a higher density (5x10⁵ cells/ml) than any of the osteogenic samples, all of the latter samples resulted in higher DNA and ALP concentrations.

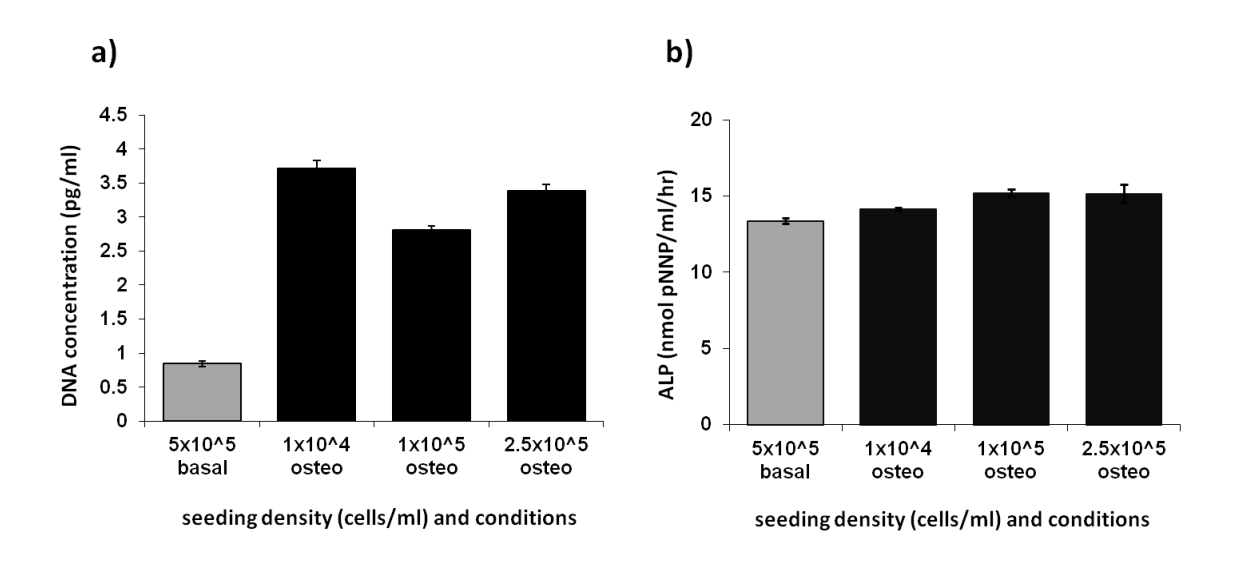


Fig. 5.13 a) DNA and b) ALP assays of ovine cells cultured with 10 mm cubes of polymer scaffold in either basal or osteogenic (osteo) conditions. Error bars denote SD, all results analysed in triplicate.

Vybrant® Green staining of scaffolds incubated for 28 days with ovine SSCs in both basal and osteogenic conditions, revealed intense staining of live cells coating the polymer. Additionally, when cultured in osteogenic conditions, the cells displayed bridging across the porous network of the scaffold and were seen to penetrate deeply within the polymer structure (Fig. 5.14).

Following these preliminary investigations, it was therefore decided that the scaffolds should be incubated with ovine cells at a concentration of 5x10⁵ cells/ml, in osteogenic medium, for 7 days prior to transfer into the *in vivo* ovine segmental defect.

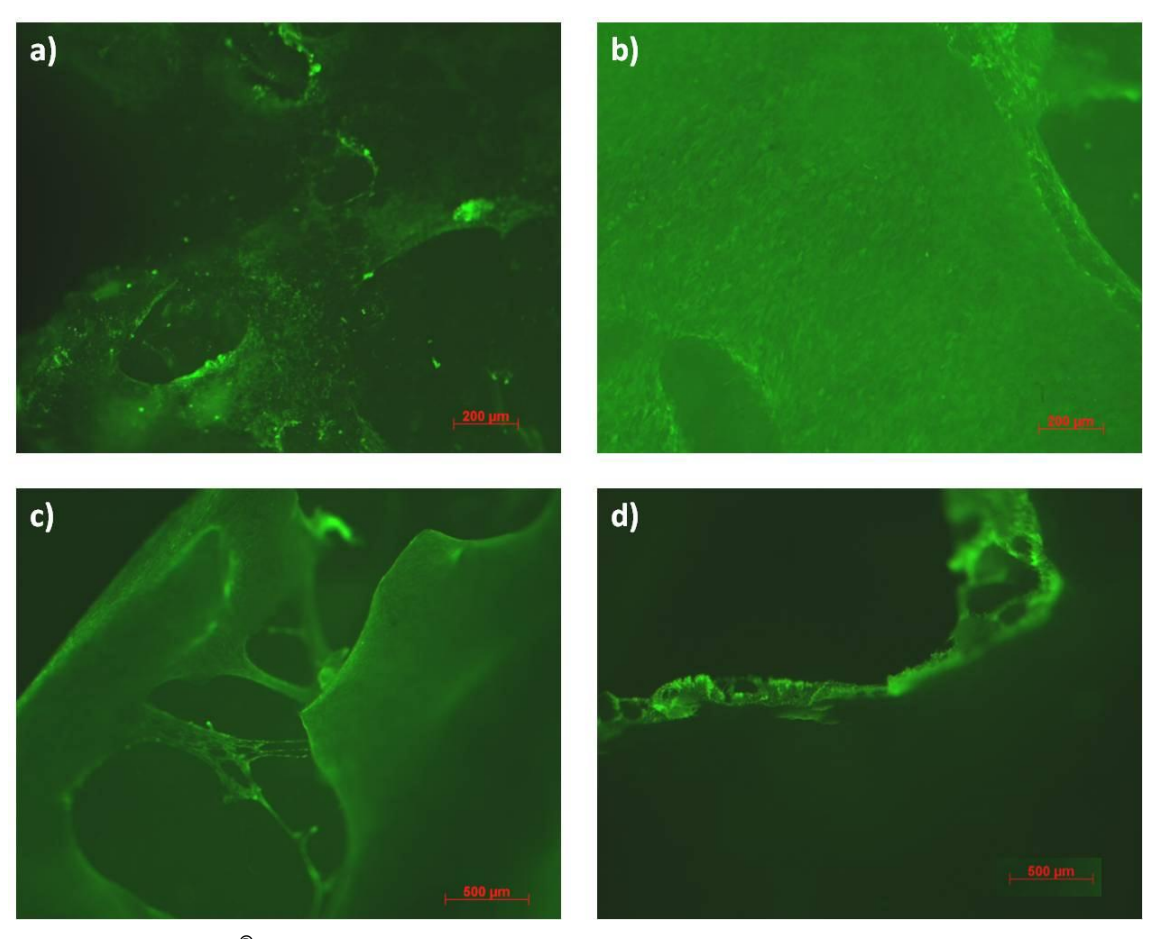


Fig. 5.14 Vybrant[®] Green cell viability analysis for ovine cells grown on polymer scaffold for 28 days, a) in basal conditions, b-d) in osteogenic conditions, c) higher magnification confirming bridging of the cells across the polymer pores, d) higher magnification of the cut surface of polymer revealing a pore in cross sectional profile, note deep penetration of cells into the pore. Scale bars: a) and b) 200 μ m, c) and d) 500 μ m

5.5.2 Ovine tibial segmental defect model

5.5.2.1 Complications of surgical procedure and anaesthesia

All aspiration, cell culture and surgical procedures were technically successful. No sample became infected during the *in vitro* stage of the study. None of the sheep suffered superficial or deep wound infection, and all ambulated and were fully weight-bearing at one week following operative intervention (Table 5.5).

Table 5.5 Summary of segmental tibial defect operative procedures in this study, presented in the order of the operative procedure

Study number	Pre-operative weight (kg)	Operative group	Analysis number	Complications/notes
5960	84	Scaffold	5	
5849	78	Empty defect	1	
5840	75	Scaffold + SSCs	9	
5962	85	Scaffold + SSCs	10	
6020	75	Scaffold + SSCs	11	
5987	65	Empty defect	2	
6003	70	Scaffold	6	
6016	60	Scaffold	7	
5922	75	Scaffold + SSCs	12	
6017	60	Scaffold	8	
5948	65	Scaffold	-	Post-operative death
5964	75	Empty defect	3	Post-operative slip of fixation
5846	80	Empty defect	4	

Analysis number refers to the number assigned to the specimen for post-mortem analysis and is henceforth indicated in this report.

There was one sheep death secondary to anaesthetic complications and one minor failure of fixation:

One sheep suffered respiratory difficulties intra-operatively during segmental defect fixation. Respiratory support could only be withdrawn slowly during recovery and the sheep suffered cardio-respiratory arrest approximately 15 minutes following extubation and could not be revived. *Post mortem* analysis revealed lungworm infestation. Another sheep from the same flock was used to take its place and maintain the original study number of 12 animals.

The external fixator of one sheep (number 3) slipped by approximately 1 mm, as noted on the second post-operative radiograph. The fixator bolts were re-tightened immediately *in situ* following recognition of this complication, and no further slip occurred. Following this, a supplementary rigid metal bar was attached between the proximal and distal body of each external fixator to avoid any undetected compression.

5.5.2.2 Radiographic analysis

Lateral radiographs of each tibia were made at incremental periods throughout the study (at day 0 and weeks 2, 6 and 12 post-operatively), using the same protocol and arranged to allow a comparison of defect size throughout the experimental period (Figs. 5.15 - 5.17).

No fracture or fixation failure was noted in any group and the fixator stability and defect size was such that union was prevented in all empty defect samples – confirmation of a critical sized defect (Fig. 5.15). Radiographic analysis however, showed little osseous formation in any sample of the polymer scaffold groups during the study period (Figs. 5.16 and 5.17).

Fig. 5.18 demonstrates the typical pattern of new bone formation in each group: in the empty defects there was minimal osteogenesis that formed into a conical pattern, mainly from the proximal cortices; in the scaffold alone group, increased bone formation was evident from both the proximal and distal bone ends that appeared more evenly throughout the structure of the scaffold polymer; in the scaffold and cells group, most bone formation occurred within the central cannulation of the scaffold. Although minor areas of calcified tissue are seen projecting particularly from the proximal bone ends in all groups (Fig. 5.18), union was not demonstrated in any specimen after 12 weeks.

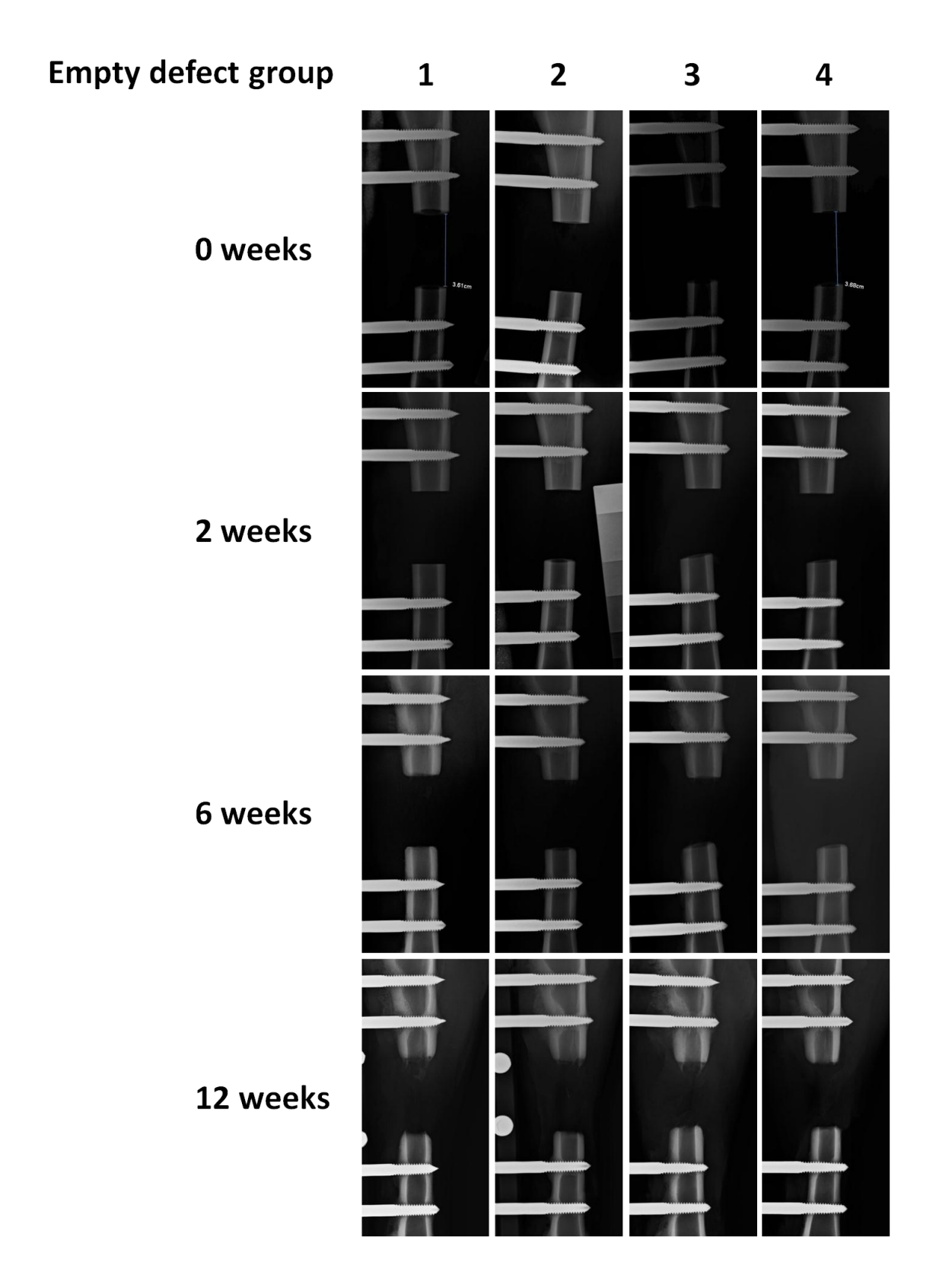


Fig. 5.15 Incremental lateral radiographic analysis of the fixated tibiae of sheep 1-4 in the empty defect group analysed immediately post-operatively (0 weeks) and at 2, 6 and 12 weeks post operatively. Images show region of interest, which includes four of the six Schanz pins and the defect. There is little new bone formation within the defect site, although after 12 weeks some calcification is visible emanating from the proximal portion of the ostectomy.

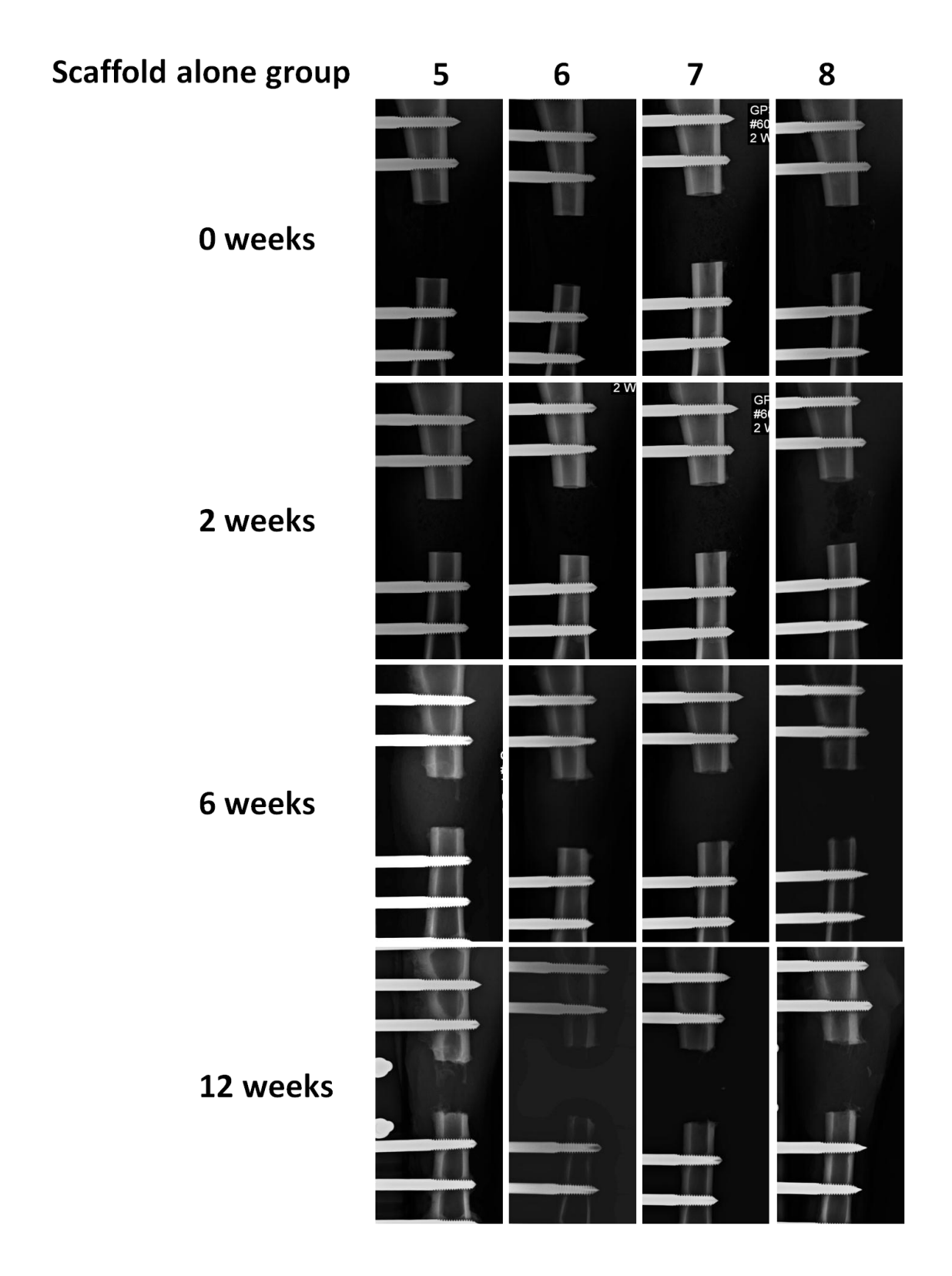


Fig. 5.16 Incremental lateral radiographic analysis of the fixated tibiae of sheep 5-8 in the scaffold alone group analysed immediately post-operatively (0 weeks) and at 2, 6 and 12 weeks post operatively. Images show region of interest, which includes four of the six Schanz pins and the defect. There is little new bone formation within the defect site, although after 12 weeks some calcification is visible emanating from the proximal portion of the ostectomy in most samples, and also the distal aspect in some specimens.

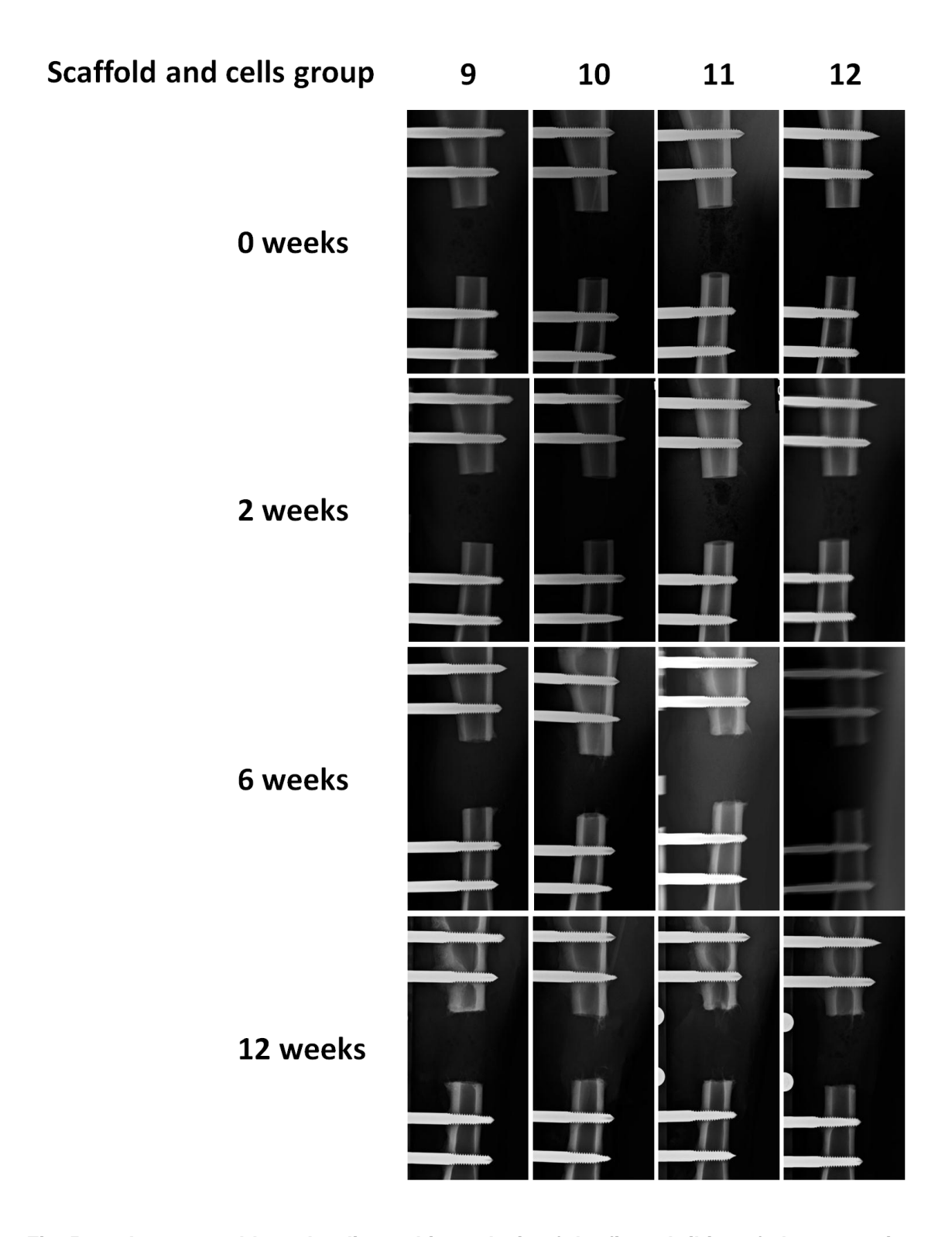


Fig. 5.17 Incremental lateral radiographic analysis of the fixated tibiae of sheep 9-12 in the scaffold and cells group analysed immediately post-operatively (0 weeks) and at 2, 6 and 12 weeks post operatively. Images show region of interest, which includes four of the six Schanz pins and the defect. There is little new bone formation within the defect site, although after 12 weeks some calcification is visible emanating from the proximal portion of the ostectomy in most samples, and also the distal aspect in some specimens.

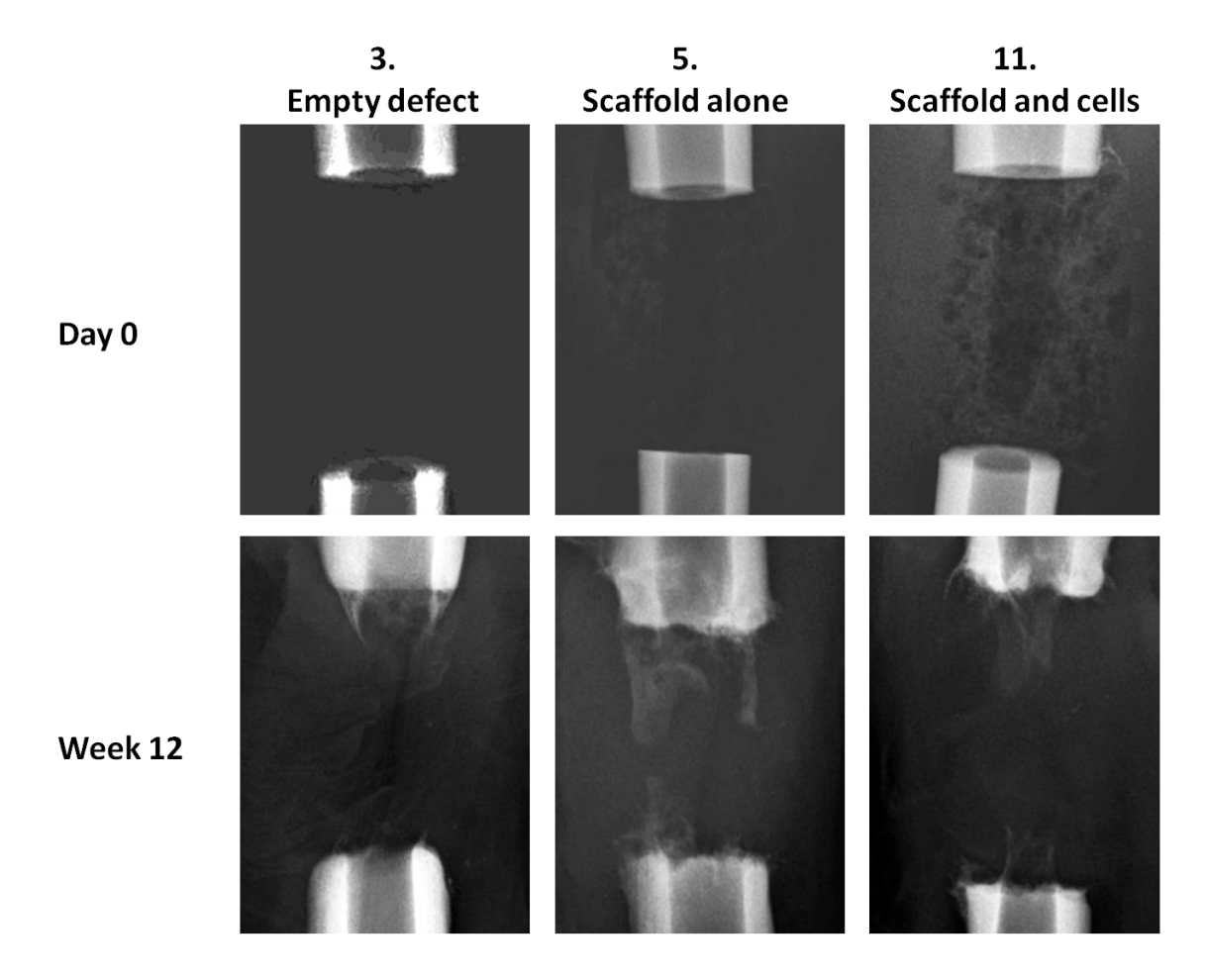


Fig. 5.18 The typical pattern of new bone formation in each group: In the empty defects (3) there was minimal osteogenesis that formed into a conical pattern, mainly from the proximal cortices; in the scaffold alone group (5), increased bone formation was evident from both the proximal and distal bone ends that appeared more evenly throughout the structure of the scaffold polymer; in the scaffold and cells group (11), most bone formation occurred within the central cannulation of the scaffold.

5.5.2.3 µCT analysis

Analysis using quantitative CT radiography techniques produced reformatted images of each specimen centred upon the defect site (Fig. 5.19). These images largely confirm the plain radiographic findings that empty defects undergo a process of atrophic non-union. There is little difference in bone formation between the two scaffold groups, although more regeneration is confirmed in these latter groups compared to empty defect controls.

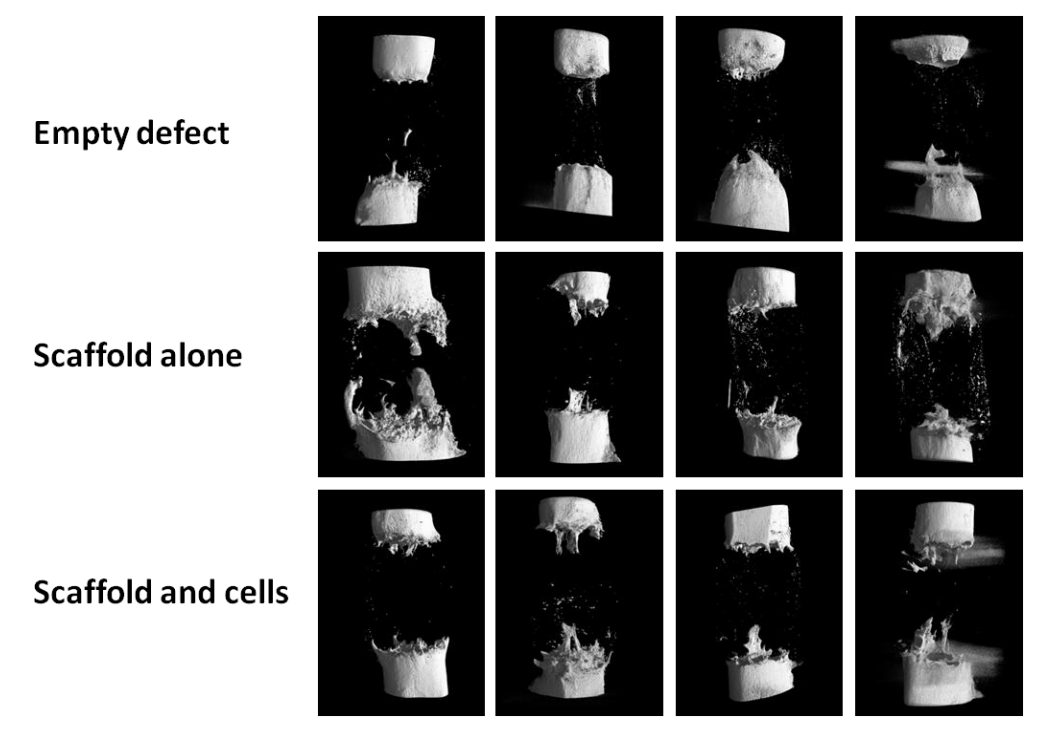


Fig. 5.19 Quantitative μ CT analysis at 12 weeks post-operation. There is minimal regenerative activity in the empty defect specimens. Some bone formation is seen in both scaffold groups, although there is no certain difference in the group with added SSCs.

Quantitative analysis of the volume of new bone formation within the ostectomy site revealed a trend towards increasing bone formation with scaffold and again with scaffold and SSCs when compared to the empty defect, however this failed to reach statistical significance (p=0.07) (Fig. 5.20).

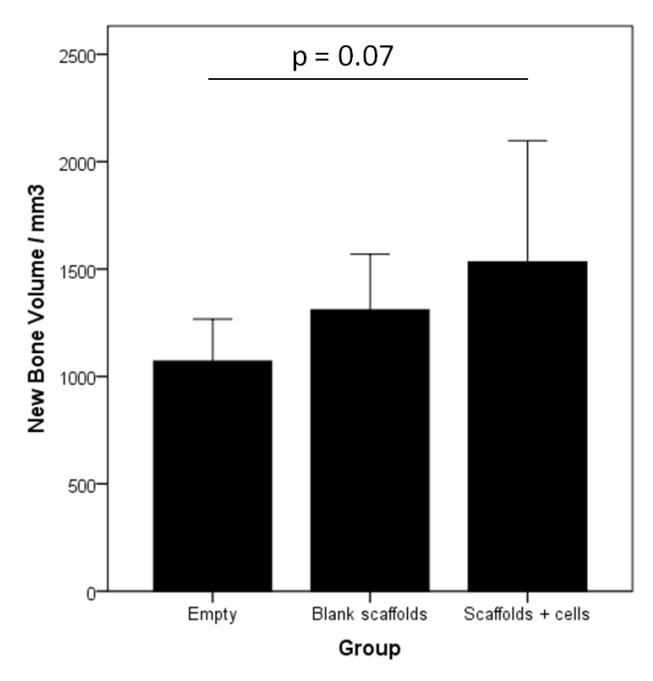
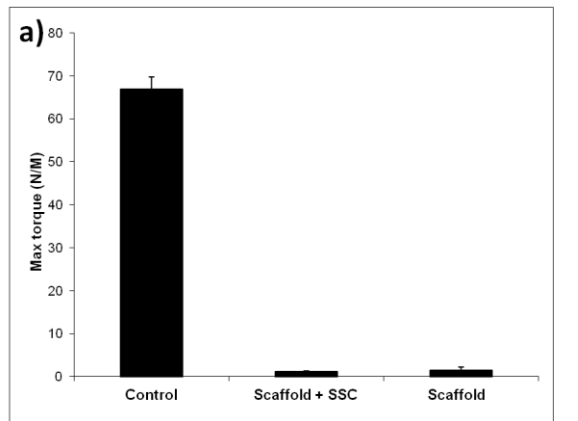


Fig. 5.20 Quantitative μ CT analysis of new bone formation after 12 weeks incubation. Error bars: SD

5.5.2.4 Mechanical testing

Bones were tested to failure at 1° per second. Only samples which demonstrated a definite failure before 40° were included in the analysis to ensure accurate values could be ascribed to a specific point of failure. This excluded all the empty defect samples and one of the scaffold-containing samples (Fig. 5.21).



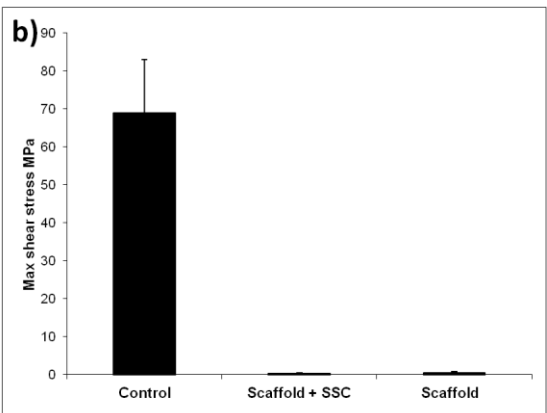


Fig. 5.21 Results of mechanical testing for the sheep tibiae under torsional compression demonstrating a) Maximum torque and b) Maximum shear stress before failure. Control refers to the contralateral intact tibia. Error bars: SD

5.5.2.5 Macroscopic analysis

Following mechanical testing, macroscopic analysis of each specimen (Fig. 5.22) confirmed atrophic non-union had occurred in every empty defect specimen. As demonstrated by plain radiographic and μ CT analysis, minimal osteogenesis had taken place in these specimens, forming a conical projection mainly from the proximal cortices. In the scaffold alone group, increased bone formation was evident from both the proximal and distal bone ends obscuring the interface between the bone and polymer scaffold, except in one case (white arrow in Fig. 5.22). Only the central portion of the scaffold exterior was visible in the remaining specimens, although this still had structural integrity. The interface between scaffold and diaphysis appeared even more indistinct in the scaffold + SSCs group, with coverage of the scaffold by soft reparative tissue in continuity with bone. In three of the four specimens in each scaffold group failure occurred through the scaffold itself, usually as a transverse or short oblique fracture line (Fig. 5.22), however failure occurred at the distal scaffold-diaphysis interface in one specimen of each scaffold group (white and black arrows, Fig. 5.22 - 8 and 11).

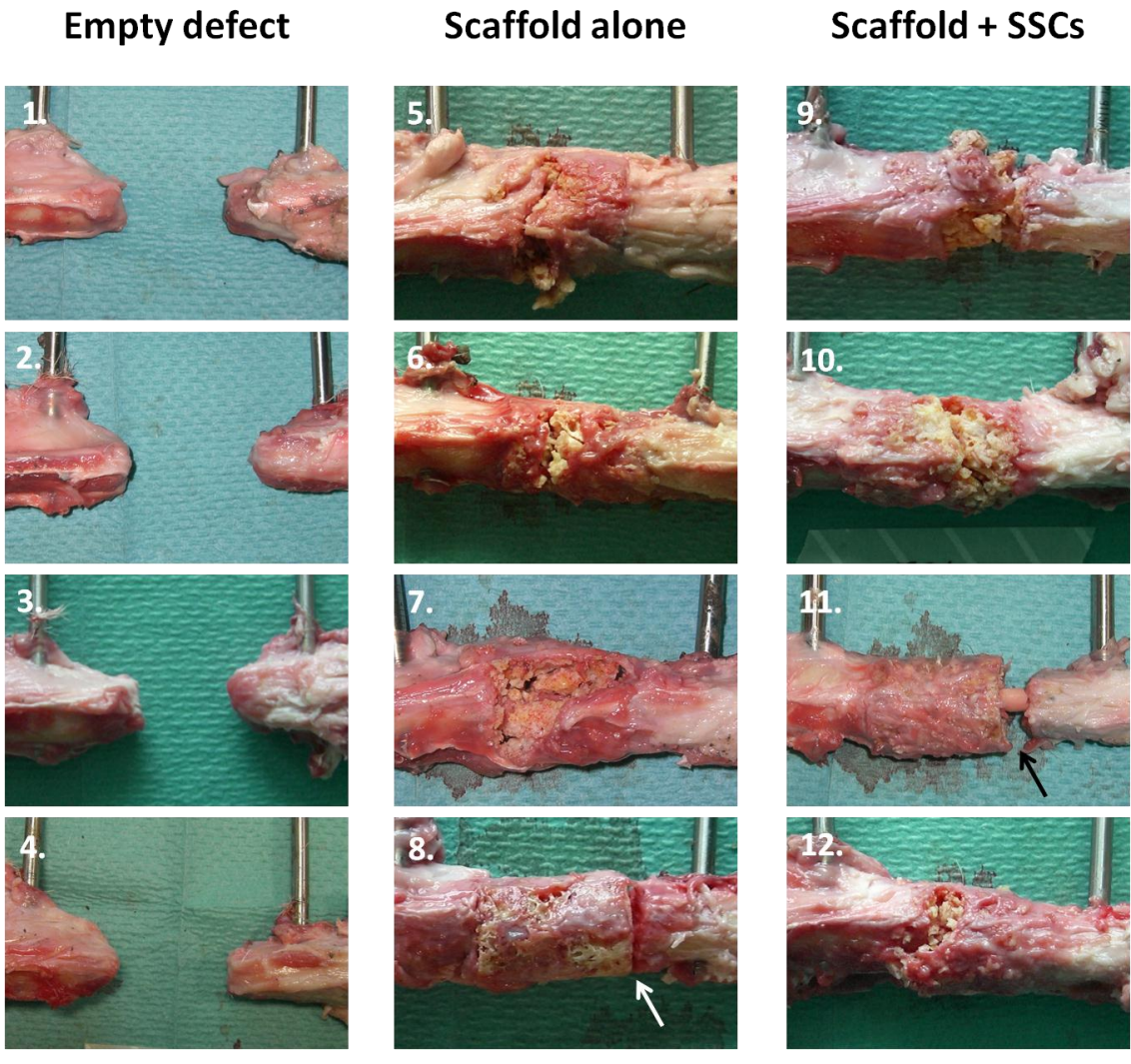


Fig. 5.22 Macroscopic specimen analysis following mechanical testing. Regions of interest in each image show the proximal diaphysis (left), the distal diaphysis (right) and defect containing no scaffold **(1-4)**, scaffold alone **(5-8)**, or scaffold with cells **(9-12)**. Failure occurred through the scaffold itself in three of the four specimens in each scaffold group; however failure occurred at the distal scaffold-diaphysis interface in one specimen of each scaffold group (arrows in 8 and 11).

A feature of new tissue growth that was seen only in specimens from the scaffold + SSCs group was intramedullary growth up the central canal of the polymer scaffold (Fig. 5.22 – 11 and Fig. 5.23). The extent of this tissue growth was not appreciated by radiographic imaging modalities as the tissue was not fully calcified and has a similar density to the surrounding polymer scaffold, but provided full continuity between the proximal and distal bone segments in these specimens.

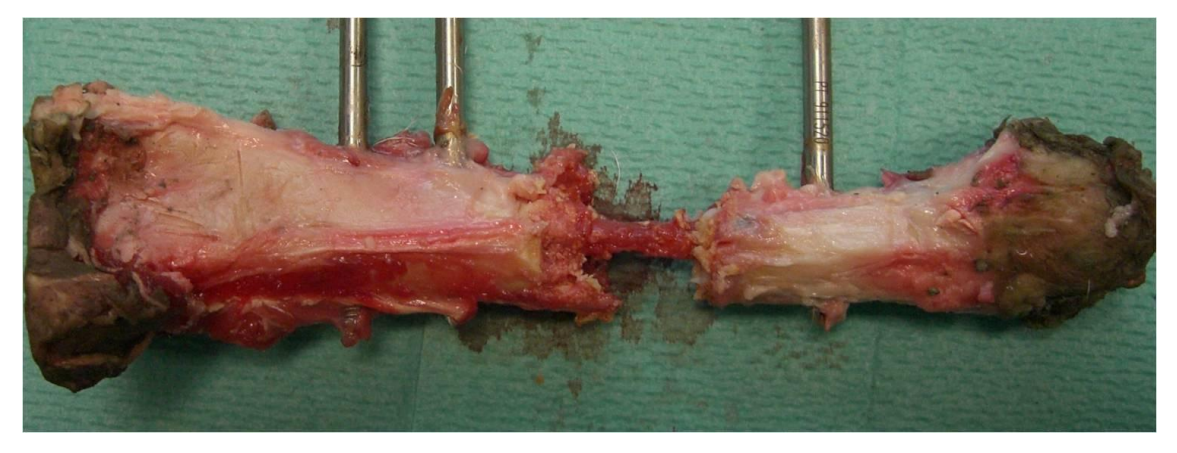


Fig. 5.23 Macroscopic image of a tibia treated in the scaffold + SSCs group (specimen 9 in Fig. 5.22). The polymer scaffold in this case was largely fragmented following mechanical testing and has been carefully removed to reveal a central bridge of new tissue formation within the medullary cavity of the scaffold. Note full continuity between the proximal and distal diaphyseal segments.

5.5.2.6 Histology

Histological examination of the three regions of interest as defined previously (Section 5.4.4.9.4) revealed a consistent pattern of tissue regeneration within the defect site in both groups containing polymer scaffold (Fig. 5.24). Insufficient tissue was formed within the empty defect group to enable histological processing and analysis. In both the scaffold alone and scaffold with SSCs specimens, there was significant infiltration of new tissue into the polymer scaffold at the bone-scaffold interface (region A), as demonstrated by staining of collagen type I with Sirius red. In this zone, most pores within the scaffold had been filled by new bone and entirely surrounded the polymer 'islands'. In region B, near the surface of the mid-section of scaffold, new osseous tissue was consistently seen in both scaffold groups, with direct contact of this red-staining tissue with the polymer and deep penetration of tissue into the porous network. Region C, within the inner face of the scaffold mid-section showed no new osseous tissue formation in either scaffold group. The polymer in this region remained intact with some surrounding cells, but no new bone formation.

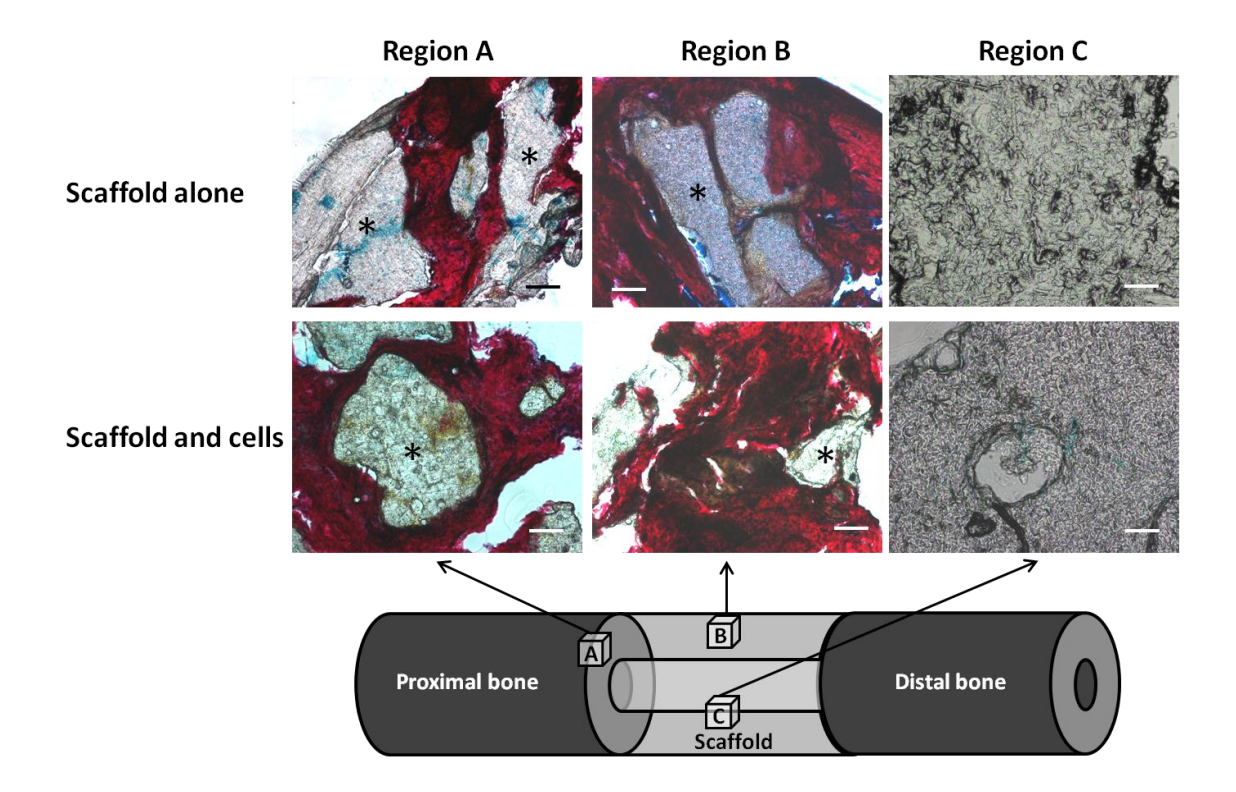


Fig. 5.24 A/S histological analysis of the ovine segmental tibial defect model after 12 weeks *in vivo* incubation. Only the scaffold groups are displayed, as insufficient tissue was formed within the empty defects for histological processing. In **region A** (bone-scaffold interface), there was significant infiltration of new tissue into the polymer scaffold at the as demonstrated by red staining of collagen type I. In **region B** (near the surface of the mid-section of scaffold), new osseous tissue was seen in both scaffold groups, with deep penetration of tissue into the porous network. **Region C** (within the inner face of the scaffold mid-section) showed no new osseous tissue formation in either scaffold group. The polymer in this region remained intact with some surrounding cells, but no new bone formation. Polymer is marked with *, scale bars: 100 μ m.

5.6 <u>Discussion</u>

The purpose of this study was to establish an appropriate large animal model that could be used consistently for the evaluation of putative tissue engineering constructs for skeletal regeneration, as a necessary prequel to potential clinical trials and subsequent clinical application. Although the initial introduction of a new large animal model into a research establishment is often fraught with difficulties, this is a pivotal and essential step towards a systematic process of product testing and development. This study therefore evaluated both the inception of a new skeletal regeneration model as well as assessing the efficacy of a binary blend polymeric scaffold (PLLA/PCL (80/20)) that had already proven successful in vitro and in a small animal in vivo model (Khan et al. 2010). Following substantial preliminary investigations to define the most appropriate animal and anatomical site for testing, an ovine tibial segmental defect model with external fixation was chosen. Sheep are readily available, economical and docile. In addition, sheep share important similarities to humans (similar body weight, bone dimensions and osseous micro-architecture), which make them useful as test subjects for musculoskeletal investigations. External fixators are particularly appropriate to this study as they are used clinically in bone defect surgery, but they have additional advantages during experimental procedures as they do not affect the defect site and allow easier radiographic and histological analysis.

Preliminary experiments to assess the polymer structure demonstrated a good network of interconnected pores with a wide range of diameters and good permeability. A thin film of polymer was noted to cover each scaffold and had to be removed manually to ensure continuity of the porous network. This is a result of the manufacture process and would have to be addressed prior to high output production of a similar polymer in future applications. Aspiration, storage and processing of ovine BMA was successful and *in vitro* growth of ovine SSCs on the polymer was rapid and appeared to penetrate deeply within the structure of the scaffold without observed cellular necrosis. Furthermore, osteoblastic activity was observed in these cells following culture in osteogenic conditions. Thus, an ovine SSC collection, seeding and *in vitro* incubation protocol has been defined for application to large polymeric scaffolds, which could be replicated in future similar studies.

Most aspects of the segmental defect operative procedure itself were successful. Apart from an explained death following general anaesthesia and a single incidence of minor fixator slippage, which was easily rectified, all aspects of sheep handling,

premedication, anaesthesia, aspiration, preparation, ostectomy, fixation, recovery, analgesia, post-operative care, radiography, termination and sample harvesting proceeded without incident.

Several aspects of *post mortem* analysis required modification to account for the large specimens resulting from the study. Consequently, some of the analysis was rationalised to allow processing within the limitations of the equipment and facilities available in our laboratories. Histological preparation in particular, was limited by a requirement to decalcify all tissue prior to processing. Consequently, only small regions could be analysed separately, rather than the ideal scenario where an entire cross-section through the un-decalcified defect would be mounted on a single slide for analysis. In order to maximise useful data, implementation of necessary equipment and expertise for this technique should be considered when planning future large animal studies.

Plain radiographic and μ CT results correlated closely: the technique has been shown to create a replicable critical sized segmental defect using all analytical modalities. Furthermore, addition of the scaffold tended to enhance bone formation when compared to the empty defect, although this did not reach statistical significance, and addition of SSCs did not demonstrably enhance bone formation. Soft tissue formation however did appear to be enhanced by the addition of SSCs to the construct and was only visualised macroscopically and on histological analysis. This may indicate a prequel to eventual osteogenesis, and although the time periods involved for this model to demonstrate complete union are too long to be clinically favourable, they do provide encouragement for future studies based on this ovine model and similar polymer blending technology.

Mechanical strength testing confirmed the contralateral (un-operated) tibiae possessed similar strength characteristics to previously published results for mammalian bone: shear moduli for human and bovine cortical bone have been published as 3.51 and 4.14 GPa respectively (Cowin 1989), which correspond with our mean ovine tibial values of 2.45 GPa (SD 0.73). The mean maximum torque for ovine tibiae in the current study was 66.82 Nm (SD 2.88), which correlates closely with previously published ovine tibia destructive tests (Jamsa and Jalovaara 1996). Additionally, torsional stiffness values are similar to those previously published for ovine tibiae (Reichel *et al.* 1998, Gao *et al.* 1997). These studies validate our methods for mechanical strength testing and justify the assumption required for calculation that the

tibiae are cylindrical. The findings that all mechanical strength modalities tested were significantly lower for the test tibiae, and that no significant increase was obtained by the addition of scaffold or scaffold and SSCs are therefore valid.

Histological analysis demonstrated several encouraging findings: 1) the polymer scaffold was still present and had maintained its structural architecture at 12 weeks incubation; 2) furthermore, in the scaffold groups, there was close apposition and penetration of tissue staining for collagen type I into the porous scaffold network. The toxic effect of by-products formed during polymer scaffold breakdown is frequently cited as a reason for failure of a tissue engineering construct, although it appears in this case not to have adversely affected the surrounding tissue. Even though little new calcified bone was seen on radiographic analysis, the histological results demonstrate regenerative tissue forming throughout the circumference of the scaffold, and penetrating to some extent into the porous scaffold substance. However, no new tissue was seen within the central scaffold area (region C). This area would be expected to regenerate last because it is located deep within the polymer, furthest away from osteogenic influences of the bone ends and periosteum, and poorly exposed to surrounding vasculature. Tissue that was formed stained uniformly with Sirius red, implying a high concentration of type I collagen. Conversely, modest Alcian blue staining was seen, confirming osteogenic rather than chondrogenic differentiation, appropriate to a skeletal regeneration strategy. The presence of abundant uncalcified matrix suggests that relatively small changes in the protocol may lead to substantial bone development.

All the analyses confirmed a trend towards increasing bone formation with the polymer scaffold when compared to the empty defect, although this effect has not been proven to be significant. Furthermore, the addition of autologous SSCs to the construct does not categorically further enhance skeletal regeneration, but may accelerate the formation of precursor tissue.

There are multiple additional factors which must be considered when up-scaling a successful small animal study, and each may account for the failure of additional regeneration seen in this study (Table 5.6). A systematic approach to critically evaluate each aspect of study design and technique is required to refine and improve future studies; however it is particularly difficult to define the cause of failure in this study as a simultaneous evaluation of multiple unknown variables was attempted – neither the validity of the large animal model, nor the efficacy of the large-scale polymer scaffold

with ovine SSCs had previously been assessed. Consequently, it is not possible to conclude whether the regenerative model, the scaffold or some technical aspect of implantation was at fault. Despite this, the failings of a technique can often only be seen in retrospect, no matter how carefully the procedure is planned and there is no substitute for direct experience when carrying out such a study.

There are particular aspects of this model that will require further confirmation, adaptation or modification before it can be adopted as a standard technique for large animal scaffold evaluation, and these will have to be undertaken prior to subsequent work. Although the scaffold was shown to have porous interconnections, work should continue to refine manufacture of these polymers to avoid the thin film of non-porous polymer coating that was encountered in this study and to maximise overall porosity and nutrient diffusion without adversely affecting its structural properties.

Assessment of cell viability and ALP activity prior to implantation confirmed the ovine SSCs adhered and grew throughout the polymer scaffold, although further work is warranted to refine ovine cell culture protocols to maximise osteogenic differentiation. Unfortunately, due to the significant transit time between the laboratory and the operating facility, scaffolds were removed from the incubator and stored in culture medium within an insulated airtight container for approximately two hours immediately prior to surgery. Therefore, it would have been useful to re-evaluate cell viability immediately prior to implantation, as this process is likely to have led to significant perioperative cell death. If such transit times cannot be avoided in future studies, attention should be turned to higher initial cell seeding density or dynamic seeding and incubation.

In common with many clinical operative procedures, a local anaesthetic agent (bupivacaine) was infiltrated around the ostectomy site to provide post-operative analgesia. Subsequent *in vitro* testing suggests significant toxicity to human SSCs following exposure to local anaesthetic agents (see Chapter VI) and this may account for the lack of enhanced regeneration seen in the scaffold and cells group.

The stiffness of the external fixation construct may have had a significant effect on the rate of bone regeneration. It is known that *relative stability* allows secondary bone healing by callus formation, whereas *absolute stability* leads to primary bone healing. Primary bone healing tends to occur most favourably when two bone ends are closely opposed and osteonal remodelling can occur by the advancement of cutting cones.

However, in a construct where a large defect is present, such as in a 35 mm segmental defect, relative stability is desirable to promote callus formation and secondary bone healing. The external fixator was applied in this study in a very stable configuration with high stiffness and little relative movement. This combined with complete removal of the periosteum, would have adversely affected both the mechanical and biological stimuli for bone healing. Although many authors suggest a defect of greater than 30 mm is required to be considered critical, it is likely, because of these factors, that our technique would produce a much smaller critical sized defect. Therefore, much less bone regeneration would be expected. This may be overcome in future by preserving periosteum, adopting a less rigid fixation construct or allowing some form of dynamisation.

Table 5.6 Factors which should be considered and modified prior to further large animal skeletal engineering biomaterial evaluation

nimal skeletal engineering biomaterial evaluation
Initial in vitro scaffold incubation
Scaffold porosity and pore interconnectivity
Absence of impermeable scaffold surface coating
Dynamic cell seeding and incubation – consider using a bioreactor
Confirmation of cell viability, differentiation and scaffold penetration prior to implantation
Reduce transit time prior to implantation
<i>In vivo</i> incubation
Size of segmental defect
Operative technique – removal of periosteum
Potential toxicity of operative adjuncts e.g. local anaesthetic infiltration
Construct stiffness, stability and micromotion
Duration of incubation
Analytical factors
Requirement for decalcification prior to analysis
Ability to analyse large specimens for microscopic and macroscopic signs of integration
Ability to differentiate between scaffold and new tissue growth

These factors highlight some of the hurdles that need to be overcome before successful outcomes can be expected from large animal trials in our laboratories. There are many unexpected factors that influence the formation of a valid tissue engineering construct and these can often only be identified in retrospect. This also serves to underline the critical importance of well-conducted large animal studies in the assessment of therapeutic products, so that any adverse factors can be resolved prior to human clinical application.

In conclusion, the first objective; to establish a consistent tibial critical defect model in sheep, has been fulfilled. The second objective; to demonstrate a living cell composite using cultured skeletal stem cells on synthetic scaffold to augment bone formation in a large animal segmental defect model, has been partially fulfilled. The null hypothesis: that the polymeric binary blend biomaterial PLLA/PCL (20/80) does not function as a suitable scaffold for skeletal regeneration strategies in an ovine tibial segmental defect model cannot be rejected, thus further work should be performed to refine the ovine segmental defect model, the polymeric scaffold and large scale analytical techniques used in these studies.

Chapter VI

Hurdles to successful clinical translation – The effect of commonly used local anaesthetics on skeletal stem cell viability and function

The *in vitro* work and analysis within this chapter was performed jointly with Mr Edward Tayton. I am also grateful to Mr Alexander Aarvold, Ms Spandan Kalra and Miss Esther Ralph whose support was crucial for successful completion of this study.

A paper containing the *in vitro* work has been published in the *Journal of Bone and Joint Surgery (Br)* under joint first authorship

A presentation based in this study was awarded first prize at the Gauvain Scientific Meeting, Southampton, 2011

6.1 Introduction

Despite some excellent recent advances in the field of tissue engineering and consistent high levels of government research funding, only a small proportion of the successful basic science research currently reaches *in vivo* analysis with a view to clinical translation. Critically, even fewer strategies are successfully scaled-up for commercial manufacture and clinical use (Mason and Manzotti 2010). This translational gap often referred to in financial venture capital circles as the 'Valley of Death' is highly relevant for the development of regenerative medicine (Hollister 2009). There is no single cause for this disparity; rather, it is the result of a complex of practical, regulatory, logistical and financial factors, which serve to ensure only the most promising strategies ultimately succeed.

One factor which may have presented a particular confounder to the successful progression of the tissue engineering strategy described in Chapter V of this thesis was the potential of local anaesthetic (LA) agents to cause toxicity to the developing cell construct. In light of this, an *in vitro* study was devised to assess the effects of these agents on the viability of SSCs.

LA infiltration is recommended in both large animal veterinary practice and in human clinical procedures for peri-operative analgesia. In regard to the large animal study (presented in Chapter V), and also for potential clinical translation of new strategies, it is of fundamental importance to establish any effects this may have on the implanted construct, particularly the SSCs contained therein. Methods of LA administration, routinely employed to ensure analgesia in orthopaedic practice, include intra-articular injection or infusion, and subcuticular wound infiltration (Moiniche et al. 1999, Scott 2010). These techniques could lead to considerable exposure of implanted tissue engineered constructs to the LA. The toxic effects of common LAs on a number of differentiated cell types have previously been documented (Piper and Kim 2008, Quero et al. 2011, Jacobs et al. 2011). Therefore any loss of viability or function of SSCs as a consequence of exposure to LA would indicate the need to seek alternative analgesic strategies. We therefore designed an *in vitro* analysis to investigate the effects of commonly used local anaesthetics on the morphology, biology, function and survival of human adult SSCs.

6.2 <u>Aims</u>

The aim of this *in vitro* study was to investigate the effects of three LAs in routine use in orthopaedic practice on SSC function and survival, in order to establish their individual toxicities over a range of physiological concentrations, and instruct the implementation of appropriate analgesia during the application of skeletal tissue engineering strategies.

6.3 Null Hypotheses

- 1. The exposure of SSCs to LA agents does not affect their function or viability.
- 2. Incubation of SSCs in basal medium following exposure to LA agents does not affect their function or viability.

6.4 Materials and methods

6.4.1 Reagents, hardware & software

Tissue culture reagents and all staining agents were purchased from Sigma, Aldrich, UK unless otherwise stated. CTG and EH-1 were purchased from Molecular Probes, Leiden, Netherlands.

6.4.2 Cell culture

Skeletal cell populations (primary passage) were obtained from the bone marrow of three patients (male aged 66 years (M66), female aged 72 years (F72) and male aged 39 years (M39)) undergoing primary THR at University of Southampton Hospital NHS Foundation Trust with the approval of the Local Research Ethics Committee (LREC 194/99) and informed patient consent as previously described (Chapter III, 3.4.2). Following isolation and monolayer culture in basal medium, cells were released using trypsin in EDTA, centrifuged and re-suspended in basal medium. The total cell count was determined using a haemocytometer. Cell populations were diluted with basal medium to a concentration of 5x10⁴ cells/ml, and 1 ml of this solution was added to each well of a standard 12 well plate. 10 plates in total were seeded for each patient (20 plates for M39, in order to perform further analysis at day 7 following LA exposure – see Section 6.4.4), giving a total of 120 wells per patient (240 wells for M39) for experimentation. The cells were then grown to confluence over a period of approximately 7 days, with PBS washes and medium changes every 2-3 days.

6.4.3 LA preparation

Three local anaesthetic solutions i) 1% lidocaine hydrochloride (Hameln pharmaceuticals Ltd, Gloucester, UK), ii) 0.5% bupivacaine hydrochloride (AstraZeneca UK Ltd, Luton, UK) and, iii) 0.5% levobupivacaine hydrochloride (Abbott Laboratories Ltd, Kent, UK) were obtained from commercial sources in their 'ready to use preparation', and diluted in basal medium to produce 50:50, 25:75, and 10:90, LA to basal medium solutions by volume.

6.4.4 Incubation in LA

Upon cell confluence, 1 ml of each of the three LA solutions at each of the three concentrations (9 groups per patient) was added to 12 wells (108 wells in total), with 1ml basal medium alone added to the remaining 12 wells to act as controls. The procedure was repeated for the second set of M39 cells. Following incubation in LA solutions for 2 hours, the LA solutions were removed, the cells washed in PBS, and then incubated overnight in basal medium before analysis. The second set of M39 cells underwent 7 days further incubation in basal medium following LA exposure, with PBS washes every 3 days prior to analysis.

In order to prevent cellular insult through lack of nutrients alone and to ensure adequate basal medium was always present for cellular metabolism and diffusion, the maximal concentration of LA used was a 50:50 (v/v) dilution.

6.4.5 WST-1 assay

Cell number and cell viability following LA exposure at the three concentrations were quantified using the WST-1 assay (9 groups per patient cell population + controls). After removal of the incubation medium and washing in PBS, 1 ml of 1:10 dilution WST-1 substrate (Roche Ltd, Welwyn Garden City, UK) was added to 4 of the 12 wells of each group. At 2 hours, three 100 µl aliquots of substrate were removed from each well and read using a BioTek ELx-800 universal microplate spectrophotometer (BioTek, Potton, UK) at a wavelength of 410 nm. An increase in absorbance value (i.e. increase in optical density of the substrate) indicated increased cell number and viability. Mean and standard deviation were calculated for the optical densities of each group and percentage reduction compared to controls.

6.4.6 DNA assay

Cell number (but not viability) was also determined using a standard DNA PicoGreen® assay. Cells were washed in PBS and fixed in 90% ethanol prior to air drying. The cells were then rewashed in PBS and lysed in 1 ml of 0.5% Triton X-100 before undergoing three freeze-thaw cycles and mechanical lysis. Cell lysate was measured for DNA content using PicoGreen® (Molecular Probes, Paisley, UK) according to routine

manufacturer protocol. 10 µl of lysate was run in triplicate for each well on a plate against standards, analysed using a BioTek FLx-800 microplate fluorescent reader.

6.4.7 Live/dead immunostaining

CTG was used to label viable cells and EH-1 for necrotic cell nuclei. The samples were washed in PBS and then incubated for 90 minutes in 1 ml of standard CTG/EH-1 solution (10 µg/ml CTG, 5 µg/ml EH-1). Samples were fixed in ethanol and stored in PBS prior to fluorescent microscopy using a standard FITC filter.

6.4.8 Alkaline Phosphatase assay

ALP assay was used as a measure of osteoblastic differentiation at seven days following LA exposure. ALP in the cell lysate (as obtained for the DNA assay) was measured using p-nitrophenyl phosphate as the substrate in 2-amino-2-methyl-1-propanol alkaline buffer solution (Sigma, Poole, UK) according to manufacturer protocol. 10 µl of lysate was run in triplicate for each well on a plate against standards, analysed using a BioTek ELx-800 microplate reader.

6.4.9 Alkaline Phosphatase stain

Cell morphology and expression of ALP was examined in the final two of 12 wells for each group. In brief, cells were fixed in 95% ethanol followed by incubation for 45 minutes in 1 ml of 40 μ l/ml naphthol AS-MX phosphate solution with 0.24 μ g/ml fast violet salt followed by rinsing prior to microscopy.

6.4.10 Statistical analysis

All experiments were run at least three times. Statistical analysis was performed using SPSS Ver. 18.0. Statistical comparison was made using Student's unpaired *t*-test with a *p* value less than 0.05 taken to be significant.

6.5 Results

6.5.1 Effect of LAs on skeletal cell proliferation

6.5.1.1 Lidocaine

Analysis of cell viability and proliferation using the WST-1 assay demonstrated a toxic effect of lidocaine on skeletal cell populations which was concentration-dependent. Negligible toxicity was observed in each of the three primary skeletal cell populations following culture in 10% lidocaine (Fig. 6.2). However, incubation in both 25% and 50% solutions resulted in a significant decrease in cell viability with a mean reduction in optical density of 33% (p=0.03) and 70% (p<0.001) respectively. Similar observations were recorded for DNA analysis (Fig. 6.3) with a reduction in measured DNA concentration for 25% and 50% solutions of 47% (p<0.05) and 74% (p<0.05) respectively. Furthermore, the inhibition of cell proliferation was maintained 7 days after LA exposure with a significant reduction of 18% (p=0.03) and 45% (p<0.001) in both the 25% and 50% solutions respectively as measured by WST-1 assay (Fig. 6.4), with a corresponding persistent drop in DNA concentration of 70% (p<0.01) and 75% (p<0.01) respectively (Fig. 6.5).

6.5.1.2 Bupivacaine

Similar concentration-dependent toxicity was observed in cells exposed to bupivacaine. As illustrated in, WST-1 assay demonstrated no significant difference in the cells exposed to the 10% solution compared to the controls (p=0.1) (Fig. 6.2). However, the drop in activity was significant for both the 25% and 50% solutions where the mean drop in activity was 68% (p<0.001) and 72% (p<0.001) respectively. These results were supported by DNA analysis (Fig. 6.3), where a mean drop in DNA concentration from the cell lysate of 59% and 61% was observed in the 25% and 50% solutions respectively (p<0.05). This appeared to be an enduring effect in those cells exposed to the 50% bupivacaine solution where a 59% reduction was measured on the WST-1 assay (p<0.001) (Fig. 6.4) and 73% decrease in DNA concentration (p<0.001) (Fig. 6.5).

6.5.1.3 Levobupivacaine

The toxic effects of levobupivacaine were not as intense as either lidocaine or bupivacaine. WST-1 assay showed no significant mean loss of cell viability in the 10% solution (p=0.14) and in both the 25% and 50% solutions the mean reduction in cell viability was only 24% (p=0.01 and p=0.002 respectively) (Fig. 6.2). This was

supported by DNA analysis (Fig. 6.3). Furthermore, the toxic effect of levobupivacaine was transient, permitting the recovery of cell viability at all LA incubation concentrations, following a 7 day recovery period. This cell recovery observed by WST-1 analysis was also seen following DNA analysis (Fig. 6.4 and 6.5).

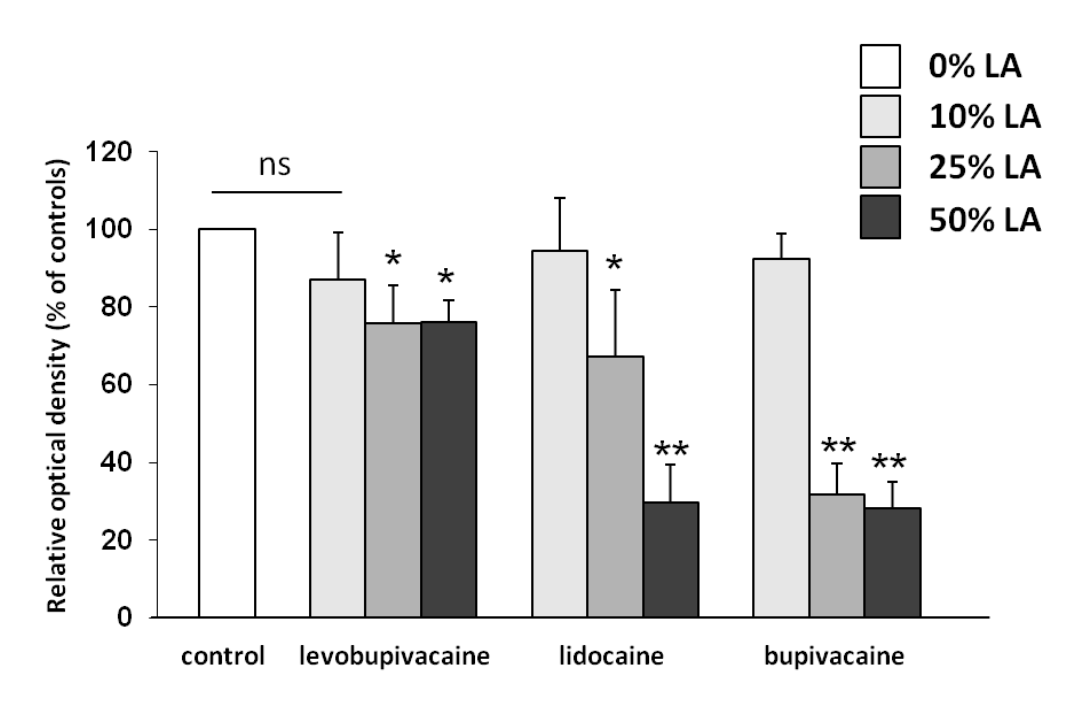


Fig. 6.1 WST-1 cell proliferation assay at 2 hours (+ SD) for the cells from three patients, 24 hours following exposure to different concentrations of LAs for 2 hours. Cell viability was reduced with increasing concentration of LA, although the effect is less marked for cells exposed to levobupivacaine (\cdot p<0.05, ns = no significant difference).

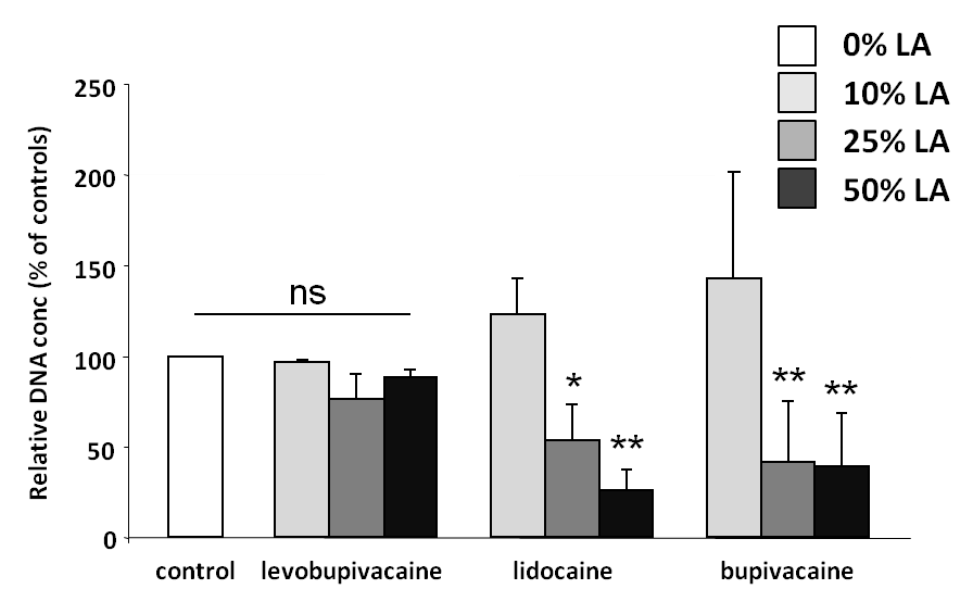


Fig. 6.2 Combined DNA assay (+ SD) of cells from all 3 patients 24 hours following exposure to different concentrations of LAs for 2 hours. A reduction in cell number with increasing concentrations of lidocaine and bupivacaine was observed (+ p<0.05). There was no significant change in DNA for cells exposed to levobupivacaine at all concentrations examined (ns).

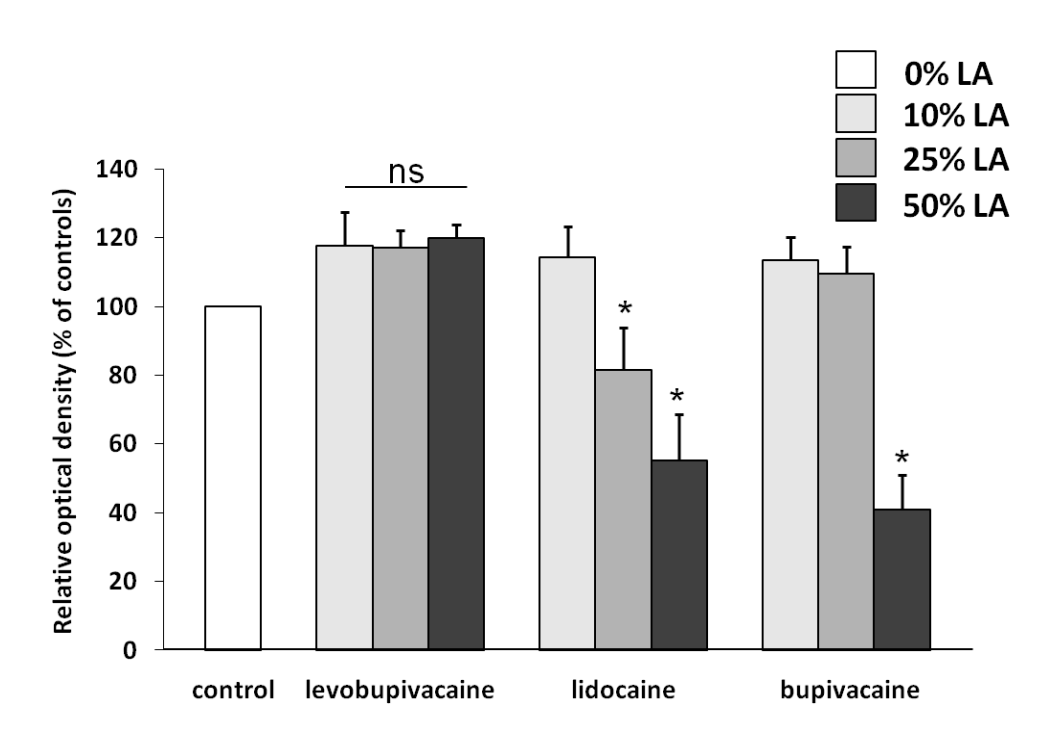


Fig. 6.3 WST-1 cell proliferation assay at 2 hours (+ SD) 7 days following exposure to different concentrations of LAs for 2 hours. A persistent reduction in cell viability was observed with increasing concentrations of lidocaine and bupivacaine. Note restoration of cell viability in cells exposed to levobupivacaine following 7 days recovery (+ p<0.05, ns = no significant difference).

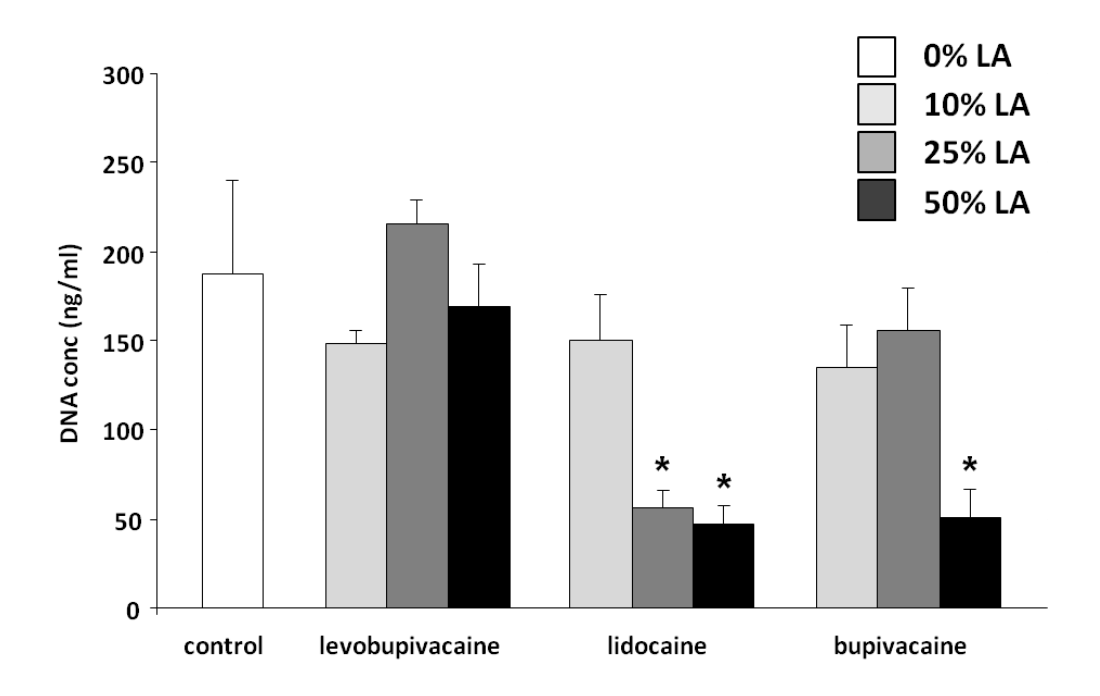


Fig. 6.4 DNA assay of cells (M39, mean + SD) following exposure to different concentrations of LAs for 2 hours and subsequent 7 days further incubation. There was a persistent reduction in cell numbers exposed to high concentrations of lidocaine and bupivacaine, but similar numbers in samples exposed to levobupivacaine compared to controls. (-p<0.01)

6.5.2 Effect of LAs on cell viability and necrosis

Cell viability and necrosis were examined using CTG/EH-1 immunocytochemistry. In all three patient skeletal cell populations examined, necrosis was observed to increase in proportion with LA concentration, as shown by the number of cell nuclei staining red with EH-1 (Fig. 6.6 and 6.7). Necrosis was exacerbated further in those cells exposed to lidocaine or bupivacaine. However, cells exposed to levobupivacaine displayed markedly reduced evidence of cell death, often limited to cytoplasmic damage.

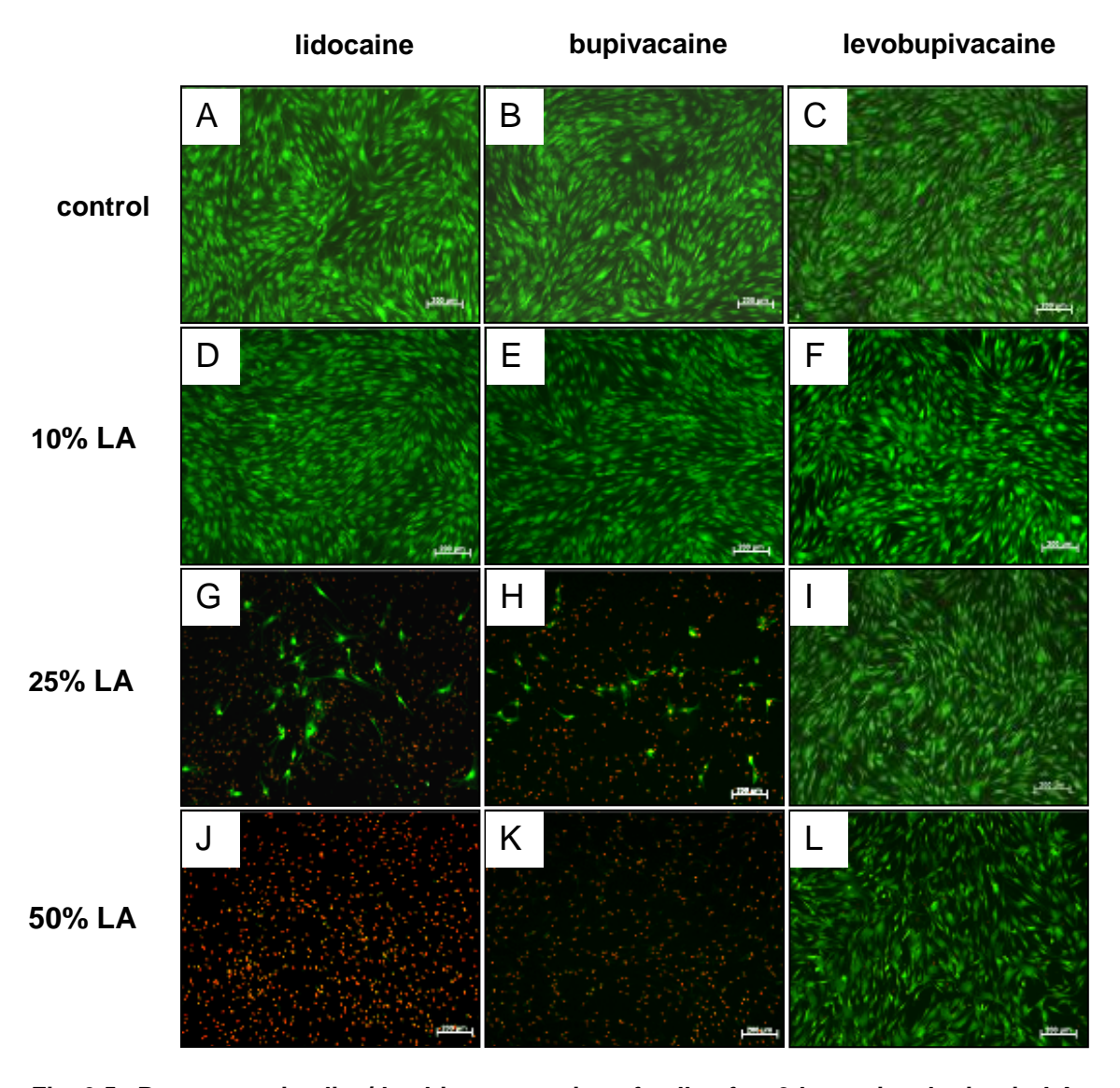


Fig. 6.5 Representative live/dead immunostains of cells after 2 hours incubation in LAs and 24 hour recovery time. The cytoplasm of live cells stain green with CTG and apoptotic cell nuclei stain red with EH-1. (A-C) controls. (D-F) cells incubated in 10% solution, showing negligible toxicity in any LA. Cells incubated in 25% lidocaine (G) and bupivacaine (H) show significant cell necrosis, whereas cells in 25% levobupivacaine (I) remain essentially viable, even at 50% concentration (L). Scale bars: 200 μm

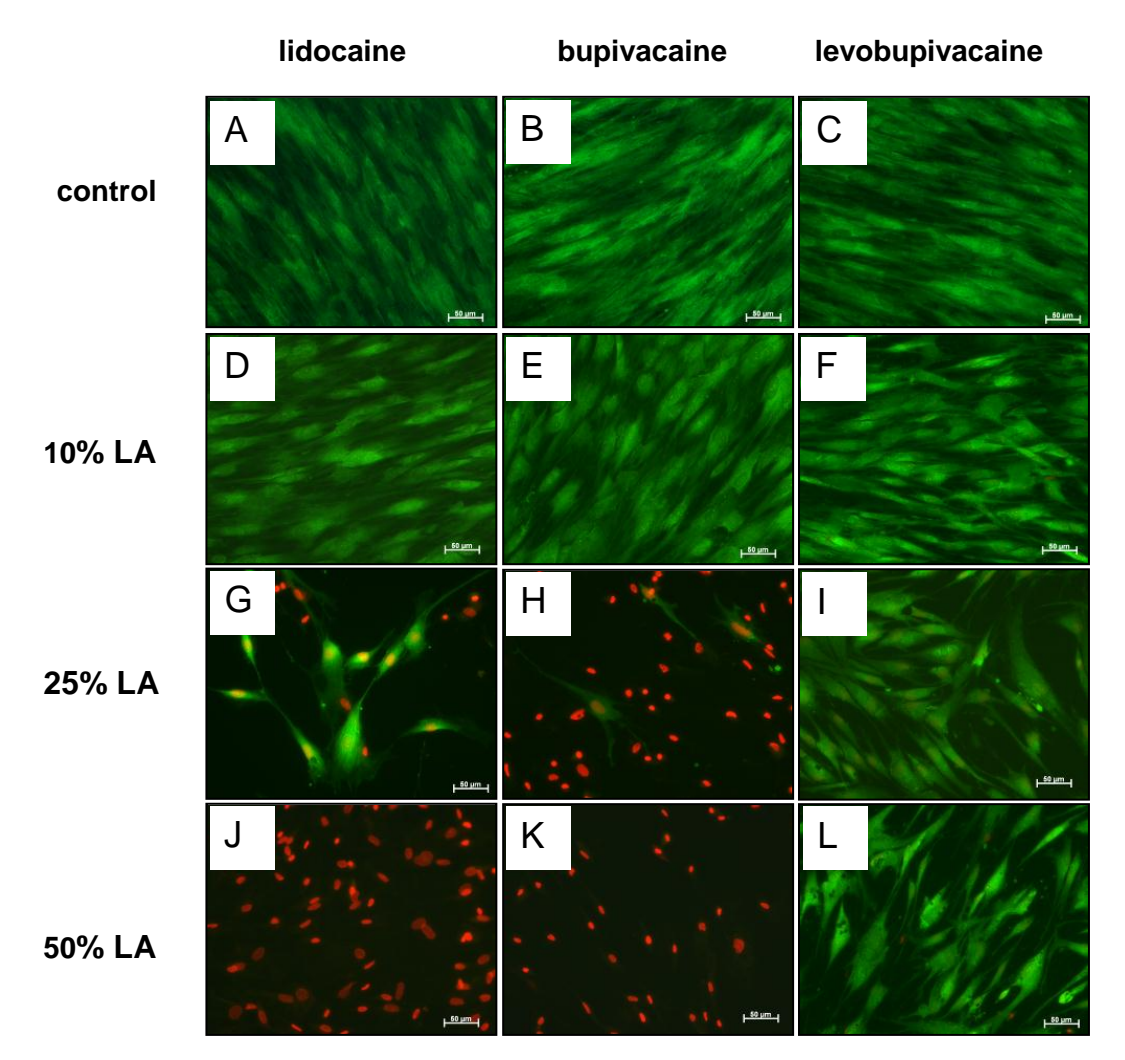


Fig. 6.6 High magnification representative live/dead immunostains of cells after 2 hours incubation in LAs and 24 hour recovery time. The cytoplasm of live cells stain green with CTG and apoptotic cell nuclei stain red with EH-1. (A-C) controls. (D-F) cells incubated in 10% solution, showing negligible toxicity in any LA. Cells incubated in 25% lidocaine (G) and bupivacaine (H) show significant cell necrosis and a change in phenotype of remaining viable cells. Cells incubated in 25% and 50% levobupivacaine (I and L) show cytoplasmic perforation within viable cells, suggesting early toxicity, although no viable cells remain in samples incubated with 50% lidocaine (J) or bupivacaine (K). Scale bars: 50 μm.

Following a 7 day period of recovery culture (Fig. 6.8), cells incubated in all the 10% LA concentrations (D-F) maintained a normal phenotype and cell growth, comparable to control samples (A-C). At 25% concentration, cells exposed to bupivacaine (H) and levobupivacaine (I) recovered to control cell densities, however cells incubated with lidocaine remained sparsely populated and phenotypically abnormal (G). There was no or limited recovery of cells after incubation with 50% lidocaine (J) or bupivacaine (K), although normal appearances with levobupivacaine (L). The absence of red nuclear staining with EH-1 in these cultures may be a consequence of repeated media changes and cell washing over a 7 day period, removing all non-adherent cells and leaving only viable cells.

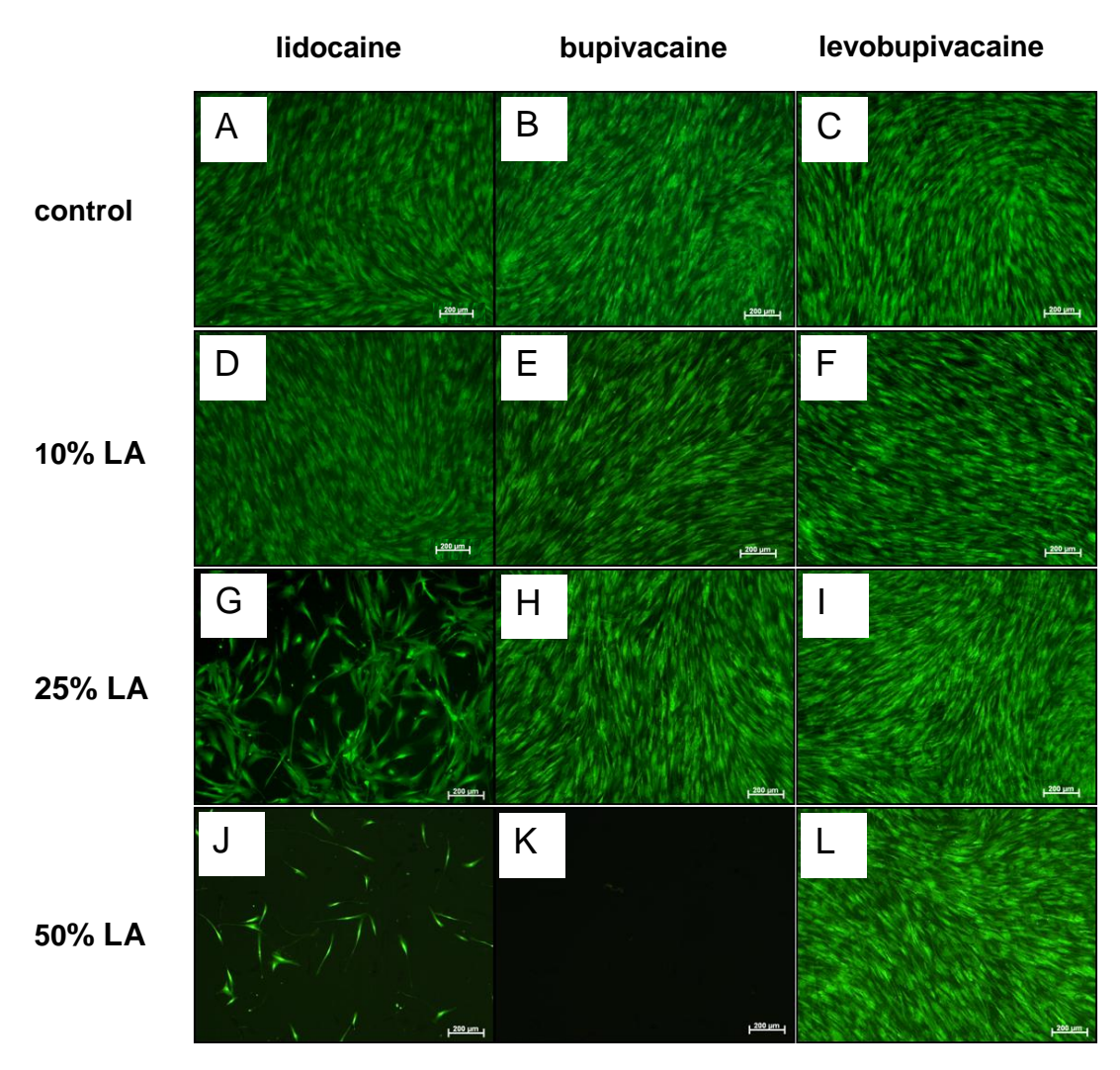


Fig. 6.7 Representative live/dead immunostains of cells after 2 hours incubation in LAs and 7 day recovery time. Note the absence of cell-nuclei staining red with EH-1. It is hypothesised that all dead cells became non-adherent and were washed away during media changes. There is no recovery in live cell number in the lidocaine 25% or 50% groups (G and J). Some recovery has occurred in the 25% bupivacaine group (H), but not at 50%, where no live cells remain (K). In contrast, cells incubated with levobupivacaine, maintain confluence, even following incubation with 25% and 50% LA (I and L). Scale bars: 200 μm.

6.5.3 Effect of LAs on cell differentiation

ALP assay was used as a measure of osteoblastic differentiation of M39 cells one week following LA exposure. There was a reduction in mean ALP activity in cells exposed to all LAs (Fig. 6.9), although this was only significant in the 25% and 50% lidocaine solutions where the reduction was 83% in both groups (p<0.05), and in the 25% and 50% bupivacaine solutions where the mean reduction recorded was 86% (p<0.05) and 100% (p<0.01) respectively.

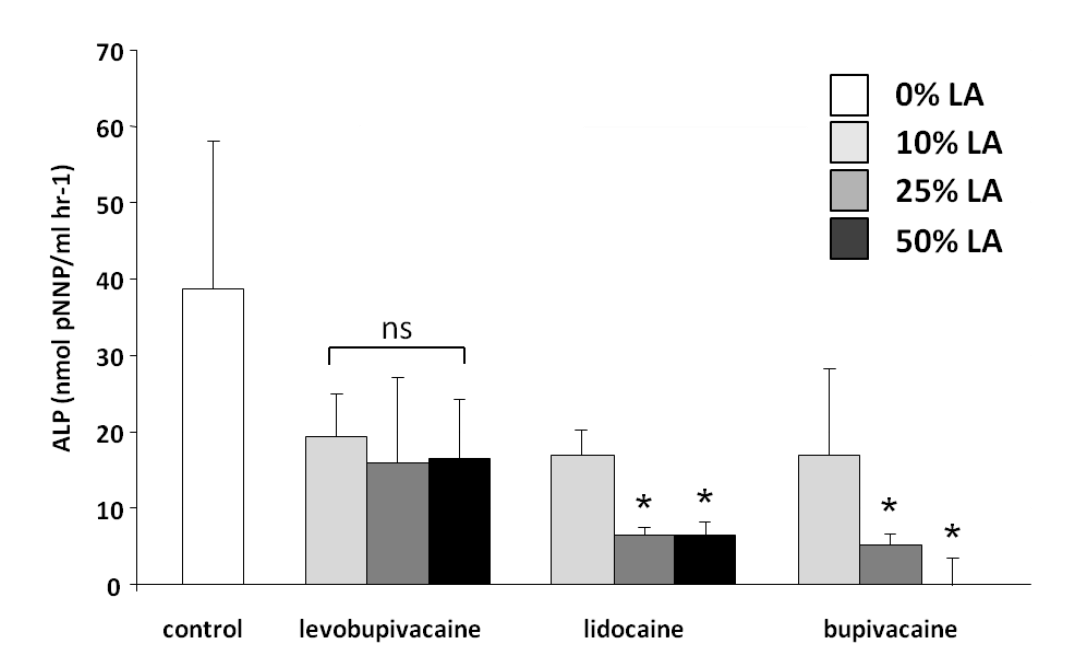


Fig. 6.8 ALP assay (+ SD) of cells following exposure to different concentrations of LAs and 7 days further incubation. There was a reduction in ALP activity in all groups following LA exposure, however this was only significant at higher concentrations of lidocaine and bupivacaine, (* p<0.05, ns = no significant difference).

These findings were also observed following analysis of ALP staining (Fig. 6.10), a measure of surviving cell number and function and further, may indicate potential mechanisms of LA toxicity through analysis of cell morphology. The concentration-dependent decrease in ALP staining is in concordance with the reduction in ALP activity detected quantitatively. Furthermore, the toxic effect was less pronounced in the cells exposed to levobupivacaine. There was also a substantial reduction in cell density corresponding to increasing concentrations of lidocaine and bupivacaine. This effect was less dramatic with levobupivacaine. In addition, altered cell morphology with condensed/ fragmented nuclei and cytoplasmic perforations were seen in higher concentrations of lidocaine and bupivacaine exposure, indicative of cell necrosis.

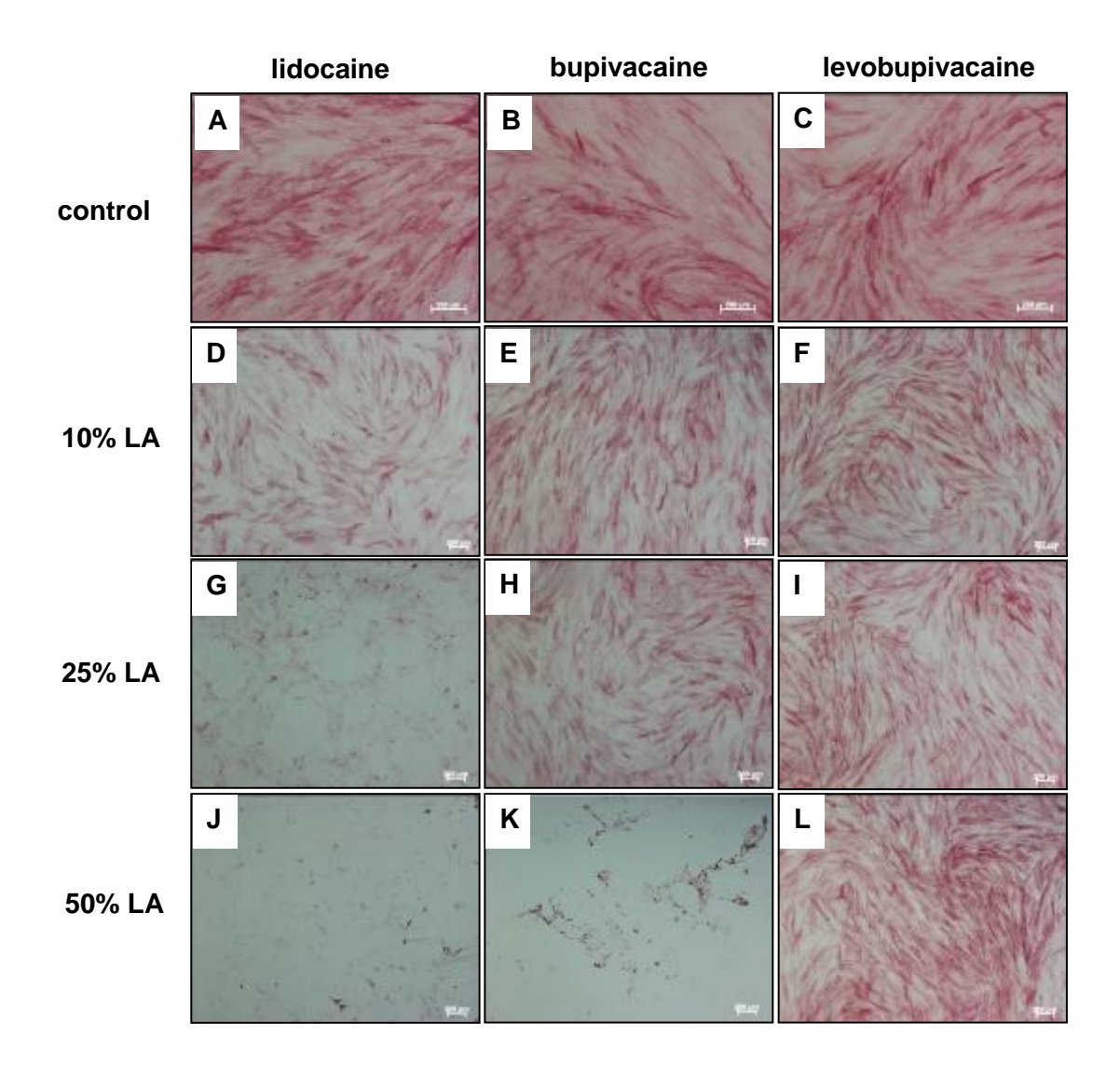


Fig. 6.9 Representative photomicroscopy of cells stained for ALP, after 2 hours incubation in LAs and 7 days recovery time. Cells incubated in 10% LA solutions (D-F), showed minor reduction in ALP staining, compared to controls (A-C). Cells incubated in 25% lidocaine (G) demonstrated significant reduction in ALP stain, whereas cells incubated in 25% bupivacaine (H) and levobupivacaine (I) showed only a slight reduction. For the 50% LA solutions, there was significant loss of cell number and ALP stain in both the lidocaine (J) and bupivacaine (K), where cells showed altered morphology and condensed/ fragmented nuclei probably due to necrosis. Note cells incubated in 50% levobupivacaine displayed robust cell density and positivity for ALP stain after 7 days recovery. Scale bars: 200 μm

6.6 Discussion

These studies indicate that certain LAs used at clinically relevant concentrations are deleterious to the survival of skeletal stem cell populations *in vitro*. Specifically, bupivacaine, the most widely used anaesthetic for post-operative intra-articular use (Moiniche *et al.* 1999), showed significant toxicity to cells following exposure for just two hours, even at 25% original concentration. Similarly, lidocaine was observed to induce toxic effects at only 25% normal clinically-used concentrations. Only levobupivacaine (the S-enantiomer of bupivacaine), displayed reduced cell toxicity compared to the other LAs, an effect maintained at 7 days culture following removal of the LA, where negligible cell toxicity was recorded in the levobupivacaine group. Thus the null hypothesis, that the exposure of SSCs to LA agents does not affect their function or viability can be rejected, although the cytotoxic effect was more pronounced for lidocaine and bupivacaine, as compared to levobupivacaine. In addition, incubation of SSCs in basal medium following exposure to LA agents *does not* appear to allow recovery of cell viability and function following toxicity.

We chose to test the LAs at the concentrations they are used clinically, rather than comparing the three LAs at the same concentrations. This provides a more suitable comparison from a clinical perspective and addresses the fact that each LA is a different drug that has been manufactured to be used within specific concentration ranges. Although this does not allow direct comparison between each LA at each individual concentration, it does enable an evaluation of each drug from a clinical viewpoint.

As the use of intra-articular constructs that incorporate SSCs becomes more commonplace, particularly during cartilage regeneration procedures (Haleem *et al.* 2010), but also in other evolving tissue engineering strategies, the choice of LA is becoming more critical. The present *in vitro* study suggests that intra-articular use of bupivacaine in such applications should be avoided. In addition, lidocaine is often used subcutaneously during minor procedures such as digital ring blocks (Reichl and Quinton 1987), and would be a prime candidate for use in a tissue engineering strategy. Despite administration of this LA several centimetres from any reparative constructs, given the concentration required to produce toxicity is so low, this may still prove harmful to the cells. Levobupivacaine is less commonly used in clinical practice, but is still indicated for local anaesthesia including infiltration, nerve block, ophthalmic, epidural and intrathecal anaesthesia in adults; and infiltration analgesia in children

(Chang *et al.* 2005). The comparatively reduced toxicity of levobupivacaine on SSCs found in the present study is consistent with the recorded reduction in cardiovascular and central nervous system toxicity in animal and human studies (Leone *et al.* 2008). Although current evidence suggests levobupivacaine exhibits a similar therapeutic profile to racemic bupivacaine, in terms of its analgesic effect and duration, further research, including *in vivo* analyses are warranted to determine if, as evidenced from these findings, levobupivacaine offers a safer LA for use in clinical procedures involving cells such as SSCs (Burlacu and Buggy 2008).

The toxic effects of LAs on a number of cell types have been extensively investigated both in vitro and in vivo. Nole et al. found reduced proteoglycan synthesis in both explanted porcine and canine cartilage when exposed to bupivacaine (Nole et al. 1985). Furthermore, Gomoll et al. showed that continuous infusion of bupivacaine into the rabbit shoulder resulted in significant histopathological and metabolic changes in the articular cartilage, advocating a cautious approach for the use of continuous postoperative analgesic infusions (Gomoll et al. 2009). From an orthopaedic perspective, reductions in specific cellular activities as a consequence of cell necrosis have also been attributed to bupivacaine exposure in myocytes and intervertebral disc cells (Quero et al. 2011, Nouette-Gaulain et al. 2009). A similar study to the present investigation was carried out by Piper and Kim, who compared the toxic effects of bupivacaine and ropivacaine (which differs only by the replacement of the butyl group with a propyl group) on human articular chondrocytes (Piper and Kim 2008). The authors found that this small change to the molecular structure resulted in significantly reduced toxicity of ropivacaine to chondrocytes, both in intact human cartilage and when cultured in vitro. However these effects were only analysed up to twenty-four hours following exposure, and a subsequent study observed toxic effects of ropivacaine when measured at 120 hours (Grishko et al. 2010).

Lidocaine has similar harmful effects to other certain differentiated cell types. Grishko et al. showed lidocaine (as well as bupivacaine and ropivacaine) exposure resulted in mitochondrial dysfunction and apoptosis in cultured human chondrocytes (Grishko et al. 2010), whereas Karpie and Chu also reported chondrotoxic effects of 1% and 2% lidocaine on bovine chondrocytes (Karpie and Chu 2007). The toxicity of lidocaine on mature human articular chondrocytes appears to be both dose and time-related in vitro (Jacobs et al. 2011). Lidocaine also has toxic effects on other cell types, including retinal ganglion cells (Grosskreutz et al. 1999) and urothelial cells (Drewa et al. 2005). Lidocaine has been shown to disrupt intercellular adherence, and this property has

been utilised to replace the use of trypsin in a tissue-culture technique, to re-plate cell suspensions with no apparent detrimental effects (Rabinovitch and DeStefano 1975). Such effects could interfere with the normal function of these cells, however, and be detrimental to tissue engineering techniques that rely on cellular adherence and replication upon a construct.

To date, the mechanisms of LA-induced cell toxicity remain unclear, although the induction of apoptosis via mitochondrial damage, caspase activation, inhibition of tyrosine kinase, and blockage of sodium channels, as well as direct necrotic effects, including altered calcium metabolism, free radical damage and changes in membrane fluidity have all been implicated (Johnson *et al.* 2002, Johnson *et al.* 2004, Klemm 1985, Werdehausen *et al.* 2007). Correlation has been made between LA lipophilicity and toxicity, as well as low LA pKa and the induction of cell apoptosis (Onizuka *et al.* 2011). Mechanisms involved in LA induced cell toxicity are thus a pivotal area warranting further examination.

To our knowledge this is the first study to report the toxic effects of LAs on skeletal progenitor cells. Kim *et al.* have examined the effects of lidocaine on rat musclederived progenitor cells (MDC) in a urinary incontinence model (Kim *et al.* 2009). The authors found minimal cytotoxicity of lidocaine at a physiologic concentration, concluding that this LA could be safely used for analgesia in a periurethral MDC injection without decreasing the efficacy of the therapy. However, this model was wholly different to the current study because only lidocaine was tested, and the cells under test were specifically cultured such that they were highly enriched for differentiated myogenic cells.

Significant progress has been made to identify and synthesise efficacious cell-scaffold combinations for tissue engineering techniques to treat skeletal pathology. Furthermore, significant resources have been invested to develop reliable, reproducible and effective therapeutic strategies to maximise the regenerative potential of such reparative constructs. As more strategies are translated to clinical use, the practical aspects necessary for delivering such successful approaches will become increasingly important. The refinement of such strategies requires a holistic understanding of the cellular science through to clinical care, and relies upon pre-emptive identification and removal of factors that may prevent optimal clinical outcomes. This study highlights an important issue for regenerative medicine. As the use of tissue engineering and regenerative clinical strategies become more commonplace, the survival of cells on a

construct will prove integral to success, and thus care with, or avoidance of the use of certain local anaesthetics in the vicinity of the construct is advocated. Such relatively simple modifications to established clinical protocols will help to ensure optimal therapeutic efficacy of the reconstructive strategy. These findings are not just important for consideration in the implementation of novel reconstructive techniques, but may have significant impacts upon the success of strategies in current use for skeletal regeneration, such as microfracture treatment, mosaicplasty and MACI (see section 1.8.1).

In conclusion, the null hypotheses that 'exposure of SSCs to LA agents and further incubation of SSCs in basal medium following exposure to LA agents does not affect their function or viability' can both be rejected. Specific LAs have a direct toxic effect to SSCs *in vitro* at clinically relevant concentrations and following exposure to a threshold concentration, these cells do not recover once the LA has been removed.

Chapter VII

Conclusions and future perspectives

7.1 <u>Conclusions</u>

Given the increasing frequency and considerable morbidity associated with damage or loss of musculoskeletal tissues, coupled with the inherent disadvantages associated with many current orthopaedic therapies, there is a clear and urgent mandate to translate musculoskeletal research into clinical use. With the advent of tissue engineering and the appreciation that its principles could be readily applied to musculoskeletal regeneration, there has been an accumulation of promising strategies to regenerate skeletal tissue. The approaches outlined in Chapter I provide a snapshot of future potential, but despite an abundance of promising *in vitro* results, the necessary validation of these strategies using robust small and large animal *in vivo* studies is scarce, with even fewer studies progressing to clinical trials. This translational gap prohibits the routine clinical use of many of these promising techniques.

The therapeutic panacea for skeletal tissue engineering would be the integration of a custom-sized immuno-modulated package containing an absorbable synthetic scaffold and impregnated with sustained-release growth factors, with viable autogenous skeletal cells (in the first instance, followed by allogeneic skeletal populations) that have been stimulated to commit to appropriate differentiation pathways. This would have to be presented within a sustained environment that provides adequate nutrition and oxygenation and removes metabolic waste products. The development of such a construct clearly requires close co-ordination within a multidisciplinary framework, involving cell scientists, biomedical engineers, mathematicians, clinicians and patients. This thesis has demonstrated how such inter-disciplinary collaborations can successfully target each of these requirements to evaluate different aspects of an evolving tissue engineering approach, including cellular concentration, and manipulation and scaffold characterisation and selection. In addition, this thesis has detailed the inception and evaluation of a large animal in vivo model for skeletal regeneration and analysed some of the hurdles preventing promising new tissue engineering strategies from reaching clinical practice.

The conclusions from each of the experimental objectives (presented in Chapter I, 1.12) are summarised below:

Chapter II: Development of an intra-operative strategy to enrich skeletal stem cells from bone marrow for orthopaedic application

Objective 1

Negative pressure filtration was demonstrated to provide an efficient and inexpensive alternative to the current clinical intra-operative strategies for administration of concentrated BMA, suitable for application with cells from an elderly cohort. This solution to cell enrichment was found to be amenable for development towards a single-use device that can be applied intra-operatively within the sterile field, thus offering considerable potential for clinical benefit.

Objective 2

The importance of BMA concentration for cell differentiation and seeding onto allogeneic bone graft was established.

Chapter III: Tantalum Trabecular Metal – Addition of human skeletal cells to an established orthopaedic implant to enhance bone-implant interface strength and clinical application

Objective 3

TTM was demonstrated to support skeletal cell growth and osteogenic differentiation comparable to allograft and autograft *in vitro*.

Objective 4

The addition of skeletal stem cells to TTM *in vitro* was shown to enhance early bone-TTM interface strength and confirmed the potential of TTM with the addition of human SSCs in tissue engineering applications as an alternative to the current accepted standard treatments for loss of skeletal tissues.

Chapter IV: *In vivo* evaluation of novel ternary polymer blend scaffolds for skeletal tissue engineering strategies using a murine model

Objective 5

In vitro and in vivo analyses for skeletal regeneration applications of candidate polymer scaffolds selected by a High Throughput screening approach, confirmed that selected polymeric ternary blend biomaterials do function as suitable scaffolds for skeletal

regeneration strategies, although it is unclear what additional effect was provided by the addition of SSCs to the construct *in vivo*.

Chapter V: *In vivo* evaluation of a candidate binary polymer blend scaffold for skeletal tissue engineering strategies using an ovine model

Objective 6

A consistent and reproducible technique was achieved for stabilisation of a 35 mm ovine tibial critical segmental defect, using an external fixator construct, for subsequent trialling of tissue regeneration strategies.

Objective 7

A living cell composite using cultured skeletal stem cells on synthetic polymeric binary blend biomaterial PLLA/PCL (20/80) scaffold was demonstrated. However this was not proven to augment bone formation in an ovine tibial segmental defect model. Practical and experimental reasons for this failure were discussed and the need for further work to refine the ovine segmental defect model, the polymeric scaffold and large scale analytical techniques, was proposed.

Chapter VI: The effect of commonly used local anaesthetics on skeletal stem cell viability and function

Objective 8

Potential hurdles to the successful implementation of tissue engineering strategies were presented with reference to bridging the translational gap. Specific *in vitro* investigations demonstrated significant dose-dependent toxic effects of three local anaesthetic agents, in routine use in orthopaedic practice, on skeletal stem cell function and survival. These findings were used to instruct the implementation of appropriate analgesia during the application of skeletal tissue engineering strategies.

The major null hypotheses that 'enriched skeletal stem cells applied as tissue engineered constructs do not augment bone formation' can therefore be rejected.

Orthopaedic surgeons are frequently required to evaluate new techniques, products or interventions, based upon information gained during research, to ensure evidence-based best practice for patients and also for professional development.

Each element of study within this research project has provided significant insight into the processes behind clinical improvement, research and product development. Furthermore, this thesis highlights the caution required before extrapolating an association seen *in vitro* to a clinical scenario, and the vast effects on experimental outcome that can be initiated by a change in a trivial or peripheral parameter. Conversely, there is also a need for caution in over-interpreting results from studies – a highly significant research finding may still translate to a relatively modest clinical benefit, and in the current economic climate of budgetary restrictions it is necessary to balance this with cost, acceptability of the treatment and alternatives.

In addition, it has been clear during the interactions with laboratory scientists throughout the preparation of this work, how important the perspective of a practising clinician is to direct research to a useful output. An understanding of the holistic needs of a patient within the context of disease is fundamental to ensuring these are appropriately met by a potential treatment, and without this understanding it is difficult to direct research to a pragmatic solution that is clinically acceptable. It has become clear that the participation of multiple personnel and agencies, with frequent discussion and feedback, is necessary to produce a coherent research protocol, targeted to answering a specific, simple question or hypothesis. Such a strategy, where the clinical applicability of any intervention or finding is constantly borne in mind, is more likely to produce findings and products with relevant outcomes and applications for therapeutic benefit.

7.2 Next steps

Although the work presented in this thesis has answered some questions and progressed the science of bone tissue engineering to a modest extent, further questions have inevitably arisen as a result of some of the findings. Therefore, several key **next steps** which require specific further investigation have been identified and are detailed below:

Chapter II: Development of an intra-operative strategy to enrich skeletal stem cells from bone marrow for orthopaedic application

In vitro analysis is required to define any additional therapeutic benefit derived from further incremental BMA enrichment.

The established importance of BMA concentration for cell differentiation and seeding onto allogeneic bone graft *in vitro* should be defined in an *in vivo* model, such as a subcutaneous mouse model. This would also enable any additional effects of host vasculature on tissue formation to be analysed.

Following refinement, the efficacy and safety of the filtration apparatus should be assessed in small and large animal skeletal regeneration models prior to clinical evaluation. This is likely to require significant multidisciplinary input and capital expenditure.

Chapter III: Tantalum Trabecular Metal – Addition of human skeletal cells to an established orthopaedic implant to enhance bone-implant interface strength and clinical application

Further enhancement of the properties of TTM should be investigated. Potential strategies could involve the incorporation of temporally-released chemical mediators or modulation of surface nanotopography to direct cellular growth and differentiation.

The enhanced biological and mechanical properties of TTM cultured with SSCs demonstrated in the current study, should be confirmed in a small animal *in vivo* study. A rabbit spinal fusion model would be particularly appropriate.

Chapter IV: *In vivo* evaluation of novel ternary polymer blend scaffolds for skeletal tissue engineering strategies using a murine model

Work on the translation of high throughput technology to larger scale clinical models (ovine condylar and segmental defects) are ongoing to validate the ternary blend biomaterials for functionality with respect to weight-bearing and remodelling capacity prior to clinical application.

Chapter V: In vivo evaluation of a candidate binary polymer blend scaffold for skeletal tissue engineering strategies using an ovine model

Work is required to refine polymer scaffold manufacturing processes, to maximise nutrient diffusion and porosity without adversely affecting structural properties.

In vitro ovine cell differentiation and culture protocols are required to define optimal conditions and techniques for seeding and osteogenic cell growth on scaffolds prior to implantation.

The effect of changing construct stability on the size of a critical-sized segmental defect should be defined in ovine tibial models.

Chapter VI: The effect of commonly used local anaesthetics on skeletal stem cell viability and function

The current study identified a significant toxic effect *in vitro* of selected local anaesthetic agents on undifferentiated SSCs. The relative sensitivity of more differentiated skeletal cells, particularly following chondrogenic and osteogenic differentiation should be assessed *in vitro*, prior to *in vivo* studies.

Investigation is required to identify other routinely used pharmaceutical or therapeutic agents that may hinder reconstructive strategies. Candidate materials for further testing include analgesics (such as non-steroidal anti-inflammatory drugs) and bone cement.

7.3 Future perspectives

Although some skeletal tissue engineering strategies have been successfully implemented in clinical practice, the rate of translation of potential new techniques remains low. In addition to the scientific and technical challenges that need to be overcome, development and manufacture of putative scaffolds and ancillary products require continued financial input, which may become harder to secure in the current fiscal climate until greater numbers of translated therapies reach the market. Seemingly peripheral concerns of finance, regulation, manufacturing and ethics are increasingly preventing some innovative and promising strategies from progressing beyond the laboratory. Efforts should therefore be made to ensure research developments are closely allied at an early stage to the processes involved in large-scale manufacture for clinical use. These processes include ethical and regulatory approval, good manufacturing practices, logistical planning, appropriate marketing and financial commitment. Clearly then, there is a need to attract appropriate personnel with an understanding of these requirements and to foster an entrepreneurial ethos within research groups to facilitate such a multidisciplinary approach.

The last ten years have seen a dramatic expansion of potentially exciting treatment options to address the increasing burden of orthopaedic morbidity. Although many of these strategies remain theoretical or in small scale development, the coordination required to effectively screen and translate the most promising options to clinical application, has now been recognised. Recent development of techniques to modulate cellular growth and differentiation, and scaffold characteristics are now being combined with analytical tools to develop constructs with appropriate physico-chemical properties for varying applications. It is likely that the wealth of experience accumulated by a variety of multidisciplinary research groups will be combined to produce an increasing catalogue of efficacious tissue engineering products for specific applications that will soon become a routine part of clinical medicine.

References

Aarvold A, Smith JO, Tayton ER, Tilley S, Dawson JI, Lanham SA, Briscoe A, Dunlop DG, Oreffo RO (2011) Taking tissue engineering principles into theatre: retrieval analysis from a clinically translated case. Regen.Med. 6:461-467

Abed YY, Beltrami G, Campanacci DA, Innocenti M, Scoccianti G, Capanna R (2009) Biological reconstruction after resection of bone tumours around the knee: long-term follow-up. J.Bone Joint Surg.Br. 91:1366-1372

Adachi N, Ochi M, Deie M, Ito Y (2005) Transplant of mesenchymal stem cells and hydroxyapatite ceramics to treat severe osteochondral damage after septic arthritis of the knee. J.Rheumatol. 32:1615-1618

Aerssens J, Boonen S, Lowet G, Dequeker J (1998) Interspecies Differences in Bone Composition, Density, and Quality: Potential Implications for in Vivo Bone Research. Endocrinology 139:663-670

Agrawal CM, Athanasiou KA (1997) Technique to control pH in vicinity of biodegrading PLA-PGA implants. J.Biomed.Mater.Res. 38:105-114

Ahlback SO, Lindahl O (1966) Hip arthrodesis. The connection between function and position. Acta Orthop.Scand. 37:77-87

Ahlmann E, Patzakis M, Roidis N, Shepherd L, Holtom P (2002) Comparison of anterior and posterior iliac crest bone grafts in terms of harvest-site morbidity and functional outcomes. J.Bone Joint Surg.Am. 84-A:716-720

Albrektsson T, Johansson C (2001) Osteoinduction, osteoconduction and osseointegration. Eur. Spine J. 10 Suppl 2:S96-101

Aldegheri R (1999) Distraction osteogenesis for lengthening of the tibia in patients who have limb-length discrepancy or short stature. J.Bone Joint Surg.Am. 81:624-634

Alhadlaq A, Elisseeff JH, Hong L, Williams CG, Caplan AI, Sharma B, Kopher RA, Tomkoria S, Lennon DP, Lopez A, Mao JJ (2004) Adult stem cell driven genesis of human-shaped articular condyle. Ann.Biomed.Eng 32:911-923

Alsousou J, Thompson M, Hulley P, Noble A, Willett K (2009) The biology of plateletrich plasma and its application in trauma and orthopaedic surgery: a review of the literature. J.Bone Joint Surg.Br. 91:987-996

Archer R, Williams DJ (2005) Why tissue engineering needs process engineering. Nat.Biotechnol. 23:1353-1355

Aronson J (1997) Limb-lengthening, skeletal reconstruction, and bone transport with the Ilizarov method. J.Bone Joint Surg.Am. 79:1243-1258

Asti A, Gastaldi G, Dorati R, Saino E, Conti B, Visai L, Benazzo F (2010) Stem Cells Grown in Osteogenic Medium on PLGA, PLGA/HA, and Titanium Scaffolds for Surgical Applications. Bioinorg.Chem.Appl.831031

Aubry D, Volcke C, Arnould C, Humbert C, Thiry PA, Delhalle J, Mekhalif Z (2009) Molecular functionalization of tantalum oxide surface towards development of apatite growth. Applied Surface Science 255:4765-4772

Augat P, Burger J, Schorlemmer S, Henke T, Peraus M, Claes L (2003) Shear movement at the fracture site delays healing in a diaphyseal fracture model. J Orthop.Res. 21:1011-1017

Augat P, Merk J, Genant HK, Claes L (1997) Quantitative assessment of experimental fracture repair by peripheral computed tomography. Calcif. Tissue Int. 60:194-199

Badiavas EV, Falanga V (2003) Treatment of chronic wounds with bone marrow-derived cells. Arch.Dermatol. 139:510-516

Badylak SF (2004) Xenogeneic extracellular matrix as a scaffold for tissue reconstruction. Transpl.Immunol. 12:367-377

Balla VK, Bodhak S, Bose S, Bandyopadhyay A (2010) Porous tantalum structures for bone implants: fabrication, mechanical and in vitro biological properties. Acta Biomater. 6:3349-3359

Barrilleaux B, Phinney DG, Prockop DJ, O'Connor KC (2006) Review: ex vivo engineering of living tissues with adult stem cells. Tissue Eng 12:3007-3019

Bedi A, Feeley BT, Williams RJ, III (2010) Management of articular cartilage defects of the knee. J.Bone Joint Surg.Am. 92:994-1009

Beitzel K, McCarthy MB, Cote MP, Chowaniec D, Falcone LM, Falcone JA, Dugdale EM, Deberardino TM, Arciero RA, Mazzocca AD (2012) Rapid isolation of human stem cells (connective progenitor cells) from the distal femur during arthroscopic knee surgery. Arthroscopy 28:74-84

Bhosale AM, Richardson JB (2008) Articular cartilage: structure, injuries and review of management. Br.Med.Bull. 87:77-95

Bianco P, Kuznetsov SA, Riminucci M, Gehron RP (2006) Postnatal skeletal stem cells. Methods Enzymol. 419:117-148

Bianco P, Robey PG (2001) Stem cells in tissue engineering. Nature 414:118-121 Block JE (2005) The role and effectiveness of bone marrow in osseous regeneration. Med.Hypotheses 65:740-747

Bloemers FW, Blokhuis TJ, Patka P, Bakker FC, Wippermann BW, Haarman HJ (2003) Autologous bone versus calcium-phosphate ceramics in treatment of experimental bone defects. J Biomed.Mater.Res.B Appl.Biomater. 66:526-531

Blokhuis TJ, Wippermann BW, den Boer FC, van LA, Patka P, Bakker FC, Haarman HJ (2000) Resorbable calcium phosphate particles as a carrier material for bone marrow in an ovine segmental defect. J Biomed.Mater.Res. 51:369-375

Bobyn JD, Poggie RA, Krygier JJ, Lewallen DG, Hanssen AD, Lewis RJ, Unger AS, O'Keefe TJ, Christie MJ, Nasser S, Wood JE, Stulberg SD, Tanzer M (2004) Clinical validation of a structural porous tantalum biomaterial for adult reconstruction. J.Bone Joint Surg.Am. 86-A Suppl 2:123-129

Bobyn JD, Stackpool GJ, Hacking SA, Tanzer M, Krygier JJ (1999) Characteristics of bone ingrowth and interface mechanics of a new porous tantalum biomaterial. J.Bone Joint Surg.Br. 81:907-914

Bobyn JD, Toh KK, Hacking SA, Tanzer M, Krygier JJ (1999) Tissue response to porous tantalum acetabular cups: a canine model. J.Arthroplasty 14:347-354

Bolland BJ, Partridge K, Tilley S, New AM, Dunlop DG, Oreffo RO (2006) Biological and mechanical enhancement of impacted allograft seeded with human bone marrow stromal cells: potential clinical role in impaction bone grafting. Regen.Med. 1:457-467

Bolland BJ, Tilley S, New AM, Dunlop DG, Oreffo RO (2007) Adult mesenchymal stem cells and impaction grafting: a new clinical paradigm shift. Expert.Rev.Med.Devices 4:393-404

Borden M, El-Amin SF, Attawia M, Laurencin CT (2003) Structural and human cellular assessment of a novel microsphere-based tissue engineered scaffold for bone repair. Biomaterials 24:597-609

Boscainos PJ, Kellett CF, Maury AC, Backstein D, Gross AE (2007) Management of periacetabular bone loss in revision hip arthroplasty. Clin.Orthop.Relat Res. 465:159-165

Bostman O, Hirvensalo E, Makinen J, Rokkanen P (1990) Foreign-body reactions to fracture fixation implants of biodegradable synthetic polymers. J.Bone Joint Surg.Br. 72:592-596

Bostman O, Hirvensalo E, Vainionpaa S, Makela A, Vihtonen K, Tormala P, Rokkanen P (1989) Ankle fractures treated using biodegradable internal fixation. Clin.Orthop.Relat Res.195-203

Bouhadir KH, Mooney DJ (2001) Promoting angiogenesis in engineered tissues. J.Drug Target 9:397-406

Boyle WJ, Simonet WS, Lacey DL (2003) Osteoclast differentiation and activation. Nature 423:337-342

Bragdon CR, Burke D, Lowenstein JD, O'Connor DO, Ramamurti B, Jasty M, Harris WH (1996) Differences in stiffness of the interface between a cementless porous implant and cancellous bone in vivo in dogs due to varying amounts of implant motion. J.Arthroplasty 11:945-951

Brinker MR, O'Connor DP (2008) Basic Sciences. In: Miller MD (ed) Review of Orthopaedics - Fifth Edition. Saunders Elsevier, Philadelphia

Brodano BG, Mazzoni E, Tognon M, Griffoni C, Manfrini M (2012) Human mesenchymal stem cells and biomaterials interaction: a promising synergy to improve spine fusion. Eur Spine J 21:3-9

Brodke D, Pedrozo HA, Kapur TA, Attawia M, Kraus KH, Holy CE, Kadiyala S, Bruder SP (2006) Bone grafts prepared with selective cell retention technology heal canine segmental defects as effectively as autograft. J Orthop.Res. 24:857-866

Buckman RWJr (2000) New Applications for Tantalum and Tantalum Alloys. JOM Journal of the Minerals, Metals and Materials Society 52:40-41

Buckwalter JA, Mankin HJ (1998) Articular cartilage: tissue design and chondrocyte-matrix interactions. Instr.Course Lect. 47:477-486

Bullens PH, Schreuder HW, Malefijt MC, Verdonschot N, Buma P (2009) The presence of periosteum is essential for the healing of large diaphyseal segmental bone defects reconstructed with trabecular metal: A study in the femur of goats. J.Biomed.Mater.Res.B Appl.Biomater. 92B:24-31

Bulstra SK, Geesink RG, Bakker D, Bulstra TH, Bouwmeester SJ, van der Linden AJ (1996) Femoral canal occlusion in total hip replacement using a resorbable and flexible cement restrictor. J.Bone Joint Surg.Br. 78:892-898

Burlacu CL, Buggy DJ (2008) Update on local anesthetics: focus on levobupivacaine. Ther.Clin.Risk Manag. 4:381-392

Burwell RG (1964) Studies in the transplantation of bone. VII. The fresh composite homograft-autograft of cancellous bone; an analysis of factors leading to osteogenesis in marrow transplants and in marrow-containing bone grafts. J.Bone Joint Surg.Br. 46:110-140

Burwell RG (1966) Studies in the transplantation of bone. 8. Treated composite homograft-autografts of cancellous bone: an analysis of inductive mechanisms in bone transplantation. J.Bone Joint Surg.Br. 48:532-566

Cahill KS, Chi JH, Day A, Claus EB (2009) Prevalence, complications, and hospital charges associated with use of bone-morphogenetic proteins in spinal fusion procedures. JAMA 302:58-66

Canalis E (2009) Growth factor control of bone mass. J.Cell Biochem. 108:769-777 Cancedda R, Giannoni P, Mastrogiacomo M (2007) A tissue engineering approach to bone repair in large animal models and in clinical practice. Biomaterials 28:4240-4250 Carano RA, Filvaroff EH (2003) Angiogenesis and bone repair. Drug Discov.Today 8:980-989

Caplan AI (2009) Why are MSCs therapeutic? New data: new insight. J Pathol. 217:318-324

Cenni E, Avnet S, Fotia C, Salerno M, Baldini N (2010) Platelet-rich plasma impairs osteoclast generation from human precursors of peripheral blood. J.Orthop.Res. Chang NS, Simone AF, Schultheis LW (2005) From the FDA: what's in a label? A guide for the anesthesia practitioner. Anesthesiology 103:179-185

Chapman MW, Bucholz R, Cornell C (1997) Treatment of acute fractures with a collagen-calcium phosphate graft material. A randomized clinical trial. J.Bone Joint Surg.Am. 79:495-502

Charbord P, Livne E, Gross G, Haupl T, Neves NM, Marie P, Bianco P, Jorgensen C (2011) Human bone marrow mesenchymal stem cells: a systematic reappraisal via the genostem experience. Stem Cell Rev. 7:32-42

Chen GQ, Wu Q (2005) The application of polyhydroxyalkanoates as tissue engineering materials. Biomaterials 26:6565-6578

Chen J, Xu J, Wang A, Zheng M (2009) Scaffolds for tendon and ligament repair: review of the efficacy of commercial products. Expert.Rev.Med.Devices 6:61-73

Chen JH, Liu C, You L, Simmons CA (2010) Boning up on Wolff's Law: mechanical regulation of the cells that make and maintain bone. J.Biomech. 43:108-118

Cheung KM, Kaluarachi K, Andrew G, Lu W, Chan D, Cheah KS (2003) An externally fixed femoral fracture model for mice. J Orthop.Res. 21:685-690

Chiroff RT, White EW, Weber KN, Roy DM (1975) Tissue ingrowth of Replamineform implants. J.Biomed.Mater.Res. 9:29-45

Chu CR, Szczodry M, Bruno S (2010) Animal models for cartilage regeneration and repair. Tissue Eng Part B Rev. 16:105-115

Cieslak P, Hedberg K, Thomas A, Kohn M, Chai F, Nainan O, Williams I, Bell B, Tugwell B, Patel P (2003) Hepatitis C virus transmission from an antibody-negative organ and tissue donor - United States, 2000-2002. MMWR Morb.Mortal.Wkly.Rep. 52:273-4, 276

Clarke B (2008) Normal bone anatomy and physiology. Clin.J.Am.Soc.Nephrol. 3 Suppl 3:S131-S139

Codivilla A (2008) The classic: On the means of lengthening, in the lower limbs, the muscles and tissues which are shortened through deformity. 1905. Clin.Orthop.Relat Res. 466:2903-2909

Coe JD (2004) Instrumented transforaminal lumbar interbody fusion with bioabsorbable polymer implants and iliac crest autograft. Neurosurg. Focus. 16:E11

Connolly J, Guse R, Lippiello L, Dehne R (1989) Development of an osteogenic bonemarrow preparation. J Bone Joint Surg.Am. 71:684-691

Connolly JF, Guse R, Tiedeman J, Dehne R (1991) Autologous marrow injection as a substitute for operative grafting of tibial nonunions. Clin.Orthop.Relat Res.259-270

Coons DA, Alan BF (2006) Tendon graft substitutes-rotator cuff patches. Sports Med.Arthrosc. 14:185-190

Coraca DC, Duek EA, Padovani CA, Camilli JA (2008) Osteointegration of poly(L: -lactic acid)PLLA and poly(L: -lactic acid)PLLA/poly(ethylene oxide)PEO implants in rat tibiae. J.Mater.Sci.Mater.Med. 19:2699-2704

Costain DJ, Crawford RW (2009) Fresh-frozen vs. irradiated allograft bone in orthopaedic reconstructive surgery. Injury 40:1260-1264

Cowin SC (1989) Bone mechanics. CRC Press, Abingdon, UK.

Cox G, Giannoudis PV, Boxall S, Buckley C, Jones E, McGonagle D (2012) Extarction of high numbers of mesenchymal stem cells (MSCS) from intra-medullary cavities of long-bones with characterisation of in vivo phenotypes. J. Bone Joint Surg.Br. 94-B:35

Cox G, McGonagle D, Boxall SA, Buckley CT, Jones E, Giannoudis PV (2011) The use of the reamer-irrigator-aspirator to harvest mesenchymal stem cells. J.Bone Joint Surg.Br. 93:517-524

Cuomo AV, Virk M, Petrigliano F, Morgan EF, Lieberman JR (2009) Mesenchymal stem cell concentration and bone repair: potential pitfalls from bench to bedside. J Bone Joint Surg.Am. 91:1073-1083

Cuthbert R, Boxall SA, Tan HB, Giannoudis PV, McGonagle D, Jones E (2012) Single-platform quality control assay to quantify multipotential stromal cells in bone marrow aspirates prior to bulk manufacture or direct therapeutic use. Cytotherapy. 14:431-440

D'Ippolito G, Schiller PC, Ricordi C, Roos BA, Howard GA (1999) Age-related osteogenic potential of mesenchymal stromal stem cells from human vertebral bone marrow. J Bone Miner.Res. 14:1115-1122

Dahabreh Z, Dimitriou R, Giannoudis PV (2007) Health economics: a cost analysis of treatment of persistent fracture non-unions using bone morphogenetic protein-7. Injury 38:371-377

Dalby MJ, Gadegaard N, Tare R, Andar A, Riehle MO, Herzyk P, Wilkinson CDW, Oreffo ROC (2007) The control of human mesenchymal cell differentiation using nanoscale symmetry and disorder. Nat Mater 6:997-1003

Dawson JI, Kanczler JM, Yang XB, Attard GS, Oreffo RO (2011) Clay gels for the delivery of regenerative microenvironments. Adv.Mater. 23:3304-3308

Deckers MM, van Bezooijen RL, van der Horst G, Hoogendam J, van Der BC, Papapoulos SE, Lowik CW (2002) Bone morphogenetic proteins stimulate angiogenesis through osteoblast-derived vascular endothelial growth factor A. Endocrinology 143:1545-1553

DeCoster TA, Gehlert RJ, Mikola EA, Pirela-Cruz MA (2004) Management of posttraumatic segmental bone defects. J Am.Acad.Orthop.Surg. 12:28-38

Deglurkar M, Davy DT, Stewart M, Goldberg VM, Welter JF (2007) Evaluation of machining methods for trabecular metal implants in a rabbit intramedullary osseointegration model. J.Biomed.Mater.Res.B Appl.Biomater. 80:528-540

Del Fattore A., Capannolo M, Rucci N (2010) Bone and bone marrow: the same organ. Arch.Biochem.Biophys. 503:28-34

Delloye C, Cornu O, Druez V, Barbier O (2007) Bone allografts: What they can offer and what they cannot. J.Bone Joint Surg.Br. 89:574-579

den Boer FC, Patka P, Bakker FC, Wippermann BW, van LA, Vink GQ, Boshuizen K, Haarman HJ (1999) New segmental long bone defect model in sheep: quantitative analysis of healing with dual energy x-ray absorptiometry. J Orthop.Res. 17:654-660

den Boer FC, Wippermann BW, Blokhuis TJ, Patka P, Bakker FC, Haarman HJ (2003) Healing of segmental bone defects with granular porous hydroxyapatite augmented with recombinant human osteogenic protein-1 or autologous bone marrow. J Orthop.Res. 21:521-528

Deng M, Kumbar SG, Nair LS, Weikel AL, Allcock HR, Laurencin CT (2011) Biomimetic Structures: Biological Implications of Dipeptide-Substituted Polyphosphazene-Polyester Blend Nanofiber Matrices for Load-Bearing Bone Regeneration. Adv.Funct.Mater. 21:2641-2651

Derwin KA, Baker AR, Spragg RK, Leigh DR, Iannotti JP (2006) Commercial extracellular matrix scaffolds for rotator cuff tendon repair. Biomechanical, biochemical, and cellular properties. J.Bone Joint Surg.Am. 88:2665-2672

Devescovi V, Leonardi E, Ciapetti G, Cenni E (2008) Growth factors in bone repair. Chir Organi Mov 92:161-168

Di Bella C., Dozza B, Frisoni T, Cevolani L, Donati D (2010) Injection of demineralized bone matrix with bone marrow concentrate improves healing in unicameral bone cyst. Clin.Orthop.Relat Res. 468:3047-3055

Di Martino A., Sittinger M, Risbud MV (2005) Chitosan: a versatile biopolymer for orthopaedic tissue-engineering. Biomaterials 26:5983-5990

Dinopoulos HT, Giannoudis PV (2006) Safety and efficacy of use of demineralised bone matrix in orthopaedic and trauma surgery. Expert.Opin.Drug Saf 5:847-866

Docquier PL, Delloye C (2005) Treatment of aneurysmal bone cysts by introduction of demineralized bone and autogenous bone marrow. J.Bone Joint Surg.Am. 87:2253-2258

Drewa TA, Wolski Z, Galazka P, Wlodarczyk Z, Wozniak A (2005) Kidney preserving solutions containing lidocaine may increase urological complication rate after renal transplantation: an in vitro study. Transplant.Proc. 37:2107-2110

Drury JL, Mooney DJ (2003) Hydrogels for tissue engineering: scaffold design variables and applications. Biomaterials 24:4337-4351

Duan X, Al-Qwbani M, Zeng Y, Zhang W, Xiang Z (2012) Intramedullary nailing for tibial shaft fractures in adults. Cochrane.Database.Syst.Rev. 1:CD008241

Ekdahl M, Wang JH, Ronga M, Fu FH (2008) Graft healing in anterior cruciate ligament reconstruction. Knee Surg.Sports Traumatol.Arthrosc. 16:935-947

Eldridge JD, Smith EJ, Hubble MJ, Whitehouse SL, Learmonth ID (1997) Massive early subsidence following femoral impaction grafting. J.Arthroplasty 12:535-540

Elisseeff J, Puleo C, Yang F, Sharma B (2005) Advances in skeletal tissue engineering with hydrogels. Orthod.Craniofac.Res. 8:150-161

Emms NW, Buckley SC, Stockley I, Hamer AJ, Kerry RM (2009) Mid- to long-term results of irradiated allograft in acetabular reconstruction: a follow-up report. J.Bone Joint Surg.Br. 91:1419-1423

Epari DR, Lienau J, Schell H, Witt F, Duda GN (2008) Pressure, oxygen tension and temperature in the periosteal callus during bone healing--an in vivo study in sheep. Bone 43:734-739

Epari DR, Schell H, Bail HJ, Duda GN (2006) Instability prolongs the chondral phase during bone healing in sheep. Bone 38:864-870

Eward WC, Kontogeorgakos V, Levin LS, Brigman BE (2010) Free vascularized fibular graft reconstruction of large skeletal defects after tumor resection. Clin.Orthop.Relat Res. 468:590-598

Fennema EM, Renard AJ, Leusink A, van Blitterswijk CA, de BJ (2009) The effect of bone marrow aspiration strategy on the yield and quality of human mesenchymal stem cells. Acta Orthop. 80:618-621

Field JR, McGee M, Wildenauer C, Kurmis A, Margerrison E (2009) The utilization of a synthetic bone void filler (JAX) in the repair of a femoral segmental defect. Vet.Comp Orthop.Traumatol. 22:87-95

Findlay DM, Welldon K, Atkins GJ, Howie DW, Zannettino AC, Bobyn D (2004) The proliferation and phenotypic expression of human osteoblasts on tantalum metal. Biomaterials 25:2215-2227

Flecher X, Paprosky W, Grillo JC, Aubaniac JM, Argenson JN (2010) Do tantalum components provide adequate primary fixation in all acetabular revisions? Orthop.Traumatol.Surg.Res. 96:235-241

Flecher X, Sporer S, Paprosky W (2008) Management of severe bone loss in acetabular revision using a trabecular metal shell. J.Arthroplasty 23:949-955

Fleming JE, Jr., Cornell CN, Muschler GF (2000) Bone cells and matrices in orthopedic tissue engineering. Orthop.Clin.North Am. 31:357-374

Fortier LA, Potter HG, Rickey EJ, Schnabel LV, Foo LF, Chong LR, Stokol T, Cheetham J, Nixon AJ (2010) Concentrated bone marrow aspirate improves full-thickness cartilage repair compared with microfracture in the equine model. J.Bone Joint Surg.Am. 92:1927-1937

Freed LE, Marquis JC, Nohria A, Emmanual J, Mikos AG, Langer R (1993) Neocartilage formation in vitro and in vivo using cells cultured on synthetic biodegradable polymers. J.Biomed.Mater.Res. 27:11-23

Friedenstein AJ (1976) Precursor cells of mechanocytes. Int.Rev.Cytol. 47:327-359

Friedenstein AY (1968) Induction of bone tissue by transitional epithelium. Clin.Orthop.Relat Res. 59:21-37

Fujibayashi S, Neo M, Kim HM, Kokubo T, Nakamura T (2004) Osteoinduction of porous bioactive titanium metal. Biomaterials 25:443-450

Fyhrie DP, Kimura JH (1999) NACOB presentation Keynote lecture. Cancellous bone biomechanics. North American Congress on Biomechanics. J.Biomech. 32:1139-1148

Gao TJ, Tuominen TK, Lindholm TS, Kommonen B, Lindholm TC (1997) Morphological and biomechanical difference in healing in segmental tibial defects implanted with Biocoral or tricalcium phosphate cylinders. Biomaterials 18:219-223

Garbuz DS, Masri BA, Czitrom AA (1998) Biology of allografting. Orthop.Clin.North Am. 29:199-204

Garcia P, Herwerth S, Matthys R, Holstein JH, Histing T, Menger MD, Pohlemann T (2011) The LockingMouseNail--a new implant for standardized stable osteosynthesis in mice. J Surg.Res. 169:220-226

Gastaldi G, Asti A, Scaffino MF, Visai L, Saino E, Cometa AM, Benazzo F (2010) Human adipose-derived stem cells (hASCs) proliferate and differentiate in osteoblast-like cells on trabecular titanium scaffolds. J.Biomed.Mater.Res.A 94:790-799

Geiger F, Bertram H, Berger I, Lorenz H, Wall O, Eckhardt C, Simank HG, Richter W (2005) Vascular endothelial growth factor gene-activated matrix (VEGF165-GAM) enhances osteogenesis and angiogenesis in large segmental bone defects. J.Bone Miner.Res. 20:2028-2035

Gerber HP, Vu TH, Ryan AM, Kowalski J, Werb Z, Ferrara N (1999) VEGF couples hypertrophic cartilage remodeling, ossification and angiogenesis during endochondral bone formation. Nat.Med. 5:623-628

Gerstenfeld LC, Cullinane DM, Barnes GL, Graves DT, Einhorn TA (2003) Fracture healing as a post-natal developmental process: molecular, spatial, and temporal aspects of its regulation. J.Cell Biochem. 88:873-884

Getgood A, Bollen S (2010) What tissue bankers should know about the use of allograft tendons and cartilage in orthopaedics. Cell Tissue Bank. 11:87-97

Getgood A, Brooks R, Fortier L, Rushton N (2009) Articular cartilage tissue engineering: today's research, tomorrow's practice? J.Bone Joint Surg.Br. 91:565-576

Ghoneem HF, Wright JG, Cole WG, Rang M (1996) The Ilizarov method for correction of complex deformities. Psychological and functional outcomes. J.Bone Joint Surg.Am. 78:1480-1485

Giannoudis PV, Dinopoulos H, Tsiridis E (2005) Bone substitutes: an update. Injury 36 Suppl 3:S20-S27

Giannoudis PV, Einhorn TA, Marsh D (2007) Fracture healing: the diamond concept. Injury 38 Suppl 4:S3-S6

Giannoudis PV, Papakostidis C, Roberts C (2006) A review of the management of open fractures of the tibia and femur. J Bone Joint Surg.Br. 88:281-289

Gloria A, De Santis R, Ambrosio L (2010) Polymer-based composite scaffolds for tissue engineering. J.Appl.Biomater.Biomech. 8:57-67

Goldstein AS, Zhu G, Morris GE, Meszlenyi RK, Mikos AG (1999) Effect of osteoblastic culture conditions on the structure of poly(DL-lactic-co-glycolic acid) foam scaffolds. Tissue Eng 5:421-434

Gomoll AH, Yanke AB, Kang RW, Chubinskaya S, Williams JM, Bach BR, Cole BJ (2009) Long-term effects of bupivacaine on cartilage in a rabbit shoulder model. Am.J.Sports Med. 37:72-77

Goodship AE, Watkins PE, Rigby HS, Kenwright J (1993) The role of fixator frame stiffness in the control of fracture healing. An experimental study. J Biomech. 26:1027-1035

Gortz S, Bugbee WD (2006) Allografts in articular cartilage repair. J.Bone Joint Surg.Am. 88:1374-1384

Goshima J, Goldberg VM, Caplan AI (1991) The osteogenic potential of culture-expanded rat marrow mesenchymal cells assayed in vivo in calcium phosphate ceramic blocks. Clin.Orthop.Relat Res.298-311

Grande R, Carvalho AJ (2011) Compatible ternary blends of chitosan/poly(vinyl alcohol)/poly(lactic acid) produced by oil-in-water emulsion processing. Biomacromolecules. 12:907-914

Green WT, Banks HH (1953) Osteochondritis dissecans in children. J.Bone Joint Surg.Am. 35-A:26-47

Griffith LG, Naughton G (2002) Tissue engineering--current challenges and expanding opportunities. Science 295:1009-1014

Grishko V, Xu M, Wilson G, Pearsall AW (2010) Apoptosis and mitochondrial dysfunction in human chondrocytes following exposure to lidocaine, bupivacaine, and ropivacaine. J.Bone Joint Surg.Am. 92:609-618

Gronthos S (2004) Reconstruction of human mandible by tissue engineering. Lancet 364:735-736

Gronthos S, Graves SE, Ohta S, Simmons PJ (1994) The STRO-1+ fraction of adult human bone marrow contains the osteogenic precursors. Blood 84:4164-4173

Gross AE, Goodman SB (2005) Rebuilding the skeleton: the intraoperative use of trabecular metal in revision total hip arthroplasty. J.Arthroplasty 20:91-93

Grosskreutz CL, Katowitz WR, Freeman EE, Dreyer EB (1999) Lidocaine toxicity to rat retinal ganglion cells. Curr.Eye Res. 18:363-367

Gudas R, Stankevicius E, Monastyreckiene E, Pranys D, Kalesinskas RJ (2006) Osteochondral autologous transplantation versus microfracture for the treatment of articular cartilage defects in the knee joint in athletes. Knee.Surg.Sports Traumatol.Arthrosc. 14:834-842

Gugala Z, Gogolewski S (1999) Regeneration of segmental diaphyseal defects in sheep tibiae using resorbable polymeric membranes: a preliminary study. J Orthop.Trauma 13:187-195

Gugala Z, Gogolewski S (2002) Healing of critical-size segmental bone defects in the sheep tibiae using bioresorbable polylactide membranes. Injury 33 Suppl 2:B71-B76

Gugala Z, Lindsey RW, Gogolewski S (2007) New Approaches in the Treatment of Critical-Size Segmental Defects in Long Bones. Macromol.Symp. 253:147-161

Gunatillake PA, Adhikari R (2003) Biodegradable synthetic polymers for tissue engineering. Eur Cell Mater. 5:1-16

Hacking SA, Bobyn JD, Toh K, Tanzer M, Krygier JJ (2000) Fibrous tissue ingrowth and attachment to porous tantalum. J.Biomed.Mater.Res. 52:631-638

Haddad FS, Thakrar RR, Hart AJ, Skinner JA, Nargol AV, Nolan JF, Gill HS, Murray DW, Blom AW, Case CP (2011) Metal-on-metal bearings: the evidence so far. J.Bone Joint Surg.Br. 93:572-579

Haleem AM, El Singergy AA, Sabry D, Atta HM, Rashed LA, Chu CR, El Shewy LT, Azzam A, Abdel Aziz MT (2010) The clinical use of human culture-expanded autologous bone marrow mesenchymal stem cells transplanted on platelet-rich fibrin glue in the treatment of articular cartilage defects. A pilot study and preliminary results. Cartilage 1:253-261

Halliday BR, English HW, Timperley AJ, Gie GA, Ling RS (2003) Femoral impaction grafting with cement in revision total hip replacement. Evolution of the technique and results. J.Bone Joint Surg.Br. 85:809-817

Harris LD, Kim BS, Mooney DJ (1998) Open pore biodegradable matrices formed with gas foaming. J.Biomed.Mater.Res. 42:396-402

Hartmann EK, Heintel T, Morrison RH, Weckbach A (2010) Influence of platelet-rich plasma on the anterior fusion in spinal injuries: a qualitative and quantitative analysis using computer tomography. Arch.Orthop.Trauma Surg. 130:909-914

Heckman JD, Sarasohn-Kahn J (1997) The economics of treating tibia fractures. The cost of delayed unions. Bull.Hosp.Jt.Dis. 56:63-72

Heliotis M, Lavery KM, Ripamonti U, Tsiridis E, di SL (2006) Transformation of a prefabricated hydroxyapatite/osteogenic protein-1 implant into a vascularised pedicled bone flap in the human chest. Int.J.Oral Maxillofac.Surg. 35:265-269

Hente R, Cordey J, Rahn BA, Maghsudi M, von GS, Perren SM (1999) Fracture healing of the sheep tibia treated using a unilateral external fixator. Comparison of static and dynamic fixation. Injury 30 Suppl 1:A44-A51

Hernigou P, Mathieu G, Poignard A, Manicom O, Beaujean F, Rouard H (2006) Percutaneous autologous bone-marrow grafting for nonunions. Surgical technique. J.Bone Joint Surg.Am. 88 Suppl 1 Pt 2:322-327

Hernigou P, Poignard A, Beaujean F, Rouard H (2005a) Percutaneous autologous bone-marrow grafting for nonunions. Influence of the number and concentration of progenitor cells. J.Bone Joint Surg.Am. 87:1430-1437

Hernigou P, Poignard A, Manicom O, Mathieu G, Rouard H (2005b) The use of percutaneous autologous bone marrow transplantation in nonunion and avascular necrosis of bone. J.Bone Joint Surg.Br. 87:896-902

Hernigou P, Poignard A, Zilber S, Rouard H (2009) Cell therapy of hip osteonecrosis with autologous bone marrow grafting. Indian J.Orthop. 43:40-45

Hibi H, Yamada Y, Ueda M, Endo Y (2006) Alveolar cleft osteoplasty using tissue-engineered osteogenic material. Int.J.Oral Maxillofac.Surg. 35:551-555

Hile DD, Kirker-Head C, Doherty SA, Kowaleski MP, McCool J, Wise DL, Trantolo DJ (2003) Mechanical evaluation of a porous bone graft substitute based on poly(propylene glycol-co-fumaric acid). J.Biomed.Mater.Res.B Appl.Biomater. 66:311-317

Histing T, Garcia P, Matthys R, Leidinger M, Holstein JH, Kristen A, Pohlemann T, Menger MD (2010) An internal locking plate to study intramembranous bone healing in a mouse femur fracture model. J Orthop.Res. 28:397-402

Hoffmann A, Pelled G, Turgeman G, Eberle P, Zilberman Y, Shinar H, Keinan-Adamsky K, Winkel A, Shahab S, Navon G, Gross G, Gazit D (2006) Neotendon formation induced by manipulation of the Smad8 signalling pathway in mesenchymal stem cells. J.Clin.Invest 116:940-952

Holinski S, Schmeck B, Claus B, Radtke H, Elgeti T, Holzhausen M, Konertz W (2011) Encouraging experience with intracardiac transplantation of unselected autologous bone marrow cells concomitant with coronary artery bypass surgery after myocardial infarction. Ann.Thorac.Cardiovasc.Surg. 17:383-389

Hollinger JO, Hart CE, Hirsch SN, Lynch S, Friedlaender GE (2008) Recombinant human platelet-derived growth factor: biology and clinical applications. J.Bone Joint Surg.Am. 90 Suppl 1:48-54

Hollister SJ (2009) Scaffold engineering: a bridge to where? Biofabrication. 1:012001 Holy CE, Shoichet MS, Davies JE (2000) Engineering three-dimensional bone tissue in vitro using biodegradable scaffolds: investigating initial cell-seeding density and culture period. J Biomed.Mater.Res. 51:376-382

Horan F, Marti RK, Sedel L, Dickson RA, Rushton N (1999) The Bone & Joint Decade - 2000 to 2010. J.Bone Joint Surg.Br. 81-B:377-379

Horas U, Pelinkovic D, Herr G, Aigner T, Schnettler R (2003) Autologous chondrocyte implantation and osteochondral cylinder transplantation in cartilage repair of the knee joint. A prospective, comparative trial. J.Bone Joint Surg.Am. 85-A:185-192

Horn P, Bork S, Diehlmann A, Walenda T, Eckstein V, Ho AD, Wagner W (2008) Isolation of human mesenchymal stromal cells is more efficient by red blood cell lysis. Cytotherapy. 10:676-685

Howard D, Partridge K, Yang X, Clarke NM, Okubo Y, Bessho K, Howdle SM, Shakesheff KM, Oreffo RO (2002) Immunoselection and adenoviral genetic modulation of human osteoprogenitors: in vivo bone formation on PLA scaffold. Biochem.Biophys.Res.Commun. 299:208-215

Hu Q, Li B, Wang M, Shen J (2004) Preparation and characterization of biodegradable chitosan/hydroxyapatite nanocomposite rods via in situ hybridization: a potential material as internal fixation of bone fracture. Biomaterials 25:779-785

Hunter RF, Broadway P, Sun SL, Niell HB, Mauer AM (1987) Detection of small cell lung cancer bone marrow involvement by discontinuous gradient sedimentation. Cancer Res. 47:2737-2740

Hutmacher DW (2000) Scaffolds in tissue engineering bone and cartilage. Biomaterials 21:2529-2543

Hutmacher DW (2001) Scaffold design and fabrication technologies for engineering tissues--state of the art and future perspectives. J.Biomater.Sci.Polym.Ed 12:107-124

Hutmacher DW, Schantz JT, Lam CX, Tan KC, Lim TC (2007) State of the art and future directions of scaffold-based bone engineering from a biomaterials perspective. J.Tissue Eng Regen.Med. 1:245-260

Innocenti M, Abed YY, Beltrami G, Delcroix L, Manfrini M, Capanna R (2009) Biological reconstruction after resection of bone tumors of the proximal tibia using allograft shell and intramedullary free vascularized fibular graft: long-term results. Microsurgery 29:361-372

Intini G (2009) The use of platelet-rich plasma in bone reconstruction therapy. Biomaterials 30:4956-4966

Jacobs TF, Vansintjan PS, Roels N, Herregods SS, Verbruggen G, Herregods LL, Almqvist KF (2011) The effect of Lidocaine on the viability of cultivated mature human cartilage cells: an in vitro study. Knee Surg.Sports Traumatol.Arthrosc. 19:1206-13

Jäger M, Herten M, Fochtmann U, Fischer J, Hernigou P, Zilkens C, Hendrich C, Krauspe R (2011) Bridging the gap: bone marrow aspiration concentrate reduces autologous bone grafting in osseous defects. J.Orthop.Res. 29:173-180

Jaiswal N, Haynesworth SE, Caplan AI, Bruder SP (1997) Osteogenic differentiation of purified, culture-expanded human mesenchymal stem cells in vitro. J Cell Biochem. 64:295-312

Jamsa T, Jalovaara P (1996) A cost-effective, accurate machine for testing the torsional strength of sheep long bones. Med.Eng Phys. 18:433-435

Jarit GJ, Bosco JA (2010) Meniscal repair and reconstruction. Bull.NYU.Hosp.Jt.Dis. 68:84-90

Jayakumar P, Di Silvio L (2010) Osteoblasts in bone tissue engineering. Proceedings of the Institution of Mechanical Engineers, Part H: Journal of Engineering in Medicine 224:1415-1440

Johnson EO, Troupis T, Soucacos PN (2011) Tissue-engineered vascularized bone grafts: basic science and clinical relevance to trauma and reconstructive microsurgery. Microsurgery 31:176-182

Johnson ME, Saenz JA, DaSilva AD, Uhl CB, Gores GJ (2002) Effect of local anesthetic on neuronal cytoplasmic calcium and plasma membrane lysis (necrosis) in a cell culture model. Anesthesiology 97:1466-1476

Johnson ME, Uhl CB, Spittler KH, Wang H, Gores GJ (2004) Mitochondrial injury and caspase activation by the local anesthetic lidocaine. Anesthesiology 101:1184-1194

Johnstone B, Hering TM, Caplan AI, Goldberg VM, Yoo JU (1998) In vitro chondrogenesis of bone marrow-derived mesenchymal progenitor cells. Exp.Cell Res. 238:265-272

Jones, A. M. H, Aarvold, A., New, A. M., Dunlop, D. G., and Oreffo, R. O. (2010) The treatment of avascular necrosis of the femoral head using impaction bone grafting and skeletal stem cells. J.Bone Joint Surg.Br. 94-B: 26-26

Jones, A. M. H, Foong, T. S., New, A. M., Bolland, B. J., Pound, J. C., Dunlop, D. G., and Oreffo, R. O. (2009) The effect of skeletal stem cells, hydroxyapatite coated stem cells and collagen coated allograft on the biomechanical properties of impacted bone graft. Eur Cell Mater. 18(Suppl. 2), 26

Kanakaris NK, Paliobeis C, Nlanidakis N, Giannoudis PV (2007) Biological enhancement of tibial diaphyseal aseptic non-unions: the efficacy of autologous bone grafting, BMPs and reaming by-products. Injury 38 Suppl 2:S65-S75

Kanczler J, Dawson JI, Aarvold A, Smith JO, Tare RS, Oreffo RO (2011) Bone Tissue Engineering. In: Cui Z, Brandon L (eds) Comprehensive Biotechnology. Elsevier, Oxford, UK

Kanczler JM, Ginty PJ, Barry JJ, Clarke NM, Howdle SM, Shakesheff KM, Oreffo RO (2008) The effect of mesenchymal populations and vascular endothelial growth factor delivered from biodegradable polymer scaffolds on bone formation. Biomaterials 29:1892-1900

Kanczler JM, Ginty PJ, White L, Clarke NM, Howdle SM, Shakesheff KM, Oreffo RO (2010) The effect of the delivery of vascular endothelial growth factor and bone morphogenic protein-2 to osteoprogenitor cell populations on bone formation. Biomaterials 31:1242-1250

Kappe T, Cakir B, Mattes T, Reichel H, Floren M (2010) Infections after bone allograft surgery: a prospective study by a hospital bone bank using frozen femoral heads from living donors. Cell Tissue Bank. 11:253-259

Karageorgiou V, Kaplan D (2005) Porosity of 3D biomaterial scaffolds and osteogenesis. Biomaterials 26:5474-5491

Karpie JC, Chu CR (2007) Lidocaine exhibits dose- and time-dependent cytotoxic effects on bovine articular chondrocytes in vitro. Am.J.Sports Med. 35:1621-1627

Karumanchi RS, Doddamane SN, Sampangi C, Todd PW (2002) Field-assisted extraction of cells, particles and macromolecules. Trends Biotechnol. 20:72-78

Kempen DH, Lu L, Heijink A, Hefferan TE, Creemers LB, Maran A, Yaszemski MJ, Dhert WJ (2009) Effect of local sequential VEGF and BMP-2 delivery on ectopic and orthotopic bone regeneration. Biomaterials 30:2816-2825

Kessler MW, Grande DA (2008) Tissue engineering and cartilage. Organogenesis. 4:28-32

Khan F, Smith JO, Kanczler JM, Tare RS, Oreffo ROC, Bradley M (2012) Discovery and Evaluation of a Functional Ternary Polymer Blend for Bone Repair - Translation from a Microarray to a Clinical Model. Advanced Functional Materials, 10.1002/adfm.201202710

Khan F, Tare RS, Kanczler JM, Oreffo RO, Bradley M (2010) Strategies for cell manipulation and skeletal tissue engineering using high-throughput polymer blend formulation and microarray techniques. Biomaterials 31:2216-2228

Khan WS, Johnson DS, Hardingham TE (2010) The potential of stem cells in the treatment of knee cartilage defects. Knee 17:369-374

Kilgore ML, Morrisey MA, Becker DJ, Gary LC, Curtis JR, Saag KG, Yun H, Matthews R, Smith W, Taylor A, Arora T, Delzell E (2009) Health care expenditures associated with skeletal fractures among Medicare beneficiaries, 1999-2005. J.Bone Miner.Res. 24:2050-2055

Kim DK, Jankowski RJ, Pruchnic R, de MF, Yoshimura N, Honda M, Furuta A, Chancellor MB (2009) In vitro and in vivo effect of lidocaine on rat muscle-derived cells for treatment of stress urinary incontinence. Urology 73:437-441

Kim TK, Sharma B, Williams CG, Ruffner MA, Malik A, McFarland EG, Elisseeff JH (2003) Experimental model for cartilage tissue engineering to regenerate the zonal organization of articular cartilage. Osteoarthritis.Cartilage. 11:653-664

King TW, Patrick CW, Jr. (2000) Development and in vitro characterization of vascular endothelial growth factor (VEGF)-loaded poly(DL-lactic-co-glycolic acid)/poly(ethylene glycol) microspheres using a solid encapsulation/single emulsion/solvent extraction technique. J.Biomed.Mater.Res. 51:383-390

Kitchel SH, Wang MY, Lauryssen CL (2005) Techniques for aspirating bone marrow for use in spinal surgery. Neurosurgery 57:286-289

Kitoh H, Kitakoji T, Tsuchiya H, Katoh M, Ishiguro N (2007a) Distraction osteogenesis of the lower extremity in patients with achondroplasia/hypochondroplasia treated with transplantation of culture-expanded bone marrow cells and platelet-rich plasma. J.Pediatr.Orthop. 27:629-634

Kitoh H, Kitakoji T, Tsuchiya H, Katoh M, Ishiguro N (2007b) Transplantation of culture expanded bone marrow cells and platelet rich plasma in distraction osteogenesis of the long bones. Bone 40:522-528

Klemm WR (1985) Comparison of known sodium-channel blockers in DFP toxicity. Toxicol.Lett. 25:307-312

Kolar R (2006) Animal experimentation. Sci. Eng Ethics 12:111-122

Koller MR, Emerson SG, Palsson BO (1993) Large-scale expansion of human stem and progenitor cells from bone marrow mononuclear cells in continuous perfusion cultures. Blood 82:378-384

Kon E, Muraglia A, Corsi A, Bianco P, Marcacci M, Martin I, Boyde A, Ruspantini I, Chistolini P, Rocca M, Giardino R, Cancedda R, Quarto R (2000) Autologous bone marrow stromal cells loaded onto porous hydroxyapatite ceramic accelerate bone repair in critical-size defects of sheep long bones. J.Biomed.Mater.Res. 49:328-337

Krych AJ, Jackson JD, Hoskin TL, Dahm DL (2008) A meta-analysis of patellar tendon autograft versus patellar tendon allograft in anterior cruciate ligament reconstruction. Arthroscopy 24:292-298

Kuttenberger JJ, Waibel A, Stubinger S, Werner M, Klasing M, Ivanenko M, Hering P, von RB, Sader R, Zeilhofer HF (2010) Bone healing of the sheep tibia shaft after carbon dioxide laser osteotomy: histological results. Lasers Med.Sci. 25:239-249

Lachiewicz PF, Soileau ES (2010) Tantalum components in difficult acetabular revisions. Clin.Orthop.Relat Res. 468:454-458

Langer R, Vacanti JP (1993) Tissue engineering. Science 260:920-926

Laurencin CT, Ambrosio AM, Borden MD, Cooper JA, Jr. (1999) Tissue engineering: orthopedic applications. Annu.Rev.Biomed.Eng 1:19-46

Lee BK, Choi SJ, Mack D, Oh SH (2011) Isolation of mesenchymal stem cells from the mandibular marrow aspirates. Oral Surg.Oral Med.Oral Pathol.Oral Radiol.Endod. 112:e86-e93

Lee CH, Cook JL, Mendelson A, Moioli EK, Yao H, Mao JJ (2010) Regeneration of the articular surface of the rabbit synovial joint by cell homing: a proof of concept study. Lancet 376:440-448

Lee MS (2004) GraftJacket augmentation of chronic Achilles tendon ruptures. Orthopedics 27:s151-s153

Leone S, Di CS, Casati A, Fanelli G (2008) Pharmacology, toxicology, and clinical use of new long acting local anesthetics, ropivacaine and levobupivacaine. Acta Biomed. 79:92-105

Leong KF, Cheah CM, Chua CK (2003) Solid freeform fabrication of three-dimensional scaffolds for engineering replacement tissues and organs. Biomaterials 24:2363-2378

Levine BR, Sporer S, Poggie RA, Della Valle CJ, Jacobs JJ (2006) Experimental and clinical performance of porous tantalum in orthopedic surgery. Biomaterials 27:4671-4681

Lin H (1998) The self-renewing mechanism of stem cells in the germline. Curr.Opin.Cell Biol. 10:687-693

Lindsey RW, Gugala Z, Milne E, Sun M, Gannon FH, Latta LL (2006) The efficacy of cylindrical titanium mesh cage for the reconstruction of a critical-size canine segmental femoral diaphyseal defect. J Orthop.Res. 24:1438-1453

Ling RS, Timperley AJ, Linder L (1993) Histology of cancellous impaction grafting in the femur. A case report. J.Bone Joint Surg.Br. 75:693-696

Lode A, Bernhardt A, Gelinsky M (2008) Cultivation of human bone marrow stromal cells on three-dimensional scaffolds of mineralized collagen: influence of seeding density on colonization, proliferation and osteogenic differentiation. J Tissue Eng Regen.Med. 2:400-407

Longo UG, Lamberti A, Maffulli N, Denaro V (2010) Tendon augmentation grafts: a systematic review. Br.Med.Bull. 94:165-188

Lord CF, Gebhardt MC, Tomford WW, Mankin HJ (1988) Infection in bone allografts. Incidence, nature, and treatment. J.Bone Joint Surg.Am. 70:369-376

Lovell-Badge R (2001) The future for stem cell research. Nature 414:88-91

Lu H, Guo L, Wozniak MJ, Kawazoe N, Tateishi T, Zhang X, Chen G (2009) Effect of cell density on adipogenic differentiation of mesenchymal stem cells. Biochem.Biophys.Res.Commun. 381:322-327

Ma H, Hu J, Ma PX (2010) Polymer Scaffolds for Small-Diameter Vascular Tissue Engineering. Adv. Funct. Mater. 20:2833-2841

Maccauro G, Iommetti PR, Muratori F, Raffaelli L, Manicone PF, Fabbriciani C (2009) An overview about biomedical applications of micron and nano size tantalum. Recent Pat Biotechnol. 3:157-165

Maissen O, Eckhardt C, Gogolewski S, Glatt M, Arvinte T, Steiner A, Rahn B, Schlegel U (2006) Mechanical and radiological assessment of the influence of rhTGFbeta-3 on bone regeneration in a segmental defect in the ovine tibia: pilot study. J Orthop.Res. 24:1670-1678

Mallick T, Mosquera A, Zinderman C, Martin L, Wise R (2011) Reported infections after human tissue transplantation before and after new food and drug administration (FDA) regulations, United States, 2001 through June, 2010. Cell and Tissue Banking DOI 10.1007/s10561-011-9253-5:1-9

Manferdini C, Guarino V, Zini N, Raucci MG, Ferrari A, Grassi F, Gabusi E, Squarzoni S, Facchini A, Ambrosio L, Lisignoli G (2010) Mineralization behavior with mesenchymal stromal cells in a biomimetic hyaluronic acid-based scaffold. Biomaterials 31:3986-3996

Mankin HJ, Gebhardt MC, Tomford WW (1987) The use of frozen cadaveric allografts in the management of patients with bone tumors of the extremities. Orthop.Clin.North Am. 18:275-289

Marcacci M, Kon E, Moukhachev V, Lavroukov A, Kutepov S, Quarto R, Mastrogiacomo M, Cancedda R (2007) Stem cells associated with macroporous bioceramics for long bone repair: 6- to 7-year outcome of a pilot clinical study. Tissue Eng 13:947-955

Marcacci M, Kon E, Zaffagnini S, Giardino R, Rocca M, Corsi A, Benvenuti A, Bianco P, Quarto R, Martin I, Muraglia A, Cancedda R (1999) Reconstruction of extensive long-bone defects in sheep using porous hydroxyapatite sponges. Calcif.Tissue Int. 64:83-90

Marder RA, Hopkins G, Jr., Timmerman LA (2005) Arthroscopic microfracture of chondral defects of the knee: a comparison of two postoperative treatments. Arthroscopy 21:152-158

Marin E, Fusi S, Pressacco M, Paussa L, Fedrizzi L (2010) Characterization of cellular solids in Ti6Al4V for orthopaedic implant applications: Trabecular titanium. J.Mech.Behav.Biomed.Mater. 3:373-381

Marino JT, Ziran BH (2010) Use of solid and cancellous autologous bone graft for fractures and nonunions. Orthop.Clin.North Am. 41:15-26

Marotti G (1993) A new theory of bone lamellation. Calcif.Tissue Int. 53 Suppl 1:S47-S55

Martin TJ, Sims NA (2005) Osteoclast-derived activity in the coupling of bone formation to resorption. Trends Mol.Med. 11:76-81

Martini L, Fini M, Giavaresi G, Giardino R (2001) Sheep model in orthopedic research: a literature review. Comp Med. 51:292-299

Mason C, Manzotti E (2010) Regenerative medicine cell therapies: numbers of units manufactured and patients treated between 1988 and 2010. Regen.Med. 5:307-313

Mastrogiacomo M, Papadimitropoulos A, Cedola A, Peyrin F, Giannoni P, Pearce SG, Alini M, Giannini C, Guagliardi A, Cancedda R (2007) Engineering of bone using bone marrow stromal cells and a silicon-stabilized tricalcium phosphate bioceramic: evidence for a coupling between bone formation and scaffold resorption. Biomaterials 28:1376-1384

Mastrogiacomo M, Scaglione S, Martinetti R, Dolcini L, Beltrame F, Cancedda R, Quarto R (2006) Role of scaffold internal structure on in vivo bone formation in macroporous calcium phosphate bioceramics. Biomaterials 27:3230-3237

Mathieu LM, Mueller TL, Bourban PE, Pioletti DP, Muller R, Manson JA (2006) Architecture and properties of anisotropic polymer composite scaffolds for bone tissue engineering. Biomaterials 27:905-916

Matsuno H, Yokoyama A, Watari F, Uo M, Kawasaki T (2001) Biocompatibility and osteogenesis of refractory metal implants, titanium, hafnium, niobium, tantalum and rhenium. Biomaterials 22:1253-1262

Matsushima A, Kotobuki N, Tadokoro M, Kawate K, Yajima H, Takakura Y, Ohgushi H (2009) In vivo osteogenic capability of human mesenchymal cells cultured on hydroxyapatite and on beta-tricalcium phosphate. Artif.Organs 33:474-481

Mayr-Wohlfart U, Waltenberger J, Hausser H, Kessler S, Gunther KP, Dehio C, Puhl W, Brenner RE (2002) Vascular endothelial growth factor stimulates chemotactic migration of primary human osteoblasts. Bone 30:472-477

Mazzocca AD, McCarthy MB, Chowaniec DM, Cote MP, Arciero RA, Drissi H (2010) Rapid isolation of human stem cells (connective tissue progenitor cells) from the proximal humerus during arthroscopic rotator cuff surgery. Am.J Sports Med. 38:1438-1447

McAllister BS, Haghighat K, Gonshor A (2009) Histologic evaluation of a stem cell-based sinus-augmentation procedure. J.Periodontol. 80:679-686

McBeath R, Pirone DM, Nelson CM, Bhadriraju K, Chen CS (2004) Cell shape, cytoskeletal tension, and RhoA regulate stem cell lineage commitment. Dev.Cell 6:483-495

McCarty RC, Gronthos S, Zannettino AC, Foster BK, Xian CJ (2009) Characterisation and developmental potential of ovine bone marrow derived mesenchymal stem cells. J.Cell Physiol 219:324-333

McDermott ID, Thomas NP, Poniatowski S, Warwick RM (2006) Soft tissue allografts in the knee: a survey of UK usage and a report of a combined user/provider collaborative group. Knee 13:72-75

McLain RF, Fleming JE, Boehm CA, Muschler GF (2005) Aspiration of osteoprogenitor cells for augmenting spinal fusion: comparison of progenitor cell concentrations from the vertebral body and iliac crest. J Bone Joint Surg.Am. 87:2655-2661

McMurray RJ, Gadegaard N, Tsimbouri PM, Burgess KV, McNamara LE, Tare R, Murawski K, Kingham E, Oreffo RO, Dalby MJ (2011) Nanoscale surfaces for the long-term maintenance of mesenchymal stem cell phenotype and multipotency. Nat Mater 10:637-644

McNamara IR (2010) Impaction bone grafting in revision hip surgery: past, present and future. Cell Tissue Bank. 11:57-73

McNamara LE, McMurray RJ, Biggs MJ, Kantawong F, Oreffo RO, Dalby MJ (2010) Nanotopographical control of stem cell differentiation. J.Tissue Eng 2010:120623

Mendias CL, Bakhurin KI, Faulkner JA (2008) Tendons of myostatin-deficient mice are small, brittle, and hypocellular. Proc.Natl.Acad.Sci.U.S.A 105:388-393

Menetrey J, Duthon VB, Laumonier T, Fritschy D (2008) "Biological failure" of the anterior cruciate ligament graft. Knee Surg.Sports Traumatol.Arthrosc. 16:224-231

Middleton JC, Tipton AJ (2000) Synthetic biodegradable polymers as orthopedic devices. Biomaterials 21:2335-2346

Mikos AG, Bao Y, Cima LG, Ingber DE, Vacanti JP, Langer R (1993a) Preparation of poly(glycolic acid) bonded fiber structures for cell attachment and transplantation. J.Biomed.Mater.Res. 27:183-189

Mikos AG, Sarakinos G, Leite SM, Vacant JP, Langer R (1993b) Laminated threedimensional biodegradable foams for use in tissue engineering. Biomaterials 14:323-330

Mitalipov S, Wolf D (2009) Totipotency, pluripotency and nuclear reprogramming. Adv.Biochem.Eng Biotechnol. 114:185-199

Mizuno M, Kuboki Y (2001) Osteoblast-related gene expression of bone marrow cells during the osteoblastic differentiation induced by type I collagen. J.Biochem. 129:133-138

Moiniche S, Mikkelsen S, Wetterslev J, Dahl JB (1999) A systematic review of intraarticular local anesthesia for postoperative pain relief after arthroscopic knee surgery. Reg Anesth.Pain Med. 24:430-437

Mooney DJ, Baldwin DF, Suh NP, Vacanti JP, Langer R (1996) Novel approach to fabricate porous sponges of poly(D,L-lactic-co-glycolic acid) without the use of organic solvents. Biomaterials 17:1417-1422

Morishita T, Honoki K, Ohgushi H, Kotobuki N, Matsushima A, Takakura Y (2006) Tissue engineering approach to the treatment of bone tumors: three cases of cultured bone grafts derived from patients' mesenchymal stem cells. Artif.Organs 30:115-118

Moroni L, Schotel R, Hamann D, de Wijn J, van Blitterswijk C (2008) 3D Fiber-Deposited Electrospun Integrated Scaffolds Enhance Cartilage Tissue Formation. Adv.Funct.Mater. 18:53-60

Mroz TE, Joyce MJ, Lieberman IH, Steinmetz MP, Benzel EC, Wang JC (2009) The use of allograft bone in spine surgery: is it safe? Spine J. 9:303-308

Muller U, Imwinkelried T, Horst M, Sievers M, Graf-Hausner U (2006) Do human osteoblasts grow into open-porous titanium? Eur.Cell Mater. 11:8-15

Muramatsu K, Ihara K, Shigetomi M, Kawai S (2004) Femoral reconstruction by single, folded or double free vascularised fibular grafts. Br.J.Plast.Surg. 57:550-555

Muschler GF, Matsukura Y, Nitto H, Boehm CA, Valdevit AD, Kambic HE, Davros WJ, Easley KA, Powell KA (2005) Selective retention of bone marrow-derived cells to enhance spinal fusion. Clin.Orthop.Relat Res.242-251

Muschler GF, Midura RJ (2002) Connective tissue progenitors: practical concepts for clinical applications. Clin.Orthop.Relat Res.66-80

Muschler GF, Nakamoto C, Griffith LG (2004) Engineering principles of clinical cell-based tissue engineering. J.Bone Joint Surg.Am. 86-A:1541-1558

Muschler GF, Nitto H, Boehm CA, Easley KA (2001) Age- and gender-related changes in the cellularity of human bone marrow and the prevalence of osteoblastic progenitors. J Orthop.Res. 19:117-125

Muschler GF, Raut VP, Patterson TE, Wenke JC, Hollinger JO (2010) The design and use of animal models for translational research in bone tissue engineering and regenerative medicine. Tissue Eng Part B Rev. 16:123-145

Nabavi A, Field JR (2009) The Utilization Of Trabecular Metal In Combination With Autograft Bone In Acetabular Reconstruction: A Preliminary Sheep Model. The Internet Journal of Orthopedic Surgery 13:1

Nade S, Burwell RG (1977) Decalcified bone as a substrate for osteogenesis. An appraisal of the interrelation of bone and marrow in combined grafts. J.Bone Joint Surg.Br. 59:189-196

Nair LS, Laurencin CT (2006) Polymers as biomaterials for tissue engineering and controlled drug delivery. Adv.Biochem.Eng Biotechnol. 102:47-90

Navarro M, Michiardi A, Castano O, Planell JA (2008) Biomaterials in orthopaedics. J.R.Soc.Interface 5:1137-1158

Nehme A, Lewallen DG, Hanssen AD (2004) Modular porous metal augments for treatment of severe acetabular bone loss during revision hip arthroplasty. Clin.Orthop.Relat Res.201-208

Newman E, Turner AS, Wark JD (1995) The potential of sheep for the study of osteopenia: current status and comparison with other animal models. Bone 16:277S-284S

Nguyen LH, Kudva AK, Saxena NS, Roy K (2011) Engineering articular cartilage with spatially-varying matrix composition and mechanical properties from a single stem cell population using a multi-layered hydrogel. Biomaterials 32:6946-6952

Nole R, Munson NM, Fulkerson JP (1985) Bupivacaine and saline effects on articular cartilage. Arthroscopy 1:123-127

Nouette-Gaulain K, Dadure C, Morau D, Pertuiset C, Galbes O, Hayot M, Mercier J, Sztark F, Rossignol R, Capdevila X (2009) Age-dependent bupivacaine-induced muscle toxicity during continuous peripheral nerve block in rats. Anesthesiology 111:1120-1127

O'Doherty DM, Butler SP, Goodship AE (1995) Stress protection due to external fixation, J Biomech, 28:575-586

O'Loughlin PF, Morr S, Bogunovic L, Kim AD, Park B, Lane JM (2008) Selection and development of preclinical models in fracture-healing research. J Bone Joint Surg.Am. 90 Suppl 1:79-84

Office for National Statistics (2010) 2008-based population projections. London, UK

Oh SH, Kang SG, Kim ES, Cho SH, Lee JH (2003) Fabrication and characterization of hydrophilic poly(lactic-co-glycolic acid)/poly(vinyl alcohol) blend cell scaffolds by melt-molding particulate-leaching method. Biomaterials 24:4011-4021

Ohgushi H, Kotobuki N, Funaoka H, Machida H, Hirose M, Tanaka Y, Takakura Y (2005) Tissue engineered ceramic artificial joint--ex vivo osteogenic differentiation of patient mesenchymal cells on total ankle joints for treatment of osteoarthritis. Biomaterials 26:4654-4661

Onizuka S, Yonaha T, Tsuneyoshi I (2011) Local anesthetics with high lipophilicity are toxic, while local anasthetics with low pka induce more apoptosis in human leukemia cells. Anesthesia and Clinical Research 2:1-6

Oreffo RO, Bennett A, Carr AJ, Triffitt JT (1998) Patients with primary osteoarthritis show no change with ageing in the number of osteogenic precursors. Scand.J Rheumatol. 27:415-424

Oreffo RO, Cooper C, Mason C, Clements M (2005) Mesenchymal stem cells: lineage, plasticity, and skeletal therapeutic potential. Stem Cell Rev. 1:169-178

Pape HC, Hildebrand F, Krettek C, Green J, Giannoudis PV (2006) Experimental background--review of animal studies. Injury 37 Suppl 4:S25-S38

Park SR, Oreffo RO, Triffitt JT (1999) Interconversion potential of cloned human marrow adipocytes in vitro. Bone 24:549-554

Patel ZS, Young S, Tabata Y, Jansen JA, Wong ME, Mikos AG (2008) Dual delivery of an angiogenic and an osteogenic growth factor for bone regeneration in a critical size defect model. Bone 43:931-940

Patil N, Lee K, Goodman SB (2009) Porous tantalum in hip and knee reconstructive surgery. J.Biomed.Mater.Res.B Appl.Biomater. 89:242-251

Pearce AI, Richards RG, Milz S, Schneider E, Pearce SG (2007) Animal models for implant biomaterial research in bone: a review. Eur Cell Mater. 13:1-10

Pederson L, Ruan M, Westendorf JJ, Khosla S, Oursler MJ (2008) Regulation of bone formation by osteoclasts involves Wnt/BMP signaling and the chemokine sphingosine-1-phosphate. Proc.Natl.Acad.Sci.U.S.A 105:20764-20769

Petite H, Viateau V, Bensaid W, Meunier A, de PC, Bourguignon M, Oudina K, Sedel L, Guillemin G (2000) Tissue-engineered bone regeneration. Nat.Biotechnol. 18:959-963 Phinney DG (2012) Functional heterogeneity of mesenchymal stem cells: implications for cell therapy. J Cell Biochem. 113:2806-2812

Piper SL, Kim HT (2008) Comparison of ropivacaine and bupivacaine toxicity in human articular chondrocytes. J.Bone Joint Surg.Am. 90:986-991

Pittenger MF, Mackay AM, Beck SC, Jaiswal RK, Douglas R, Mosca JD, Moorman MA, Simonetti DW, Craig S, Marshak DR (1999) Multilineage potential of adult human mesenchymal stem cells. Science 284:143-147

Playford MP, Bicknell D, Bodmer WF, Macaulay VM (2000) Insulin-like growth factor 1 regulates the location, stability, and transcriptional activity of beta-catenin. Proc.Natl.Acad.Sci.U.S.A 97:12103-12108

Porter RM, Liu F, Pilapil C, Betz OB, Vrahas MS, Harris MB, Evans CH (2009) Osteogenic potential of reamer irrigator aspirator (RIA) aspirate collected from patients undergoing hip arthroplasty. J Orthop.Res. 27:42-49

Quarto R, Mastrogiacomo M, Cancedda R, Kutepov SM, Mukhachev V, Lavroukov A, Kon E, Marcacci M (2001) Repair of large bone defects with the use of autologous bone marrow stromal cells. N.Engl.J.Med. 344:385-386

Quero L, Klawitter M, Nerlich AG, Leonardi M, Boos N, Wuertz K (2011) Bupivacaine-the deadly friend of intervertebral disc cells? Spine J. 11:46-53

Rabinovitch M, DeStefano MJ (1975) Use of the local anesthetic lidocaine for cell harvesting and subcultivation. In Vitro 11:379-381

Rahaman MN, Mao JJ (2005) Stem cell-based composite tissue constructs for regenerative medicine. Biotechnol.Bioeng. 91:261-284

Rath SN, Arkudas A, Lam CX, Olkowski R, Polykandroitis E, Chroscicka A, Beier JP, Horch RE, Hutmacher DW, Kneser U (2012) Development of a pre-vascularized 3D scaffold-hydrogel composite graft using an arterio-venous loop for tissue engineering applications. J.Biomater.Appl. 27:277-289

Ravaglioli A, Krajewski A, Celotti GC, Piancastelli A, Bacchini B, Montanari L, Zama G, Piombi L (1996) Mineral evolution of bone. Biomaterials 17:617-622

Regauer M, Jurgens I, Kotsianos D, Stutzle H, Mutschler W, Schieker M (2005) [Newbone formation by osteogenic protein-1 and autogenic bone marrow in a critical tibial defect model in sheep]. Zentralbl.Chir 130:338-345

Reichel H, Lebek S, Alter C, Hein W (1998) Biomechanical and densitometric bone properties after callus distraction in sheep. Clin.Orthop.Relat Res.237-246

Reichert JC, Epari DR, Wullschleger ME, Saifzadeh S, Steck R, Lienau J, Sommerville S, Dickinson IC, Schutz MA, Duda GN, Hutmacher DW (2010) Establishment of a preclinical ovine model for tibial segmental bone defect repair by applying bone tissue engineering strategies. Tissue Eng Part B Rev. 16:93-104

Reichert JC, Saifzadeh S, Wullschleger ME, Epari DR, Schutz MA, Duda GN, Schell H, van GM, Redl H, Hutmacher DW (2009) The challenge of establishing preclinical models for segmental bone defect research. Biomaterials 30:2149-2163

Reichl M, Quinton D (1987) Comparison of 1% lignocaine with 0.5% bupivacaine in digital ring blocks. J.Hand Surg.Br. 12:375-376

Richter W (2009) Mesenchymal stem cells and cartilage in situ regeneration. J.Intern.Med. 266:390-405 Ridgway J, Butcher A, Chen PS, Horner A, Curran S (2010) Novel technology to provide an enriched therapeutic cell concentrate from bone marrow aspirate. Biotechnol. Prog. 26:1741-1748

Rivron NC, Liu JJ, Rouwkema J, de BJ, van Blitterswijk CA (2008) Engineering vascularised tissues in vitro. Eur.Cell Mater. 15:27-40

Robey PG, Boskey AL, ASBMR (The American Society for Bone and Mineral Research) (2008) Chapter 6. The Composition of Bone. Primer on the Metabolic Bone Diseases and Disorders of Mineral Metabolism. John Wiley & Sons, Inc., Washington, USA

Rodan GA (1992) Introduction to bone biology. Bone 13 Suppl 1:S3-S6

Rose FR, Oreffo RO (2002) Bone tissue engineering: hope vs hype. Biochem.Biophys.Res.Commun. 292:1-7

Rougraff BT, Kling TJ (2002) Treatment of active unicameral bone cysts with percutaneous injection of demineralized bone matrix and autogenous bone marrow. J.Bone Joint Surg.Am. 84-A:921-929

Rowley JA, Madlambayan G, Mooney DJ (1999) Alginate hydrogels as synthetic extracellular matrix materials. Biomaterials 20:45-53

Rozbruch SR, Pugsley JS, Fragomen AT, Ilizarov S (2008) Repair of tibial nonunions and bone defects with the Taylor Spatial Frame. J.Orthop.Trauma 22:88-95

Rozen N, Bick T, Bajayo A, Shamian B, Schrift-Tzadok M, Gabet Y, Yayon A, Bab I, Soudry M, Lewinson D (2009) Transplanted blood-derived endothelial progenitor cells (EPC) enhance bridging of sheep tibia critical size defects. Bone 45:918-924

Rush SM (2010) Trinity Evolution: mesenchymal stem cell allografting in foot and ankle surgery. Foot Ankle Spec. 3:140-143

Rush SM, Hamilton GA, Ackerson LM (2009) Mesenchymal stem cell allograft in revision foot and ankle surgery: a clinical and radiographic analysis. J.Foot Ankle Surg. 48:163-169

Russell WMS, Burch RL, Hume CW (1959) The principles of humane experimental technique. Methuen London, UK

Sachlos E, Czernuszka JT (2003) Making tissue engineering scaffolds work. Review: the application of solid freeform fabrication technology to the production of tissue engineering scaffolds. Eur.Cell Mater. 5:29-39

Sagomonyants KB, Hakim-Zargar M, Jhaveri A, Aronow MS, Gronowicz G (2011) Porous tantalum stimulates the proliferation and osteogenesis of osteoblasts from elderly female patients. J.Orthop.Res. 29:609-616

Sah RL, Ratcliffe A (2010) Translational models for musculoskeletal tissue engineering and regenerative medicine. Tissue Eng Part B Rev. 16:1-3

Salgado AJ, Coutinho OP, Reis RL (2004) Bone tissue engineering: state of the art and future trends. Macromol.Biosci. 4:743-765

Salzmann GM, Niemeyer P, Steinwachs M, Kreuz PC, Sudkamp NP, Mayr HO (2011) Cartilage repair approach and treatment characteristics across the knee joint: a European survey. Arch.Orthop.Trauma Surg. 131:283-291

Sammer DM, Chung KC (2009) Tendon transfers: part I. Principles of transfer and transfers for radial nerve palsy. Plast.Reconstr.Surg. 123:169e-177e

Sarkar MR, Augat P, Shefelbine SJ, Schorlemmer S, Huber-Lang M, Claes L, Kinzl L, Ignatius A (2006) Bone formation in a long bone defect model using a platelet-rich plasma-loaded collagen scaffold. Biomaterials 27:1817-1823

Schaefer D, Martin I, Shastri P, Padera RF, Langer R, Freed LE, Vunjak-Novakovic G (2000) In vitro generation of osteochondral composites. Biomaterials 21:2599-2606

Schantz JT, Lim TC, Ning C, Teoh SH, Tan KC, Wang SC, Hutmacher DW (2006) Cranioplasty after trephination using a novel biodegradable burr hole cover: technical case report. Neurosurgery 58:ONS-E176

Schell H, Epari DR, Kassi JP, Bragulla H, Bail HJ, Duda GN (2005) The course of bone healing is influenced by the initial shear fixation stability. J Orthop.Res. 23:1022-1028

Schep N, van Lieshout E, Patka P, Vogels L (2009) Long-term functional and quality of live assessment following post-traumatic distraction osteogenesis of the lower limb. Strategies in Trauma and Limb Reconstruction 4:107-112

Schimming R, Schmelzeisen R (2004) Tissue-engineered bone for maxillary sinus augmentation. J.Oral Maxillofac.Surg. 62:724-729

Schindeler A, McDonald MM, Bokko P, Little DG (2008) Bone remodeling during fracture repair: The cellular picture. Semin.Cell Dev.Biol. 19:459-466

Schmelzeisen R, Schimming R, Sittinger M (2003) Making bone: implant insertion into tissue-engineered bone for maxillary sinus floor augmentation-a preliminary report. J.Craniomaxillofac.Surg. 31:34-39

Schneiders W, Reinstorf A, Biewener A, Serra A, Grass R, Kinscher M, Heineck J, Rehberg S, Zwipp H, Rammelt S (2009) In vivo effects of modification of hydroxyapatite/collagen composites with and without chondroitin sulphate on bone remodeling in the sheep tibia. J Orthop.Res. 27:15-21

Schreurs BW, Bolder SB, Gardeniers JW, Verdonschot N, Slooff TJ, Veth RP (2004) Acetabular revision with impacted morsellised cancellous bone grafting and a cemented cup. A 15- to 20-year follow-up. J.Bone Joint Surg.Br. 86:492-497

Schreurs BW, Keurentjes JC, Gardeniers JW, Verdonschot N, Slooff TJ, Veth RP (2009) Acetabular revision with impacted morsellised cancellous bone grafting and a cemented acetabular component: a 20- to 25-year follow-up. J.Bone Joint Surg.Br. 91:1148-1153

Schroeder JE, Weil YA, Khoury A, Liebergall M, Mosheiff R (2010) Thermal tibial osteonecrosis: a diagnostic challenge and review of the literature. Injury 41:235-238 Schultz O, Sittinger M, Haeupl T, Burmester GR (2000) Emerging strategies of bone and joint repair. Arthritis Res. 2:433-436

Scott NB (2010) Wound infiltration for surgery. Anaesthesia 65 Suppl 1:67-75

Semenov MV, He X (2006) LRP5 mutations linked to high bone mass diseases cause reduced LRP5 binding and inhibition by SOST. J.Biol.Chem. 281:38276-38284

Sengers BG, Dawson JI, Oreffo RO (2010) Characterisation of human bone marrow stromal cell heterogeneity for skeletal regeneration strategies using a two-stage colony assay and computational modelling. Bone 46:496-503

Sengers BG, Please CP, Taylor M, Oreffo RO (2009) Experimental-computational evaluation of human bone marrow stromal cell spreading on trabecular bone structures. Ann.Biomed.Eng 37:1165-1176

Seong JM, Kim BC, Park JH, Kwon IK, Mantalaris A, Hwang YS (2010) Stem cells in bone tissue engineering. Biomed.Mater. 5:062001

Shapiro F (2008) Bone development and its relation to fracture repair. The role of mesenchymal osteoblasts and surface osteoblasts. Eur.Cell Mater. 15:53-76

Sharma P, Solomon KR, Hauschka PV (2006) High-throughput tool for discovery of bone regulating factors. Biotechniques 41:539-40, 542

Shearer JR, Roach HI, Parsons SW (1992) Histology of a lengthened human tibia. J.Bone Joint Surg.Br. 74:39-44

Shimko DA, Nauman EA (2007) Development and characterization of a porous poly(methyl methacrylate) scaffold with controllable modulus and permeability. J.Biomed.Mater.Res.B Appl.Biomater. 80:360-369

Shimko DA, Shimko VF, Sander EA, Dickson KF, Nauman EA (2005) Effect of porosity on the fluid flow characteristics and mechanical properties of tantalum scaffolds. J.Biomed.Mater.Res.B Appl.Biomater. 73:315-324

Shin H, Jo S, Mikos AG (2003) Biomimetic materials for tissue engineering. Biomaterials 24:4353-4364

Shrestha LB, Heisler EJ (2011) The changing demographic profile of the United States. Congressional Research Service, Washington, USA

Simmons PJ, Torok-Storb B (1991) Identification of stromal cell precursors in human bone marrow by a novel monoclonal antibody, STRO-1. Blood 78:55-62

Simon JL, Roy TD, Parsons JR, Rekow ED, Thompson VP, Kemnitzer J, Ricci JL (2003) Engineered cellular response to scaffold architecture in a rabbit trephine defect. J.Biomed.Mater.Res.A 66:275-282

Simonds RJ, Holmberg SD, Hurwitz RL, Coleman TR, Bottenfield S, Conley LJ, Kohlenberg SH, Castro KG, Dahan BA, Schable CA, . (1992) Transmission of human immunodeficiency virus type 1 from a seronegative organ and tissue donor. N.Engl.J.Med. 326:726-732

Singh PK (2009) Occurrence of low grade concentration of niobium and tantalum in the granites of Eastern Uis region of Namibia: An exploration based study. Journal of Geology and Mining Research 1:67-75

Slooff TJ, Huiskes R, van HJ, Lemmens AJ (1984) Bone grafting in total hip replacement for acetabular protrusion. Acta Orthop.Scand. 55:593-596

Smith JO, Aarvold A, Tayton ER, Dunlop DG, Oreffo RO (2011) Skeletal Tissue Regeneration: Current Approaches, Challenges, and Novel Reconstructive Strategies for an Aging Population. Tissue Eng Part B Rev. 17:307-20

Smith JO, Oreffo RO, Clarke NM, Roach HI (2003) Changes in the antiangiogenic properties of articular cartilage in osteoarthritis. J.Orthop.Sci. 8:849-857

Smith JO, Sengers BG, Aarvold A, Tayton ER, Dunlop DG, Oreffo RO (2012) Tantalum trabecular metal - addition of human skeletal cells to enhance bone implant interface strength and clinical application. J.Tissue Eng Regen.Med.

Southwood LL, Frisbie DD, Kawcak CE, McIlwraith CW (2004) Delivery of growth factors using gene therapy to enhance bone healing. Vet.Surg. 33:565-578

Spiegelberg BG, Sewell MD, Aston WJ, Blunn GW, Pollock R, Cannon SR, Briggs TW (2009) The early results of joint-sparing proximal tibial replacement for primary bone tumours, using extracortical plate fixation. J.Bone Joint Surg.Br. 91:1373-1377

Stenderup K, Justesen J, Eriksen EF, Rattan SI, Kassem M (2001) Number and proliferative capacity of osteogenic stem cells are maintained during aging and in patients with osteoporosis. J Bone Miner.Res. 16:1120-1129

Stevenson S, Emery SE, Goldberg VM (1996) Factors affecting bone graft incorporation. Clin.Orthop.Relat Res. 324:66-74

Stewart K, Walsh S, Screen J, Jefferiss CM, Chainey J, Jordan GR, Beresford JN (1999) Further characterization of cells expressing STRO-1 in cultures of adult human bone marrow stromal cells. J.Bone Miner.Res. 14:1345-1356

Stiehler M, Lind M, Mygind T, Baatrup A, Dolatshahi-Pirouz A, Li H, Foss M, Besenbacher F, Kassem M, Bunger C (2008) Morphology, proliferation, and osteogenic differentiation of mesenchymal stem cells cultured on titanium, tantalum, and chromium surfaces. J.Biomed.Mater.Res.A 86:448-458

Stolzing A, Jones E, McGonagle D, Scutt A (2008) Age-related changes in human bone marrow-derived mesenchymal stem cells: consequences for cell therapies. Mech. Ageing Dev. 129:163-173

Sutherland AG, Raafat A, Yates P, Hutchison JD (1997) Infection associated with the use of allograft bone from the north east Scotland Bone Bank. J.Hosp.Infect. 35:215-222

Taichman RS (2005) Blood and bone: two tissues whose fates are intertwined to create the hematopoietic stem-cell niche. Blood 105:2631-2639

Takahashi Y, Tabata Y (2004) Effect of the fiber diameter and porosity of non-woven PET fabrics on the osteogenic differentiation of mesenchymal stem cells. J.Biomater.Sci.Polym.Ed 15:41-57

Tang QO, Shakib K, Heliotis M, Tsiridis E, Mantalaris A, Ripamonti U, Tsiridis E (2009) TGF-beta3: A potential biological therapy for enhancing chondrogenesis. Expert.Opin.Biol.Ther. 9:689-701

Tare RS, Babister JC, Kanczler J, Oreffo RO (2008) Skeletal stem cells: phenotype, biology and environmental niches informing tissue regeneration. Mol.Cell Endocrinol. 288:11-21

Tare RS, Kanczler J, Aarvold A, Jones AM, Dunlop DG, Oreffo RO (2010) Skeletal stem cells and bone regeneration: translational strategies from bench to clinic. Proc.Inst.Mech.Eng H. 224:1455-1470

Tare RS, Khan F, Tourniaire G, Morgan SM, Bradley M, Oreffo RO (2009) A microarray approach to the identification of polyurethanes for the isolation of human skeletal progenitor cells and augmentation of skeletal cell growth. Biomaterials 30:1045-1055

Taylor CJ, Bolton EM, Bradley JA (2011) Immunological considerations for embryonic and induced pluripotent stem cell banking. Philos.Trans.R.Soc.Lond B Biol.Sci. 366:2312-2322

Taylor GI, Miller GD, Ham FJ (1975) The free vascularized bone graft. A clinical extension of microvascular techniques. Plast.Reconstr.Surg. 55:533-544

Taylor WR, Ehrig RM, Heller MO, Schell H, Seebeck P, Duda GN (2006) Tibio-femoral joint contact forces in sheep. J Biomech. 39:791-798

Taylor WR, Heller MO, Bergmann G, Duda GN (2004) Tibio-femoral loading during human gait and stair climbing. J Orthop.Res. 22:625-632

Teixeira CR, Rahal SC, Volpi RS, Taga R, Cestari TM, Granjeiro JM, Vulcano LC, Correa MA (2007) Tibial segmental bone defect treated with bone plate and cage filled with either xenogeneic composite or autologous cortical bone graft. An experimental study in sheep. Vet.Comp Orthop.Traumatol. 20:269-276

Terella A, Mariner P, Brown N, Anseth K, Streubel SO (2010) Repair of a calvarial defect with biofactor and stem cell-embedded polyethylene glycol scaffold. Arch.Facial.Plast.Surg. 12:166-171

Thein-Han WW, Misra RD (2009) Biomimetic chitosan-nanohydroxyapatite composite scaffolds for bone tissue engineering. Acta Biomater. 5:1182-1197

Thomson RC, Yaszemski MJ, Powers JM, Mikos AG (1995) Fabrication of biodegradable polymer scaffolds to engineer trabecular bone. J.Biomater.Sci.Polym.Ed 7:23-38

Tilley S, Bolland BJ, Partridge K, New AM, Latham JM, Dunlop DG, Oreffo RO (2006) Taking tissue-engineering principles into theater: augmentation of impacted allograft with human bone marrow stromal cells. Regen.Med. 1:685-692

Tomford WW (1995) Transmission of disease through transplantation of musculoskeletal allografts. J.Bone Joint Surg.Am. 77:1742-1754

Tourniaire G, Collins J, Campbell S, Mizomoto H, Ogawa S, Thaburet JF, Bradley M (2006) Polymer microarrays for cellular adhesion. Chem.Commun.(Camb.)2118-2120

Triffitt JT (2002) Osteogenic stem cells and orthopedic engineering: summary and update. J.Biomed.Mater.Res. 63:384-389

Trikha SP, Singh S, Raynham OW, Lewis JC, Mitchell PA, Edge AJ (2005) Hydroxyapatite-ceramic-coated femoral stems in revision hip surgery. J.Bone Joint Surg.Br. 87:1055-1060

Tsuchiya H, Tomita K, Minematsu K, Mori Y, Asada N, Kitano S (1997) Limb salvage using distraction osteogenesis. A classification of the technique. J.Bone Joint Surg.Br. 79:403-411

Tuan RS, Boland G, Tuli R (2003) Adult mesenchymal stem cells and cell-based tissue engineering. Arthritis Res.Ther. 5:32-45

Tyllianakis M, Deligianni D, Panagopoulos A, Pappas M, Sourgiadaki E, Mavrilas D, Papadopoulos A (2007) Biomechanical comparison of callus over a locked intramedullary nail in various segmental bone defects in a sheep model. Med.Sci.Monit. 13:BR125-BR130

Ueda M, Yamada Y, Ozawa R, Okazaki Y (2005) Clinical case reports of injectable tissue-engineered bone for alveolar augmentation with simultaneous implant placement. Int.J.Periodontics.Restorative.Dent. 25:129-137

Vacanti CA, Bonassar LJ, Vacanti MP, Shufflebarger J (2001) Replacement of an avulsed phalanx with tissue-engineered bone. N.Engl.J.Med. 344:1511-1514

van der Donk S, Buma P, Slooff TJ, Gardeniers JW, Schreurs BW (2002) Incorporation of morselized bone grafts: a study of 24 acetabular biopsy specimens. Clin.Orthop.Relat Res.131-141

van Haaren EH, Heyligers IC, Alexander FG, Wuisman PI (2007) High rate of failure of impaction grafting in large acetabular defects. J.Bone Joint Surg.Br. 89:296-300

Venkatesan J, Kim S (2010) Chitosan Composites for Bone Tissue Engineering—An Overview. Mar.Drugs 8:2252-2266

Wallace AL, Draper ER, Strachan RK, McCarthy ID, Hughes SP (1991) The effect of devascularisation upon early bone healing in dynamic external fixation. J Bone Joint Surg.Br. 73:819-825

Wallace AL, Makki R, Weiss JB, Hughes SP (1995) Measurement of serum angiogenic factor in devascularized experimental tibial fractures. J Orthop.Trauma 9:324-332

Wang Y, Wan C, Deng L, Liu X, Cao X, Gilbert SR, Bouxsein ML, Faugere MC, Guldberg RE, Gerstenfeld LC, Haase VH, Johnson RS, Schipani E, Clemens TL (2007) The hypoxia-inducible factor alpha pathway couples angiogenesis to osteogenesis during skeletal development. J.Clin.Invest 117:1616-1626

Warnke PH, Springer IN, Wiltfang J, Acil Y, Eufinger H, Wehmoller M, Russo PA, Bolte H, Sherry E, Behrens E, Terheyden H (2004) Growth and transplantation of a custom vascularised bone graft in a man. Lancet 364:766-770

Warnke PH, Wiltfang J, Springer I, Acil Y, Bolte H, Kosmahl M, Russo PA, Sherry E, Lutzen U, Wolfart S, Terheyden H (2006) Man as living bioreactor: fate of an exogenously prepared customized tissue-engineered mandible. Biomaterials 27:3163-3167

Watt FM, Driskell RR (2010) The therapeutic potential of stem cells. Philos.Trans.R.Soc.Lond B Biol.Sci. 365:155-163

Weiner S, Traub W (1992) Bone structure: from angstroms to microns. The FASEB Journal 6:879-885

Welldon KJ, Atkins GJ, Howie DW, Findlay DM (2008) Primary human osteoblasts grow into porous tantalum and maintain an osteoblastic phenotype. J.Biomed.Mater.Res.A 84:691-701

Werdehausen R, Braun S, Essmann F, Schulze-Osthoff K, Walczak H, Lipfert P, Stevens MF (2007) Lidocaine induces apoptosis via the mitochondrial pathway independently of death receptor signaling. Anesthesiology 107:136-143

Whang K, Thomas CH, Healy KE, Nuber G (1995) A novel method to fabricate bioabsorbable scaffolds. Polymer 36:837-842

Widmer MS, Gupta PK, Lu L, Meszlenyi RK, Evans GR, Brandt K, Savel T, Gurlek A, Patrick CW, Jr., Mikos AG (1998) Manufacture of porous biodegradable polymer conduits by an extrusion process for guided tissue regeneration. Biomaterials 19:1945-1955

Widuchowski W, Lukasik P, Kwiatkowski G, Faltus R, Szyluk K, Widuchowski J, Koczy B (2008) Isolated full thickness chondral injuries. Prevalance and outcome of treatment. A retrospective study of 5233 knee arthroscopies. Acta Chir Orthop.Traumatol.Cech. 75:382-386

Wildemann B, Sander A, Schwabe P, Lucke M, Stockle U, Raschke M, Haas NP, Schmidmaier G (2005) Short term in vivo biocompatibility testing of biodegradable poly(D,L-lactide)--growth factor coating for orthopaedic implants. Biomaterials 26:4035-4040

Wilson CG, Nishimuta JF, Levenston ME (2009) Chondrocytes and meniscal fibrochondrocytes differentially process aggrecan during de novo extracellular matrix assembly. Tissue Eng Part A 15:1513-1522

Yamasaki T, Yasunaga Y, Ishikawa M, Hamaki T, Ochi M (2010) Bone-marrow-derived mononuclear cells with a porous hydroxyapatite scaffold for the treatment of osteonecrosis of the femoral head: a preliminary study. J.Bone Joint Surg.Br. 92:337-341

Yang PJ, Temenoff JS (2009) Engineering orthopedic tissue interfaces. Tissue Eng Part B Rev. 15:127-141

Yang XB, Green DW, Roach HI, Clarke NM, Anderson HC, Howdle SM, Shakesheff KM, Oreffo RO (2003) Novel osteoinductive biomimetic scaffolds stimulate human osteoprogenitor activity--implications for skeletal repair. Connect.Tissue Res. 44 Suppl 1:312-317

Yang XB, Webb D, Blaker J, Boccaccini AR, Maquet V, Cooper C, Oreffo RO (2006) Evaluation of human bone marrow stromal cell growth on biodegradable polymer/bioglass composites. Biochem.Biophys.Res.Commun. 342:1098-1107

Yin Z, Chen X, Chen JL, Ouyang HW (2010) Stem cells for tendon tissue engineering and regeneration. Expert.Opin.Biol.Ther. 10:689-700

Yoshimoto H, Shin YM, Terai H, Vacanti JP (2003) A biodegradable nanofiber scaffold by electrospinning and its potential for bone tissue engineering. Biomaterials 24:2077-2082

Young RG, Butler DL, Weber W, Caplan AI, Gordon SL, Fink DJ (1998) Use of mesenchymal stem cells in a collagen matrix for Achilles tendon repair. J.Orthop.Res. 16:406-413

Younger EM, Chapman MW (1989) Morbidity at bone graft donor sites. J.Orthop.Trauma 3:192-195

Zellin G, Linde A (2000) Effects of recombinant human fibroblast growth factor-2 on osteogenic cell populations during orthopic osteogenesis in vivo. Bone 26:161-168

Zhang ZY, Teoh SH, Hui JH, Fisk NM, Choolani M, Chan JK (2012) The potential of human fetal mesenchymal stem cells for off-the-shelf bone tissue engineering application. Biomaterials 33:2656-2672

Zimmermann G, Wagner C, Schmeckenbecher K, Wentzensen A, Moghaddam A (2009) Treatment of tibial shaft non-unions: bone morphogenetic proteins versus autologous bone graft. Injury 40 Suppl 3:S50-S53

Zippel N, Schulze M, Tobiasch E (2010) Biomaterials and mesenchymal stem cells for regenerative medicine. Recent Pat Biotechnol. 4:1-22

Appendices

- Anaesthetic protocol for sheep
- -Peri- and post-operative protocol for sheep
- Selected publications related to this thesis

Anaesthetic protocol for sheep

Pre-medication

Rompun 2% (Xylazine) - 0.1 mg/kg

Bayer Health Care

Strawberry Hill

Newbury

Berkshire

RG14 1JA

Induction

Ketaset (Ketamine) - 2mg/kg

Fort Dodge Animal Health Ltd

Southampton

SO30 4QH

Hypnovel (Midazolam) - 2.5mg flat rate

Roche Products Ltd

Welwyn Garden City

Hertfordshire

AL7 3AY

Maintenance

Isoflurane (IsoFlo) - approx 2% inhaled in pure oxygen

Abbott Laboratories Ltd.

Abbott House

Vanwall Road

Maidenhead

Berkshire

SL6 4XE

Peri- and post-operative protocol for sheep

Analgesic

Durogesic 75mcg/hr (Fentanyl) – 2 patches, 12 hrs before and 60hrs after surgery

Janssen-Cilag

50-100 Holmers Farm Way

High Wycombe

Bucks

HP12 4EG

Vetergesic (Buprenorphine) – 0.6mg approximately 72hrs after second application of fentanyl patches

Alstoe Animal Health

Pera Innovation Park

Nottingham Road

Melton Mowbray

LE13 0PB

Antibiotic Cover

Betamox LA (Amoxicillin) 150mg/ml – 15mg/kg given preoperatively

NorbrookLaboratories (GB) Limited

The Green

Great Corby

Carlisle

CA4 8LR

Ceporex (Cefalexin) – at 5ml/animal for four days

Schering-Plough Animal Health

Division of Schering-Plough Ltd

Welwyn Garden City

AL7 1TW

Euthanasia

Pentobarbital solution 20% – 0.7mg/kg (approx 40mg per sheep)

Pharmasol Ltd.

North Way

Andover

Hampshire

SP10 5AZ